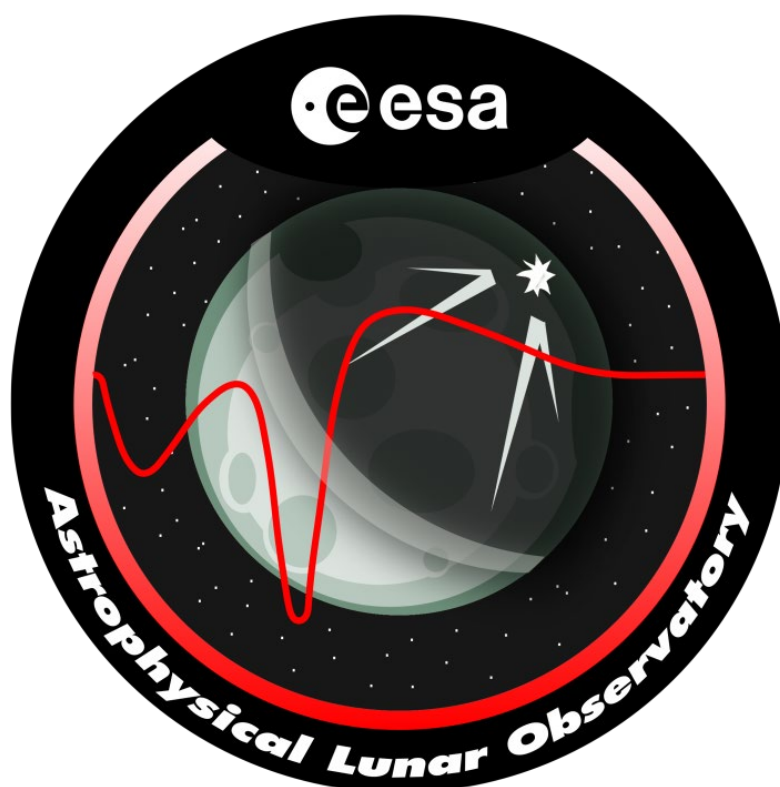

CDF Study Report

ASTROPHYSICAL LUNAR OBSERVATORY

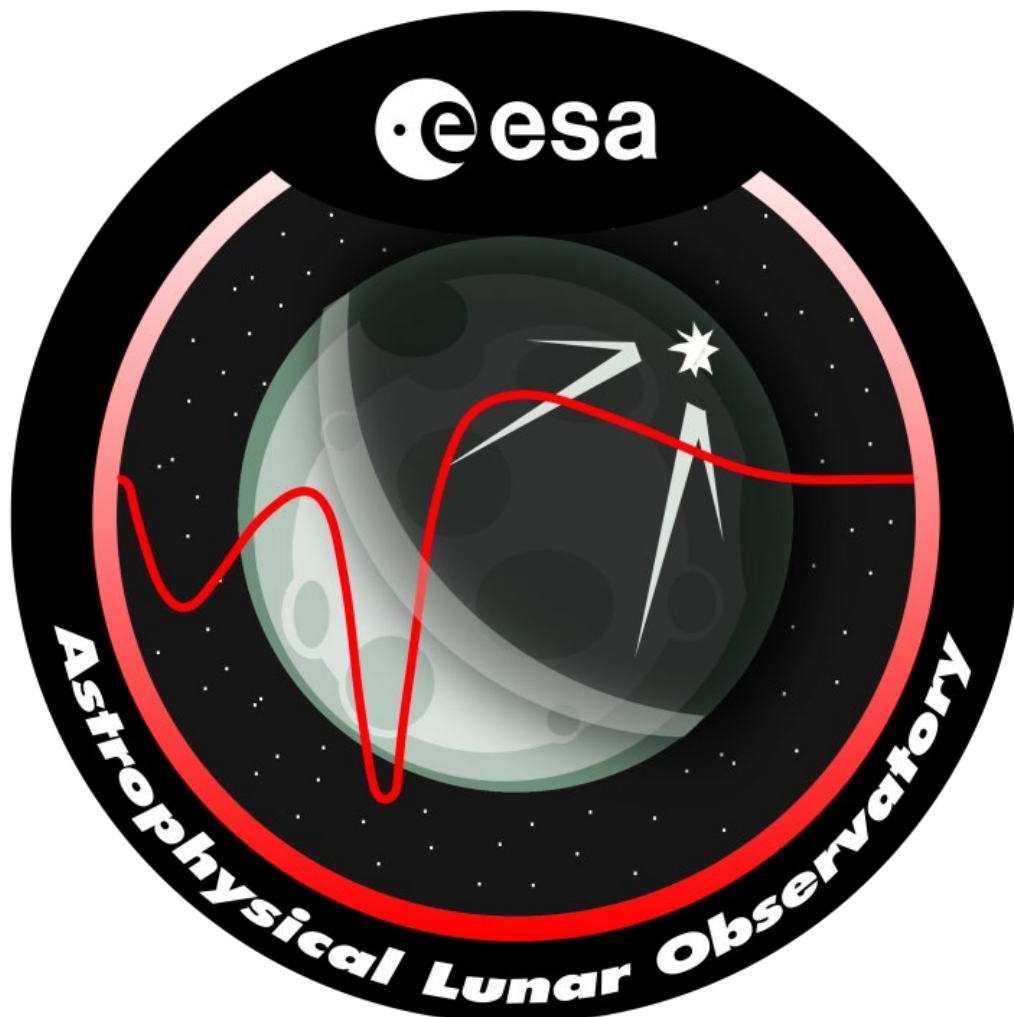
**Assessment of an Astrophysical Lunar Observatory
on the farside of the Moon**



CDF Study Report

ALO

Assessment of an Astrophysical Lunar Observatory on the farside of the Moon



Disclaimer:

This version of the CDF report **CDF-219(C)_December 2024** was generated in response to a specific request. The only modifications made, compared to the previous version, were the removal of names from the team list and the exclusion of the Risk and Cost chapters. No updates have been made with regard to the study itself.

This study report, created in 2021, was not intended for public release. As such, the content of this report should not be shared or used outside the scope of the agreed-upon activity, and therefore its content shall not be distributed online.

FRONT COVER

A stylised logo showing the far side of the
moon

STUDY TEAM

This study was performed in the ESTEC Concurrent Design Facility (CDF) by the following interdisciplinary team:

TEAM LEADER	TEC-SYE		
SPACE ENVIRONMENT	TEC-EPS	PAYLOAD / ANTENNA	TEC-EFA
COMMUNICATIONS	TEC-EST	POWER	TEC-EPM
CONFIGURATION	TEC-MSS	PROGRAMMATICS/ AIV	TEC-MXC
STRUCTURES	TEC-MSS	RISK	TEC-QQD
COST	TEC-SYC	MISSION ANALYSIS	OPS-GFA
ROBOTICS	TEC-MMA	GS&OPS	OPS-OPD
DATA HANDLING	TEC-EDD	SYSTEMS	TEC-SYC
MECHANISMS	TEC-MSM	THERMAL	TEC-MTT

Under the responsibility of:

HRE-E, Study Manager

With the scientific support of experts from:

ESA

Radboud University Nijmegen

RUG

ASTRON

TU Delft

The editing and compilation of this report has been provided by:

TEC-SYE, Technical Author

Please note that all names of the ALO CDF study team members have been deliberately removed from this version of the report.

This study is based on the ESA CDF Open Concurrent Design Tool (OCDT), which is a community software tool released under ESA licence. All rights reserved.

For further information regarding the report please contact:

J. Grenouilleau
ESA/ESTEC/HRE-E
Postbus 299
2200 AG Noordwijk
The Netherlands
Jessica.Grenouilleau@esaint

For further information on the Concurrent Design Facility please contact:

I. Roma
ESA/ESTEC/TEC-SYE
Postbus 299
2200 AG Noordwijk
The Netherlands
Ilaria.Roma@esa.int



TABLE OF CONTENTS

1	INTRODUCTION	12
1.1	Background	12
1.2	Objective.....	12
1.3	Scope	13
1.4	Document structure	13
2	EXECUTIVE SUMMARY	14
2.1	Study flow	14
2.2	Study objectives.....	14
2.3	Requirements and design drivers	14
2.4	Observatory architecture	15
2.5	Baseline design – Single EL3 mission	16
2.6	Considerations for scalability	18
2.6.1	General considerations and known limitations	19
2.6.2	Scaling law summary and conclusions	19
2.7	General conclusions and options.....	20
3	STUDY BACKGROUND	22
3.1	European exploration programme context.....	22
3.2	Lunar exploration programme context	22
3.3	EL3 applicable context.....	25
4	SCIENCE OBJECTIVES AND OBSERVATORY DESCRIPTION	26
4.1	Science case for an Astrophysical Lunar Observatory	26
4.1.1	Introduction	26
4.1.2	Science performance indicators.....	28
4.1.3	High-level goals	33
4.1.4	ALO in the context of other observatories.....	33
4.2	Key drivers and trade-offs.....	34
4.2.1	Architecture – the case for an interferometer.....	34
4.2.2	Antenna level	36
4.2.3	Array level.....	49
4.3	Proposed Observatory description.....	62
4.4	Technology and analysis roadmap	64
4.4.1	ALO analysis topics	65
4.4.2	Dedicated TRL activities (industrial activities).....	67
5	PAYLOAD ANTENNA.....	68
5.1	General considerations and initial assumptions.....	68
5.2	Requirements and Design Drivers	68
5.3	Key drivers and challenges.....	69
5.4	Technology Needs.....	70

6	ENVIRONMENT	72
6.1	Lunar Ionosphere	72
6.2	Plasma Environment and Lunar Surface Charging	72
6.3	Radiation Effects and Main Sources of Radiation Environment	74
6.3.1	The Radiation Belts	74
6.3.2	Solar Particle Events	74
6.3.3	Galactic Cosmic Rays	75
6.3.4	Transfer environment and Surface Phase	75
6.3.5	Total Ionising Dose (TID)	77
6.3.6	Magnetic anomalies	78
6.4	Lunar dust environment	80
6.4.1	Natural dust transport	80
6.4.2	Anthropogenic Dust Transport	81
6.4.3	Dust Accumulation Impact On Sensitive Elements	82
7	MISSION ANALYSIS	84
7.1	General considerations and initial assumptions	84
7.2	Landing site	84
7.2.1	Baseline selection	84
7.2.2	Horizon mask analysis	85
7.2.3	Terrain slope analysis	86
7.3	Communications relay analysis	87
7.3.1	Moonlight/LCNS	88
7.3.2	Lunar Gateway	89
7.3.3	Lunar Pathfinder	91
8	SYSTEMS	92
8.1	General considerations and initial assumptions	92
8.1.1	Key drivers and challenges	92
8.1.2	Harness considerations	93
8.2	Antennas to Base Station	93
8.2.1	Antennas to Hubs to Base Station	93
8.2.2	Antenna concept	95
8.3	Observatory architecture	95
8.3.1	Observatory architecture baseline	98
8.3.2	Observatory data resources	98
8.4	Observatory description	99
8.4.1	Baseline observatory – Single EL3	99
8.4.2	List of Equipment	102
8.5	Considerations for scalability	106
8.5.1	General considerations and known limitations	107
9	DATA HANDLING	112
9.1	General considerations and initial assumptions	112
9.1.1	Key drivers and challenges	112
9.2	Baseline Description	113

9.2.1	On-Board Computer	113
9.2.2	Payload Processing Unit.....	114
9.2.3	Mass Memory	114
9.2.4	HUB Electronics and Data Transfer hardware	114
9.2.5	List of Equipment.....	115
9.3	Trade-Offs and alternative options.....	116
9.4	Considerations for scalability	117
9.5	Technology Needs.....	117
10	TELECOMMUNICATIONS.....	118
10.1	General considerations and initial assumptions.....	118
10.1.1	Subsystem Requirements.....	118
10.1.2	Key drivers and challenges.....	118
10.2	Baseline Description	119
10.2.1	S-band Link.....	120
10.2.2	Ka-band Link.....	122
10.2.3	List of Equipment.....	124
10.3	Trade-Offs and alternative options.....	125
10.3.1	Ka-band transmit-only.....	125
10.3.2	Ka-band multiple antennas	126
10.4	Wireless communication proposal	127
10.5	Considerations for scalability	129
10.6	Technology Needs.....	129
11	MECHANISM	132
11.1	General considerations and initial assumptions.....	132
11.1.1	Key drivers and challenges.....	132
11.2	Baseline Description	132
11.2.1	Cross-dipole payload antenna	132
11.2.2	Antenna Pointing Mechanism	135
11.2.3	List of Equipment.....	137
11.3	Trade-Offs and alternative options.....	137
11.3.1	Cross-dipole payload antennas trade-off	137
11.3.2	Passive deployment trade-off	140
11.4	Considerations for scalability	141
11.5	Technology Needs.....	142
12	ROBOTICS.....	144
12.1	General considerations and initial assumptions.....	144
12.1.1	Key drivers and challenges.....	144
12.2	Baseline description.....	145
12.2.1	Approach	145
12.2.2	High level subsystem components	145
12.2.3	Deployment steps	153
12.2.4	Other considerations.....	156
12.2.5	List of Equipment.....	158

12.3 Trade-Offs and alternative options	158
12.3.1 Robotic arm types on lander and rover.....	158
12.3.2 Different deployment pattern	159
12.4 Considerations for scalability.....	160
12.5 Technology Needs	161
13 THERMAL.....	162
13.1 General considerations and initial assumptions	162
13.1.1 Thermal lunar surface conditions	163
13.1.2 Impact of lunar dust on TCS.....	164
13.1.3 Key drivers and challenges	165
13.2 Baseline Description.....	166
13.2.1 Antenna	167
13.2.2 Hub.....	169
13.2.3 Base	171
13.2.4 List of Equipment.....	172
13.3 Trade-Offs and alternative options	174
13.3.1 Antenna	174
13.3.2 Hub.....	175
13.3.3 Base	176
13.4 Considerations for scalability.....	177
13.5 Technology Needs	178
14 POWER.....	180
14.1 General Considerations and Initial Assumptions.....	180
14.1.1 Key Drivers and Challenges	180
14.1.2 Power System Requirements	181
14.2 Trade-Offs and Analyses.....	181
14.2.1 Local and Central Power System Options	181
14.2.2 Solar Array Attitude Trade-Off	183
14.2.3 Solar Array Mechanical Configuration Trade-Off.....	185
14.2.4 Solar Array Concept Trade-off.....	188
14.2.5 Electrochemical Energy Storage Trade-Off.....	189
14.2.6 Regenerative Fuel Cell System	189
14.2.7 Antenna Power Feed and Cabling Options	191
14.2.8 Parallel Individual Feed	192
14.2.9 Parallel Common Feed.....	192
14.2.10 Series DC Feed	193
14.2.11 Series AC Feed (as selected in the NASA-JPL FARSIDE study RD[109])	193
14.2.12 Antenna Power Feed Conclusions.....	194
14.3 EPS Model and Baseline Sizing Results	194
14.3.1 EPS Model Description.....	194
14.3.2 EPS Model Inputs and Assumptions	195
14.3.3 EPS Model Results	195
14.3.4 EPS Model Timeline	196

14.3.5 List of Equipment.....	197
14.4 Considerations for scalability	198
14.4.1 Nuclear Power – Radioisotope Systems.....	198
14.4.2 Nuclear Power – Space Fission Reactor Systems.....	199
14.5 Technology Needs.....	201
15 CONFIGURATION	202
15.1 General considerations and initial assumptions.....	202
15.1.1 Key drivers and challenges.....	203
15.2 Baseline Description	204
15.3 Internal and External accommodation	205
15.4 Overall Dimensions.....	207
16 STRUCTURES	208
16.1 General considerations and initial assumptions.....	208
16.1.1 Key drivers and challenges.....	208
16.2 Baseline Description	209
16.2.1 List of Equipment.....	210
16.3 Considerations for scalability	211
16.4 Technology Needs.....	211
17 GROUND SEGMENT AND OPERATIONS.....	212
17.1 General Considerations and Initial Assumptions	212
17.1.1 Assumptions for the Rover Operations Phase	213
17.1.2 Assumptions for the Observatory Operations Phase	214
17.2 Specific Considerations for Operations.....	215
17.2.1 Considerations for Contingencies	216
17.2.2 Considerations for Hibernation	217
18 PROGRAMMATICS/AIV	218
18.1 General considerations and initial assumptions.....	218
18.2 Baseline Description	218
18.3 Technology Requirements.....	218
18.3.1 Generalities.....	218
18.4 TRL Assessment	219
18.5 Technology Needs.....	221
18.6 Development Approach	222
18.7 Summary and Recommendations.....	226
19 RISK ASSESSMENT	228
20 COST.....	229
21 CONCLUSIONS	230
21.1 Representativeness of results	230
21.1.1 Dipole/antenna concept	230
21.1.2 Harness budget	231

21.1.3 Magazine concept for deployment.....	231
21.1.4 Solutions for power supply and thermal control.....	231
21.1.5 Communications architecture for relay systems	231
21.2 Feasibility considerations	232
21.3 Main outcome of the study	232
21.3.1 Technology showstoppers.....	233
21.4 Study objectives achievement.....	233
21.5 Further study areas	233
22 REFERENCES.....	235
23 ACRONYMS	245
A APPENDIX A - TECHNOLOGY READINESS LEVELS TABLE	251

This Page Intentionally Left Blank

1 INTRODUCTION

The Astrophysical Lunar Observatory (ALO) mission is notionally the 3rd mission concept being studied in the context of the European Large Logistic Lander (EL3) project, currently in phase A/B1 aiming at program subscription at ESA Ministerial Council in 2022.

1.1 Background

TEC-SYE was requested by HRE-E to perform a CDF Study on a mission concept to deploy and operate a low radio frequency interferometric array on the far side of the Moon, building on the capabilities of the EL3 system.

The study was carried over 8 plenary sessions with Kick-off on 8 June 2021 and Internal Final Presentation on 8 July 2021. These sessions were supplemented with additional topical meetings and, throughout the whole process, the study benefited of the invaluable participation and support of the ALO science team community.

The observatory aims at providing the capability to image the entire sky extending down two orders of magnitude below bands accessible to ground-based radio astronomy.

The lunar farside can simultaneously provide isolation from terrestrial radio frequency interference, auroral kilometric radiation and plasma noise from the solar wind, representing a unique location within the inner solar system from which sky noise limited observations can be carried out at sub-MHz frequencies.

1.2 Objective

The CDF ALO Study aimed at supporting the consolidation of the mission and payload concepts and the preparation of any potential pre-phase A industrial activities, for which the following study objectives were defined:

- Consolidate payload concept, needs and constraints, together with the ALO science team
- Identify options for the payload architecture and deployment (number of antennas, positioning area, etc.)
- Define mission concepts implementing the payload deployment and operation, and identify potential gaps with respect to current EL3 capabilities
- Identify key technology developments to be further addressed through industrial studies
- Assess the mission risk and schedule risks while ensuring alignment with EL3 programmatic constraints

1.3 Scope

The study scope included the following activities:

- Critical review of the observatory requirements derived from the science objectives, science requirements, and preliminary observatory definition to assess the maturity of the payload concept
- Characterisation of main observatory parameters (topology, performances, etc.) driving its deployment and operation, and its impact on the overall science return
- Comprehensive assessment of the state of the art for all required technologies based on the possible system architectures, identifying gaps and potential solutions to implement the ALO mission
- Consolidation of potential mission and observatory concepts compatible with EL3 programmatic context, identifying mission and schedule risks and proposing mitigation actions when possible
- Preliminary cost assessment based on general EL3 and specific ALO considerations, including economy of scales for recurrent costs
- Identification of potential areas for international collaboration

The results of the study were presented to the customer and ALO science team at the Internal Final Presentation (RD[1]), and detailed in this Technical Report and the Cost Report (RD[2]).

1.4 Document structure

The layout of this report of the study results can be seen in the Table of Contents. The Executive Summary chapter provides an overview of the study; details of each domain addressed in the study are contained in specific chapters.

Due to the different distribution requirements, the costing information is published in a separate document (RD[2]).

2 EXECUTIVE SUMMARY

2.1 Study flow

The Astrophysical Lunar Observatory (ALO) mission study, requested by HRE-E and funded by the General Studies Programme (GSP) office, is a multidisciplinary study performed in the Concurrent Design Facility (CDF) by an interdisciplinary team of experts from across ESA and supported by the ALO science team community carried over 8 plenary sessions with Kick-off on 8 June 2021 and Internal Final Presentation on 8 July 2021.

2.2 Study objectives

The CDF ALO Study was aimed at supporting the consolidation of the mission and payload concepts and the preparation of any potential pre-phase A industrial activities, for which the following study objectives were defined:

- Consolidate payload concept, needs and constraints, together with the ALO science team
- Identify options for the payload architecture and deployment (number of antennas, positioning area, etc.)
- Define mission concepts implementing the payload deployment and operation, and identify potential gaps with respect to current EL3 capabilities
- Identify key technology developments to be further addressed through industrial studies
- Assess the mission risk and schedule risks while ensuring alignment with EL3 programmatic constraints

2.3 Requirements and design drivers

The Lunar Descent Element (LDE) is the actual EL3 lander. As payloads may not formulate requirements towards the LDE, it is considered outside the definition scope of this study. The Cargo Platform Element (CPE) is the interface between the LDE and the EL3 payload, which can provide functions requested by the user. In this study, the CPE is considered integral part of the mission payload and therefore within the scope of the study.

The ALO mission aims at landing, deploying and operating a low radio frequency observatory on the far side of the Moon to support the following scientific experiments:

- **Imaging Array**
 - Regular interferometric array of antennas (smallest: 32 x 32, optimal: 128 x 128)
 - Dense distribution e.g. antenna centres ~ 5.15 m apart from each other
 - Placement location accuracy in the order of 0.1 to 1 m (TBC)
 - Placement orientation accuracy in the order of 10 deg rms (TBC)
- **Global Detection**
 - 1 antenna [or preferably 2 or 3 independent ones]
 - Large distance to base station (> 1 km) & any other antennas to minimize noise interference

NOTE: Due to low maturity of the antennas design for these experiments, it was assumed that both experiments could share a common detector design and thus it was considered as a black box (in particular, by analogy with existing heritage, it was assumed 200 x 200 x 200 mm³ in stowed configuration with up to 2 kg of mass and 2 W of power consumption).

The main driving mission requirements are:

- Goal: Deploy and operate 1000-16000 antennas
- Observatory located on the far side of the moon
- Mission Lifetime of 4 years
- Lunar Environment: Radiation, dust, plasma, Lunar night @ ~ -170 °C and Lunar day @ ~ 100 °C for ~ 14 Earth days (near equatorial)
- One single EL3 as dedicated lunar landing system
- Observatory data generation rate (up to ~ 20 Mbit/s)

2.4 Observatory architecture

The potential architectures for the observatory have been formulated based on a functional decomposition of the end-to-end science data processing flow over the following three subsystems:

- The Antenna subsystem
- The Network subsystem
- The Base Station subsystem

		Network has Hubs		Digitization			Processing	
		NO	YES	@ antenna	@ hub	@ base	@ hub	@ base
Scenario	1	✓				✓		✓
	2	✓		✓				✓
	3		✓			✓		✓
	4		✓		✓			✓
	5		✓	✓				✓
	6		✓		✓		✓ (pre)	✓ (final)
	7		✓	✓			✓ (pre)	✓ (final)

Table 2-1: Main Features of each System Architecture Scenario

In particular, out of the 7 identified options presented in Table 2-1, the preferred architecture (Scenario 4) considers the following allocation of functions to each subsystem:

- Array antennas are grouped in clusters and assigned to a central hub
- Each antenna within a cluster sends analog signals to their respective hub
- Each hub digitizes all analog signals of the cluster, bundles them, and sends a digital signal to the base station
- All data processing is done at the base station

A diagram of the observatory architecture baseline is shown in Figure 2-1.

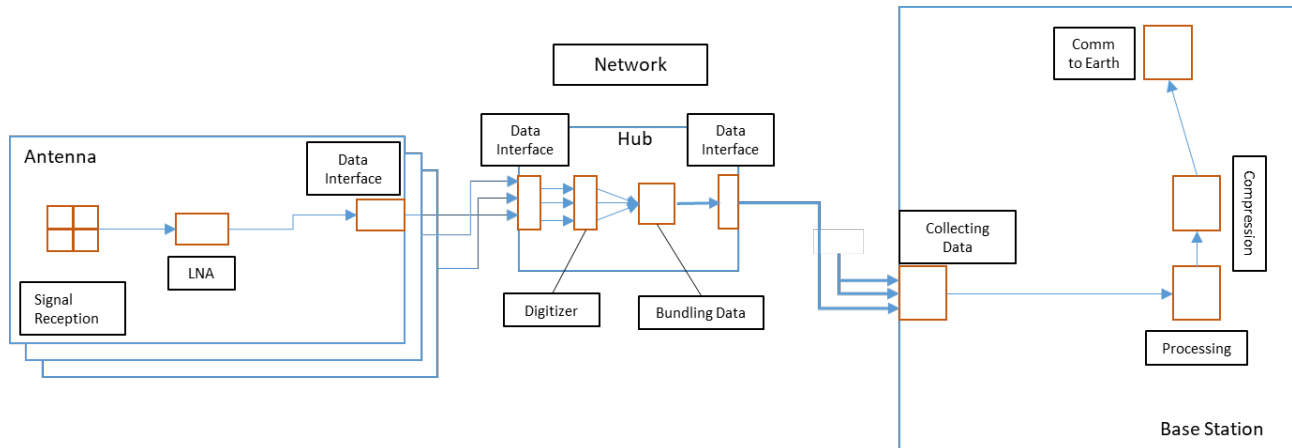


Figure 2-1: Observatory Architecture Baseline

2.5 Baseline design – Single EL3 mission

Based on the initial assumptions for the antenna detector, an observatory array in the ~ 1,000 to ~ 16,000 units range would have a mass between 2 and 33 t and power needs between 2 and 33 kW, in addition to all housekeeping supporting subsystems and kilometres of harness for power and data. This largely surpasses the capacity of a single EL3 mission.

The study baseline is therefore the “smallest reasonable observatory”, still fully representative of a larger scale one, that allows identifying and characterising the different design thresholds as function of the observatory size.

From a first sizing iteration, the following system level assumptions were made for an observatory compatible with a single EL3 mission:

- One single Imaging Array cluster of 16 antennas and 1 hub, with Global Detection experiment done with some antenna(s) of the array (different operation mode)
- Wired power and data transfer between antennas and hub, and between hub and base station, plus wireless data transfer between hub and base station as demonstrator
- Central power supply with solar panels and Regenerative Fuel Cell (RFC)
- Lunar night survival with heaters and hibernation
- One single rover using a magazine-like concept for deployment of the antennas (after antennas are deployed, the magazine is also deployed remaining as hub for the cluster)

The ALO mission baseline design is summarised in Table 2-2 and shown in Figure 2-2.

(Nominal) Mass	<p>ALO Payload (incl. CPE): 984.6 kg</p> <ul style="list-style-type: none"> - Antenna subsystem: 29.6 kg - Network subsystem: 58 kg incl. 7.6 kg of harness - Base Station subsystem: 503.5 kg - Rover: 393.4 kg incl. 43.5 kg antenna deployment arm
(Nominal) Power	<p>Night survival system demand: ~225 W</p> <p>Nominal day operation system demand: ~250 W</p>
Observatory	<p>16x antenna units</p> <p>1x magazine hub</p> <p>1x Science Data Processing Unit</p>
Data Handling	OBC+RTU, SSMM
Communications	<p>Ka-band (1x HGA, 2x RX/TX, 2x TWTA, 1x RFDN)</p> <p>S-band (2x LGA, 2x RX/TX, 2x TWTA, 1x RFDN)</p> <p>On-ground wireless network</p>
Mechanisms	<p>Solar array HDRMs and hinges</p> <p>HGA Pointing Mechanism</p> <p>Rover Unloading Mechanism</p>
Robotics	Hub deployment arm
Thermal Control	<p>Antennas: MLI, heaters, washers, white paint/SSM/OSR</p> <p>Hub: louvers, MLI, heaters, washers, white paint/SSM/OSR</p> <p>Base Station: louvers, MLI, heaters, washers, white paint/SSM/OSR, heat pipes, loop heat pipes (TBC), RHU (TBC)</p>
Power	8.1 m ² Solar array, RFC, Battery, PCDU
Structures	<p>Primary structure (LDE I/F):</p> <ul style="list-style-type: none"> - Ø 2.121 m x 0.2 m CFRP core / Al skin honeycomb sandwich central cylinder with Aluminium ring - CFRP core / Al skin honeycomb sandwich rover deck <p>Secondary structure (Rover garage):</p> <ul style="list-style-type: none"> - CFRP core / Al skin honeycomb sandwich side walls Al core / Al skin honeycomb sandwich roof with shear support <p>NOTE: Deck extensions serves as rover driveway</p> <p>Robotic arm support, equipment I/Fs, brackets and inserts</p>

Table 2-2: ALO Payload Design Overview

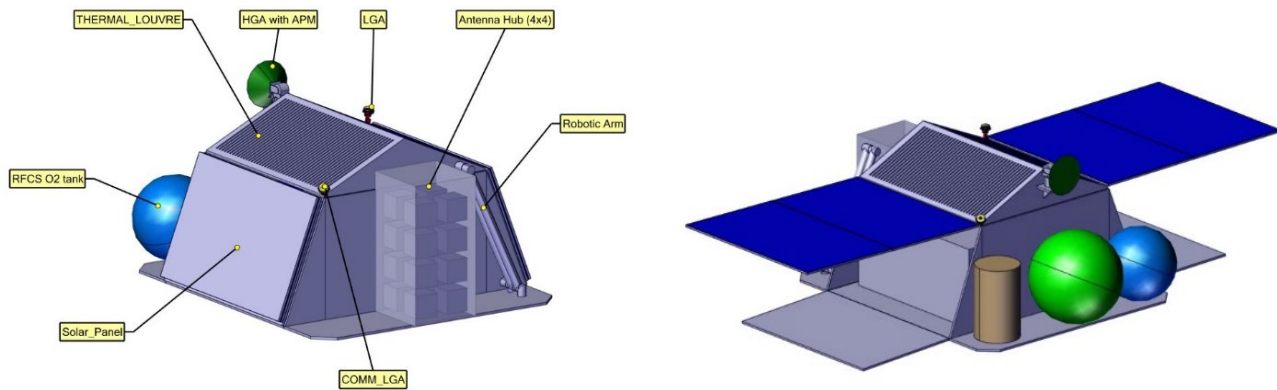


Figure 2-2: ALO Payload in Stowed and Deployed Configuration

An observatory duty cycle has been defined for the system sizing based on a sensitive balance between power demand during day and night, between science data generation and downlink, and between observation time and mission operation overheads while ensuring consistency with observatory efficiency (25% over 4 years lifetime). Table 2-3 provides the observatory operational modes and their time allocation assumed over a full lunar day.

Mode	Duration [h]	Description & Rationale
Standby	35	Residual buffer for idle state. Only minimal necessary units are active. Antennas and hubs are off.
Observation	288	Main science operation mode. Max. time window including time to recharge fuel cell. All antennas and hub operational. Base station processing and storing science data.
Communication	15	Transmitting science data and mission housekeeping to Earth and receiving mission telecommands from Earth via relay. Communication units on Antennas and hubs are off.
Hibernation	370	Hibernation time for lunar night survival (incl. margin). All units off except for thermal control (i.e. PCPU, RFC and OBC/RTU at minimum).

Table 2-3: Baseline Observatory Conceptual Schedule

2.6 Considerations for scalability

This section presents and discusses the system budgets of different scaled arrays based on the extrapolation of the baseline system presented in Section 2.5. Given that not all design assumptions can be directly extrapolated, these results shall be considered in terms of orders of magnitude and not as precise results of additional design iterations.

2.6.1 General considerations and known limitations

The volume available and required for accommodation of units has not been assessed in scaled missions. Therefore, while mass-wise a certain array might be compatible with a given number of EL3s, accommodation feasibility has not been confirmed for such system in that number of EL3s.

The mass of the power subsystem is scaled with the power demand, although the baseline solution (solar panels plus RFC) is not suitable for large arrays with demands above ~ 1 kW during lunar night.

Similarly to the volume, the thermal control of the base station has not been assessed in scaled missions since geometric impact cannot be directly extrapolated.

The potential need or benefits of using a larger number of rovers has not been assessed in scaled missions (maintained at 1 for all cases). This is expected to be sufficient for small arrays but not likely for large arrays if deployment time wants to be kept to a reasonable minimum.

The harness length is approximated only in orders of magnitude, based on some general observatory topologies, while the thresholds –assuming feasibility- to implement some wireless solutions could not be established.

The number of antennas per hub is fixed at 16 based on the selected reference antenna unit concept and the observatory deployment strategy, but larger arrays would require more efficient and compact stowed configurations with likely larger number of antennas per hub.

2.6.2 Scaling law summary and conclusions

Table 2-4 presents a summary of all budgets and -as reference- a simple estimation, based on the overall observatory mass, of the potentially required number of EL3 missions.

Array Size	Mass [t]	Max. Power [kW]	Comp. Power [Mflops]	Data Rate [kbit/s]	Number of EL3s
4 x 4 = 16	0.98	0.25	102	0.6	1
8 x 8 = 64	1.43	0.7	614	5	~ 1
16 x 16 = 256	3.2	2.7	3,277	40	~ 2–3
32 x 32 = 1024	10.5	11	16,384	300	~ 7
64 x 64 = 4096	39.7	42	78,643	2,400	~ 25
128 x 128 = 16384	157.8	170	367,000	19,500	~ 90

Table 2-4: Summary of Observatory Budgets Scaling with Array Size

Considering, that these numbers are nominal values without system margins and limited redundancy (e.g. no redundancy for harness), the baseline observatory (4 x 4) is likely the largest array that can be delivered by a single EL3 without any significant improvement of the

assumptions considered for this study. Therefore, it is well suited as a precursor mission to demonstrate feasibility of instruments and the observatory architecture.

For the slightly larger cases, in addition to the potential accommodation feasibility issues, the available capacity of each EL3 might be quickly reached once all margins and redundancy requirements are considered. Furthermore, if multiple EL3s are required, since all data must be delivered to and processed at a single base station, this requires different dedicated EL3s designs (one as base station, the others just providing additional antenna and hubs to be deployed and connected to the common base station). These alternative mission concepts were not assessed in this study.

2.7 General conclusions and options

The study highlighted the challenges of the ALO mission and could not confirm feasibility for the minimum required observatory size due to the extremely large number of antenna detectors required for the interferometric array observatory (starting at ~1,000 antennas for a minimal array size of 32 x 32 up to ~16,000 antennas for an optimal array size of 128 x 128).

The study results present the “smallest reasonable observatory”, still fully representative of a large scale one, as study baseline plus the considerations for scalability that allows establishing a) a long-term development plan addressing technology showstoppers and enablers, and b) the scoping of the mission in the overall context of the European Lunar Exploration strategy and, in particular, the EL3 program.

The extrapolation for any given observatory size suffers from some limitations and lack of representativeness for certain design assumptions, which have been thoroughly identified and described to ensure an adequate interpretation of the results.

Overall, the study allowed to consolidate the observatory concept, payload performances and resources needs, to identify and characterise the support capabilities such as deployment and housekeeping infrastructure needs, and to establish the possible observatory architectures, including feasibility considerations and limitations in terms technology showstoppers.

Nevertheless, a number of areas for further consolidation are proposed:

- Antenna specification and implementation options, including confirmation of a single antenna design suitability for both science cases
- Alternative deployment strategies for full-scale observatory, including confirmation of full autonomous robotic deployment compared to potential hybrid approaches involving human supported by robotic assets
- Harness characterisation and specification
- Foreseen capabilities of Lunar relay and navigation services

As well as potential Technology Development Activities to further enable larger observatories:

- Low power electronics
- Passive thermal control designs for night survival, including
 - Tolerance to very low [non-operational] temperatures
- Wireless on-ground comms (10-100 Gbps @ 100-1000m)
- Low mass cryogenic harness for radiofrequency, digital data and power distribution
 - Low power losses and voltage drop over long distances
- Large scale lunar power supply

- Super-computing (data storage and processing) in space

Finally, two potential follow up studies are recommended:

- Global Detection + small array for Imaging Array precursor mission
- Dedicated Global Detection mission
 - Possibility also in coordination with other EL3 missions

3 STUDY BACKGROUND

3.1 European exploration programme context

ESA's future for human spaceflight and robotic exploration is a sustainable and international endeavour to visit new places and discover new things. Exploring space is about travelling farther and coming back with new experiences and knowledge to help us on Earth.

The Human and Robotic Exploration (HRE) strategy, described in the European Exploration Envelope Programme (E3P), includes three destinations where humans will work with robots to gather new knowledge: low-Earth orbit on the International Space Station, the Moon and Mars. The three destinations share a common horizon goal, namely human presence on Mars.

In the medium term, the exploration programme includes Europe's service module for NASA's Orion spacecraft, a landing on the Moon with Roscomos' Luna and drilling into Mars with ESA's ExoMars rover. A Gateway farther afield than the International Space Station will see significant European contribution in terms of architecture elements (notably I-HAB, ESPRIT, and CLTV). Moonlight/LCNS, an exciting new way of buying services for exploration, will provide for communication and navigation support to lunar exploration missions. These combined shall constitute a springboard for a sustainable lunar surface exploration and preparing for the next big leap to Mars.

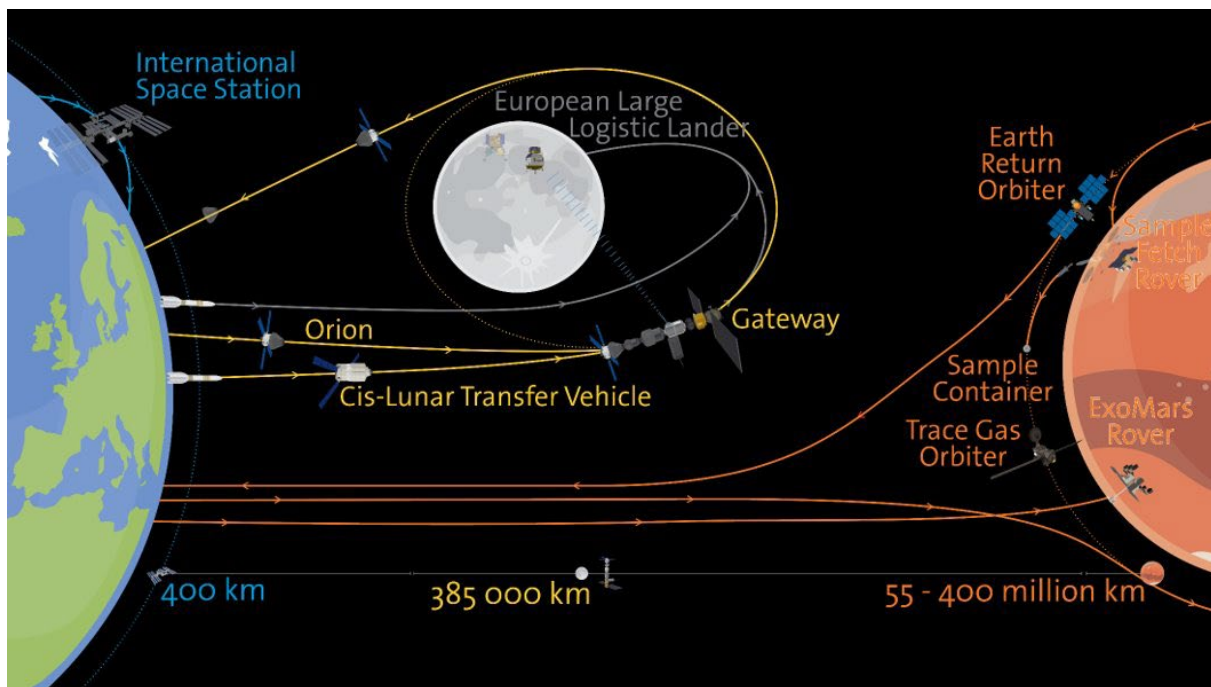


Figure 3-1: Summary of E3P major current activities by destination: LEO, at Moon and Mars

3.2 Lunar exploration programme context

The interest in the Moon exploration has grown substantially in the last years, positioning the Moon as an attractive place to develop the required technologies and capabilities for human Deep Space exploration. The Moon exploration is therefore now emerging as the next global strategic priority in space exploration and the latest developments are expected to further support highly ambitious government and commercial missions.

Moon missions of opportunity provide for:

- Early research opportunities for lunar surface science
- Development of key instrumentation capabilities
- Increased opportunities for lunar surface research outside of ESA led missions
- Consolidate partnerships and cooperation opportunities with lunar exploration partners

The European Large Logistics Lander (EL3) is a strategic contribution to international lunar surface exploration efforts. It will provide complete European autonomy for standalone, large and ambitious robotic lunar surface missions, including launch on Ariane 64EVO.

The inherent capabilities of EL3 ensures that the vehicle can support key lunar exploration needs, both in the context of the evolving Artemis architecture as well as broader international lunar exploration efforts. As such, it complements NASA's Artemis architecture by delivering payload to any location on the surface of the moon, accessing sites which will be difficult for a Human Landing System (HLS) or would not warrant a dedicated HLS mission. Furthermore, the payload capability of EL3 is substantially higher than the currently foreseen Commercial Lunar Payload Services (CLPS) landers providing the capability to support more complex robotic surface exploration mission. Finally, EL3 could deliver critical infrastructure elements (e.g. ahead of lunar surface expeditions) for human surface operations such as power systems or navigation systems.

In 2020, ESA organised a Call For Ideas (CFI) for exploring the Moon with EL3. The purpose of the call for ideas was to gather novel ideas for ways to utilise the capabilities of a large European lunar lander, and to leverage this information to support programmatic decisions. Out of the many ideas which were submitted, 6 overarching science mission concept themes emerged from the call for further study. Several virtual expert workshops were consequently held during Q4 of 2020, providing continued engagement with the science community as a next step following the call for ideas. Subsequently a number of scientific Topical Team proposals have been received, via the continuously open research announcement for Topical Teams. The CFI resulted in a set of Future mission concepts to be advanced by the Exploration Preparation, Research & Technology (ExPeRT) team through Concurrent Design Facility (CDF) studies and/or industrial studies:

- A power plant which could provide energy to a lunar human surface infrastructure
- An In-Situ Resource Utilisation (ISRU) pilot plant
- A biological sciences mission to investigate the effects of the integrated lunar environment on biological systems of different complexities
- An astrophysical observatory to be located on the lunar farside and which primarily observes in long wavelength radio
- A lunar geosciences mission, which performs in situ sample analysis with mobility

The aim of these studies of future projects and capabilities is to identify which potential concepts could be developed into missions in subsequent programme periods, along with the maturation of the required mid-TRL technologies for these missions. It is necessary in the early project phases (0, A, B1 and B2) to spend adequate effort to define a technology plan and the technology readiness status list to properly support the assessment of the mission achievable performance, the overall project schedule and the related costs and risk. From these, realistic plans are refined to ensure a timely implementation of the mission selection process.

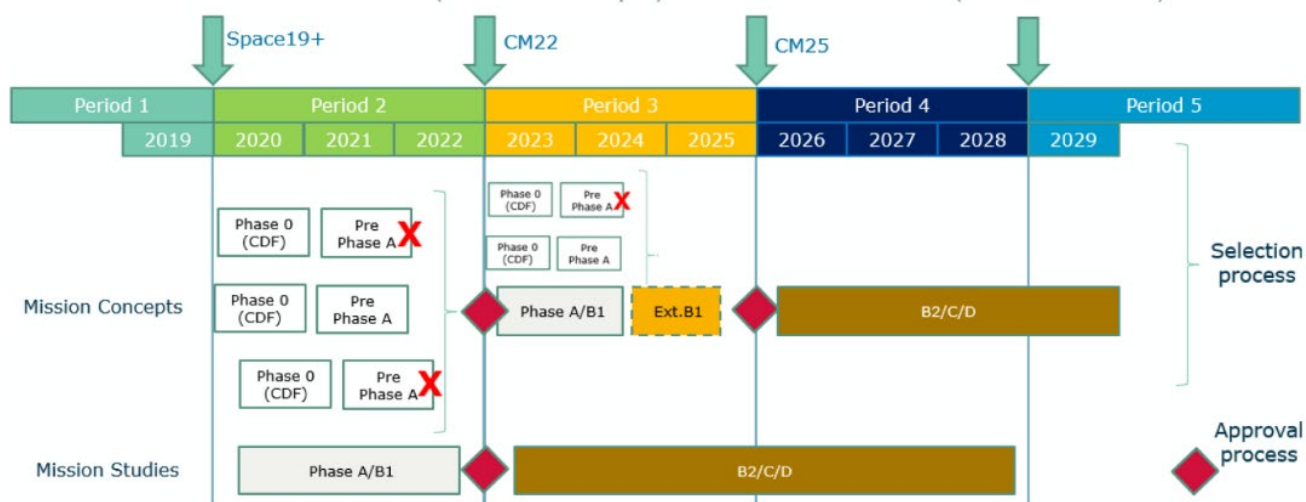


Figure 3-2: Mission selection process overview

It is foreseen to perform the first EL3 mission in 2029, which could potentially be a cargo logistic flight in support of Artemis, a scientific mission or a hybrid logistic / science mission. Following the EL3 Maiden mission, additional flights in the 2030-2040 timeframe are foreseen, typically in a 3 missions batch procurement approach at approximately 3 years interval.

The study described in this report focuses upon one of the identified missions, the Astrophysics Lunar Observatory (ALO), aiming at landing the elements needed for a radiotelescope in order to carry out specific astrophysical science investigations from the lunar farside.

Notionally (see Figure 3-3), the concept behind ALO is simple. However, it is well known that radio-telescopes on Earth are (very) large and (very) complex projects, usually the fruit of international collaboration. As such it was anticipated quite early that this study, instead of trying to establish a set design, should rather aim at exploring the trade-space with the science team, explore the possible architecture options and identify the design drivers. Central to the work of the study team, was the goal to reach a collecting area as large as possible and identify how to scale the observatory.

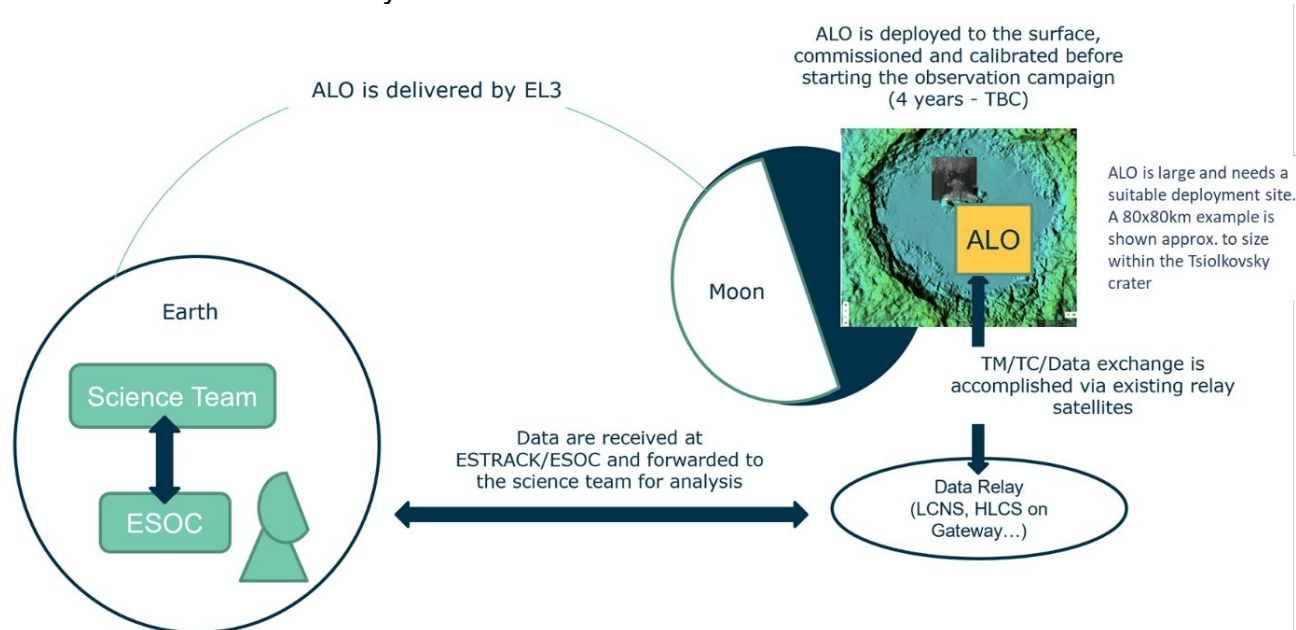


Figure 3-3: ALO notional overview

3.3 EL3 applicable context

The EL3 will be a significant and visible contribution to the international sustainable exploration of the lunar surface. It will provide an entirely autonomous European capability – with a launch by Ariane 64 – for large robotic surface missions for an extended duration.

As a robotic vehicle able to land anywhere on the Moon, EL3 missions will provide access to the surface for substantial scientific payloads and technology demonstrations (static or with surface mobility).

To support a variety of different missions the EL3 consists of a modular design, including the following elements:

- The Lunar Descent Element (LDE) is the core lander vehicle with a fully recurrent production which can support all of the basic requirements of the different missions
- The Cargo Payload Element (CPE) which provides an interface to the different payloads and some common services
- Mission Specific Payloads may include scientific instruments or technical demonstrators, robotic rovers, logistics cargo or infrastructure elements

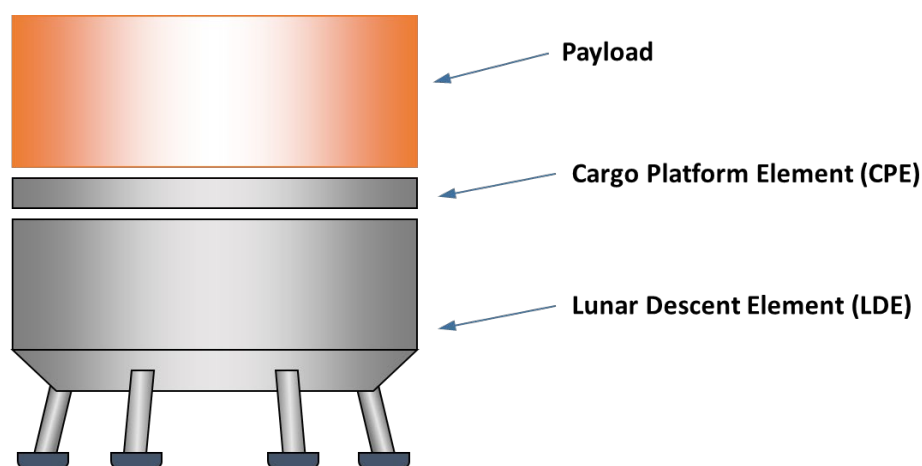


Figure 3-4: EL3 combined stack

Several CDF, pre-phase A and phase A/B1 have already been undertaken, thereby allowing to rely upon existing knowledge and to make assumptions for the study of ALO.

- EL3 LEOP and Transit are out of scope for the study; the mission starts post-landing
- EL3 is capable of landing up to 1700 kg of payload (incl. CPE)
- EL3 can land anywhere on the Moon, including equatorial areas with an accuracy of 250x50 meters; azimuth is not controlled during landing
- The LDE design is taken for granted; only if critically required, very minimal adjustments could be proposed
- CPE is an integral part of the trade-space; CPE design and services are being investigated, as is the scheme of a deeper integration between CPE and LDE; the CPE can be notionally custom-fit for purpose
- Launch in mid 2030's, as part of EL3 mission batch 2

4 SCIENCE OBJECTIVES AND OBSERVATORY DESCRIPTION

4.1 Science case for an Astrophysical Lunar Observatory

4.1.1 Introduction

Following the detection of gravitational waves, and taking into account the wealth of astronomical instrumentation across the electromagnetic spectrum, the radio frequency range below ~30 MHz remains the last virtually unexplored frequency domain. The Earth's atmosphere reflects back all radiation from space below its ionospheric plasma frequency (around 20 MHz), and the turbulent ionosphere gives rise to "radio seeing", making ground-based radio observations of the sky more difficult at frequencies below ~100 MHz but certainly prohibiting observations at the lowest frequencies. An additional complication at lower radio frequencies is that strong man-made Radio Frequency Interference (RFI) levels close to Earth require either locations which provide partial or complete obscuration of the Earth, or locations that are sufficiently remote so that the RFI levels are significantly attenuated. In addition, stable temperature and gain conditions are essential to allow for careful calibration of the radio antennas. These requirements are met only for a number of locations of which the lunar far side, the lunar north- and south poles and the lunar orbit seem to be the most promising ones.

Hence the ESA EL3 plans to allow for scientific infrastructure to be placed on the Moon, and in particular the lunar far side, will allow to **open up the last, virtually unexplored, window on the universe**.

There is a wealth of science to be addressed in the low-frequency radio regime, ranging from the study of Solar and Jovian emission to the detection of exo-planets, but the real treasure trove is the **detection and imaging of the redshifted 21-cm line emission from the neutral Hydrogen in the pristine periods of the universe known as the Dark Ages¹ (DA) and the Cosmic Dawn² (CD; see e.g. RD[47]; RD[44]; RD[32]; RD[31]; RD[48]).**

The only conceivable signal from the CD and DA comes from the hyperfine 21-cm (1.4 GHz) line from neutron Hydrogen caused by the spin flip of the electron. The high redshift involved causes this emission to redshift into the frequency range between 1.4 – 140 MHz, with the **Global³ DA and CD signals** peaking around 30 MHz and 70 MHz, respectively, and being rather broad, hence requiring space-based or lunar-based low-frequency radio instrumentation. See Figure 4-1 for a sketch of the evolution of the Global signal over time.

¹ Dark Ages refers to the epoch in the very early Universe's history after it has recombined and become neutral (about 380000 yrs after the Big Bang) and during which ordinary matter starts to condense by gravity, but no stars have formed yet. See Figure 4-1.

² Cosmic Dawn refers to the epoch when the first stars, black holes, and galaxies in the Universe formed, starting about 50 million years after the Big Bang and ending about one billion years later, by which time diffuse intergalactic Hydrogen in the Universe is again fully ionized. Figure 4-1.

³ "Global signal" refers to the average of the signal over all directions in the sky and focuses on extracting a globally averaged spectrum.

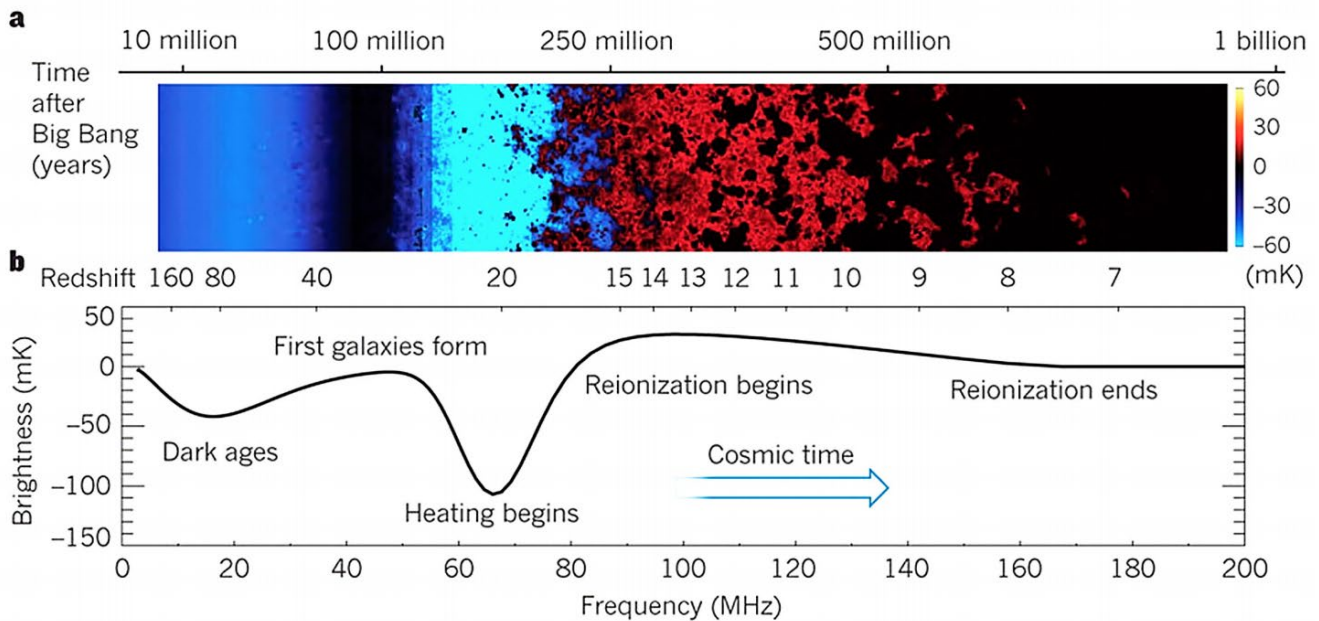


Figure 4-1: The top panel shows a sketch of the evolution of the spatial structure of diffuse neutral hydrogen in the Universe. The lower panel shows the brightness of the 21 cm “global signal” as it evolves over time, showing general features of the Dark Ages and Cosmic Dawn spectral dips, according to standard physical models [RD[31]].

Scientific interest in observations of the neutral hydrogen distribution in the early universe is high as no other channel is available to study that epoch in the universe’s history, before and around the formation of the first stars in the universe. By tracing the history of the global signal of neutral hydrogen emission we can study the discrepancy between the thermal temperature and the spin temperature of the neutral gas (making it appear either in emission or in absorption), which in turn contains information on the history of structure formation in the universe. With this information, the role of dark matter in structure formation is made clearer, providing stronger tests of the Λ -CDM cosmological model.

In addition to the global signal, it is extremely interesting to measure the *spatial* variations of the 21-cm emission from hydrogen. Measurements of the **angular power spectrum** of fluctuations provide information on the scales at which clustering is prominent at different high redshifts, which helps us understand the picture of how Galaxies initially formed and what was the history of their activity. Finally, **tomography** is about actually mapping out the three-dimensional structure of the redshifted neutral hydrogen emission across slices of redshift, providing an almost direct view of the morphology of large-scale structures in the early Universe and their evolution. For a more in-depth look at the science of this epoch, see RD[29].

In summary, we identify (e.g. RD[47]; RD[3]) the following main scientific measurements to be addressed in this study:

- **Global 21-cm line emission:** measurement of the spatially-averaged redshifted 21-cm hydrogen emission from the Dark Ages epoch and from the Cosmic Dawn epoch.
- **Angular-Power-Spectrum 21-cm analysis:** performing arc-minute to degree scale analysis of the spatial variations in distribution of the hydrogen gas and by inference of dark matter;

- **Tomography of the 21-cm line:** imaging the distribution of the Hydrogen and Dark Matter by observing the 21-cm line at different frequencies and hence different look-back times, in this way generating a “movie” of the evolution of the infant universe.

Of the three objectives, the third one is the most challenging. As explained by RD[44], achieving this requires a large **lunar far side radio distributed interferometer** covering the 1-80 MHz regime with ultimately several arcminute-scale spatial resolution and the ability to detect cosmological milli-Kelvin brightness fluctuations.

Next to providing a Herculean observational breakthrough and providing fundamental limits on the signal from the Epoch of Reionization, Cosmic Dawn and Dark Ages, a radio interferometric observatory (the Astrophysical Lunar Observatory or ALO) on or around the moon can address the following additional radio science cases:

- Non-thermal (exo-)planetary magnetospheric radio emission - Jupiter & Saturn and exoplanets;
- Solar Emission (eruptions and CMEs) and Space Weather;
- Extrasolar transient phenomena - pulsars, gamma-ray bursts, fast-radio bursts, supernovae, and accreting black holes and neutron stars (XRBs), AGNs;
- Low-frequency radio sky map – mapping the synchrotron emission in the Galaxy;
- Extra-galactic surveys - high-redshift galaxies and quasars, AGNs;
- Cosmic Rays and High-Energy Neutrinos – using the moon to detect the Askaryan emission from impacts in the lunar interior;
- Earth emissions – AKR, RFI, lightning effects;
- LF radio lunar environment study - lunar exosphere, the lunar radio background spectrum, the effect of high-energy cosmic rays, micro-meteorites and Solar-wind that interact with the lunar surface and the study of the lunar dust.

4.1.2 Science performance indicators

Having defined at high level the science objectives we wish to address, we need to describe in more detail the performances which we aim to obtain for each of the measurements to be carried out.

4.1.2.1 Global 21-cm signal

Detection of the Global signal from redshifted hydrogen is driven by sensitivity and therefore by integration time. The Global DA Signal, being the most challenging of the two Global measurements, is expected to be strongest (deepest absorption) around 20-30 MHz (see Figure 4-1). However, RD[47] shows that even with one dipole antenna (under low-RFI and stable temperature and gain conditions) the signal can be detected at a 5σ level within integration times of the order of one year. Similar arguments show that the CD signal can be detected with a signal antenna in periods of weeks to months.

However, sensitivity is not the only factor because of the presence of foreground signals. Indeed, the Global DA signal is $\sim 10^6$ below the foreground signal. Foreground mitigation and/or subtraction is a key part of the measurement.

Because the foregrounds for the ALO are spectrally smooth and the 21-cm signal is not, one approach for foreground removal is to separate their contributions by Fourier transforming the

frequency direction and applying a (baseline-dependent) filter that removes the foreground including part of the 21-cm signal. This is called “foreground avoidance”, and has been used by the PAPER, MWA and HERA teams, but it loses part of the signal and signal-to-noise RD[39]. The foregrounds can also be modelled and removed via a combination of spectrally-smooth model components (e.g. point sources, Gaussians, shapelets) and Gaussian Process Regression methods that separate the two signals, a technique pioneered by the LOFAR team RD[40] and adopted for SKA. Foreground removal needs to include a full-Stokes model including Faraday rotation due to instrument polarisation leakage. This can be mitigated at higher frequencies RD[41], and is expected to be of smaller concern at lower frequencies where depolarisation is expected.

4.1.2.2 Power-Spectral 21-cm analysis

Characterising the power spectrum of the distribution of neutral redshifted hydrogen in the early universe involves measuring its fluctuations over different scales, using all three spatial dimensions. Two of these manifest as angular dimensions on the sky, and the third (corresponding to line-of-sight depth) manifests in the frequency dimension because of the relation between redshift and lookback distance. Each of these dimensions are transformed into the spatial frequency domain (see Figure 4-2), and data is integrated over shells of spatial frequency to derive a measurement for the correlated power as a function of linear comoving distance (see Figure 4-3). The comoving distance scales are typically indicated using the wavenumber k , in units of cycles per comoving megaparsec. The sensitivity with which the power spectrum is measured is thus a function of the total integration time per k -shell in this mixed angle/frequency space.

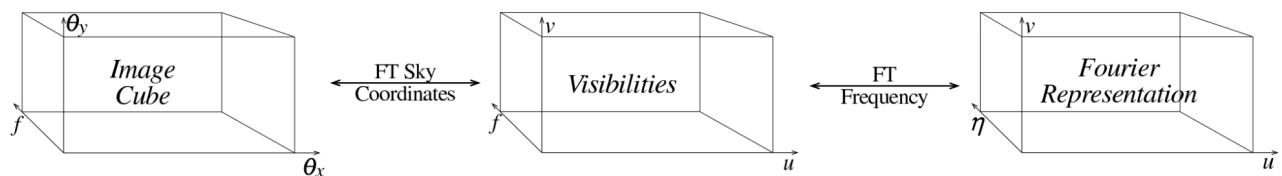


Figure 4-2: An interferometer measures visibilities (center box), which can be transformed into an image cube(left), which corresponds to mapping the emission, or to a full Fourier representation (right) which is used for the power spectrum measurement. Figure from RD[30].

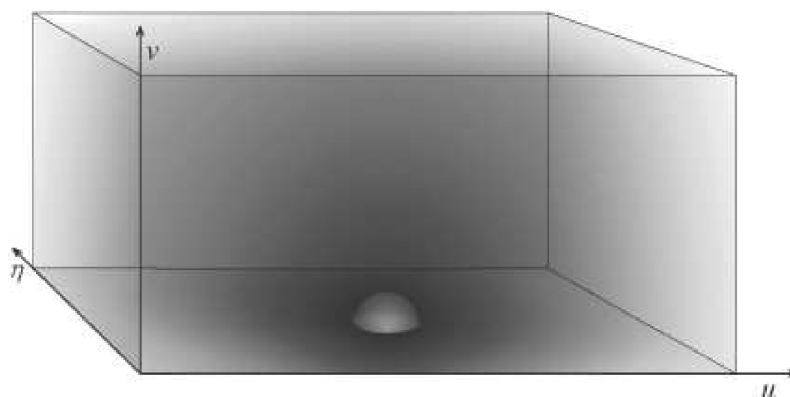


Figure 4-3: illustration of the spherical shell symmetry of the power spectrum signal. The bubble sits at the zero-frequency location in the Fourier cube, and measurement of the power spectrum involves integrating the received power over successive shells in this space. Figure from RD[30].

When measuring the power spectrum for the distribution of neutral hydrogen in the early universe, the measured data needs to be treated in separate ‘slices’ of redshift. This is because the process of structure formation in the universe has been active throughout its evolution, and so any snapshot of the power spectrum, centred around a given redshift value, has only a limited redshift range that can be taken into account if the measurement is to represent the hydrogen distribution at a particular limited duration in time. The range of comoving distance scales that we can sample for any redshift slice is thus limited by the frequency range we can use (i.e. the effective redshift range forming the ‘thickness’ of our slice) and by the range in angular scales that our observatory setup affords us.

4.1.2.3 Tomography of the 21-cm line

Mapping of the distribution of neutral hydrogen in the early universe goes one step beyond measuring the power spectrum, as we no longer sum the distribution properties in terms of power per scale bin. This makes tomography a more challenging measurement than the power spectrum measurement. For this science case, sensitivity in the standard sense (integration time, collecting area and uv sampling coverage) is again the suitable way to measure performance.

4.1.2.4 Non-thermal (exo-)planetary magnetospheric radio emission

Magnetospheric emissions from exoplanets are expected to be very faint (below 1 Jy from 0.5 to 40 MHz). Being transient sources, integration time does not have any bearing on their detectability. Collecting area (for lowering the noise floor) and uv-coverage (for rejection of foregrounds) are the primary factors that determine detectability for these signals.

For Solar system planetary emissions, which are orders of magnitude stronger, the required sensitivity is more modest. As these emissions typically have a strong circularly polarised component, polarisation detection is an important capability to have in this context.

4.1.2.5 Solar Emission (eruptions and CMEs) and Space Weather

Solar emissions, specifically those associated with Solar flares, are among the brightest phenomena in the low-frequency radio regime. Of interest are the arrival directions of these emissions, and the time-variable spectral signature they exhibit. Relevant performance metrics for this measurement are therefore uv-coverage and polarisation detection capability.

4.1.2.6 Extrasolar transient phenomena

Emissions from accreting objects (neutron stars, black holes), pulsars, GRBs, FRBs, AGN and supernovae at low radio frequencies all share the characteristic of strong dispersion, traveling through the interstellar medium on their way to us. For short pulses, high time resolution and fine frequency resolution are needed for successful dedispersion and detection. While array sensitivity (collecting area) again is an important metric, the proper signal processing infrastructure for dedispersion, flagging and detection is also an important component.

4.1.2.7 Low-frequency radio sky map

Good uv-coverage is of importance for this science case: ideally, the same range of angular scales is probed for any direction on the sky. Placement of the observatory on the Lunar surface will likely mean that no full-sky mapping can be done, and the geometry of projection will mean that not all look directions will have the same effective resolution. The sky brightness at low radio frequencies is actually dominated by the stationary structures of the Galactic synchrotron emission across almost the full sky, so sensitivity is not as critical for this science case. Accurate characterisation of this foreground is important for its removal in the context of the redshifted HI power spectrum and tomography measurements, however.

4.1.2.8 Extra-galactic surveys

This science case hinges on a capability to detect relatively compact sources against the much larger structures of the Galactic emission. High angular resolution is of importance to resolve out the (dominant) foregrounds and retain detection capability of these compact sources.

4.1.2.9 Cosmic Rays and High-Energy Neutrinos

The detection of high-energy cosmic rays hinges on the Askaryan effect, which occurs when these energetic particles interact with the Lunar regolith. From any given point at the Lunar surface, the volume from which the radio pulse emission can be detected is expected to be modest: down to a depth of several wavelengths ($\sim 100\text{m}$), and within an angle of ~ 45 degrees from the local nadir. Besides the monitored physical volume, another important array capability that determines the feasibility of this science case is the possibility to trigger waveform capture upon reception of pulses in the time domain that have the correct signature.

4.1.2.10 Earth emissions

Lightning and RFI emissions from Earth are severely attenuated on the Lunar far side, in a frequency-dependent way. Array locations close to the Lunar limb may see some leakage at the lower frequencies (sub-MHz).

4.1.2.11 LF radio lunar environment study

This science case is the 'catch-all' case, which does not aim to look for specific sources but instead aims to characterise the aggregate spectrum and how it may change over time. No fixed performance is required here, besides the duty cycle: a regular measuring cadence that covers the transition from Lunar day to Lunar night in multiple measurements is desired, at a sensitivity that is high enough to detect the variations over one Lunar cycle.

4.1.2.12 Figures of merit summary

In Table 4-1 we summarise the performance indicators described in the text above.

Science case	Defining characteristics	Figure of merit to use
21-cm global signal	Very well understood instrument response. Foreground mitigation and/or subtraction.	Sensitivity per frequency bin
21-cm power spectrum	Much weaker than foreground, expected variations over k-scales from $1e-3$ to 1 h Mpc^{-1} , expresses power as a function of comoving scale	Integrated sensitivity per k-shell
21-cm tomography	Same measurement as the power spectrum but without integration over k-shells: this is direct mapping	Sensitivity per pixel element per frequency bin
(exo)planetary magnetospheres	Very weak emission, requiring long integration times and subtraction of other components	Sensitivity per pixel element
Solar emissions	Bursts lasting from minutes to hours depending on frequency, very strong emission, lower frequencies delayed w.r.t. higher ones	Polarisation measurement capability
Extrasolar transients	Dispersed pulses that likely require channel stacking for detection	Sensitivity per pixel element, de-dispersion capability
Low-frequency sky map	Large angular sizes of flux density contribution expected, with point-like, variable sources superimposed	Sensitivity per pixel element
Extra-galactic surveys	Point-like sources	Sensitivity per pixel element
Cosmic rays and neutrinos	Short pulses of emission, nanosecond scale	Catchment volume, triggering capability
Earth emissions	Strongly attenuated (in a frequency-dependent way), sub-second variability	Location on Lunar surface, time and frequency resolution
LF Lunar radio environment	Unknown	Time and frequency resolution

Table 4-1: Summary figures of merit for the different science cases

4.1.3 High-level goals

Among all the science cases included in Table 4-1, we consider the measurement of the 21-cm power spectrum in the early universe to be the top science case for ALO: it is one of the more challenging science cases, but also one with the largest scientific impact that is made uniquely possible by locating the array on the Lunar far side. Designating this science case as paramount does imply that array performance will be suited to the pursuit of several other science cases as well, since it puts stringent requirements on performance.

With the top science case being the global redshifted hydrogen spectrum, the required properties of a suitable instrument will need to be:

- The instrument should have the capability of reaching a high sensitivity per k-bin (described in Section 4.1.1) in an efficient way. This means that measurements pertaining to particular angular scales and directions on the sky should be performed in parallel (between many pairs of antennas simultaneously) and repeated often. This sensitivity will be reached more easily for relatively large angular scales, as these correspond to short baselines which have longer dwell times in each uv-cell as the Moon provides aperture synthesis through its rotation.
- We wish to sample a range of k-values spanning 2 dex, centred around $k=0.1 \text{ h Mpc}^{-1}$, as the matter distribution (and 21-cm signal) power spectrum is expected to show a maximum there. This k-value sits at the transition from large scale cosmology to smaller-scales of astrophysical interest, allowing us to probe various aspects of cosmology and astrophysical structure formation in the early Universe RD[3],RD[35].

For the global signal, a well-modelled instrument response is crucial. Imperfectly understood and modelled chromatic effects will ‘contaminate’ the recorded spectrum, which makes the subtraction of foreground components more problematic. Hence, influences from the environment (lander platform, other antennas) should be kept to a minimum or else should be understood with a high degree of precision. This makes the global signal measurement challenging to do with a dense array, requiring extensive calibration strategies.

The requirement on measurement of the global cosmic dawn and dark ages signals is to reach a noise level of 10 mK across a redshift range from $z = 20$ to $z = 50$. This sensitivity value is set because it allows for the characterisation of the expected features in the global spectrum, which have depths of several tens of mK to ~a hundred mK according to standard physics (see Figure 4-1).

4.1.4 ALO in the context of other observatories

Naturally, there are existing arrays on Earth that include in their aims to perform similar measurements on the redshifted neutral hydrogen signal (MWA, PAPER, LOFAR) as well as planned Earth-based facilities that aim to address this science case (SKA). The main difference with ALO is that the accessible frequency range is limited from Earth, and as such these arrays focus on a different epoch in the evolution of the early Universe, namely the Epoch of Reionization (EoR). This epoch ranges roughly from $z = 20$ to $z = 6$. Their approach is similar to ALO in the sense that they use dense arrays that optimise the measurement of the power spectrum of the signal of interest.

The unique advantage of ALO is that it will have access to the low-frequency part of the radio spectrum that is not measurable from Earth due to blockage by the Earth's ionosphere. From Earth, frequencies below 50 MHz (corresponding to redshifts above $z = 28$) are increasingly severely affected by the behaviour of the ionosphere which attenuates and scatters radio waves, making it extremely impractical or downright impossible to do astrophysical measurements from the ground in that regime. As can be seen in the previous subsection, while the global signal detection using single antennas is feasible up to high redshifts like $z = 50$ and beyond (frequencies of 28 MHz and below), power spectrum measurements in this range are only feasible with extended arrays of at least 32×32 elements.

Currently many attempts are made by new and existing ground-based facilities to push for sensitive observations at frequencies below ~ 50 MHz in an attempt to measure the 21-cm line emission from the Cosmic Dawn. Single, well calibrated instruments such as EDGES attempt to measure the global 21-cm line emission from the neutral Hydrogen from the Cosmic Dawn (RD[44]). The EDGES claim for the initial detection is still much disputed and cannot be explained with current standard cosmological models.

However, the Netherlands-China Low frequency Explorer (NCLE; PI KleinWolt/Falcke), following the Radio Astronomy Explorers (RAE) 1 and 2 missions in the 1970s, is currently the only space-based low-frequency radio observatory and is considered a **path-finder instrument** for any future large low-frequency radio facility in space or on the moon.

Other proposals for lunar-based radio observatories have been made, notably FARSIDE RD[33]. Making a comparison to the proposed FARSIDE array architecture, we see that FARSIDE uses a sparse array architecture where the full array consists of four 'petals' that have 32 antennas each, deployed along one shared cable for each petal. FARSIDE addresses multiple other science cases (exoplanet magnetospheres, heliophysics, radio emissions from the outer Solar system planets, lunar sub-surface sounding, ISM tomography), but regarding the redshifted neutral hydrogen measurement the aim is to provide a high-fidelity measurement of the Dark Ages 'trough' global signal below 30 MHz. Foreground subtraction, which involves contributions from sources that are much stronger than the signal of interest, is done by using interferometry to characterise the sky distribution of these sources. Note that FARSIDE does not aim to measure the power spectrum of redshifted neutral hydrogen, and as such does not require a dense array. In fact, the large spacing of the antenna elements helps in getting clean measurements from the individual antennas.

4.2 Key drivers and trade-offs

4.2.1 Architecture – the case for an interferometer

At low frequencies dishes are not practical, discrete antennas or arrays of discrete aperture array antennas are much more cost effective RD[13]. Moreover, discrete antennas basically can 'see' the entire sky, with FoVs nearing the full hemisphere visible from the lunar surface. Such a large instantaneous FoV is needed for the cosmology science cases of the mission. Using an array has additional calibration advantages, moreover it allows spatial radio interference mitigation.

Aperture arrays are dense (antenna spacing $\sim \lambda/2$) or sparse, depending on the science requirements, frequency range to be covered, aperture diameter, and sidelobe levels. Earth-based aperture arrays can for example consist of Vivaldi antennas [RD[14], RD[15]], inverted vee dipoles on a ground plane RD[4], or log-periodic antennas RD[14]. Single antenna systems

aiming to detect radio signals from the early universe typically are 'fat' dipoles above a large ground plane RD[17].

Figure 4-4 shows the core area of the distributed LOFAR aperture array telescope, based on phased-array telescope stations RD[4]. Visible are groups of 96 dual polarization LBA 10-90 MHz antennas, and groups of 24 HBA antenna tiles (black rectangular boxes), each consisting of 4x4 110-240 MHz antennas.



Figure 4-4: Aerial photograph of the LOFAR superterp circular area, and several additional core stations, credit: ASTRON

Figure 4-5 shows a close-up of the LBA antennas, inverted vee crossed dipoles above a ground plane (left), and 'fat' triangle shaped crossed dipoles embedded in a polystyrene structure above a ground plane in a dense array configuration.



Figure 4-5: LOFAR LBA inverted vee crossed dipole antennas above a ground plane with amplifier on top (left) and a HBA crossed dipole antenna above a ground plane in a dense 4x4 tile array supported by a polystyrene structure covered with weather resistant foil, credit: ASTRON

In order to achieve the sensitivity levels envisioned for investigating the Dark Ages and Cosmic Dawn era, and for supporting other radio science cases, an interferometric array must be considered of hundreds up to thousands of antennas. Such a large number of antennas implies that they must be light weight and easily deployable. However, it is very likely that a large interferometer must be built in stages. The ability to carry out a staged implementation approach, i.e. first deploying a smaller sub-array which can subsequently gradually be increased to larger numbers of antennas, is therefore considered as a fundamental design requirement.

4.2.2 Antenna level

4.2.2.1 Individual antenna design

In principle, apart from environmental condition considerations, the Earth based aperture array antenna concepts would be usable on the lunar surface. Indeed, for a single antenna or a small number of antennas, such a configuration may be optimal. However, when deploying many more antennas there are several drawbacks. The first is that the current earth-based concepts are too heavy to transport to the lunar surface. Furthermore, among antenna concepts used in Earth-based arrays, some would require a vertical support structure (inverted vee dipole, or logger) as shown for example in RD[4], RD[23], increasing mass and deployment complexity. Such approaches are to be avoided. An additional concern is that deploying and connecting the antennas is very complex and would require a very long time. Finally, the environmental conditions on the Moon are very harsh, and different antenna concepts need to be adapted accordingly. For example, the ambient temperature of an amplifier on top of a LOFAR antenna (at a height of 1.8 m) would be much easier to control if buried a few centimetres into the regolith.

A specific issue is that Earth-based aperture arrays typically use ground planes to define a fixed interface with the ground, avoiding variation over time of RF properties such as dielectric constant (rain) and limiting variation between different deployment locations. A ground plane also has the advantageous effect that the antenna gain in the direction of the horizon is highly attenuated, thus suppressing radio interference from fixed transmitters. Another important advantage of a ground plane is that it allows to route all galvanic connections behind the ground plane, avoiding coupling effects on the beam shape. Given that the observation wavelengths are very long, the ground plane need not be solid, it usually is constructed as a mesh with a relatively large pitch.

A difference between Earth soil and lunar regolith is that the latter is relatively transparent for low-frequency radio waves, while the Earth soil is much less transparent and its electromagnetic properties vary significantly over time due to weather influences (rain, humidity). The effect of a ground plane on Earth is that it provides a stable electromagnetic environment for the antennas. It also influences the antenna beam patterns, but this effect is included in the overall antenna design. As the lunar regolith electromagnetic properties are to a large extent constant over time, ground planes are not strictly needed for providing stability. Also, at low frequencies the thermal noise contributions from the soil is negligible compared to the sky noise, therefore a ground plane screen is not needed to suppress it. At some depth, the bedrock layer will reflect part of the celestial radio waves, impinging on the array from below. This effect however can be mitigated by calibration and post processing (TBC).

Considering the difficulties of deploying ground planes on the Moon, we conclude therefore that – although including a ground plane has important advantages – it is not strictly required.

Ideally three crossed antennas, e.g. three dipoles (tripole), can optimally capture the electromagnetic field from the celestial hemisphere, including its polarization state RD[27], RD[23]. There is however some redundancy when combining (auto and cross correlating) all $3 \times N_{ant}$ signals from all antennas in an array of N_{ant} tripole antennas. Using two crossed antennas is in principle sufficient to estimate the spatial distribution of the impinging power flux including the polarization state, albeit with somewhat reduced sensitivity compared to the tripole case. An array of single dipole antennas, provided their main gain lobes (physical orientations) are distributed over multiple directions, can in principle also be used. Drawbacks of this concept are that the infrastructure probably is not efficiently used, and the calibration of this non co-located concept becomes rather complex.

Dual (dipole) antenna systems and triple (dipole) antenna systems usually are co-located. This often makes production and calibration relatively easy. There however exist non co-located antenna systems (dense aperture arrays RD[23] and (dense) focal plane arrays RD[34]) in which the two orthogonal antenna elements are separated at half a wavelength. In RD[34] it is shown that for a non co-located focal plane array the Stokes leakage is below 2% at a distance of 1 FWHMP width from the pointing centre. It is assumed that a similar polarization leakage limit is achievable for aperture arrays (TBC). This however has not been demonstrated, and it would require a special calibration strategy (TBD). An additional complexity of non co-located antenna elements may arise if the two orthogonal elements are deployed separately. In that case it may be complicated to connect the two elements 'galvanically'. Isolated elements in crossed (dipole) antennas have different beam patterns compared to antennas for which the grounds are connected.

Considering all of the above, the simplest antenna concept that we can consider to use is a **horizontal planar dual polarization dipole configuration without a ground plane**. As the regolith is to a large extent transparent to radio waves, the planar antenna can be located on the surface.

4.2.2.2 Detailed RF considerations

Given mass constraints, polymer composite foils with copper antenna patterns deposited on them could form suitable antennas. The detailed shape of the copper deposit determines the angular response of the antennas and can be optimized for different purposes. Such an optimization is best done by detailed simulations.

An important related issue is that powering antenna receivers and transporting the received signal and data communication usually requires galvanic connections (which could also be printed on the same foil that the antenna is), and their presence can influence the antenna gain patterns. (Note: in Earth-based designs, the galvanic lines are located under the ground-plane).

Another design consideration is that the aperture array needs to be rather dense in order to be able to effectively calibrate it for the envisioned main science cases. When antennas are placed close to each other, their individual RF responses are mutually influenced. As the main scientific signals lie many orders of magnitude below the instantaneous noise levels, it is of vital importance that the array complex gains are well understood, including the effects of galvanic lines and nearby antennas or structures. In order to assess such effects, a few initial antenna and array simulations have been conducted, including investigating:

- the influence of dipole length on antenna gain and polarization,
- the polarization properties of a 4x4 crossed 1.5 m dipole array,
- the antenna response of a 5 m crossed dipole compared with a 'fat' blade antenna, and

- the polarization properties of a 3x3 crossed dipole array of 1m dipoles compared with 5 m dipoles, and the influence of solar panels and cables.

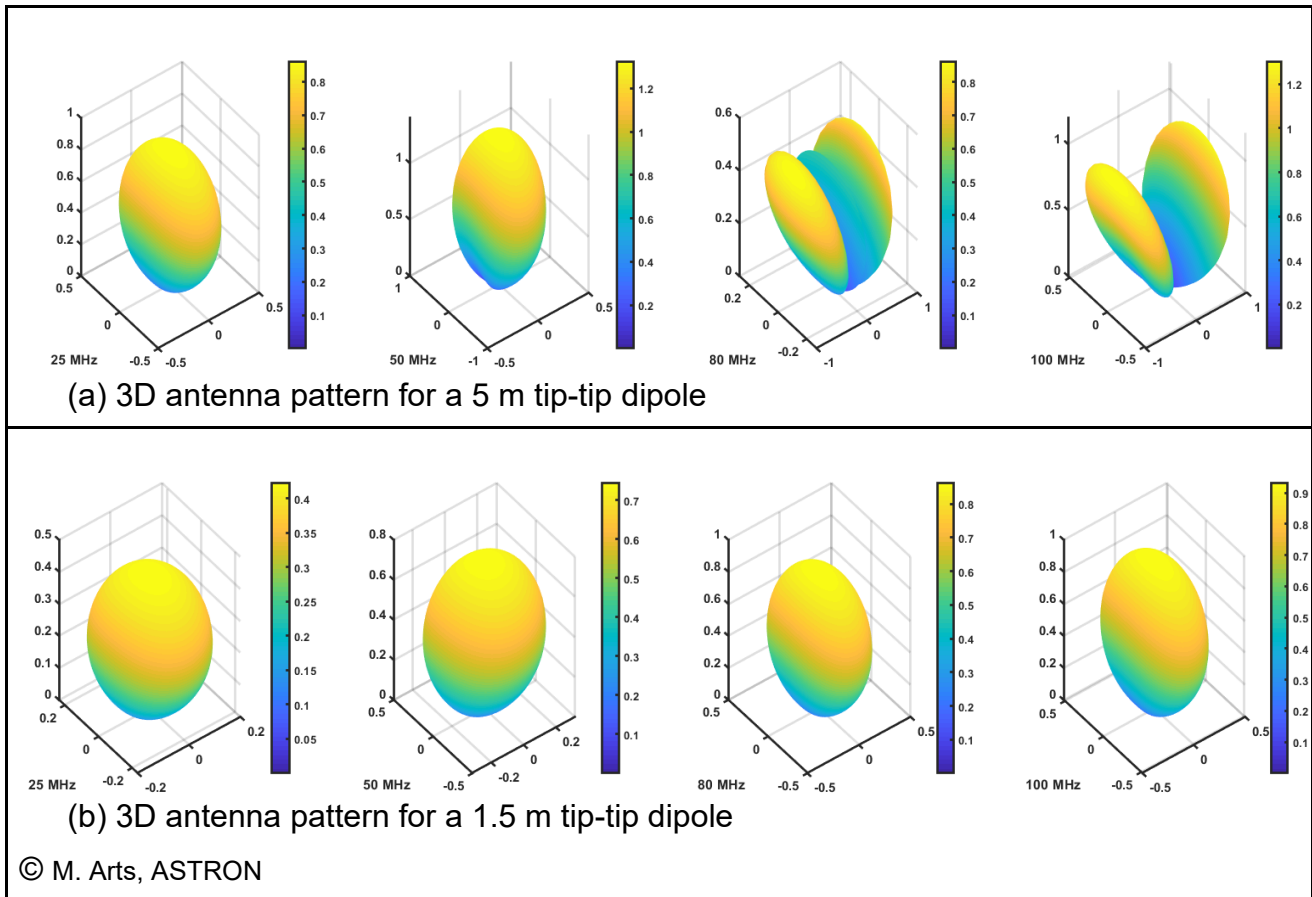


Figure 4-6: Element patterns for a dipole in a horizontal plane at the lunar surface with an assumed dielectric constant $\epsilon_r = 2$ for the regolith and $\tan(\delta) = 0.01$. Simulated frequencies are (left to right) 20, 50, 80 and 100 MHz, gain uses a linear scale

Influence of dipole length on antenna gain and polarization

The first simulation considers dipoles of length (tip-tip) 1.5 m and 5 m, placed in a horizontal plane on the lunar surface. The lunar surface regolith is assumed to have a dielectric constant $\epsilon_r = 2$ and electromagnetic loss $\tan(\delta) = 0.01$ [RD16]. The aim for the beam patterns is to be as smooth as possible. For 1.5 m dipoles up to 100 MHz, the dipole element patterns are smooth, but for 5 m length a split in the pattern is clearly visible at frequencies above 50 MHz (Figure 4-6).

Figure 4-7 shows the antenna impedance for both dipoles for different values of ϵ_r and $\tan(\delta)$. Also here it is clear that the shorter dipole gives a spectrally smoother response than the 5 m dipole. A drawback of short dipoles however is, that these give a lower system sensitivity, especially at lower frequencies.

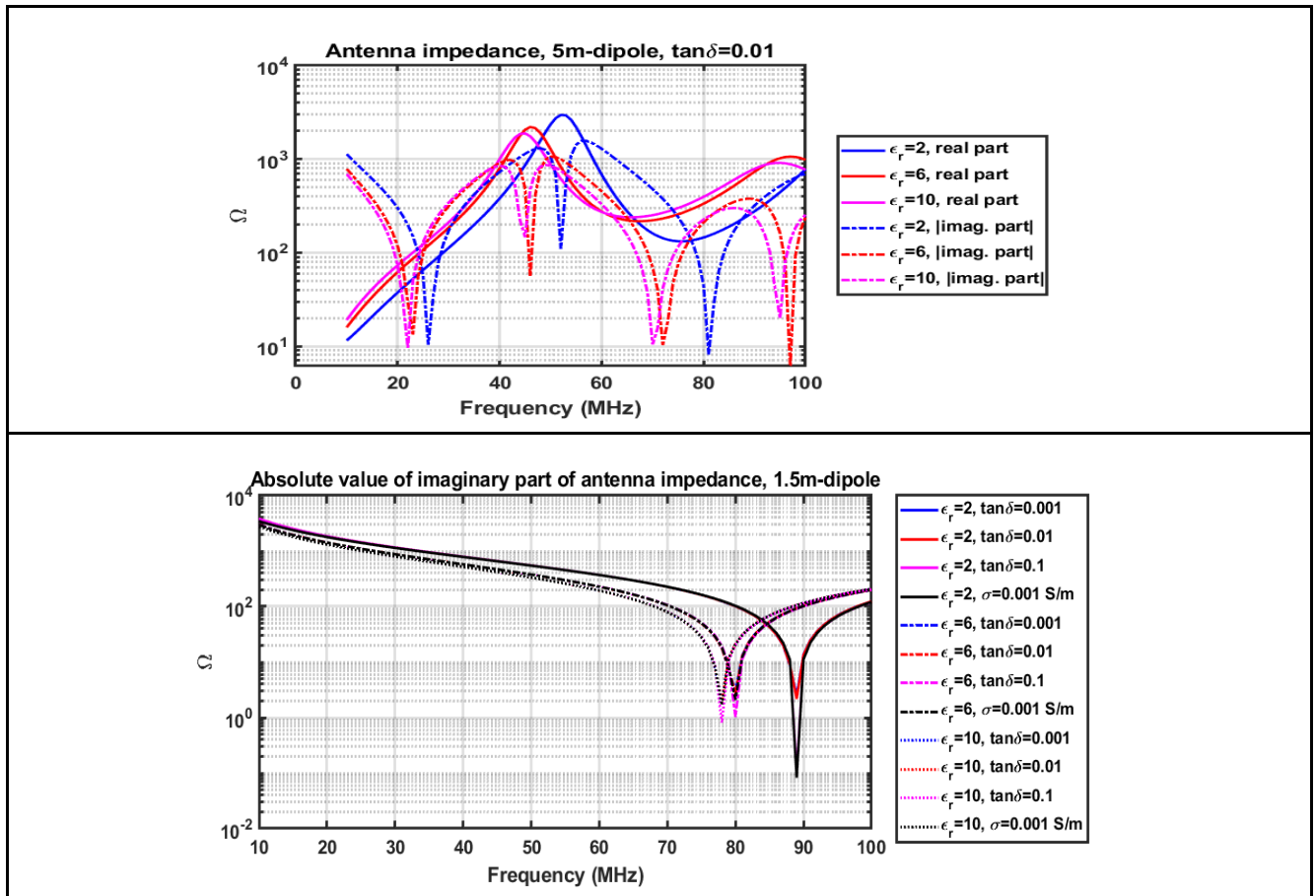


Figure 4-7: Antenna impedance for a dipole in a horizontal plane at the lunar surface with different values for the dielectric constant ϵ_r for the regolith for electric losses $\tan(\delta)$. The longer dipole shows a smoother response.

Polarization properties of a 4x4 element 1.5 m crossed dipole array

Due to coupling effects, a dense antenna array has a different response compared to simply geometrically expanding the element patterns. To investigate an array, often the intrinsic cross-polarization ratio (IXR) is used as a figure of merit RD[19]. A low IXR (say below about 20 dB) means that there is ‘leakage’ of one polarization state to the other. High IXRs mean that this leakage is small.

This simulation assumes a regular 4x4 array (16 antenna elements) of 1.5 m length co-located crossed dipoles placed with a pitch of 1.6 m. The height above ground is 10 mm for x-polarized elements, and 15 mm for y-polarized elements, allowing some mechanical deployment support, but this does not significantly influence the antenna electromagnetic properties. In the simulations the elements excited by a voltage source of 1 V, and one broadside beam for both polarizations is computed. Note: for practical reasons, the simulations assume that the height above ground is finite; however, due to the electrically short distance simulated between the antennas and the lunar surface - as compared to the operating wavelength - little deviation from these results are expected if the height of the antennas are altered slightly.

Figure 4-8 (a) shows the IXR of the array for different values of ϵ_r and $\tan(\delta)$. Up to about 70 MHz the beam response is smooth, but at 79 MHz a resonance is visible. This is also visible in (b) with a rapidly changing IXR beam pattern around 79 MHz. This means there is a direction

dependent antenna gain, smooth over frequency up to about 70 MHz, but with a relatively strong frequency dependence above 70 MHz. The calibration of the array needs to take this into account.

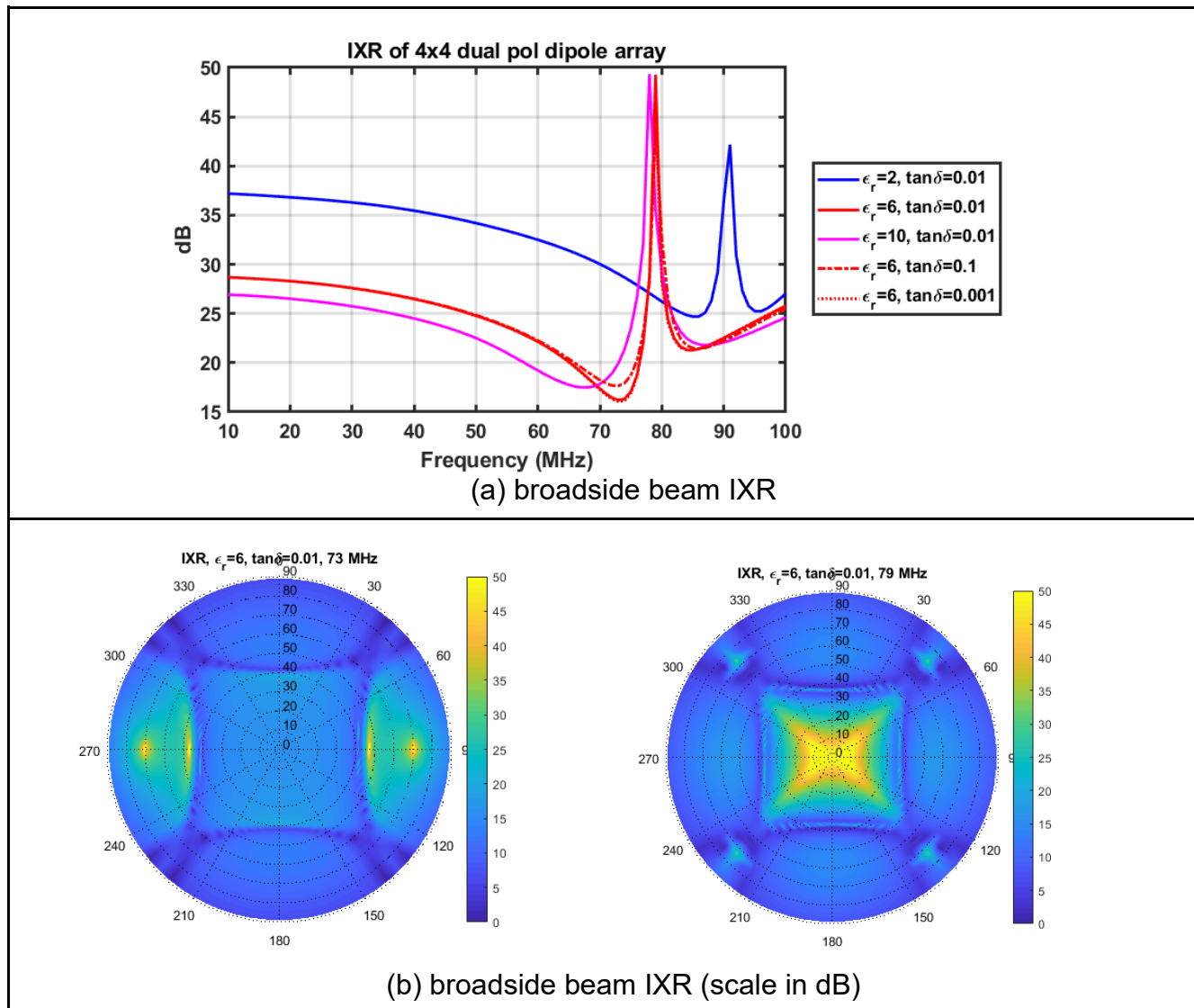


Figure 4-8: Antenna IXR for a dense 4x4 array of 1.5 m length dipoles (upper), and broadside beam IXR at 73 MHz (lower left) and 79 MHz (lower right)

Antenna response of a 5 m crossed dipole compared with a 'fat' blade antenna

As the simulation above assumes thin dipoles, a question is whether perhaps using thicker/wider antennas may yield a smoother beam response over frequency. Lightweight foils can be relatively easily provided with arbitrarily shaped copper patterns. Figure 4-6 for example shows a Vivaldi 2-PAD foil antenna for the 300-1000 MHz range RD[20]. The pattern is printed with silver ink, and copper is deposited using an electro-chemical plating process. Thickness 2 micron (middle) to 10 micron (edges). In the second simulation a simplified EDGES design RD[21] is used, without impedance correction measures (at the antenna pattern rim). Figure 4-9 shows the planar blade antenna layout, a 'fat' structure with the same length, 5 m tip-tip,

as the crossed dipole antenna. This simulation assumes $\epsilon_r = 6$ and $\tan(\delta) = 0.01$. The height of both blade and dipole antenna is 10 cm above the lunar soil.

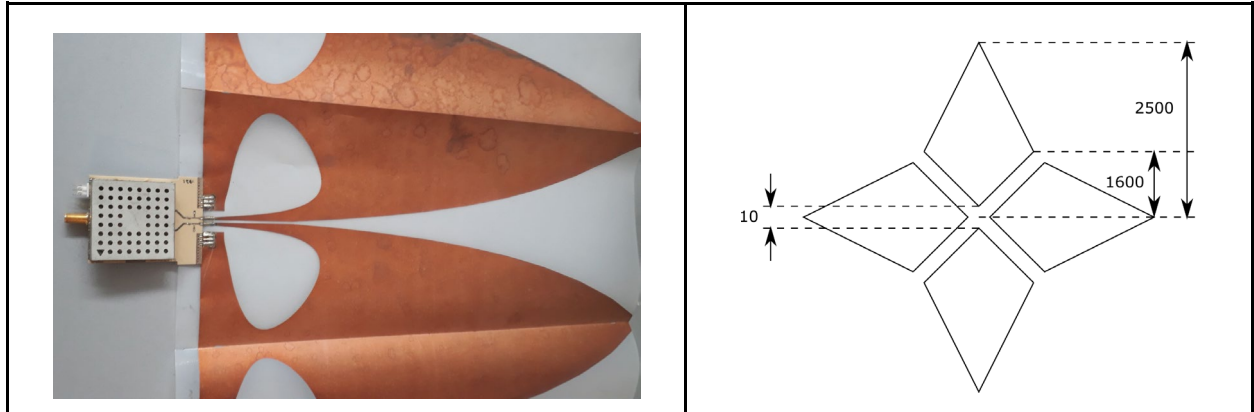
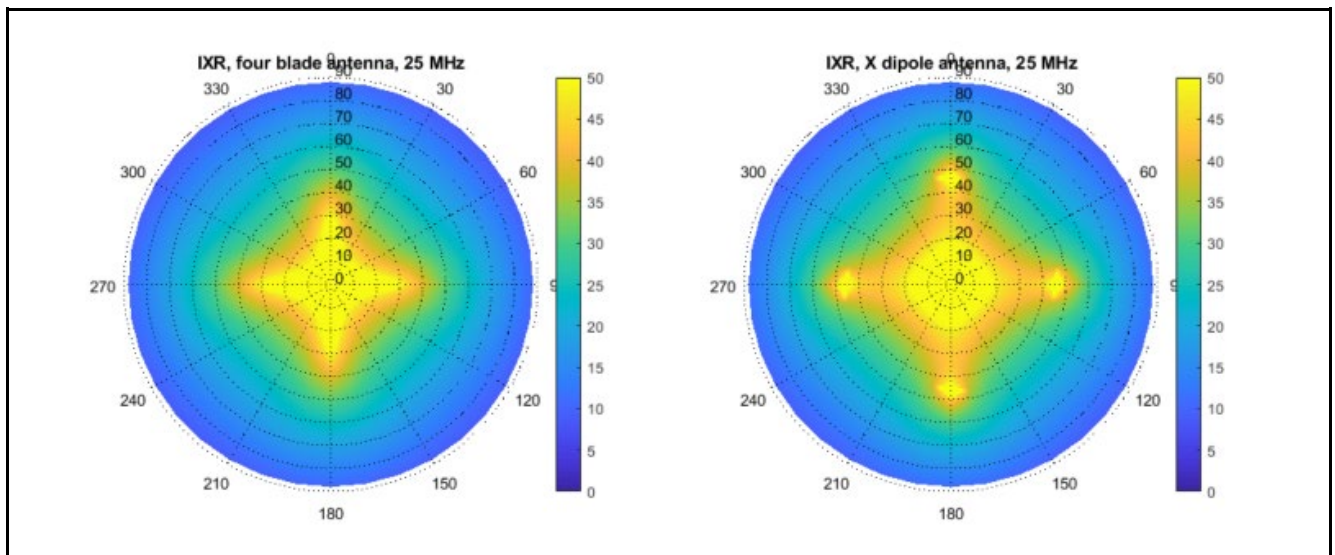


Figure 4-9: A 300-1000 MHz Vivaldi foil antenna RD[20] (left) demonstrating the efficacy of foil antenna technology, and blade antenna configuration 10-100 MHz located in a horizontal plane 10 cm above the lunar surface (right)

The simulations show little difference at low frequencies (below about 20 MHz), but significant differences at higher frequencies. The smoothness of both concepts however seem comparable. As an example, figure 10 shows IXR broadside beam responses for both antennas at respectively 25 and 50 MHz.



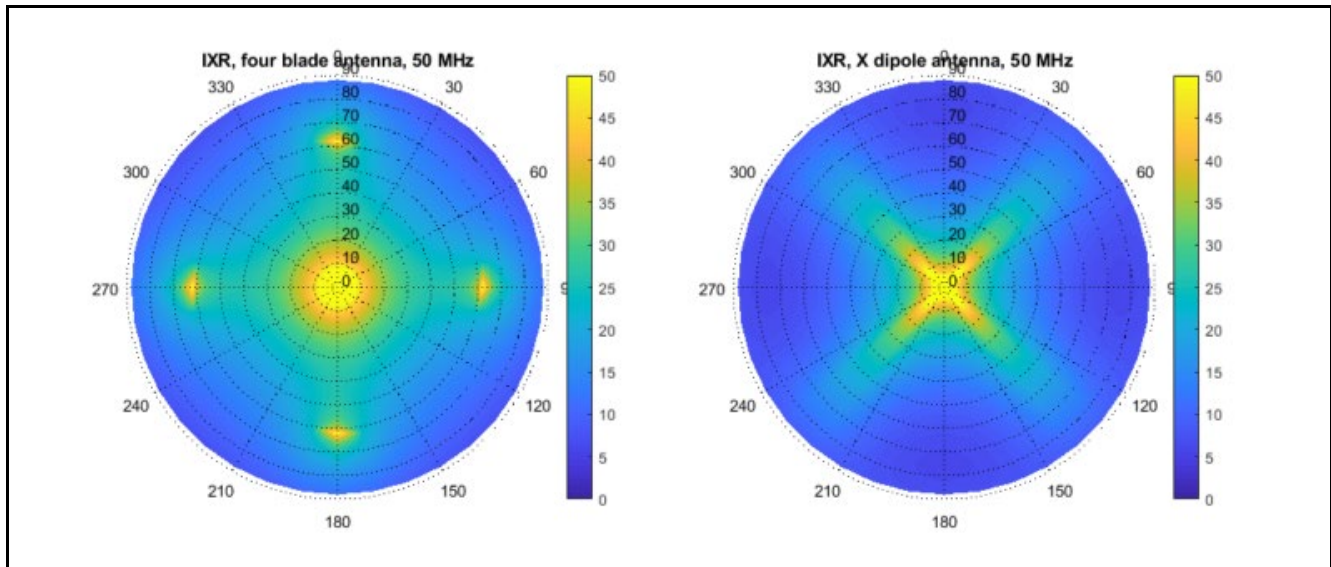


Figure 4-10: IXR broadside beam response for a Blade antenna (left figures) and crossed dipole antenna (right figures) for 25 MHz (upper figures) and 50 MHz (lower figures)

To illustrate the wide-field properties of both antenna types, Figure 4-11 shows the antenna gains in the E-plane and H-plane as a function of zenith angle theta. Up to about 60 MHz the gains are similar to the figure on the left. At higher frequencies the gains behave more irregularly.

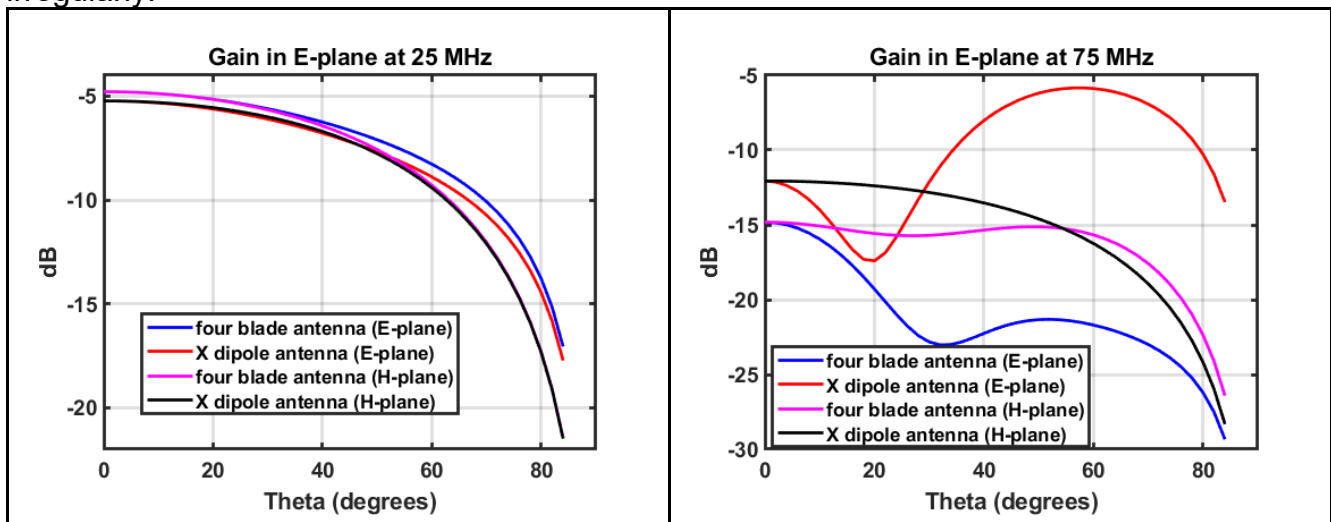


Figure 4-11: Gain of the crossed dipole antenna as a function of zenith angle compared with the blade antenna, at 25 MHz (left) and 75 MHz (right)

Polarization properties of a 3x3 crossed dipole array of 1 m dipoles compared with 5 m dipoles, and influence of solar panels and cables

As mentioned above, galvanic connections will influence the antenna properties of the lunar array. To assess the (order of magnitude) effect, a 3x3 array configuration is considered with cabling and solar panel configuration as shown in Figure 4-12. Of course, alternative configurations are possible as well. The 3x3 configuration has the advantage (over 4x4) that it is more symmetric, making the cabling routing easier.

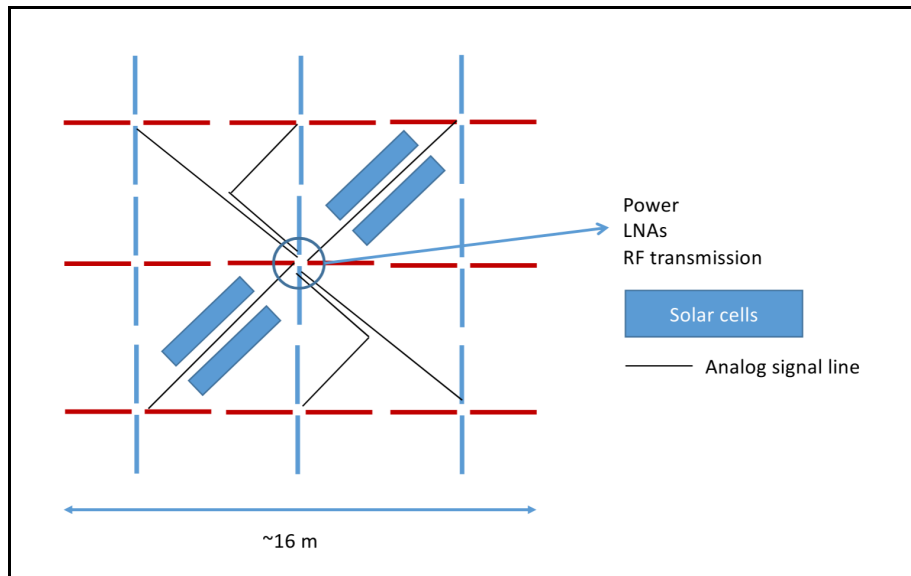
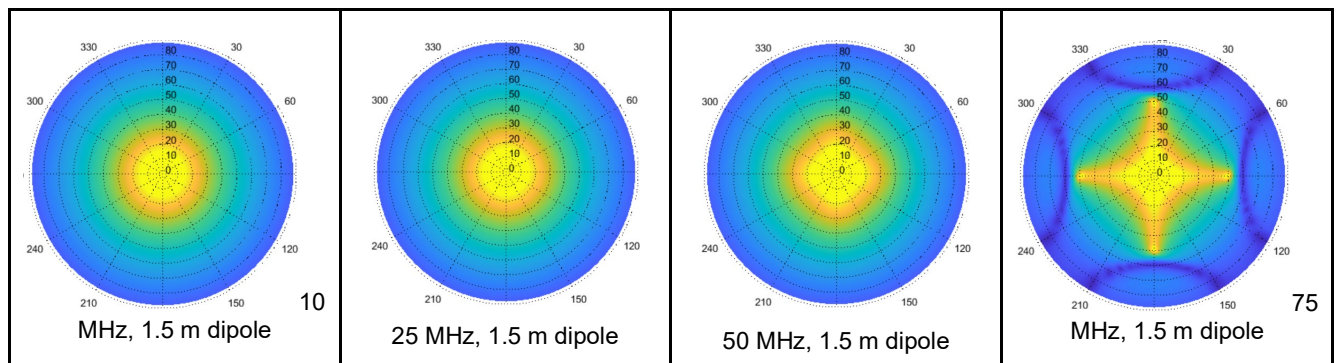


Figure 4-12: A 3x3 crossed dipole array with galvanic power connections

Before simulating the influence of solar panels⁴ and the galvanic connections, first a simulation without these was done for both 1.5 m and 5 m dipoles on a pitch of 5.3 m. Figure 4-13 shows the IXR broadside beam response results. Up to about 60 MHz the 1.5 m dipole configuration shows a constant pattern (over frequency), but the 5 m array shows already complex patterns starting from about 25 MHz.



⁴ We simulate the presence of solar cells to power the antenna receiver, as simple metallic rectangles deposited on the same foil as the antennas themselves.

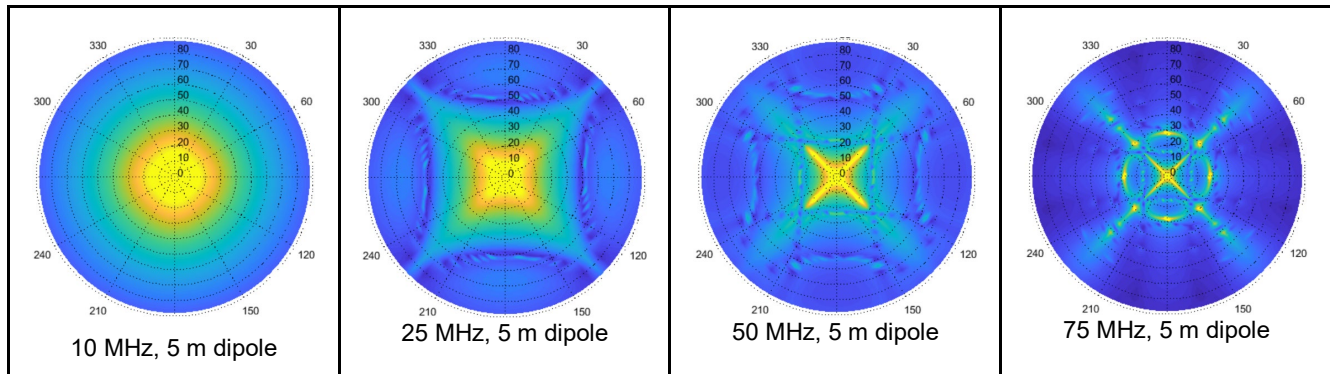


Figure 4-13: IXR broadside beam response for a 3x3 crossed dipole array for 1.5 m elements (upper row) and 5m elements (lower row), scale 0-50 dB

Figure 4-14 shows the influence of galvanic connections and solar panels (assumed to be metal patches in the simulations) on the 3x3 array IXR response. It is clear these additions have significant effects and need to be carefully modelled. Solar panels and electronics probably can be mounted on top or below the copper patterns of the antenna foils thus improving the antenna patterns, but the cabling routing and RF design of it needs careful attention.

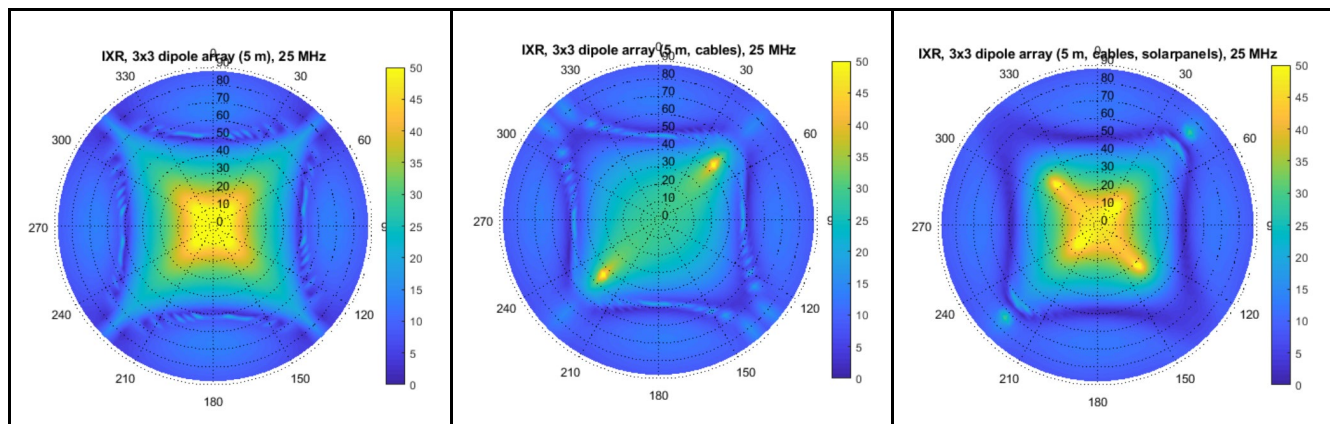


Figure 4-14: IXR broadside 25 MHz beam response for a 3x3 crossed dipole array for 5 m elements without cables and solar panels (left), with cables (middle), and with cables and with solar panels (right)

4.2.2.3 Radio interference

This subsection briefly discusses the maximum allowable radio interference (RFI) levels for a single antenna system at the Lunar surface aimed at detecting the global DA/CD signal. Please note that the levels mentioned below are only initial indications, for a proper assessment a more rigorous study is needed.

For detecting the global sky signal, expected to lie in the range 0-200 mK sky temperature range, one would allow error signals that lie at least one order of magnitude below the expected signal. For example RD[22] assumes maximum RFI levels of 5 mK for a 5 kHz wide band. Radio interference can to some extent be mitigated, usually down to the level that it can be detected. But often the interference that is not detectable at short integration times may build

up and become a hampering factor after long integration over time. Also, RFI mitigation consumes degrees of freedom in the processing, making the instrumental and scientific calibration harder. Therefore it is best to tackle the problem at the source: avoid interference being generated. Please also note that all RF interference (both from transmitters and spurious signals from electronics) are highly time variable.

4.2.2.3.1 *Emissions*

For electronics emissions, as a reference, one could use the CENELEC EMC emission standard EN55022 RD[37] which specifies a limit of 30 dBuV/m (or 40 dBuV/m depending on class) at 10 m distance. According to RD[24] this corresponds to 30-84.8 = -55 dBm at the emission source (e.i.r.p.). RD[22] assumes electronic emissions of -80 dBm per 5 kHz band. This is 25 dB less power than the maximum allowable by EN55022. The maximum value will occur probably only in one or a few frequency bins, the -80 dBm value probably will occur much more frequently throughout the frequency band.

Assuming transmitters similar to Earth based systems are deployed on the lunar surface, and assuming that the carrier frequencies of e.g. 4G or 5G mobile base stations are outside the DA/CD frequency range, how much spurious will leak into ALO? Earth base station spurious emission maximum levels are typically -36 dBm / 10 kHz for $f < 30$ MHz and -36 dBm / 100 kHz for $f > 30$ MHz RD[24].

4.2.2.3.2 *ALO susceptibility*

The sky noise limited system temperature ranges between about 1000 K (80 MHz) and 300.000 K (10 MHz) RD[23]. RD[22] assumes a maximum allowable electronics spurious power of -80 dBm in a 5 kHz band. The sky noise power is given by $10 \cdot \log_{10}(k \cdot T \cdot bw) + 30$ dBm, which is -181.6 dBm for a 5 kHz band and maximum 10 mK 'sky noise' contribution. The difference, 101.6 dB is the required faraday cage attenuation. With proper signal filtering this is in principle doable. The memo specifies more details (also more stringent isolation), but these are strongly design dependent. Placing electronics at distances of 100 m to a km reduces the required attenuation, but a Faraday cage still would be needed.

In radio astronomy susceptibility studies usually a 0 dBi antenna sidelobe effective area is assumed ($A_{iso} = \lambda^2 / (4\pi)$ m²). Assuming free-space attenuation, a transmitter at a distance d with e.i.r.p. spurious power of -36 dBm is attenuated by the path loss $20 \cdot \log_{10}(4\pi d / \lambda)$. A maximum 5 mK contribution as mentioned above would require the transmitter to be at least at a 250 km distance (at 50 MHz). Being located (envisioned) in a crater, there will be natural shielding, but additional assessments need to be carried out for transmission systems deployed on the lunar surface (and above).

4.2.2.4 **Strawman antenna concept**

In summary, given the need to balance the following for a lunar array:

- as many antennas as possible for better sensitivity, better calibration accuracy (more net degrees of freedom), more RFI mitigation options
- a lightweight and stable antenna structure
- a scalable antenna concept
- a dual polarization array, fully calibrated

- very short dipoles as this ensures smooth spectral gain behaviour
- very long dipoles (half wavelength at the lowest frequency) as this ensures the best sensitivity
- a dense large aperture array to allow calibration to a high dynamic range, and
- a solid EMI and grounding philosophy with a careful design of galvanic connections (including control and data transport, and power generation and distribution) in relation to antenna gain properties and self-generated interference

the following **strawman antenna concept** is proposed: planar dual polarization elements of 5 m length (optimizing sensitivity), configured in antenna-foil tiles containing 2x2 (or 3x3) co-located dipoles with a central local hub for power distribution and signal transport. The antenna elements are 'fat' co-located dipoles. The concept does not have a ground plane, the foil antennas are located either directly on the lunar surface or elevated a few centimetres if that is more convenient for deployment. If solar panels are used, these are then located contiguous to the fat dipoles (locating them between the elements is also possible but this would put additional constraints on the antenna RF design). The maximum distance between LNA and antenna centre is 50 cm. The LNA and processing electronics could be buried several 10s of cm into the regolith to limit the thermal cycling.

The main next step is to further investigate the scalable lightweight antenna concept that meets the requirements mentioned above, and to increase its TRL level. Figure 4-15 below schematically shows an example of a possible scalable four-element foil antenna. The dual polarization antennas are depicted as lines, but these may have a much broader shape, possibly with a solar panel printed on the same foil. The galvanic connections of power and the amplifier to the antenna foil metal shape are filtered to ensure an optimal antenna gain pattern. Data can be transported to a local hub for example using fibres or wireless via LiFi. At these low frequencies, and high sky temperatures, the amplifier could be located up to about half a metre into the regolith to dampen the day-night thermal cycling, without significantly compromising the performance. Reliability needs to be addressed as well. A full array would allow some 'graceful degradation', how much is yet to be defined.

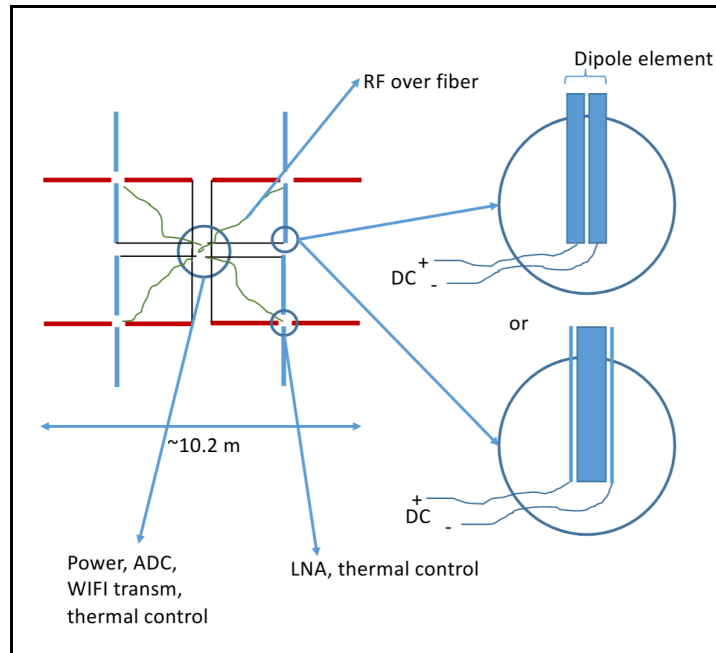


Figure 4-15: Foil antenna tile concept with four crossed dipoles, wireless (or optical) data transmission, and powering via (filtered) antenna patterns. Control and data transport is directed via a nearby hub

4.2.2.5 Amplifiers and receiver electronics

Each antenna in ALO needs a corresponding receiver which conditions (filters, amplifies, etc) the astronomical signals before they are transported and digitized for further processing and combination. A typical layout of the receiver is shown in the Figure below, which is taken from the NCLE instrument RD[50]. Some considerations for the design of ALO receivers are described below.

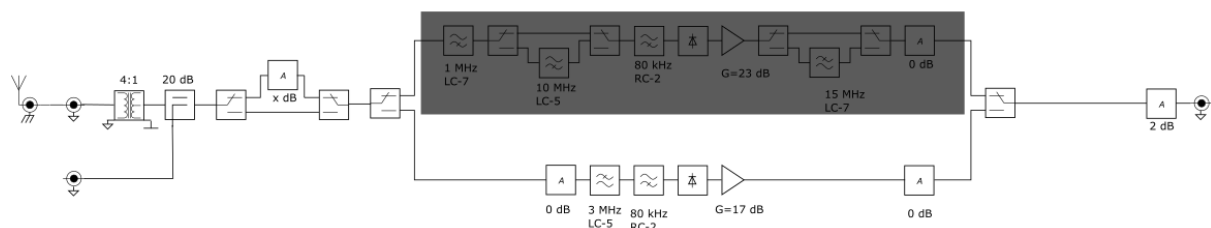


Figure 4-16: example diagram of a low-frequency RF receiver (the depicted system is from the NCLE instrument). The signal is received by the antenna depicted on the far left, and passes through a balun, calibration signal inserter, a switchable LNA, and a switchable band filter with further amplifier stage.

Given the fact that the sky is rather ‘hot’ at low frequencies RD[7], receiver systems are sky noise limited for typical pre-amplifiers (<10 nV/ $\sqrt{\text{Hz}}$). There are however a few considerations to take into account when designing pre-amps and receivers at low frequencies.

One concern is that the electronics need to be properly shielded to avoid EMC emissions to deteriorate the sky signal. This has been solved for Earth based low-frequency systems, even for DC-DC converter emissions, but this needs to be carefully taken into account for the lunar

situation. This analysis needs to be conducted in parallel to the antenna design, together with the galvanic layout and RF filtering.

A second consideration is that most low-frequency technology heritage RD[51], RD[52] uses relatively narrow bands. When using instantaneous very wide bands three issues will arise: maintaining linearity will become more difficult, an equalizer is needed to 'flatten' the input band, and special attention is needed to keep the system sky noise limited over the entire band.

Technology wise, using direct sampling in the first or second Nyquist zone is preferred because of its relative simplicity. However, RF filters at low frequency are very bulky due to the 'physics' involved. It may be very advantageous mass-wise if after the first amplifier stage(s) the signals are up-converted using mixers. The added complexity may be well outweighed by the advantages of using integrated components at higher frequencies.

The power needed for the RF electronics strongly depends on the EMI environment. For NCLE RD[50] for example, the design was optimized for linearity in harsh EMI conditions. For this reason, the input band was split into several bands, switchable filters and attenuators were used, and multiple PCB boards were needed, as well as multiple control systems. Because of linearity considerations, the LNA uses relatively large currents, as do the switches. But as it is envisioned that a lunar array will reside in a shielded area, man-made EMI levels will be very low. This means that the LNA power (per RF channel) for a lunar array can be much lower than for NCLE. Also, assuming only one input band is used, the switches and attenuators can be discarded, or at least greatly reduced in number. In case switches are needed then they probably will require less energy than for the NCLE case.

For ALO, the power of an amplifier will use of the order of 100 mW. This number can perhaps be reduced somewhat but given that the system needs to remain sky noise limited, that it is wide-band (~1 to ~80 MHz), and that it needs to remain linear, it probably cannot be reduced much. We assume 100 mW per channel as an upper limit.

The upper power limit of the other receiver components per RF channel up to the ADC for other receivers (e.g. NCLE) is of order 0.7 W. However, the number for ALO probably can be significantly reduced as the NCLE RF system is more complex (wider frequency bands, equalization needed, multiple bands, multiple boards) than ALO needs to be. An initial estimate leads us to adopt a typical level of 200 mW for other receiver components, which implies that the entire receiver (up to digitization) requires ~300 mW in operation.

As there probably will not be electronics available that can withstand the surface temperature variations, the assumption is that all electronics needs to be thermally shielded, giving it an operational range of -10 to 50 C (TBC). This for example could be achieved by burying the electronics several tens of cm into the regolith. In this way it could also survive the lunar night.

4.2.2.6 Number of ADC bits and data rate

In radio astronomical imaging and spectral line observations (non-transient science) the signals are assumed to be Gaussian. The astronomical signals of interest typically are buried deep in the instantaneous noise. Only after auto- and cross correlation, and integrating in time and (to some extent) in frequency the SNR exceeds one. As explained in [RD4] digitizing with 1, 2, or 3 bits gives a 'loss' of about 30%, 13%, or 4% respectively. This is only true for measuring Gaussian noise. Best would be to use 4 or more bits, but 2 bits may be acceptable as the outcome of a trade-off study with other design parameters.

If there is strong interference, then the number of bits should be equal to the number of bits required to fully cover the RFI induced ADC voltage swing plus a few bits (1 to 4) for the 'noise dynamic range'. For example, in LOFAR (10-90 MHz and 110-240 MHz) twelve ADC bits are used to account for strong pager signals RD[4]. These 12 bits are reduced to 4 or 8 bit after channelization (200 MHz wide channels) and discarding the few frequency channels with strong RFI. In this way, Gaussianity of the signals is ensured for a very large fraction of the recorded data samples.

The observable power of man-made radio interference from Earth at Lunar distance is up to 20 to 40 dB above the sky (galactic) background RD[9]-RD[12]. Natural phenomena (AKR, lightning, QTN, solar bursts) at the same location may be observed with a power similar to interference. According to RD[7] solar burst peak powers may lie at least 50 dB above the sky background.

Another aspect influencing the choice of number of ADC bits is the skewness of the input frequency band, or in other words the frequency dependent gain. If there is a large difference in gain at both extremes of the input band then the number of bits required to represent the signal is larger than for a 'flat' band.

And finally, ADCs are not perfect, and the 'effective' number of bits typically is somewhat lower, typically one to two bits, than the actual number of bits. With 6 dB power per ADC bit one would typically need 8 bits for 50 dB RFY dynamic range plus say 2 bit for the astronomical signal plus 2 bits for band skewness plus 2 'effective' bits. These ~14 bits may be reduced significantly in case the array location is a far side lunar crater, or if a certain fraction of intermittent data drop-out is acceptable.

As indicated above, the number of signal bits may be reduced after digitization by filtering techniques (temporal, spectral, spatial), but this requires processing capacity close to the ADCs.

Using a fiducial number of 200 Msps and 4 bits per sample with 2 cross-dipole elements per antenna, we get a raw data rate of 1.6 Gbps per antenna.

4.2.3 Array level

4.2.3.1 Topology

In order to work out the optimal topology (antenna placement and array structure) for ALO from the DA/CD science cases, we can make use of expression 5.1 from RD[3] that describes the thermal noise power spectrum from fundamental array properties:

$$\Delta^2_{Noise} = \left(\frac{2}{\pi}\right) k^{3/2} [D_c^2 \Delta D_c \Omega_{FoV} / N_b]^{1/2} \left(\frac{T_{sys}}{\sqrt{B t_{int}}}\right)^2 \left(\frac{A_{core} A_{eff}}{A_{coll}^2}\right)$$

In the above expression, Δ^2_{Noise} is the thermal noise (expressed in Kelvin) at a particular comoving scale k (expressed in cycles per comoving Mpc), D_c is the comoving distance to the redshift slice under consideration (in Mpc), ΔD_c is the comoving thickness of the redshift slice in Mpc, Ω_{FoV} is the field of view of the array in steradians, N_b is the number of independent beams in the FoV when multi-beaming is used, T_{sys} is the system temperature in Kelvin, B is the bandwidth associated with the comoving thickness, t_{int} is the integration time in seconds,

A_{core} is the area of the array within which uniform uv-coverage is provided, A_{eff} is the effective antenna aperture for a single element, and A_{coll} is the total effective collecting area for the full array.

The thermal noise power for a particular k-bin thus follows the following scaling relation (equation 5.2 in RD[3]):

$$\Delta^2_{Noise} \propto \left(\frac{A_{core}}{\sqrt{N_{stat}} A_{coll}^{3/2}} \right)$$

where N_{stat} is the number of antennas in the array and where $A_{coll} = N_{stat} A_{eff}$ is assumed. This expression tells us that it is advantageous to keep the array core size as small as possible given the number of elements involved, but also that the sensitivity scales with the square of the number of elements. A compact array, as large as possible, is the optimal topology for our top science case.

The requirements stated in section 4.1.3, which address the two science cases of measuring the redshifted hydrogen power spectrum and global signals, therefore motivate having two components for ALO:

- 1) A **compact array** with a high filling factor, which provides a large number of visibility measurements per uv-cell per given time span. A regularly spaced array (grid-like) maximises the possible filling factor that can be reached for a given array size, whereas an irregularly spaced array will incur a penalty. A compact, regularly gridded setup maximises the sensitivity per k-cell for a given array size. Scaling the number of antennas in this array impacts the range of redshifts that are reachable in a given mission lifetime.
- 2) At least one **outrigger antenna** with an accurately known antenna pattern and sensitivity properties, spatially separated from the main array to avoid any extraneous influence on its properties. Multiple outrigger antennas reduce the total required integration time and provide the capacity for cross-checks, at the cost of increased system mass and complexity. The trade-off regarding the optimal number of outriggers to use depends on the degree to which antenna and receiver performance can be modelled, monitored, controlled and corrected.

For the compact array, an array size of ~1000 antennas allows us to probe the moderately higher redshifts (up to $z=30$) for exotic physics in the early Universe. This provides a clear benefit over a much more modest array size of 16 antennas, which probes a limited redshift range up to $z=20$ and overlaps in frequency space with current and planned Earth-based facilities.

An integration time of 10000 hours has been used for our simulated array performances. The duty cycle is likely below 50% because of limitations imposed by the Lunar night, and could be reduced somewhat further to accommodate commissioning and intermediate calibration efforts. Assuming a duty cycle of 30%, this translates to a total mission lifetime of 4 years.

Regular vs irregular array (FFT telescope vs Correlation telescope)

If standard data processing is performed for the array, meaning that all individual baselines are correlated separately and simultaneously, data processing requirements quickly become unfeasible: for an array of 32x32 antennas, the number of baselines is $1024 * (1024 - 1)/2 = 523776$, a number far beyond the capacity of any correlator system envisioned to date. A solution to this is to employ a regularly spaced array, with all antennas laid out in a grid pattern where the separations between neighbouring antennas are constant. This regular spacing enables us to greatly simplify the data processing architecture by replacing the correlation step with a spatial 2D FFT, where the points used are matching spectral bins per antenna. The processing therefore starts with generating simultaneous spectra at each antenna (1D FFT), followed by a 2D FFT for each of the spectral bins generated in the first step. The result is a 'data cube', with dimensions $N_{chan} \times \sqrt{N_{ant}} \times \sqrt{N_{ant}}$. This data product can be averaged in time over time scales where the Lunar sky does not shift appreciably. The time frame for this is defined by the shortest time it takes for one visibility measurement to move to a different uv-cell, which is defined as: $t_{int} = D_{Min} / (\omega_{Moon} \cdot D_{Max})$, where t_{int} is the maximum integration time that can be used without getting uv-smearing, ω_{Moon} is the angular velocity of the Moon.

4.2.3.2 Location on lunar surface and sky coverage

The choice of placement of ALO on the Lunar surface, when considered from the point of view of its impact on the science we can do, is dictated by two factors. The first factor is that we wish to be adequately shielded from Earth RFI emissions by ~80 dB RD[42], which requires placement far enough away from the Lunar limb on the far side. This also implies that ALO will need to be located away from the Lunar poles. The second factor governing array placement is that we wish to obtain good uv-coverage through aperture synthesis using the Lunar rotation. Sites on the Lunar equator do not offer good uv-coverage, as many directions on the sky remain unsampled in that case. Therefore, mid-latitudes on the Lunar far side (ranging from ~20 to ~50 degrees North or South) offer the best scientific return for ALO.

4.2.3.3 Array size

In the following, we consider the ability of different array scales to achieve the 21-cm power spectrum measurement, and we present an overview of the general performance of these different scales.

Using the scaling relations as presented in RD[3] (section 5.1) combined with the predicted power spectrum from (Anastasia Fialkov, Rennan Barkana, Daan Meerburg, priv. comm.), we have calculated the performance of arrays of various sizes in measuring the 21-cm power spectrum at different redshifts. Maximum array density (filling factor) has been assumed, as that yields the best performance for this science case for a given array size (number of antennas). Examples of these calculated performances are shown here, and they are summarised in the table below.

For our calculations, we have assumed a compact array using cross-dipole antennas laid out in a regular grid pattern. The integration time was set at 10000 hours, a time span that corresponds to a mission lifetime of 4 years when a limited duty cycle (day only) is taken into account along with some overhead. The observing frequency corresponding to a given redshift z is calculated as $\nu = \frac{1421}{1+z}$ MHz. The frequency bandwidth involved in each of the redshift slices was set at half of the observing frequency.

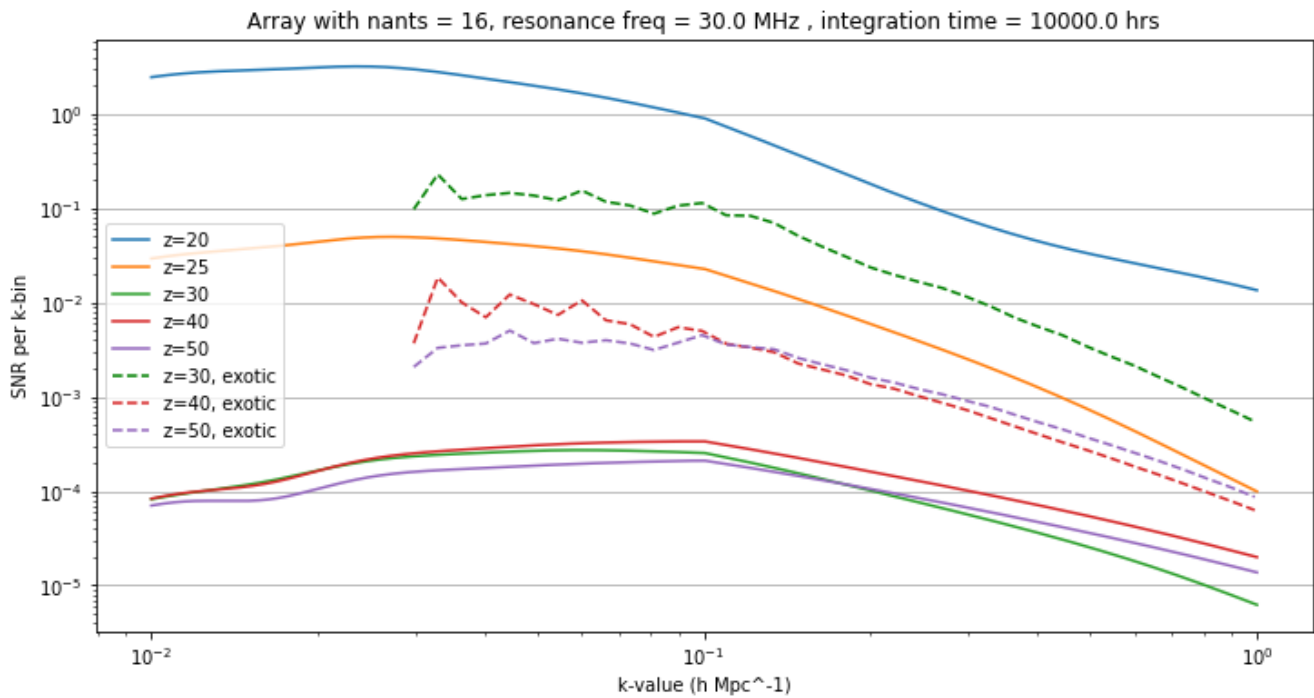


Figure 4-17: SNR per k-bin for a compact array of 4x4 antennas at different redshifts. Beyond $z = 20$, no measurements of the power spectrum are feasible within the given integration time.

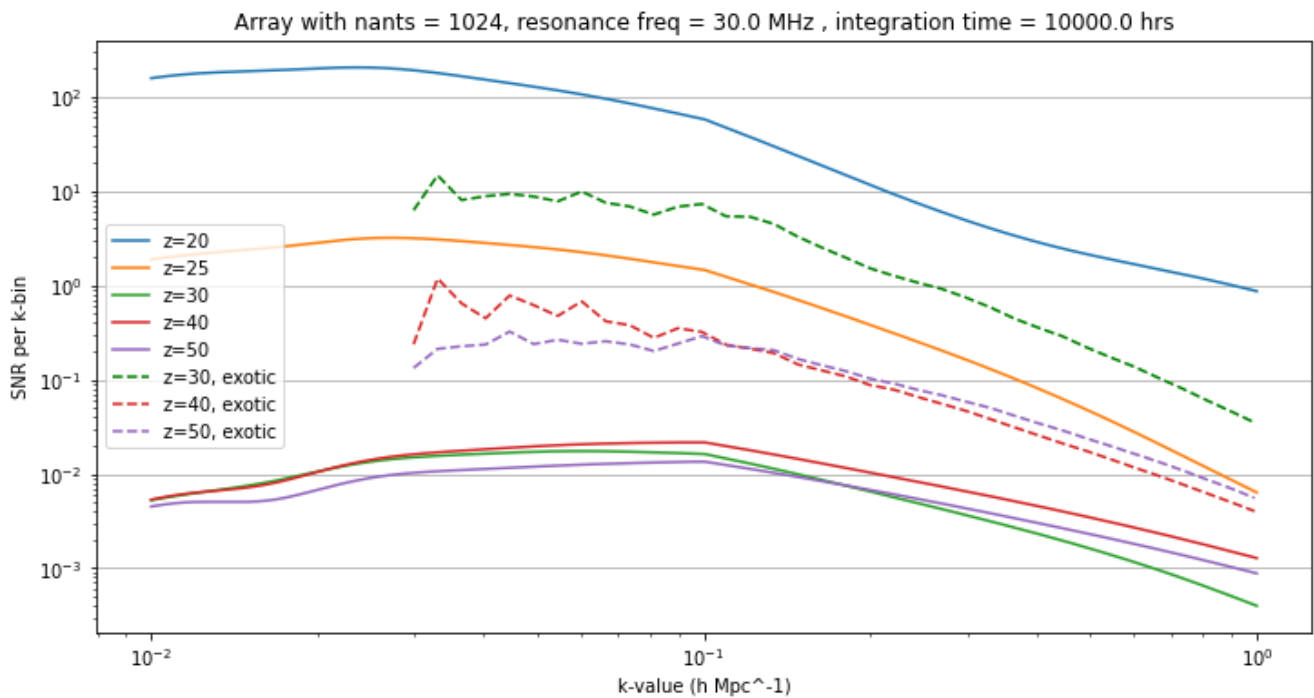


Figure 4-18: As Figure 4-16, but with 32x32 antennas. Assuming standard physics, measurements up to $z = 25$ are possible over a limited range of k-values. However, models of structure formation in the early Universe involving different physics can yield much stronger predictions for the power spectrum: for this model, the array has discriminating power up to $z = 30$.

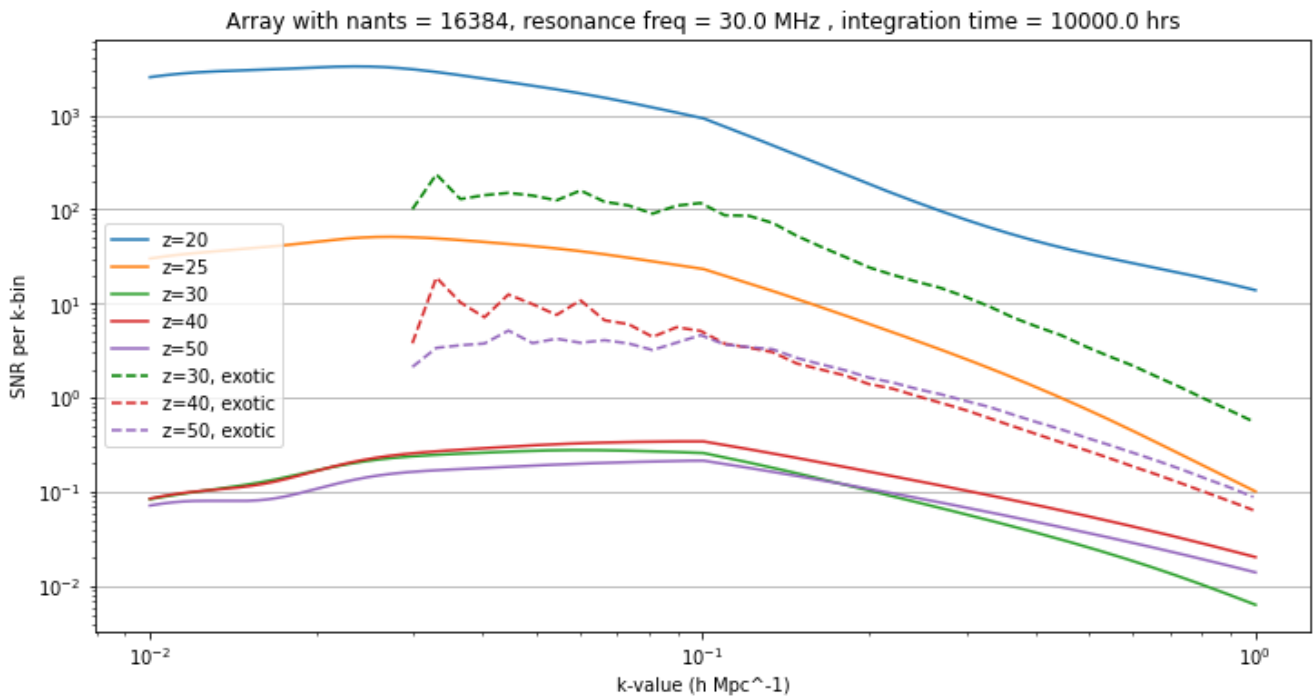


Figure 4-19: As Figure 4-16, but with a much larger compact array of 128x128 antennas. The SNR for $z = 20$ and $z = 25$ is dramatically enhanced compared to the 4x4 array, making the 21-cm power spectrum measurement feasible for the full Cosmic Dawn redshift range. When models with different physics are considered, these can be tested up to a redshift of $z = 50$.

We see from Figure 4-13 and Figure 4-14 that measuring the power spectrum at low redshifts (around $z = 20$) is already viable with a modest array of 4x4 antennas, but only over a limited range of comoving distances ($k = 1e-3$ to $1e-2$ h Mpc⁻¹). To probe deeper into the history of the Universe, the array needs to be of a significantly larger size. We therefore also show what a 32x32 element array can measure, as well as a 128x128 element array (Figure 15).). With a 32x32 array one can start to perform imaging at higher redshifts, up to $z = 25$ (i.e. at around 50 MHz), something which **cannot** be done from Earth given limitations caused by the atmospheric cut-off and RFI (noise) conditions. Another big new capability for such an array is that it can start to discriminate between different predictions for the Cosmic Dawn power spectrum, based on various models. While the prediction from standard cosmology at redshifts of $z = 30$ and higher is still too weak to measure with a 32x32 array, predictions from other candidate theories yield much stronger power spectra in several cases. These theories can therefore be tested at this scale.

Moving to a 128x128 element array, the SNR for the ‘later’ Cosmic Dawn power spectrum gets much stronger ($SNR > 10$ for $z = 25$ and below), while the limiting redshift for which detections are expected goes up to $z = 28$. As the dependence of the signal of interest on redshift is extremely steep ($\Delta T \propto z^{-5.1}$), probing farther into the early Universe will require arrays that are multiple orders of magnitude larger than what is considered feasible for EL3. One such large configuration is included in Table 4-2 for reference, together with the other array sizes.

Nr. of antennas	Dark Ages Power Spectra (DA)	Cosmic Dawn Power spectra (DP)
4 x 4	S/N << 1	S/N > 1 for z = 20, k from 0.003 to 0.1
8 x 8	S/N << 1	S/N > 1 for z = 22, k from 0.003 to 0.1
16 x 16	S/N << 1	S/N > 1 for z = 22, k from 0.003 to 0.2
32 x 32	S/N << 1	S/N > 1 for z = 25, k from 0.003 to 0.1
64 x 64	S/N << 1	S/N > 1 for z = 27, k from 0.003 to 0.1
128 x 128	S/N < 1	S/N > 1 for z = 28, k from 0.003 to 0.1
1024 x 1024	S/N ~ 10 for z = 50, k from 0.002 to 0.2	S/N ~ 10 for z = 28, k from 0.003 to 1

Table 4-2: Overview of Power Spectrum measurement capabilities for different array sizes

The second science case that has high priority is the global detection of the 21-cm signal from the early universe. This science case presents a requirement that differs from the power spectrum measurements in the sense that this hinges on an antenna and receiver system that are very well isolated from any sources of EMI, as well as very carefully calibrated. The reason that this is necessary is that this measurement does not make use of correlated signals and as such is extra susceptible to variations in total power in the receiver signal chain from interfering sources. The antenna will need to be located many wavelengths away from any potentially interfering systems, translating to a physical separation from the lander of hundreds of meters.

Performed from a quiet location on the Lunar far side, given a mission life time of multiple years and with the added benefit of having the compact antenna array available for foreground modelling and subtraction capability, measurement of the global redshifted 21-cm signal should be possible over a wide range of redshifts. We have used a general expression for the required integration time for detection of the global signal (Koopmans, priv. comm.):

$$t_{int} = 17 \text{ hr} \times \left(\frac{\nu}{70 \text{ MHz}}\right)^{-5.1} \left(\frac{\Delta\nu}{1 \text{ MHz}}\right)^{-1} \left(\frac{\delta T}{10 \text{ mK}}\right)^{-2}$$

The steep dependence of the required integration time for detection of the global signal on the redshift (and thus on the observing frequency) means that there is quite a striking difference between the lower end of the redshift range of interest and the upper end. For z = 20, and given a quiet environment and instrument, detection only requires an integration time of approximately 17 hours. Looking at z = 80, firmly in the domain of the Dark Ages global signal, requires an integration time that is more than 100 times as long as that, at 2000 hours - and this is with a bandwidth that is 10 MHz as well.

Thus, while measurement of the global signal for the Dark Ages is much more challenging than it is for the Cosmic Dawn, it is still within reach for a small number of well-calibrated, well-

isolated antennas. A summary of performances for different numbers of outrigger antennas on the global signal measurement of DA and CD is shown below in Table 4-3.

Nr. of antennas	Global Dark Ages signal (DA)	Global Cosmic Dawn signal (CD)
1	For $z = 80$ (17.5 MHz), bandwidth 10 MHz, $\Delta T = 10$ mK: $t_{\text{int}} = 2000$ hours.	For $z = 20$ (70 MHz), bandwidth 1 MHz, $\Delta T = 10$ mK: $t_{\text{int}} = 17$ hours.
2	For $z = 80$ (17.5 MHz), bandwidth 10 MHz, $\Delta T = 10$ mK: $t_{\text{int}} = 1400$ hours.	For $z = 20$ (70 MHz), bandwidth 1 MHz, $\Delta T = 10$ mK: $t_{\text{int}} = 12$ hours.
3	For $z = 80$ (17.5 MHz), bandwidth 10 MHz, $\Delta T = 10$ mK: $t_{\text{int}} = 1150$ hours.	For $z = 20$ (70 MHz), bandwidth 1 MHz, $\Delta T = 10$ mK: $t_{\text{int}} = 10$ hours.
4	For $z = 80$ (17.5 MHz), bandwidth 10 MHz, $\Delta T = 10$ mK: $t_{\text{int}} = 1000$ hours.	For $z = 20$ (70 MHz), bandwidth 1 MHz, $\Delta T = 10$ mK: $t_{\text{int}} = 8.5$ hours.

Table 4-3: Required integration times for global signal detection with different numbers of outrigger antennas

The above considerations indicate that significant power spectrum science can be obtained with a 4x4 array and 10000 hrs integration although limited in redshift space (up to $z = 20$), but the important leap will be achieved with an array of order 32x32 antennas: such an array configuration will be capable of discerning models with new physics over redshifts up to $z = 30$, a redshift range that is not feasible to observe from Earth. For the global signal, a small number (<4) of isolated antennas can achieve important science with observing times of order 2000 hrs, all the way up to $z = 80$ – again, reaching far beyond what Earth-based observations are capable of and accessing an unobserved epoch in the history of the early Universe.

4.2.3.4 Roll-out considerations

The architecture and the deployment strategy for a lunar array requires a radically different approach compared to Earth based systems. For example, the LOFAR array roll-out procedure briefly described below is, for several reasons, not possible on the moon.

The LOFAR station antenna deployment included flattening the phased-array terrains, each of order 100 m diameter. This was done using a tractor, and also manually using shovels, and it was guided by a laser beacon. The antennas were placed using markers / stakes that were placed using GPS-referenced theodolites. The orientation accuracy achieved was about 1.5 to 3 degrees rms. The LBA antennas were fixed using herrings RD[4]. The HBA antenna orientation was done by orienting the polystyrene tile, and inside the tile the antennas were aligned by a rotating mechanism. Cabling from the antenna arrays (48 to 96 pairs) was trenched, cable lengths were several tens of metres.

4.2.3.5 Antenna array clock and synchronization

Given an array of low-frequency antennas for which each antenna is connected to an analogue to digital converter (ADC), the synchronization requirement relates to the fact that the (sky) signals need to be combined coherently. This is done by ensuring that the ADCs receive a stable frequency reference for the sampler, and a distributed pulse for time synchronization. For the array let us consider the following two scenarios.

The first scenario assumes that each ADC is equipped with its own clock. As mentioned in [RD3], the stability requirement for the clock (frequency reference) is such that the rms phase error remains less than one radian: $2 \pi f \sigma(\tau) \tau < \sim 1$, with τ the coherence time (s) and $\sigma(\tau)$ the Allan variance. Figure 4-5 (right) in RD[5] shows the maximum integration times before re-calibration is needed, for different clocks and for different frequencies. So with most clocks listed, integration times up to half an hour are possible without needing re-calibration (syncing with a pulse). At 80 MHz for example, and a coherence time of 1 hour, the clock would need an Allan variance of about 5.5×10^{-13} . The time drift then would be 2 ns. As a reference, the LOFAR telescope stations RD[4] use a GPS conditioned Rubidium clock that can drift up to 20 ns in 20 minutes, but the LOFAR integration times typically are less than the envisioned Lunar array, in the order of a second to a minute.

A second scenario is the case in which there is one central clock which signal is distributed along the array. Given that there is one central clock the stability requirements are much less stringent than for the first case. A simple crystal clock probably will do. This however assumes that the transport path of this central signal is 'stable', otherwise a phase calibration scheme would be needed. Please note however that, also for the first case, there are other stability requirements as well such as jitter, relating to the effective number of bits for the ADCs, cf Figure 4-5 (left) in RD[5].

Both scenarios mentioned above are possible, the choice depends on system level design choices, for example relating to the physical transport layer of the data and control signals (coax, fibre, RF, or free space optical). In case (not envisioned now) the lunar radio array is used in interferometric mode with another telescope, for example on Earth, one would obviously need a high quality central clock similar to the one in the first scenario.

4.2.3.6 Antenna location and orientation accuracy/knowledge considerations

Crossed antenna element reference points

The two orthogonal antenna elements in a crossed dipole can be either located at a common spatial reference point, or located with a separation of about half a wavelength RD[26]. Although the latter may have advantages concerning deployment, the common reference point is chosen as it has advantages concerning beam response (better control of galvanic/RF

environments), calibration (would require artificial sources), and galvanic connections (due to separation of the x- and y- dipoles).

Crossed antenna element ‘intrinsic’ orthogonality

In Earth based systems, dipoles can be made orthogonal well within 1 degree, but due to different instrumental effects, the polarization leakage typically is of the order of 1 percent, corresponding roughly to 1 degree offset from orthogonality. Although RD[35] suggests that larger orthogonality offsets may be possible, here the maximum 1 degree offset is the requirement for the lunar array.

Antenna 3D orientation

Following the Measurement Equation formalism RD[27], the power, phase, and polarization state of waves impinging on an aperture array are accounted for by modelling the instrument and (RF) signal paths using Jones and Mueller vectors and matrices. Given a proper calibration strategy, instrumental effects such as antenna orientation offsets (errors) can be corrected for by transformation matrices RD[28]. In theory, antenna orientation offsets in any of the three unit directions can be corrected for, but as orientation calibration consumes degrees of freedom that cannot be used for other calibration tasks, it is desirable to keep the offsets as small as realistically possible. Currently the assumption is that the deployment accuracy is 10 degrees, such that angular offsets remain below 10 degrees and random throughout the array, and that the residual error after calibration is one degree. This 10 degree is assumed to hold both for the azimuthal orientation uncertainty as well as for the surface inclination uncertainty for each antenna

Antenna deployment location, accuracy in horizontal plane

The 5 m length antennas (tip to tip) are deployed in a dense grid with a pitch of 5.2 m with a deployment accuracy of 2 cm.

Antenna deployment location, accuracy in the vertical direction

The deployment area needs to be smooth (cf array flatness below), with a vertical deployment accuracy of 5% of the wavelength at the highest frequency: 20 cm.

Array inclination

Antenna tilt/inclination can in principle be estimated by calibration, preferably at higher frequencies (>30 MHz) using a sky model and parameterized antenna beam responses. Once estimated the tilt can be compensated for in the post processing.

Array flatness

The preferred observational mode of the lunar array is the 2D FFT mode as it minimizes processing load. The lunar deployment location surface is required to be smooth, in absolute sense, before calibration. Moreover, it is required that the surface shape can be modelled with up to second order spatial terms, while the variation in height (relative to the plane tilt) is

maximum about two lambdas. When these requirements are met then the 2D-FFT processing and calibration can account for the non-flatness (TBC).

4.2.3.7 Calibration

Concerning calibration, Earth based telescopes often use strong point-like astronomical sources for calibration purposes. As the power of point sources at low frequencies may be relatively weak compared to higher observation frequencies, it may be advantageous to consider artificial calibration sources as well.

RD[43] have shown that 21-cm arrays such as LOFAR and SKA are calibratable if the number of calibration directions $Q < (K/(N+1))(P-1)/2$, where P is the number of receivers, N is the number of parameters describing the frequency dependence of the gains and K is the number frequency channels. For a 4x4 regular array, for example, $P=16$, $K \sim 400$ (say ~ 50 kHz channels at 20 MHz), $N \sim 3$ over ~ 10 MHz (as for LOFAR), hence Q must be less than few hundred. Given that a compact 4x4 array has at most 16 spectrally-smooth independent viewing directions in the sky, this means that if a decent sky model can be constructed the system is calibratable. For $P > 4 \times 4$, this will also hold. This argument weakens a little since the sky model needs to be built from the same data as is used for calibration, but the system will remain calibratable given the low number of independent parameters needed to describe the sky and the very large number of spectral channels.

The approach to calibrate the global signal system is quite different (RD[49]) and often involves signal switching and internal noise-calibration sources. State of the art here are the EDGES RD[44] and SARAS RD[45] approaches. RD[46] have shown that foreground and global signal are separable as well, as long as the instrument is spectrally smooth.

4.2.3.8 Antenna signal to central hub(s) transmission considerations

We consider a situation where the signals from all individual antennas are transported to a central hub for processing, possibly with an intermediate hub.

There are several ways to send data to an intermediate hub or subsequently to a central hub for further processing. The first option is to send the analogue RF signal after amplification over coax to a hub that contains the ADCs. This requires, per antenna, hundreds of metres of coax, and is impractical because of its mass and deployment complexity.

Another option is to send analogue RF signals via RF over fibre (RfF) to central hubs. The dynamic range of fibres and RfF converters is limited, and possibly cannot handle strong transmitter signals in the vicinity (in the bands of interest). Given the envisioned radio quietness this may not be a big problem. The synchronization / stability of the RF over fibre signals may be an issue. These need to be stable within a fraction of a wavelength, but can this be guaranteed when there are huge temperature jumps every two weeks? Or is it a matter of calibration? 'Equalization' (just after the LNA) needs to be considered in case the dynamic range of the fibre systems are limited. This option has a much lower mass budget compared to coax, but still is complex in deployment.

Sending digital signals over fibres is a fourth option, but this requires digitization at the antenna, and requires proper EM shielding as the digital circuitry is very close to the antenna.

A fifth option is using wireless (wifi/lifi/5G-6G) RF free space data transmission, or optical without fibre. Wireless RF probably has to be combined in a hybrid form with intermediate hubs,

as for the full 128^2 array the bandwidth simply is not large enough. Free space optical transmission currently is too bulky for deployment for the full array, but future systems may be applicable in a hybrid form including intermediate hubs.

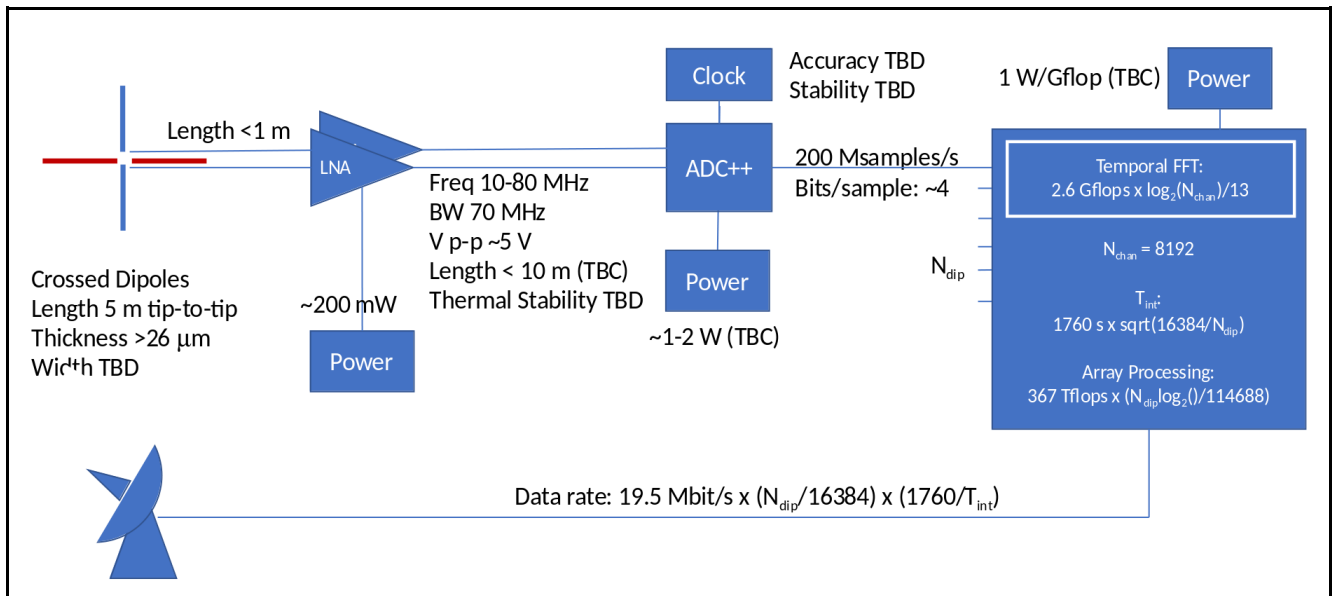


Figure 4-20: Top-level system overview of lunar aperture array, signals from crossed dipoles, amplified (LNA), digitized (ADC), channelized, correlated, integrated, and sent to Earth for further processing

4.2.3.9 Data rate estimates

Two extreme cases for the array geometry are either to have a fully regularly gridded array or to have an array designed to provide the best coverage of the uv-plane (an irregular array). Both of these alternatives do require that the array be dense ($\sim 2 \lambda$ separation between neighbouring antennas) in order that the array's sensitivity over the relevant angular scales on the sky be optimised. However, these alternatives have very different requirements regarding the local processing power, and possibly the downlink data bandwidth, that will be necessary.

In general, the sampled data from each antenna will need to be transformed into the frequency domain before further processing takes place. This is done by performing FFTs on successive chunks in the sample stream. For a sample rate of 200 Msps, covering frequencies up to 100 MHz, an FFT size of 16384 points gives a frequency resolution of ~ 12 kHz. The data rate associated with the 200 Msps per-antenna stream depends on the bit depth used for the sampling. For 8-bit sampling, this per-antenna data rate comes to 1.6 Gbps. To limit this data rate, the sampling bit depth can be reduced at a penalty in sensitivity, but bear in mind that additional requirements on passband flatness and the absence of RFI are relevant here (weaker signals can 'drown' more easily in a quantized sample series if other signal components dominate the voltages). One-bit sampling incurs a 36% reduction in sensitivity compared to the theoretical un-quantized performance, while 2-bit sampling comes with a 12% reduction.

For the *gridded*, or *regular array*, a 2D FFT is then performed along the axes of the antenna grid for every frequency bin from all antenna elements. For instance, for a 128×128 antenna array these are 128×128 FFTs, executed for every frequency channel. These 'FFT maps' per frequency bin can then be accumulated over time as long as the uv-coverage does not change

significantly over that time scale. This time scale depends on the length of the longest baseline in the array - as a guide, it is close to 15 minutes when this maximum length is about 1 km.

For the *irregular array*, all baselines will need to be correlated. For a 128 x 128 antenna array, there are $16384 \times (16384 - 1)/2$ unique baselines, so this quantity scales very fast with array size. The same integration time can be used for the resulting correlation products as for the regular array, but the associated data rate is orders of magnitude larger. This will necessitate further central processing of the generated data within the instrument itself, before sending the resulting sky maps (which will have a data rate comparable to the case for the FFT regular-grid telescope) out.

For the global signal, the estimate on the raw data rate per antenna is simply:

$$D = N_{chan} \cdot N_{pol} \cdot N_{bpc} / T_{int},$$

where D is the raw data rate in bits per second, N_{chan} is the number of frequency channels (8192, as for the power spectrum measurement), N_{pol} is the number of polarisations (2 for a cross-dipole antenna), N_{bpc} is the number of bits per frequency channel (32 for standard IEEE754 floats) and T_{int} is the integration time in seconds. Choosing an integration time of 1 second together with the values mentioned, the raw data rate comes out as $D = 0.5$ Mbit/s.

4.2.3.10 Data Processing estimates

Following RD[25], the processing requirements to first order are expressed in terms of multiplication operations. Additions are assumed to be second order operations and are not considered.

Channelizing

This concerns the required data processing per antenna data stream, which holds for any array geometry: it will always be necessary to perform. The sampled data from each antenna will need to be transformed into the frequency domain ('channelized'), using an FFT. Following the paper mentioned above (equations 4 and 19), the number of required DFT multiplications N_{fft} is given by:

$$N_{fft} = 4 \left(\Delta f - N_{bins} \right) (0.5 N_{bins}) \log_2(N_{bins}),$$

With $\Delta f = 100$ MHz, and $N_{bind} = 8192$ this yields $N_{fft} = 2.6 \times 10^9$ multiplications per second for each antenna and for each polarization. For $N_{ant} = 128^2$ and $N_{pol} = 2$ this yields in total 85×10^{12} multiplications per second. Note that this computational requirement is independent of the style of correlation chosen for the array (FFT telescope or full-visibility array). Possible ways to reduce this aggregate computational effort include:

- Reduction of the number of total antenna elements
- Reduction of instantaneous bandwidth
- Reduction of the number of bits per sample
- Beamforming of groups of antenna elements

Cross-correlation, FX, irregular array

The number of (real) multiplications for correlation per frequency channel for the irregular array equals, where we multiply the number of baselines by the number of multiplications per frequency channel per baseline (two complex numbers, so 4 real multiplications needed):

$$N_{corr,irreg} = 0.5 N_{ant} (N_{ant} - 1) \cdot 4 \approx 2 N_{ant}^2$$

This is done at a rate f_s / N_f , with f_s the sampling frequency and N_f the number of frequency channels. For N_{stokes} channels this gives:

$$N_{corr} = 2 N_{ant}^2 (f_s / N_f) N_f N_{stokes}$$

real multiplications. For an array of 128 x 128 antennas, a sampling frequency $f_s = 200$ Msps (and a channel width of 12 kHz or 8192 frequency bins) and full Stokes this yields a total of $N_{corr} = 2.3 \times 10^{17}$ multiplications per second. This is independent of channel width.

Cross-correlation, regular array

For this case, we make use of the regularity of the array to simplify the correlation process drastically. The channelized data from the antennas can now be processed using a 2D FFT for each channel. Such a 2D FFT involves an FFT along each dimension, which has $K \log_2(K)$ complexity (where K is the number of grid points along one dimension, which we can express as $K = \sqrt{N_{ant}}$). This FFT along one axis needs to be performed K times (once for every row in the grid), and this exercise is repeated for the second dimension. So, for the full 2D FFT we get (four real multiplications per complex product):

$$N_{mult,1} = 2 \sqrt{N_{ant}} \log_2(\sqrt{N_{ant}}) \sqrt{N_{ant}} \cdot 4$$

complex multiplications. Again using $N_{ant} = 128^2$, and all Stokes products we get:

$$N_{corr} = 2 \cdot 4 \cdot N_{ant} \log_2(\sqrt{N_{ant}}) \cdot (f_s / N_f) \cdot N_f \cdot N_{stokes}$$

real multiplications. Using the same numbers as for the earlier expression, this gives $N_{corr} = 3.67 \times 10^{14}$ multiplications per second.

A potential advantage for the regular array lies in the fact that the FFT algorithm can be performed in a distributed fashion. If the FFT can be evaluated at the subgrid-level (e.g. for 8 x 8 antennas in some hierarchical node structure), the products from this operation can be passed on to a central data processing stage where the number of incoming data streams is significantly reduced compared to the direct antenna-to-base station architecture. However,

the viability of this option is currently being investigated - time-averaging at the subgrid level may destroy information needed for higher-resolution sky map generation.

As of 2020, consumer GPU hardware offers performance figures beyond 50 GFLOPS/Watt RD[38]. We here use the figure of 50 GFLOPS/Watt as a fiducial estimate for the performance of computing hardware for ALO. With a **regular** 128x128 array, the total computation requirements are dominated by the correlation. With correlation requiring $N_{\text{corr}} = 3.67 \times 10^{14}$ multiplications per second, this means that consumed power would be on the order of 8 kW. Compare this to the power required for the correlation stage of a 128x128 **irregular** array, which amounts to approximately 4.6 Megawatts (!).

4.2.3.11 Operations concept

ALO will effectively be generating sky maps for all frequency channels from the 2D FFT data processing stage, and as such we envision ALO to observe in one consistent mode throughout its operational life. This means that no frequent commands are required in remote operation – instead, ALO is kept running with a certain set of configuration parameters for days or even weeks at a time. Periodically, new antenna calibration parameters may be uploaded to ALO based on recent measurement results taken over timescales of days if necessary.

From a science point of view, the ideal case is to have as large a duty cycle as possible for ALO that includes both day- and night-time operation. Available power considerations may limit the duty cycle to daytime operation only, although night-time operation would actually be preferred because of the absence of strong Solar emission and improved sensitivity characteristics of the signal chain at low temperature during night-time. Limited battery capacity could extend the duty cycle to include the transition from daytime into night-time, where measurements may still be performed if the response of the instrument changes sufficiently smoothly and slowly with local temperature and plasma conditions.

Depending on the achievable performance of the receiver system over the wide range of frequencies needed for the combined DA/CD science cases, a split-spectrum system might be necessary if the appropriate spectral sensitivity cannot be reached by a single receiver chain. If this is the case, operation of ALO will involve switching between the DA and CD modes, with the DA mode focusing on frequencies below 45 MHz and the CD mode on frequencies above 45 MHz. For this case, the DA mode will take up the most integration time if the goal is to reach similar aggregate sensitivity for both science cases over the mission lifetime.

4.3 Proposed Observatory description

Resulting from the above high-level trade-offs, we propose for this study a configuration for ALO which consists of the following elements:

1. Global detection experiment

For the global signal measurement of the redshifted hydrogen spectrum from the early Universe, carefully characterised and calibrated antennas are needed. These antennas therefore need to be placed away from other antennas and systems, as outriggers. We recommend placing these outrigger antennas several hundreds of meters away from any other array elements. The global detection antennas should have a well-behaved and thoroughly understood antenna pattern for the frequency range of interest.

2. Imaging array experiment

For measurement of the power spectrum of the Cosmic Dawn and the possibility to identify scenarios with different physics for the Dark Ages, we consider a compact and regularly spaced array of 32x32 elements optimal. The compactness ensures that we make the most effective use of our uv-coverage, with large dwell times per uv-cell. The regularity enables greatly simplified data processing at a fraction of the capacity that would be needed for an irregularly spaced array. The antennas transmit data to a Hub where (FFT-type) data processing is carried out before transmission to Earth. Table 4-4 summarizes the main requirements for each of these elements.

We specify the instrument requirements separately for the DA and CD science cases in this table, while the aim is to address both of these science cases with a single receiver chain as well as a single recording mode.

		Global signal		Power spectrum	
		DA	CD	DA	CD
Spectral					
	frequency range (MHz)	18 - 45	45 - 80	18 - 45	45 - 80
	bandwidth (MHz)	27	35	27	35
	Frequency resolution (kHz)	12	12	12	12
Temporal					
	Total integration time	2000 hrs		10000 hrs	
	Time resolution	1 s		1760 s	
Physical					
	Nant	≥1	≥1	128x128	32x32
	Antenna type	Crossed fat-dipoles, 5m tip-to-tip No ground plane		Crossed fat-dipoles, 5m tip-to-tip No ground plane	
	Location accuracy (antenna)	-		Lambda/20 (~30 cm at 45 MHz)	Lambda/20 (~19 cm at 80 MHz)
	array type	Spatially separate antenna element		regular fully filled 2D array	
	location	Isolated from RF srcs and other antennas		On flat area, at mid-range Lunar latitudes (20 to 50 degrees)	
	Array location accuracy	-	-	deviation from planarity <30cm per antenna	deviation from planarity <19cm per antenna

Power per antenna	~300 mW	~300 mW	~300 mW	~300 mW
Data rate per antenna	1.6 Gbps	1.6 Gbps	1.6 Gbps	1.6 Gbps
Common clock reqt	-	-	1e-11	1e-11
Processing power (hub)	-	-	3.67e5 GFLOPS	1.15e4 GFLOPS
Power to hub			>8 kW	>250 W
Data rate to Earth	0.5 Mbps per cross-dipole	0.5 Mbps per cross-dipole	305 kbps aggregate	19.5 Mbps aggregate

Table 4-4: Summary of instrument requirements for DA and CD science cases

4.4 Technology and analysis roadmap

While a detailed scientific roadmap is beyond the scope of this document, from the material presented in this chapter it has become clear that a low-frequency radio array on the moon has a strong and visible lead science case: the detection of the global signal and mapping of the redshifted neutral Hydrogen to uniquely study the pristine Universe before the first stars were formed. In fact, many attempts are already being made with Earth based facilities to push observations to higher and higher redshifts. Currently projects like LOFAR, MWA and in the future for instance SKA, will attempt to map the neutral hydrogen emission in the redshift ranges from $\sim 6-25$ (i.e. corresponding to 200-50 MHz), but these experiments are extremely difficult and will not be able to push to higher redshifts due to the ionospheric cut-off. SKA will be the dominant of these experiments in the years to come, but will be limited to tomography of the Epoch of Reionization ($z=6-10$) and power spectra from the Cosmic Dawn ($z=10-25$) and will be completely blind to the Dark Ages. Similarly, Earth-based single-detection experiments such as EDGES aiming to detect the global 21-cm line emission are already struggling to constrain the measurement of the spectrally broad Cosmic Dawn signal, while the Dark Ages signal will remain well beyond their reach. In order to reach the higher redshifts, i.e. probe further back into the early history of the Universe, and start to attempt to constrain the signal from the Dark Ages and produce tomographic maps of the Cosmic Dawn, an array on the Lunar far side is crucial.

ALO is the first coordinated effort to detail a concept design for such a facility in the context of the ESA EL3 program, with the goal to identify the key technological drivers and push for coordinated efforts for TRL activities, which will need to happen in **parallel** to the ground-based efforts referred to above. A key element in this will be the **step-wise approach and scalability** of the concept. This is inherent to the concept of an interferometric array, and in this case a first single element would already provide new science from day one (global detection from a far side location) while each addition to the array will allow to go to higher redshifts (earlier times) and smaller cosmological scales.

The EL3 concept can in principle accommodate this approach. The first of the EL3 missions to the Lunar South Pole equipped with a one- or two-element precursor instrument can serve as the technological demonstration of the antenna concept and the effect of the Lunar environment, the concept of interferometry, and provide essential measurements of the local

radio background spectrum, the RFI and EMI conditions, and attempt to measure the global signal in preparation for a dedicated far side mission. As the EL3 program currently foresees repeated Lunar missions, and assuming that a modest low-frequency array (4x4 or 32x32 antennas) would fit into a single dedicated EL3 mission, the ALO concept can be scaled up with subsequent missions. Finally, note that this also provides opportunities for international collaborations in the context of human and science exploration of the Moon, as multiple, similar sub-arrays can be connected via a central (European?) hub, in the same way for instance as now the central LOFAR station in the Netherlands is connected to the other European stations in France, Germany, the UK, Poland, Sweden, Ireland, Latvia and Italy.

The focus of the work in the ALO topical team should be on refining and clarifying the requirements on ALO, and on technological developments that are needed to prepare for a precursor instrument and possible future far side array, in the context of the EL3 program, and also following the EL3 program timeline. From the CDF sessions a number of key topics were identified that require a follow-up: either as a dedicated ALO topical team activity, or via dedicated industrial activities; of course in both cases to the extent that it is possible depending on availability of resources and within the timescale of the topical team activity. Here we provide an overview of these topics.

4.4.1 ALO analysis topics

- **Antenna design** – for the design of the antenna we have now selected a baseline but there are a number of open questions which need to be addressed in further studies. The major topics are:
 - ALO focuses on two science cases: the global detection and the mapping of the 21-cm line emission, the first requires at least one well-calibrated single antenna placed at a remote (low-noise) location, while the second requires a compact, regular array of identical elements. For now, we have assumed that the basic antenna design is the same for both cases, i.e. a “fat-dipole”, but this needs to be studied in more detail, in particular to make sure that the design meets the science requirements, i.e. is optimised for these two different type of detections. Within the ALO topical team activities we will perform more detailed antenna simulations and perform prototype tests to characterise these types of antennas in more detail (beam pattern, polarization response, sensitivity, etc.).
 - We need to analyse in more detail if non co-located antennas can be used and how issues like galvanic connection constraints and calibration can be solved.
 - The total mass of the antennas in the array is one of the most limiting factors in the ALO concept, hence we need to push for alternative light-weight antenna designs. In the CDF the concept of printed antennas on Kapton film was discussed. We propose here to further investigate existing designs (e.g. available at ASTRON) and further develop a concept design for ALO. This will be an ALO activity which will be closely connected to design work that is currently ongoing in the Center for Astronomical Instrumentation (CAI, an initiative of the Radboud University and the Technical University Eindhoven).

- **Calibration and characterisation** – as discussed above, the calibration of the individual antennas and the whole array is critical for the 21-cm detection, as the signal-to-noise ratio is high and foreground emission (by known and unknown sources) needs to be removed. Calibration is a major topic in the ALO topical team activity, and summarising we propose to focus on the following sub topics:
 - The antennas will need to be placed directly on the Lunar surface, with no ground plane. This is possible as the Lunar regolith is expected to have suitable dielectric properties. However, at some depth, the bedrock layer will reflect part of the celestial radio waves, impinging on the array from below. How this effect can be mitigated by calibration and post-processing requires further study.
 - The spectral properties of all the noise components at the Lunar surface and their temporal behaviour needs to be determined, this includes the RFI from Earth, EMI from the spacecraft and other future infrastructure, the Lunar background spectrum and the foreground emission. This can be done by detailed modelling, but also by using data from existing measurements from the ground (e.g. measurement by LOFAR of the lunar radio emission) and from the Lunar environment (e.g. existing measurements by the Chinese lunar missions, Cassini, Solar Orbiter). Based on this, a RFI/EMI mitigation plan will be developed as part of the ALO topical team.
 - Particular attention needs to be given to EMI and the ALO team will define the requirements for the EL3 mission and will push for a low-frequency radio protected zone at the Moon.
 - Within the ALO context, a concept calibration plan will be defined for the flux calibration strategy and need for artificial noise sources, at (or close to) the Moon, for calibration purposes.
 - An additional noise source will come from the influence of galvanic lines/solar cells. Within the ALO activity these levels will be characterised and a concept plan to minimize their effect, at antenna and array levels, will be presented.
 - Related to the RFI and the gain and temperature stability of the antennas, we will investigate the optimal location for the array within the boundaries of the EL3 missions, and determine the location and orientation requirements. These can include ray-tracing simulations of RFI emission around the moon.
- **Receiver & data** – another major driver identified in the CDF is the power consumption and mass of the harness need to transport and process the data created by ALO. This can be directly related to the following topics:
 - Receiver design, mass and power minimisation: within the ALO topical team and the CAI initiative we are investigating ways to optimise the receiver design to allow for high-performance processing with less power. One of the topics that is will be addressed is the possibility of using a dedicated ASIC chip and smart algorithms for the data processing.

- The options for distributed processing on the moon will be investigated in more detail, in order to optimise the data processing and power needs, and find the right balance between which data products will be produced where.
- To reduce the mass of the harness, alternative data transport options will be identified, for example optical communication.
- Related to the high power requirement and the antenna design, we will investigate the option to integrate the antenna and solar panel systems into one single design.
- Finally, in order to deal with the high data rates and volumes compared to the available downlink, we will study means for data compression.

4.4.2 Dedicated TRL activities (industrial activities)

Following the proposed ALO topical team activities on the identified critical enabling technologies, we provide here an overview of some of the areas on which urgent TRL-increasing activities are needed:

- Printing planar antennas on foils;
- Deployment of individual antenna elements or small groups of antennas, e.g. inflatable or unrollable planar units;
- Low-mass low-power receiver units, including their survivability in Lunar night conditions;
- Power distribution via non-conventional means, e.g. RF transmission;
- Integration of receivers and processing electronics into deployable units;
- Low-mass, low-power data processing units.

Within the ALO Topical Team activities we will address these topics further and define a feasible development plan with a clear timeline.

5 PAYLOAD ANTENNA

5.1 General considerations and initial assumptions

The array of antennas chosen for the ALO CDF is an Aperture array.

An aperture array is a cluster of a large number of fixed antenna elements which can be arranged in a regular or random pattern on the ground. Because of the relatively long wavelength of the ALO frequencies, the number of elements required for a given effective aperture (A_{eff}) is a practical configuration for this CDF case (the higher the frequency, the higher the number of elements and the more expensive).

The amplitude and phase at the antenna levels are measured for two orthogonal polarizations.

Independent beams can then be created simultaneously in post processing, yielding very large field of view. Each beam is formed and steered by combining the received signal after appropriate time delays for phase alignment.

Thus, the number of beams produced or total Field of View (FoV) is essentially limited by signal processing, data communications and computing capacity.

5.2 Requirements and Design Drivers

The objective of this section is to derive the requirements for the design of the antenna subsystem from the requirements as set at the beginning of the CDF study.

In order to define the drivers for the antenna design, top-level specifications of a radio telescope are enumerated, and the ones affected by the antenna and array design are simplified in antenna engineering terms.

Top level specifications RD[53]:

1- System sensitivity $\left(\frac{A_{eff}}{T_{sys}}\right)$ as a Function of Frequency

In radio astronomy, the sensitivity is proportional to the telescope's effective aperture area over the system noise temperature. Both these terms are dependent on the antenna front end.

- Impact of array configuration: total size of the array, density of the array and size of the antennas is the main contribution.
- Single antenna radiation efficiency (η_{rad}): affects both the incoming desired wave ($G = \eta D$) and the system noise (It affects the system noise by directly weighting the undesired Sky noise temperature). It does not include impedance mismatch but represents the antenna losses (due to the presence of non-perfect electric conductors in the antenna and the presence of ground soil).

2- Accessible Field-of-View as a function of frequency and Baseline

- The main contributor for the definition is in the simplest case the "Element Pattern" or the shape of the pattern of a single element of the array. The elements could have very directive pattern and hence a narrow accessible FoV. Those would perform with great sensitivity at zenith but would underperform at large

angles from zenith. For smaller antennas or elements with omnidirectional patterns like dipoles, the accessible FoV is larger.

3- Processed Field-of-View as a Function of Baseline

- It is the angular region mapped from the sky, after post-processing of the data collected by the elements of the array. It highly depends on the baselines (distance between the antennas in the array) and the sub-arrays selected for imaging.

4- Survey Speed as a Function of Frequency (traditional metric for survey capability)

- It is defined as proportional to $\frac{A_{eff}}{T_{sys}} \times (procssed\ FoV) \times (Processed\ Bandwidth)$
- Dependent on the geometrical configuration of the array. A trade-off between processed FoV and $\left(\frac{A_{eff}}{T_{sys}}\right)$ (Longer baselines gives smaller FoV, but larger effective aperture).

5- Angular Resolution as a Function of Frequency

- Defined by the maximum baseline in the array.

6- Polarisation Purity

- Defined by the IXR* (intrinsic axial ratio) of a single element of the array, as well as the effect of the environment and the coupling from neighbouring antenna elements and the feed lines).

*The IXR can be calculated by post-processing the simulation results of the antennas in a commercial software

7- Total Bandwidth and Spectral resolution

- Not directly dependent on the antenna or array design.

8- Imaging Dynamic Range

- Not directly dependent on the antenna or array design.

5.3 Key drivers and challenges

In summary, Table 5-1 shows the modelling drivers for the antenna element and the array configuration:

Key drivers – Antenna: Single element			
Ref.	Parameter	Requirement	Impact
1.	High antenna efficiency	TBD%	Sensitivity (spec 1)
2.	Choice of antenna element: size and type of antenna	Maximizing the directivity and radiation efficiency within \pm TBD ($^{\circ}$). (A hemispherical pattern has been chosen as a baseline for this study: $\pm 90^{\circ}$) Reduced sensitivity of the pattern to coupling with neighbouring element	Accessible FoV (spec 2)
3.	Polarization characteristics of the single element and the coupling effect on it	TBD	Polarisation Purity (Spec 6)

Table 5-1: Key antenna drivers

The following topology has been chosen for the geometry of the array in accordance with the science team: 128x128 antenna elements in a 640m x 640m = 0.410 km² area. Table 5-2 shows the Antenna array parameters and their impact of the top-level specifications.

Key drivers – Antenna Array			
Ref.	Parameter	Requirement	Impact on top level specification
1.	A_{eff} : total size of the array, density of the array (number of antennas and their location) and size of the antennas (Baseline of regular array of 128x128)	TBD (depends on trade-offs)	Sensitivity (spec 1)
2.	Distance and location of the array elements (Baseline of regular array 128x128)	TBD (Deg^2)	Processed FoV (spec 3)
3.	Trade-off between A_{eff} and baselines	TBD	Survey Speed (spec 4)
4.	Longest distance between the antennas (905km per the chosen topology)	TBD For the chosen topology : $\frac{\lambda}{9.05 \times 10^5}$ (rad)	Angular Resolution (spec 5)

Table 5-2: Key Array drivers

5.4 Technology Needs

The requirements of the ALO instrument call for an antenna design capable of delivering excellent performance in radiation patterns (quasi-hemispherical pattern) and polarization purity over a wide angular beam and in a wide-band frequency range (1-100MHz).

The challenge is that the technology used to deploy the elements of the array will condition the choice of the antenna type.

Moreover, the design of the antenna should be done taking into account the characteristics of the Lunar soil and the coupling with the feed lines (A solution to study could be the creation of a controlled meshed ground plane and the integration of the feed lines into the mesh.)

After performing this CDF activity, it became clear that the design of the antenna could not be done independently from the science requirements, as many of the parameters are subject to trade-offs and should be checked with the science team regarding the calibration and post-processing capacities and limits. For example, the CDF study emphasised that accurate precision was needed for the alignment of the antenna elements (crossed dipoles). A looser alignment could be tolerated as long as combined with a precise knowledge of the misaligned geometry. However, this would come at the cost of increased data processing.

Therefore, it is recommended to perform additional studies, for the design of innovative antennas with double orthogonal polarization and a wide angular beam with high polarization purity beam, including studies on the reduction of effects of coupling with neighbouring elements and feed cables. It is also recommended to perform a study on the characterization of the Lunar soil in antenna modelling software's in order to be sure to have models that are representative of the Lunar conditions.

6 ENVIRONMENT

6.1 Lunar Ionosphere

The Moon has an ionosphere that originates from the interaction between the solar wind, solar photons and the lunar exosphere (a tenuous neutral background). Since the ALO mission main objective is to observe radio waves (in the MHz range), the potential interference between the lunar ionosphere and the radio waves was investigated. Measurements made by Chandrayaan-1 provide the electron column density at various altitudes, as shown in Figure 6-1. Around 20-30 km altitude the electron density sharply increases and has a range of 100 to 300 cm^3 . The electron density column in the lunar ionosphere is quite low with respect to the Earth ionosphere (10^4 - 10^6 cm^3). The plasma frequency around the Moon is of the order of 30-150 kHz. ALO radio waves spectrum is in the MHz range, leading to the conclusion that ALO observation will not be affected.

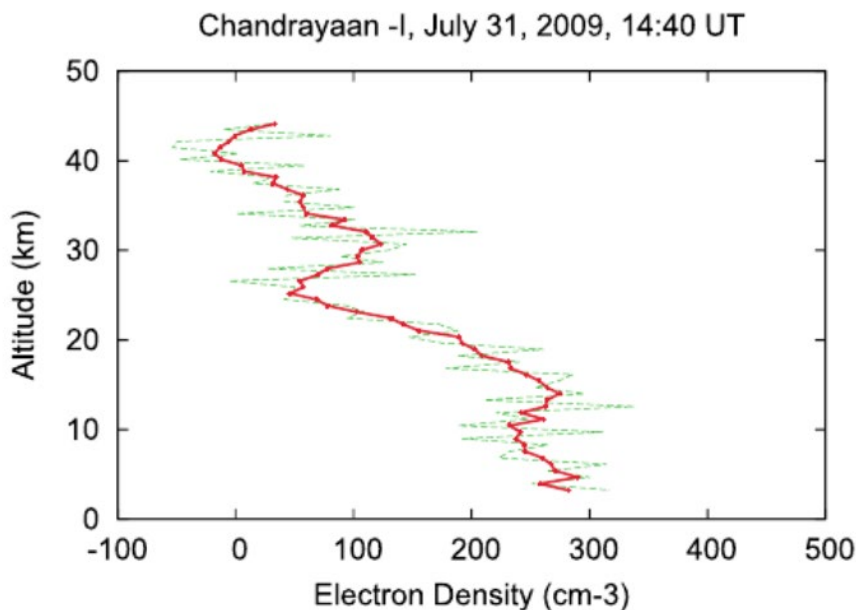


Figure 6-1: Altitude variation of the electron density averaged measured by Chandrayaan-1 S-band radio occultation experiment RD[54]

6.2 Plasma Environment and Lunar Surface Charging

The plasma environment around the Moon can be highly variable, it depends on the lunar latitude, lunar orbital position, lunar local topology, solar illumination conditions, solar wind conditions and local magnetic anomalies (if any).

In nominal solar wind conditions, the photoelectron current is the main driver that charges the surface positively to a few Volts. On the dayside, the lunar surface charges positively due to the photoelectron current being dominant. While on the nightside, the lunar surface charges negatively due to the electron current being the most prominent.

As the Moon passes through the Earth magnetotail lobes and the plasma sheet, the plasma temperature increases, and the lunar surface potential can charge up to hundred or to thousand Volts respectively. Moreover, the solar wind conditions can have transient conditions, due to Coronal Mass Ejection (CME) for instance, that may charge the lunar surface to thousand Volts. A summary of the different plasma environment and lunar surface potential is presented in Figure 6-2.

	Tail Lobe	Plasma Sheet	Solar Wind	Lunar Wake	SEP Event
Electron density	0.001-0.5 cm ⁻³	0.01-1 cm ⁻³	0.5 – 10 cm ⁻³	0.001-0.1 cm ⁻³	0.001-0.1 cm ⁻³ in wake
Electron temperature	<100eV	100eV to 2keV	5-30eV	50-150eV	50 eV to 1keV in wake
Electrostatic surface Potential	~+200V (Day) / -150 to 0V (Night)	-1000 to 0V	<20 V	-200 to 0V	-1000 to -4000 V in wake

- Electrons accelerated by surface potentials : LP/ER (US)
- SW Ions reflected by surface potentials / magnetic anomalies: Kaguya (JAXA), Chandrayaan-1 (IRSO), ARTEMIS (US)

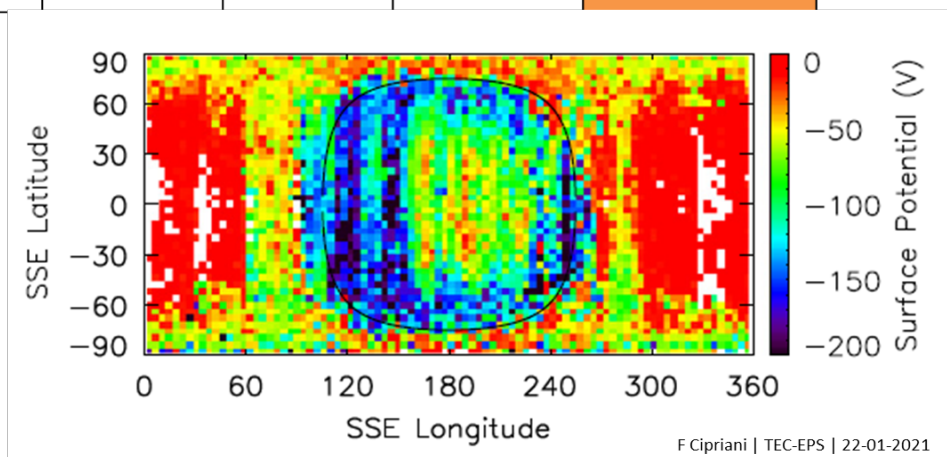


Figure 6-2: Typical lunar surface potentials and plasma properties. The lunar surface potential map was measured by the Electron Reflectometer on-board the Lunar Prospector RD[55]

In the context of ALO, the selected deployment location is Tsiolkovsky crater. Tsiolkovsky crater coordinates are 20.4°S 129.1°E, located on the lunar farside. The precise deployment location may influence ALO operations. The local lunar topography influences the local lunar surface potential and plasma conditions.

For instance, close to Tsiolkovsky crater rims the plasma conditions could be extreme during sunrise and sunset. Close to sunrise or sunset, the solar wind is almost parallel to the local surface and the crater rim can create a plasma expansion. Electrons have a much higher thermal velocity compared to ions. Electrons thus can reach the inner walls of the crater, while ions are unable to. This forms an electron cloud that may charge the local lunar surface to high negative potentials. Electrostatic Discharge (ESD) is a potential risk that may arise and needs to be further investigated later. ESD risks depends on many factors (environment, spacecraft design, materials, etc.) that are not fully characterized yet for ALO.

The current deployment location and the solar illumination conditions are shown in Figure 6-3. The local plasma environment at this area should be further investigated to prevent any potential environmental risk not considered in the study.

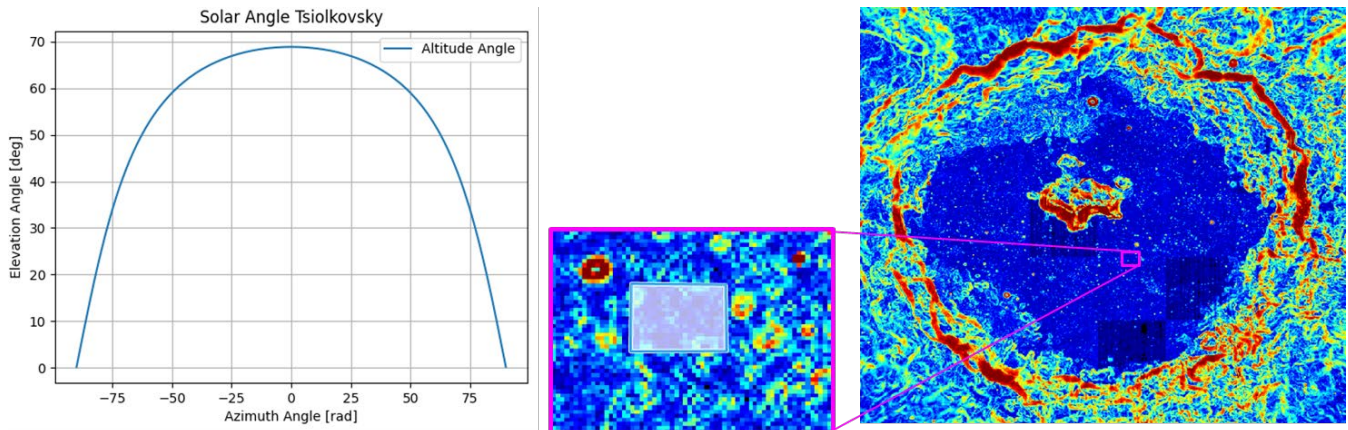


Figure 6-3: Solar illumination conditions at Tsiolkovsky crater and the current ALO deployment location.

6.3 Radiation Effects and Main Sources of Radiation Environment

In the context of ALO, the radiation environment effects were not investigated. The ALO mission had high uncertainty on many subsystems, and the limited time available in CDF study did not allow the opportunity to investigate further radiation effects. Nevertheless, the radiation environment has been characterised using EL3 environment specification and is present below.

In general, the energetic particle environment consists of geo-magnetically trapped charged particles, solar protons and galactic cosmic rays. It is the penetrating particles that pose the main problems, which include upsets to electronics, payload interference, degradation and damage to components and solar cells. The main components of the radiation environment are:

6.3.1 The Radiation Belts

These encircle the Earth and contain electrons and protons that are trapped in the geomagnetic field. An inner relatively stable belt contains mostly protons with energies up to several hundred MeVs. An outer highly dynamic belt consists primarily of energetic electrons with energies up to a few MeVs. The MEO orbit is particularly severe with respect to radiation since it is located at the heart of the outer electron belt. In this case, since the mission will quickly leave the Earth magnetosphere and never cross it again, the total effect of the trapped protons and electrons will be minimal in comparison to the other sources.

6.3.2 Solar Particle Events

Events of strongly enhanced fluxes of primarily protons originate from the Sun, usually with a duration in the order of a couple of days. These events occur randomly and mainly during periods of solar maximum (~7 years of the 11 year solar cycle). The events are also accompanied by enhanced fluxes of heavy ions. The geo-magnetic field can provide an element of shielding from these particles in equatorial zones at lower altitudes but for the same reasons as above and given the absence of such magnetosphere around the Moon over a significant part of its orbital trajectory, the mission will not benefit from any planetary shielding.

The protons contained in the constant solar wind and the enhanced solar event particles will induce displacement damage (Non-Ionising Dose) in silicon matrices such as solar cells and photodetectors, inducing in both cases a loss of performance.

6.3.3 Galactic Cosmic Rays

A continuous flux of very high energy particle radiation is received from outside the heliosphere. Although the flux is very low, it includes heavy ions capable of causing intense ionisation as they pass through matter. Although their contribution to the total dose is insignificant, they are important when analysing single event effects. The geomagnetic field can provide an element of shielding of these particles in equatorial zones at lower altitudes.

6.3.4 Transfer environment and Surface Phase

The trapped particle effects, are taken into account and proceed from the AP-8 and AE-8 models from protons and electrons, respectively taken at solar minimum and maximum. They are presented in Figure 6-4.

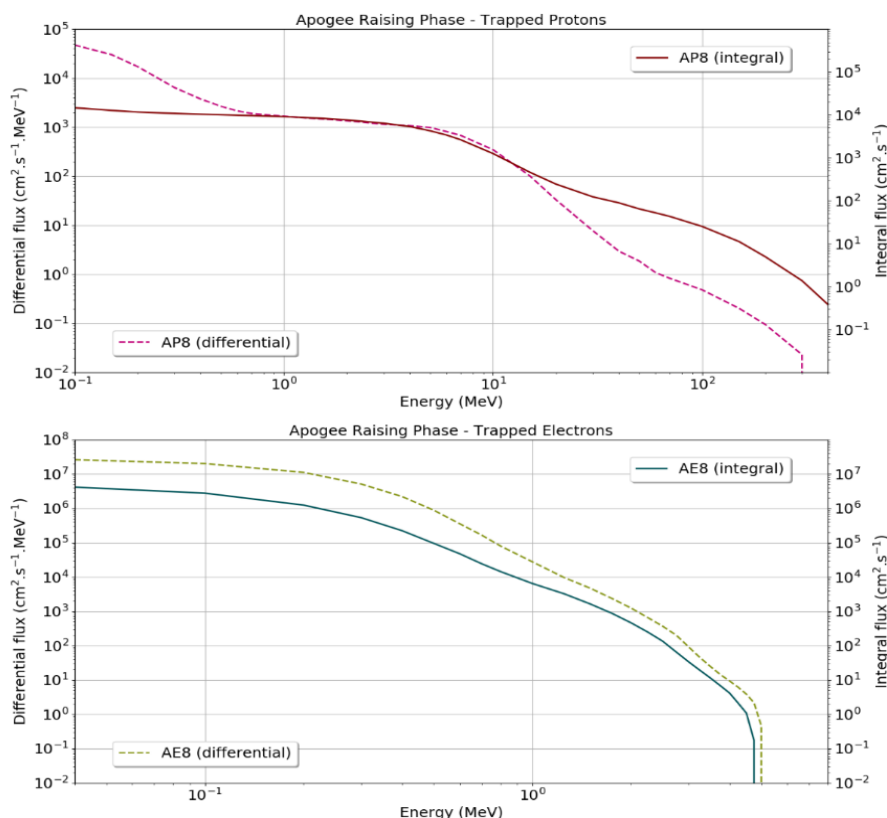


Figure 6-4: The average proton flux according to the AP8MIN model (top) and average electron flux according to the AE8MAX model (bottom) for the transfer trajectory (scaled by factor 2 E-RDM)

The cumulative radiation effects are calculated for solar protons from the ESP-PSYCHIC model (protons only with 95% confidence level) and Galactic Cosmic Rays from the ISO 15390 model (ion range Hydrogen to Uranium from the 1996 solar minimum data).

When running the ESP-PSYCHIC model, the conservative assumption that the maximum possible time will be spent during solar maximum (assuming a solar cycle of 11 years with a 4 years of minimum between each maximum) is applied. The contribution from the solar minimum period is small in comparison to the solar maximum fluence but is considered in the ESP model output. The result of this is that particle fluence increases at a lower rate from 7-11 years than over the first 7. The Solar Energetic Particles (SEP) integral mission cumulative fluence for protons ($Z=1$) are given in Figure 6-5.

Galactic Cosmic Rays fluxes from the ISO 15390 model are provided in Figure 6-6.

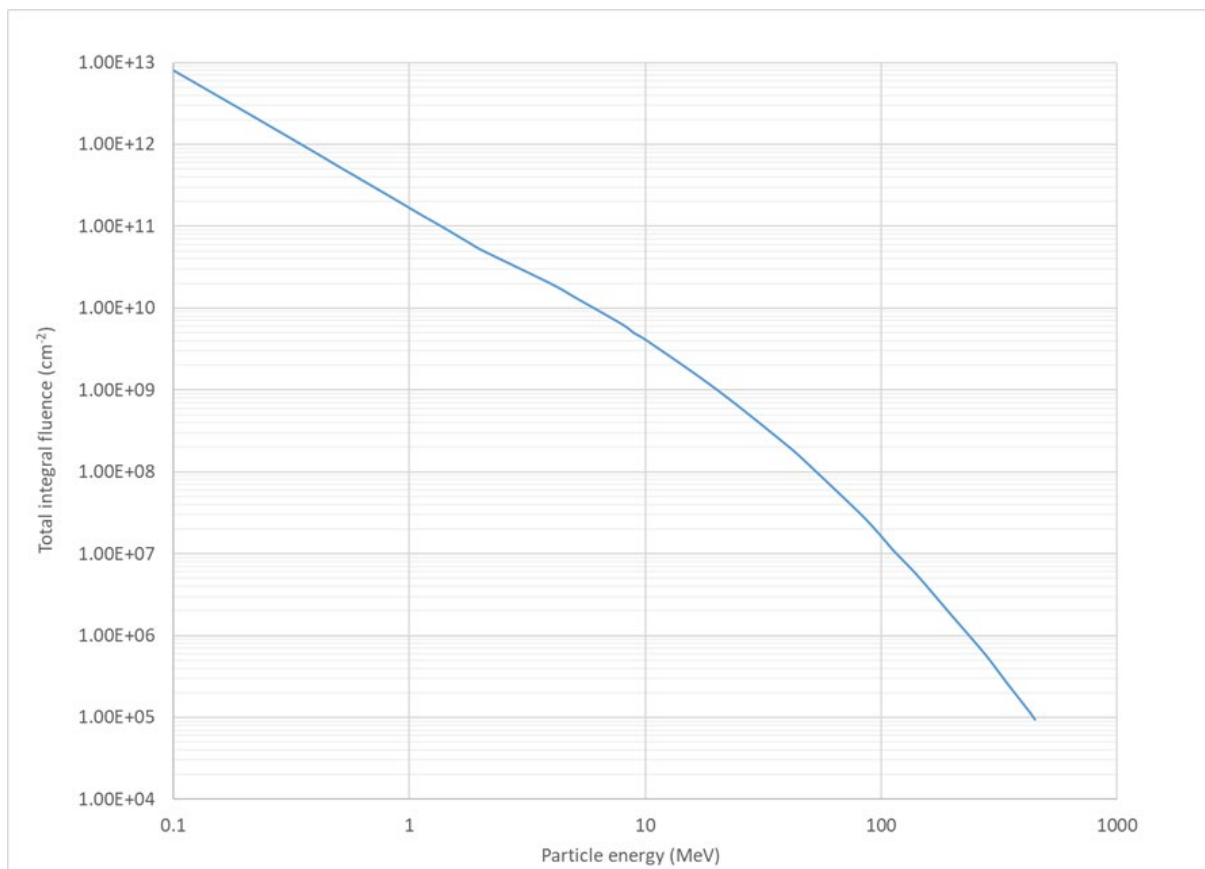


Figure 6-5: Integral mission (1 yr.) cumulative solar proton for the lunar segment.

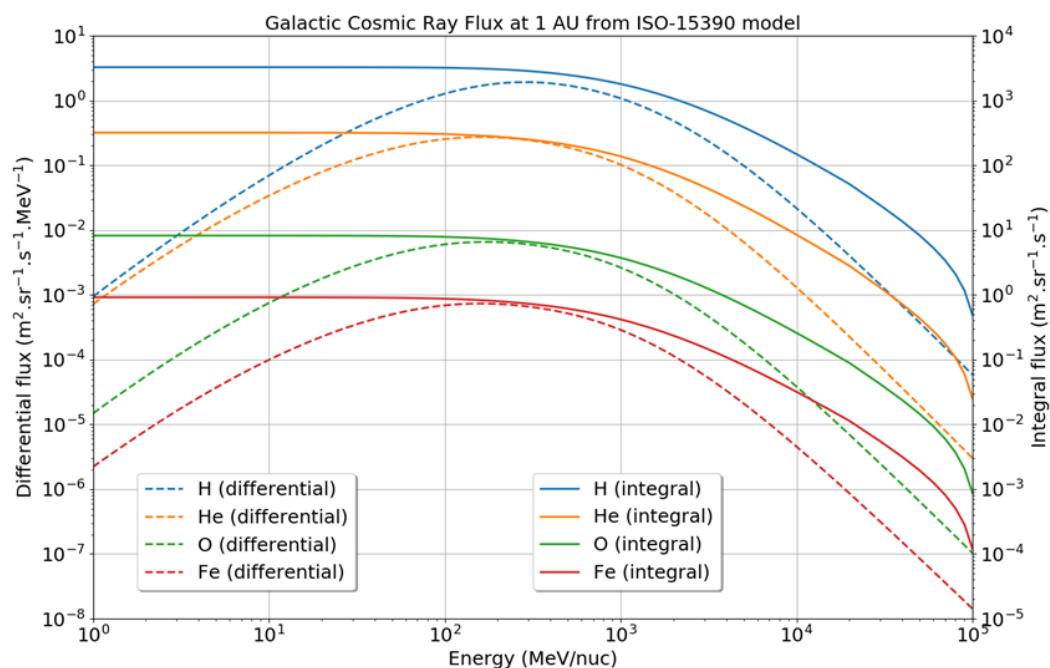


Figure 6-6: The galactic cosmic ray flux according to the ISO15390 model at 1 AU.

6.3.5 Total Ionising Dose (TID)

Figure 6-7 shows the specified Total Ionizing Dose (TID) calculated using the SHIELDOSE-2 update assuming a silicon target at the centre of an Aluminium sphere as a function of aluminium shielding thickness in units of millimetres for the Earth orbit segment and the lunar segment.

Typical Electrical, Electronic and Electromechanical (EEE) parts with about 1 krad(Si) TID sensitivity would require a shielding of about 10 mm of aluminium equivalent (without any margins).

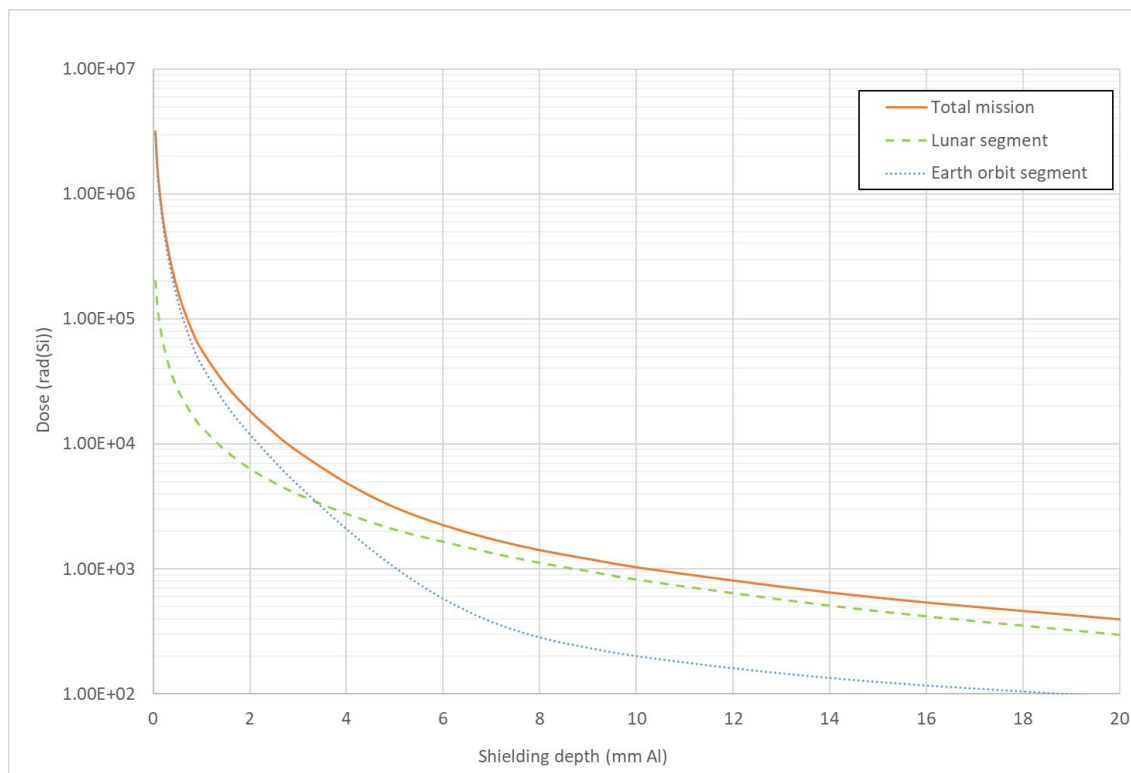


Figure 6-7: Total ionising dose for the carriers and landers during transfer

6.3.6 Magnetic anomalies

The Moon does not have a global magnetic field but there are local lunar locations that have a magnetic field. A global map of the magnetic anomalies present on the Moon is shown in Figure 6-8. Some of these regions are well-known for their peculiar shape, such as Reiner-Gamma. Reiner-Gamma and other lunar swirls remain enigmatic lunar features. Some explanations for their peculiar shape are associated to space weathering (solar wind interacts with magnetic field) or lunar dust motion (charge dust interacts with magnetic field).

The surface potential at lunar magnetic anomalies may charge to high positive potential due to ion currents. With a sufficiently strong magnetic field, solar wind electrons are deflected and do not reach the lunar surface. In comparison, ions have a sufficiently high mass to reach the surface under lunar magnetic field strength. The lunar surface charges positively due to the ion current and the photoelectron current. Since these locations are still not fully characterised, and some features remain enigmatic, it is wise to avoid these locations for ALO deployment.

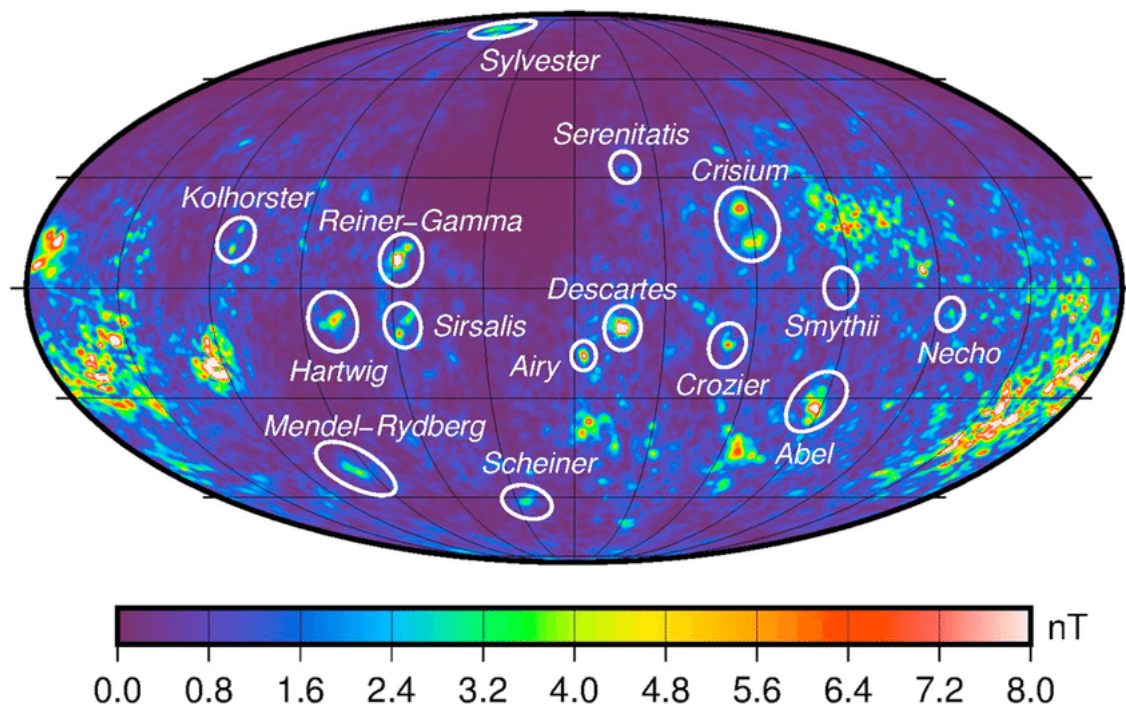


Figure 6-8: Global lunar map of magnetic anomalies and highlighting lunar swirls on the lunar near-side. The lunar southern far-side anomalies correspond to the red areas in the map edges.

In Figure 6-9, the southern farside anomalies and the two candidates landing location are highlighted. The location of Tsiolkovsky crater is far enough from the southern farside anomalies to avoid any interference that might affect ALO operations.

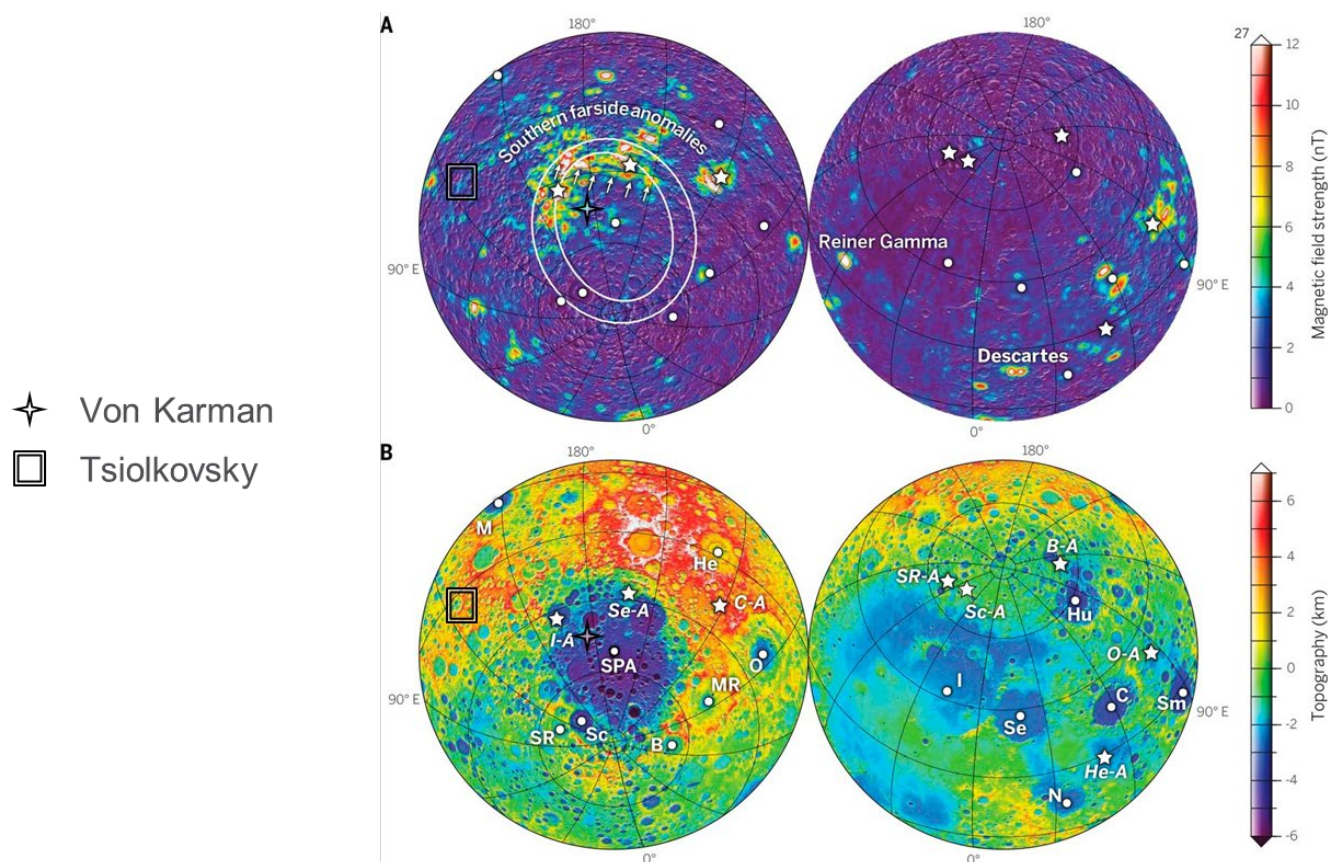


Figure 6-9: Southern far side anomalies and the location of the landing site investigated during this study. Von Karman crater is highlighted as a cross, south of the southern far side anomalies. Tsiolkovsky crater is highlighted as a square, north west of the southern far side anomalies.

6.4 Lunar dust environment

Lunar dust has proven to be one of the main environmental hazards by previous lunar missions. Dust accumulation can highly degrade power and thermal systems, which are vital for long-term missions on the lunar surface. Dust can also degrade optical systems performances and their high abrasiveness can wear sensitive mechanisms. During this CDF, the degradation of power and thermal systems by lunar dust was the main concern.

Lunar dust transport can be categorised as either natural or anthropogenic source.

6.4.1 Natural dust transport

The first phenomena is linked to micrometeoroid secondary ejecta. RD[56] estimated as an average dust flux of $10 \mu\text{g}/\text{cm}^2$ per year linked to micrometeoroid impact.

The second natural dust transport mechanism is electrostatic dust levitation. Electrostatic potential difference is generated between sunlit and shadowed areas. On the sunlit areas, photoelectrons are generated which produce a positive potential. While the shadowed areas are getting negatively charged by the solar wind electrons. The voltage difference is sufficient to break the cohesive forces and gravitational force to levitate dust.

O'Brien & Hollick RD[57] have estimated the electrostatic dust transport using the data from the Dust Detector Experiments (DDEs) from Apollo 12, 14 and 15. The DDEs are solar cells with different coverglass shielding. They separated the degradation linked to solar radiation to non-radiation degradation and estimated a $100 \mu\text{g}/\text{cm}^2$ of lunar dust per year.

Chang'E 3 measured an annual dust deposition of $21.4 \mu\text{g}/\text{cm}^2$ using a quartz crystal microbalance RD[58]. Chang'E-3 landing site is a young mare basalt region with a thin regolith layer, and this can explain partially the difference between Apollo and Chang'E-3 measurements RD[58].

	Ref.	Measurements
Meteoroid dust transport	RD[56]	$10 \frac{\mu\text{g}}{\text{cm}^2} \text{ per year}$
Electrostatic dust transport	Apollo RD[57]	$100 \frac{\mu\text{g}}{\text{cm}^2} \text{ per year}$
	Chang'E 3 RD[58]	$21 \frac{\mu\text{g}}{\text{cm}^2} \text{ per year}$

Table 6-1: Natural dust transport estimates summary

6.4.2 Anthropogenic Dust Transport

The anthropogenic dust transport is dust movement generated by human/spacecraft activities. Any motions, such as astronaut walking, rover wheels, mining activities and landing/ascent rocket exhaust, produces dust movement that can self-contaminate sensitive components.

The main concerning anthropogenic dust transport that can self-contaminate ALO is landing rocket exhaust blowing lunar dust (in the full-scale context).

The only data available linked to dust accumulation during landing is from Surveyor III. During Apollo 12, astronauts disassembled Surveyor III components and brought them back to Earth for further analysis.

Analysis of Surveyor III components measured a dust thickness from 3.6 to 8.7 μm . Presumably these values are under-estimating the dust accumulation for several reasons. In the context of ALO, the number of lander was not clarified. Due to the uncertainty on this aspect, the landing dust contamination was not included in the performance degradation. If several landers are expected to land close to each other, the dust accumulation on sensitive elements needs to be revised.

Another anthropogenic dust transport source that may increase dust accumulation is the rover motion during antenna deployment. Lunar rover wheel motion induces dust motion that was investigated during the Apollo era RD[56]. Katzan and Edwards have developed a mathematical model to estimate the dust accumulation from the site of ejection. In Figure 6-10, the dust accumulation and distance from ejection was estimated for the Lunar Rover Vehicle (LRV). The Lunar Rover Vehicle (LRV) rover wheel speed is 3.56 m/s and ejected considerable amount of dust. Wheel fences were used on the LRV to minimize dust ejection on sensitive elements.

In the context of ALO, the rover wheel speed is 0.1 m/s. Compared to LRV, the wheel speed is very low and the dust ejected by the rover should be negligible. Therefore, dust transport by

rover motion was not considered. Only a recommendation to include wheel fences was considered.

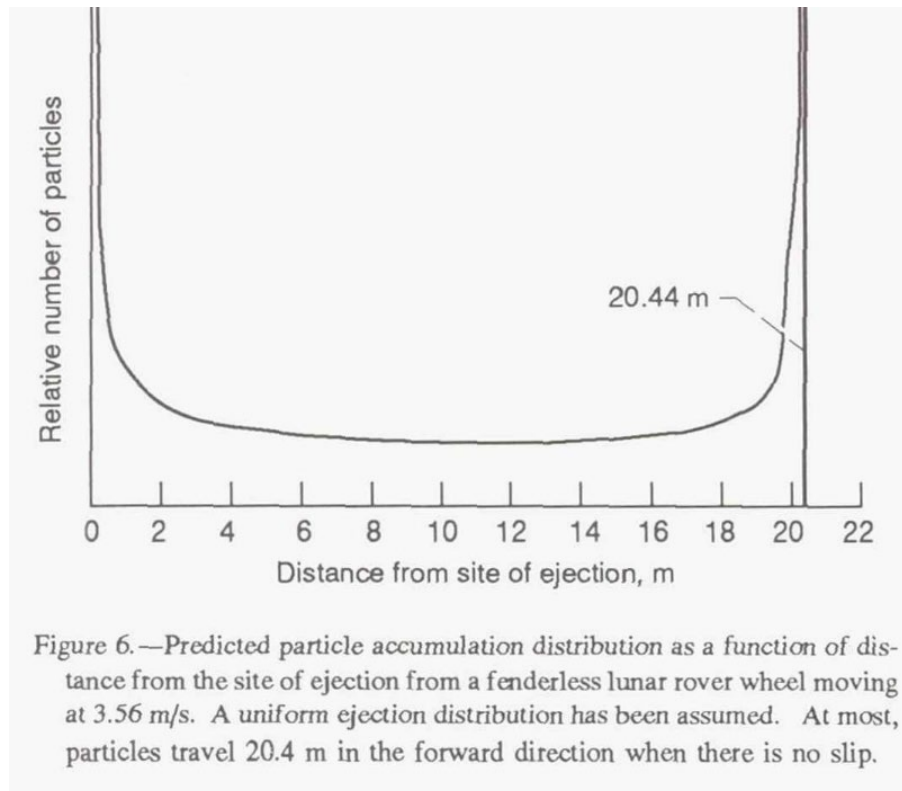


Figure 6-10: Katzan and Edwards mathematical model results for the dust induced motion by the LRV. The LRV rover wheel speed is 3.56 m/s

Let us note that a continuous rover operation during several lunar days may be a driver for further dust ejection. Even at low speed, the dust ejected may levitate due to the electrostatic environment, and could potentially levitate towards sensitive antenna elements. No studies were found to support this claim.

6.4.3 Dust Accumulation Impact On Sensitive Elements

The results of the previous section can be used to estimate the performance degradation of the sensitive elements. ALO mission is planned to operate for 4 years. Using the data presented in Table 6-1, the dust accumulated over the whole mission duration can be estimated. The results of this extrapolation is presented in Table 6-2.

The dust accumulation measurements available are at different height, latitude, local topography and lunar soil. The limited amount of data, led to the decision to present a worst-case scenario corresponding to the Apollo DDEs measurements as a baseline. While the best-case scenario corresponds to the Chang'E-3 measurements, the degradation associated to this measurement is presented to be exhaustive.

	4 years (Apollo DDEs @ $h = 100\text{ cm}$)	4 years (Chang'E-3 @ $h = 190\text{ cm}$)
Natural dust transport	$3.12\text{ }\mu\text{m}$	$0.655\text{ }\mu\text{m}$
Micrometeoroid dust transport	$0.312\text{ }\mu\text{m}$	
Total dust thickness	$3.43\text{ }\mu\text{m}$	$0.96\text{ }\mu\text{m}$
SA performance	$\sim 80\%$	$\sim 95\%$

Table 6-2: Dust accumulation estimation and performance degradation estimate based on RD[56]

The solar array performance degradation is estimated using the cubic particle curve from RD[56]. Radiator performance degradation can also be estimated using Katzan and Edwards.

7 MISSION ANALYSIS

7.1 General considerations and initial assumptions

Initial assumptions	
Ref.	Assumptions
1.	ALO will be delivered to surface by EL3 (no orbital analysis was performed during the CDF study)
2.	The considered relay satellites (Moonlight/LCNS, Gateway, Lunar Pathfinder) will be available when ALO will be deployed
3.	Tsiolkovsky crater has been identified as baseline landing option (no landing site trade-off was performed during the CDF study)

Table 7-1: Initial assumptions

7.2 Landing site

7.2.1 Baseline selection

Figure 7-1 depicts the altitude profile of the lunar farside. For ALO, two primary candidates were initially identified as landing sites:

- Tsiolkovsky crater ($20.4^{\circ} S$, $129.1^{\circ} E$, magenta in Figure 7-1). This has been selected as **baseline** for the ALO CDF study.
- Von Kármán crater ($44.8^{\circ} S$, $175.9^{\circ} E$, blue in Figure 7-1). This option is provided to show additional possibilities and open the way to future trade-offs.

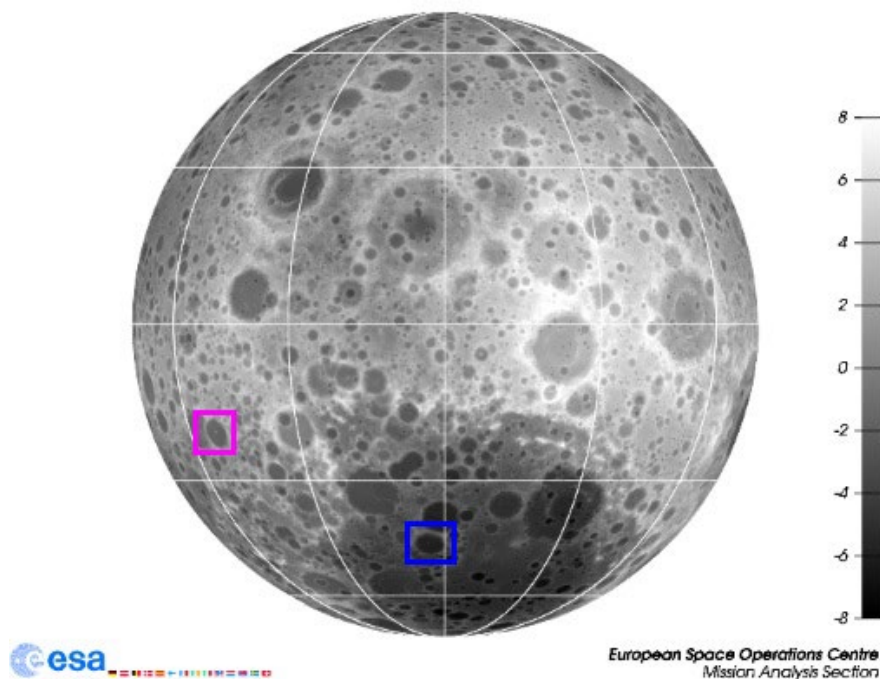


Figure 7-1: Lunar farside – topographic grayscale view (km)

Both sites show similar topographic features and solar illumination profiles, as depicted in Figure 7-2 and Figure 7-3.

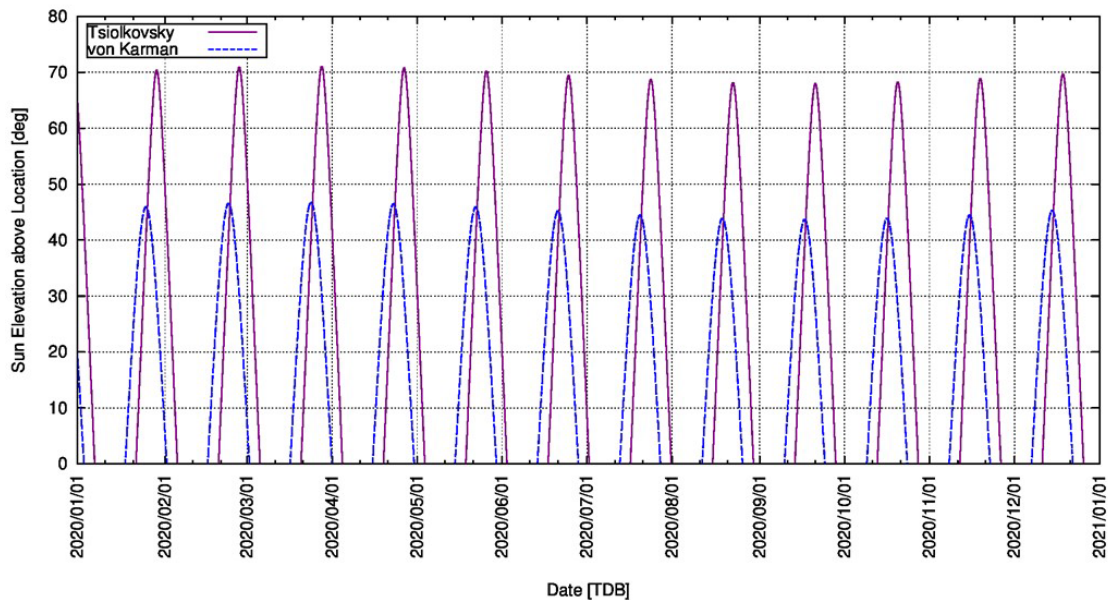


Figure 7-2: Maximum Sun elevation profile

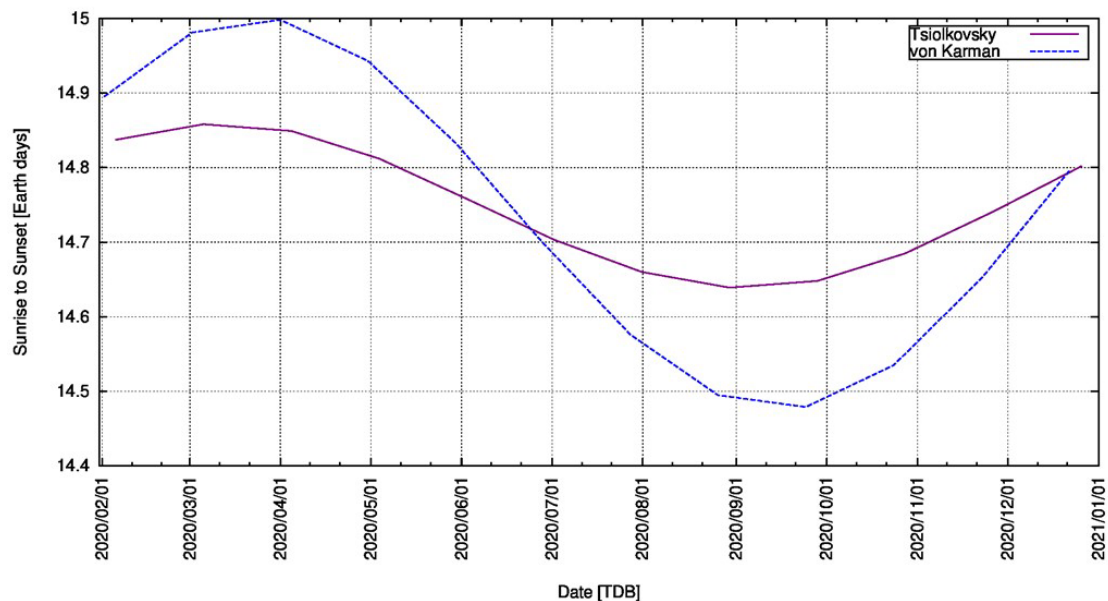


Figure 7-3: Daylight duration profile

7.2.2 Horizon mask analysis

Once the landing region is selected, the exact location inside the crater can be chosen, according to the terrain topography. In particular, it is important to analyse the horizon mask profile, as it influences the solar illumination and the access to relay satellites. The analysis performed during the CDF study shows the procedure and the tools to identify a suitable location within the selected crater.

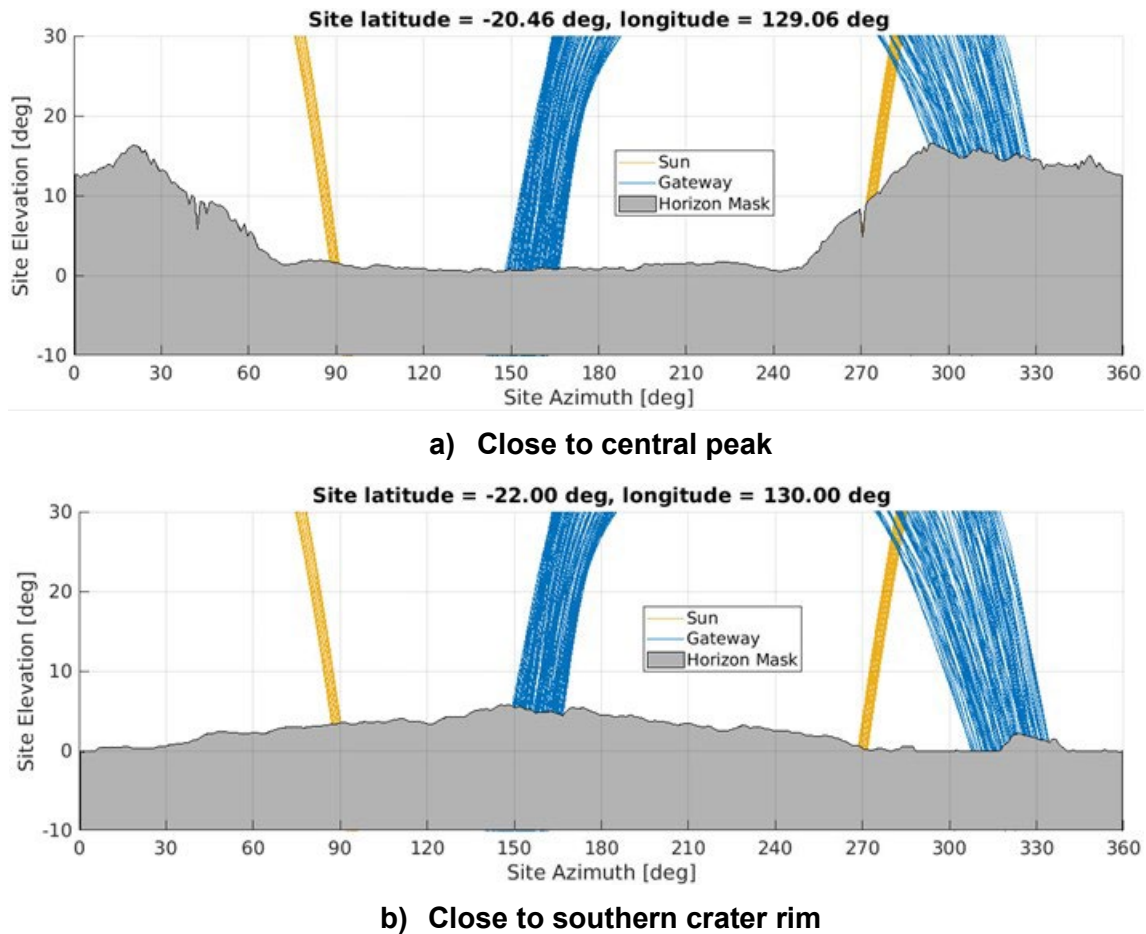


Figure 7-4: Horizon mask examples at two different locations – Tsiolkovsky crater

Figure 7-4 depicts an example of horizon mask analysis. The location in Figure 7-4 a) is close to the crater centre, and shows significant horizon masking to North and West, due to the central peak. Conversely, the location shown in Figure 7-4 b) is farther towards the South and closer to the crater rim; this yields a light masking in the South direction, whereas the rest of the azimuth span is mask-free.

Nevertheless, at a near-equatorial location the horizon masking has a minor impact on the available sunlight: the Sun rises and sets with an angular velocity of roughly 0.5 deg/hour, hence even if directly masked, the daylight duration is not significantly shortened. This is no longer valid for landing sites close to the poles, where the Sun elevation rate is much slower.

Figure 7-4 also shows the effect of the horizon mask on spacecraft visibility. Assuming the lunar Gateway as relay (further spacecraft are investigated in Section 7.3), the South masking is more critical due to the orbit aposelene location. This effect is particularly important for libration point orbits, whose geometry is nearly fixed with respect to the lunar surface.

7.2.3 Terrain slope analysis

Although not thoroughly investigated in the CDF study, the terrain slope shall be analysed, in order to identify the suitable area to correctly deploy the ALO components.

An illustrative example of such analysis is reported in Figure 7-5:

- The colour scale represents the terrain slope;
- The blue rectangle identifies a sample 1x1 km area with an average slope < 5 degrees

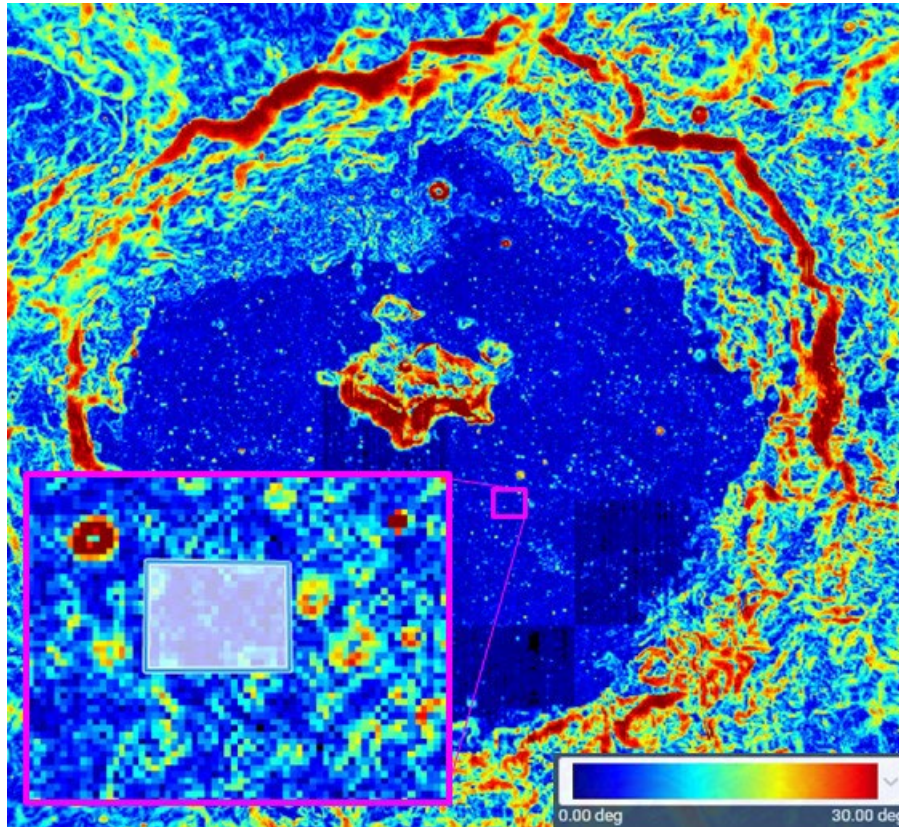


Figure 7-5: Tsiolkovsky crater slope

These type of analyses are performed with ESA tools and publicly available elevation models. Figure 7-5 is generated using QuickMap and the SLDEM2015 elevation model (RD[60], RD[61]).

Further studies may be directed to identify and trade-off different deploying areas according to surface topology and system requirements.

7.3 Communications relay analysis

Assuming the reference landing site at $22^{\circ} S, 130^{\circ} E$, analysed in Figure 7-4 b), the following spacecraft are investigated as possible relay for communications:

- Moonlight/LCNS (ESA CDF): a three-SC constellation in Elliptical Lunar Frozen Orbits (ELFO), analysed in RD[62]. The constellation was designed and optimised to provide maximum south pole coverage. Two additional spacecraft were envisaged to enhance the constellation navigation performance, with a further optimization of the baseline constellation parameters RD[63].
- Lunar Gateway (NASA): located in a Near Rectilinear Halo Orbit in cislunar space, towards Earth-Moon L2 libration point.

- Lunar Pathfinder (SSTL): commercial lunar navigation service, orbital parameters taken from reference manual RD[64].

	Lunar Gateway	LCNS 1	LCNS 2	LCNS 3	LCNS 4	LCNS 5	Lunar Pathfinder
Alt. perilune (km)	1,600	1,190					500
Alt. apolune (km)	70,000	14,800					7,500
Inclination (deg)	-	63.5					57.8
RAAN (deg)	-	0	120	240	120	240	-
AoP (deg)	-	90					90
True anomaly (deg)	-	0	164	196	245	184	-

Table 7-2: Relay assets orbital parameters

Table 7-2 reports the orbital parameters of the relay spacecraft used for the analysis. Note that the Gateway is in a non-Keplerian NRHO, hence the classical Keplerian parameters definition cannot be applied.

7.3.1 Moonlight/LCNS

The LCNS constellation was designed to optimise coverage of the Southern hemisphere. The orbital planes are separated by 120 degrees, maximising the spread in the sky. Furthermore, the true anomaly spread has been optimised to improve the overall communication and navigation performance (RD[63]).

The baseline 3-spacecraft constellation offers good coverage, with an average visibility gap of 3 hours. Augmenting LCNS to 5 spacecraft allows continuous 1-fold coverage.

The sky coverage at the selected landing site is reported in Figure 7-6. The full sky is covered, except for a region towards the South, due to the inclination of the ELFO. Additionally, Figure 7-7 depicts the angular rate, underlining the important issue of tracking from the surface. Figure 7-8 provides the angular rate of the three spacecraft as function of time, showing the regular superposition pattern and the visibility gaps.

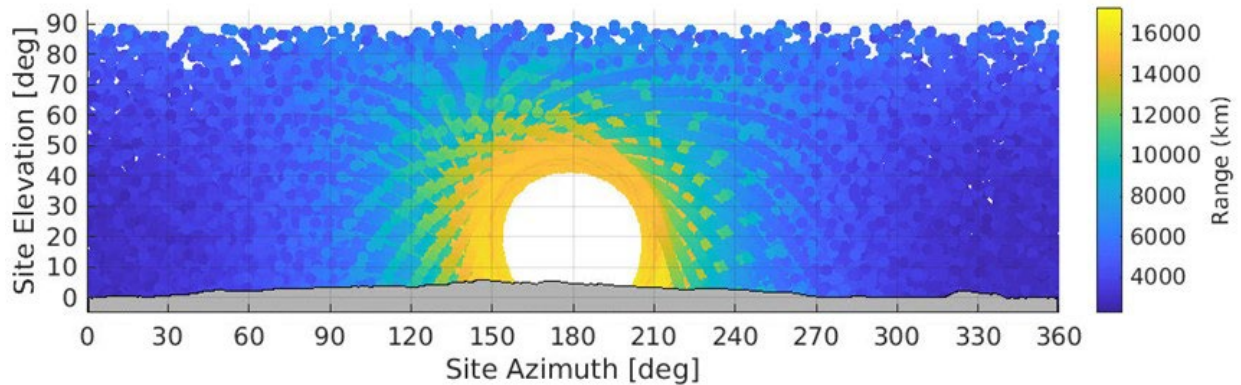


Figure 7-6: LCNS constellation sky coverage – range

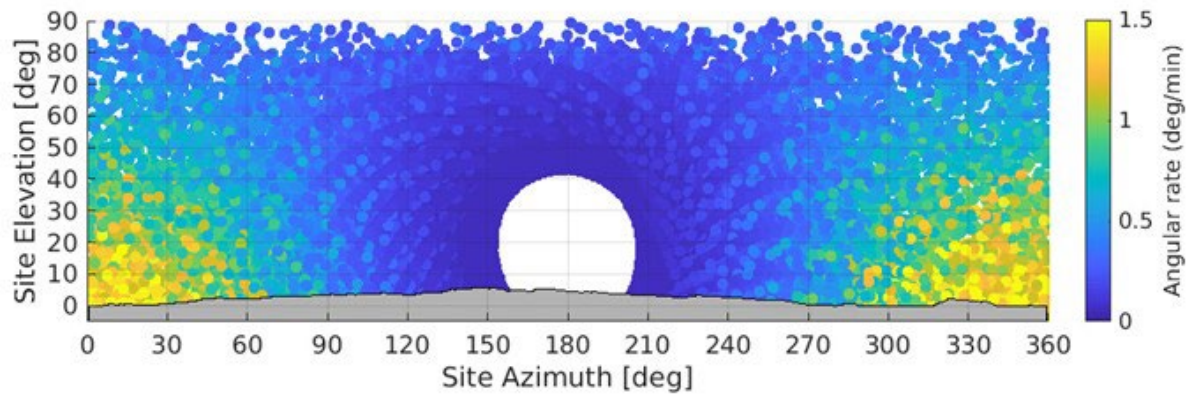


Figure 7-7: LCNS constellation sky coverage – angular rate

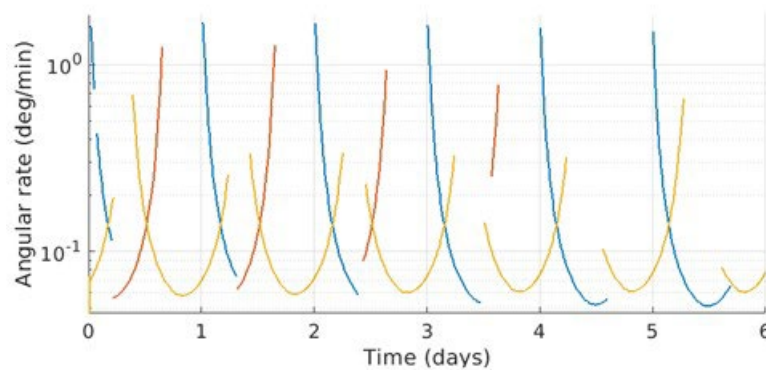


Figure 7-8: LCNS constellation – angular rates vs. time

7.3.2 Lunar Gateway

The orbit of the Gateway is a NRHO, belonging to the EML2 Halo family. This entails that its geometry remains fixed with respect to the lunar surface, thanks to the tidal lock of the Moon in its orbit. This is evident in Figure 7-9 and Figure 7-10, depicting respectively the range and the angular rate as seen from the ALO landing site. Figure 7-11 additionally shows the angular rate as function of time, noting the very fast passage over the periselene.

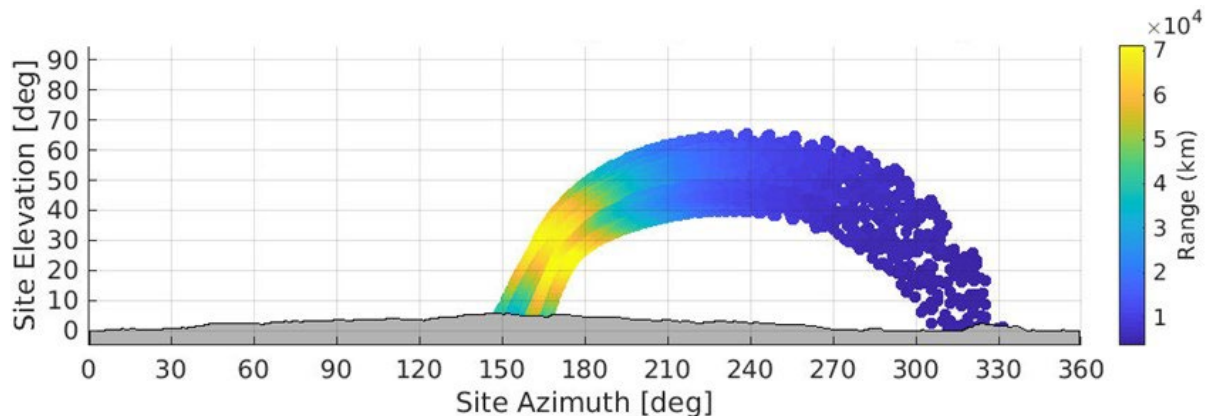


Figure 7-9: Lunar Gateway sky coverage – range

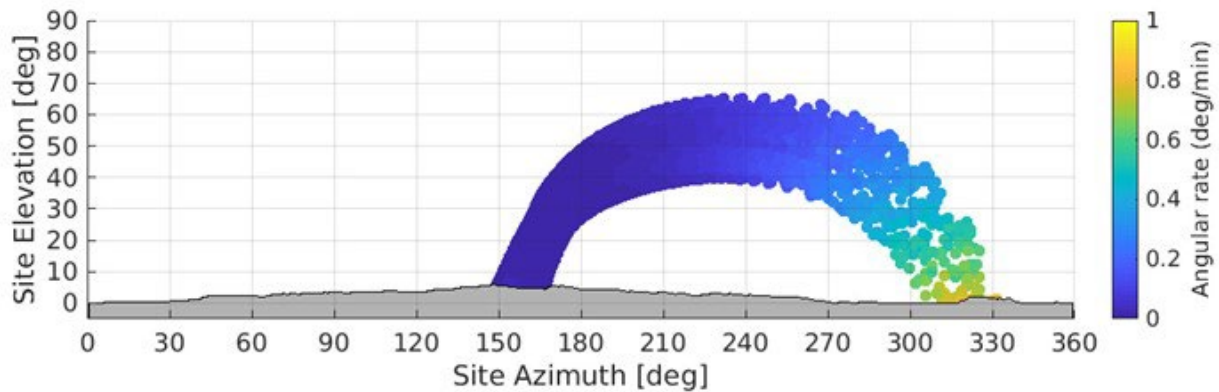


Figure 7-10: Lunar Gateway sky coverage – angular rate

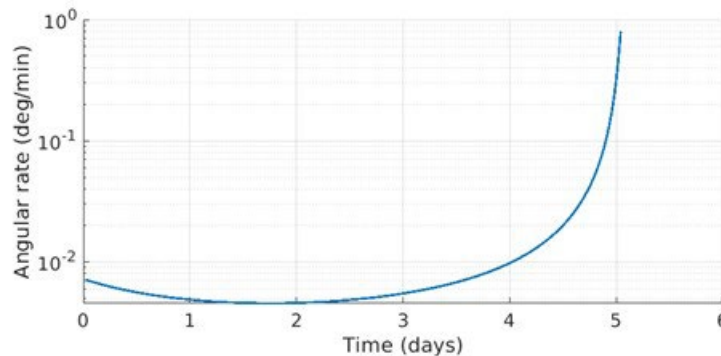


Figure 7-11: Lunar Gateway – angular rate vs. time

The NRHO has a period of 6.5 days; the majority of time is spent at the aposelene, in the South direction from the landing site.

The Gateway has a permanent direct-to-Earth link capability. With respect to the landing site, it provides long periods of coverage, with a periodic 21 hours occultation every orbit, since its periselene is above the lunar North pole.

7.3.3 Lunar Pathfinder

Lunar Pathfinder's orbit is similar to that of LCNS; both belong to the same family of ELFOs. This being a single satellite instead of a constellation, the rotation of the orbital plane entails 5 days visibility gaps every 11 days. Figure 7-12 shows the sky coverage and the range. The angular rate pattern is analogous to LCNS, hence it's possible to refer to Figure 7-7 and Figure 7-8 to draw preliminary conclusions.

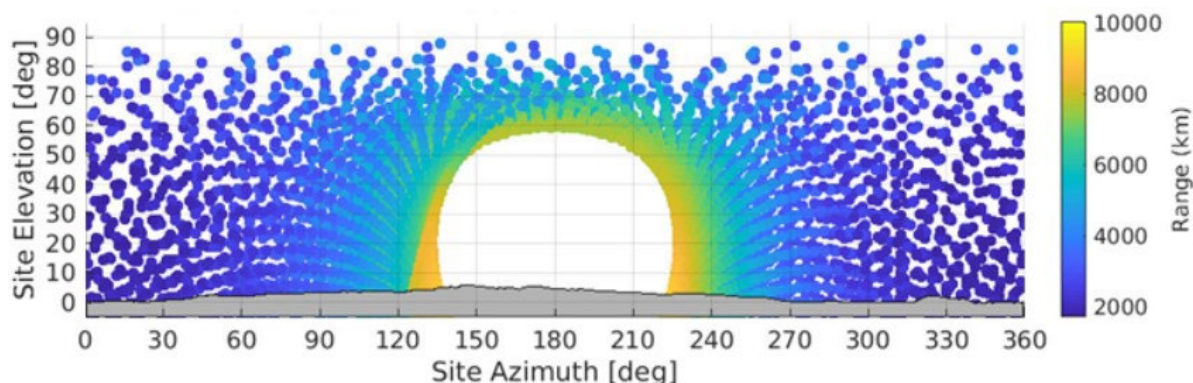


Figure 7-12: Lunar Pathfinder sky coverage – range

8 SYSTEMS

8.1 General considerations and initial assumptions

Initial assumptions	
Ref.	Assumption
1.	Near-equatorial observatory location: Tsiolkowski crater (20.4 S; 129.1 E) as baseline and Von-Karman (44.8 S; 175.9 E) as back-up. Near-equatorial is preferred to achieve maximum celestial sky-coverage.
2.	Antenna unit consists of 2x orthogonally crossed dipoles with a length of 5 m tip-to-tip.
3.	Both experiments, the Imaging Array and the Global Detection, ideally can use the same type of antenna.
4.	Imaging Array Observatory Topology: <ul style="list-style-type: none"> Regular array of antennas (smallest: 32 x 32, optimal: 128 x 128) Dense distribution e.g. antenna centres ~ 5.15 m apart from each other Placement location accuracy in the order of 0.1 to 1 m (TBC) Placement orientation accuracy in the order of 10 deg rms (TBC)
5.	Global Detection Observatory Topology: <ul style="list-style-type: none"> 1 antenna [or preferably 2 or 3 independent ones] Large distance to base station (> 1 km) & any other antennas to minimize noise interference
6.	A single antenna unit has a mass of ~ 1 to 2 kg and consumes ~ 1 to 2 W of power.
7.	The European Large Logistic Lander (EL3) as defined in RD[65] is the reference lander for this study.
8.	A single EL3 launched with an Ariane 64 EVO can achieve a payload mass capacity of 1.8 t with an available payload volume of Ø4000 x 2000 mm
9.	The Cargo Platform Element (CPE) of the EL3 is considered custom for this mission and integrated with the base station as a single element, differentiated from the rover and other payload deployable units (i.e. hubs/antennas). The custom CPE and base station are designed and procured by a single prime, responsible for the overall ALO system stack integration and verification.

Table 8-1: Initial Assumptions

8.1.1 Key drivers and challenges

Key drivers		
Ref.	Key driver	Impact
1.	Goal: Deploy and operate 1000-16000 antennas	Huge mass, power, data volume and processing needs.
2.	Observatory located on the far-side of the moon	No direct communication link to Earth. Operational and Data link constraints.
3.	Mission Lifetime of 4 years	Lunar night survival necessary. Higher radiation resistance necessary then for short term mission (~ 14 Earth days).

4.	Lunar Environment: Radiation, dust, plasma. Lunar night @ ~ -170 °C and Lunar day @ ~ 100 °C for ~ 14 Earth days (near equatorial)	Large temperature differences between day and night over long periods. Challenging lunar night survival.
5.	EL3 as dedicated lunar landing system	Mass and volume constraint.
6.	Observatory data generation rate (up to ~ 20 Mbit/s)	Mission efficiency (maximum observation time depending on relay capabilities and allowed data volume downlink)

Table 8-2: Key Drivers

8.1.2 Harness considerations

From the start of the study, the harness was considered a complex and potentially driving part of the system. For the worst case estimate, it was assumed that each antenna needs a dedicated connection. The formulas derived here define the ***harness distance*** between an element and the base station. The ***total harness length*** depends on the number of lines required between element and base station (e.g. redundant power or data lines, dedicated fibre optic cables, etc.).

8.2 Antennas to Base Station

The first formula derived estimates the total harness length required to connect the base station to n antenna units. Considering only regular arrays (square), the distance d between each antenna is equal to the tip-to-tip distance (5 m). Thus, for one antenna, the distance to the base station can be approximated as the sum of vertical and horizontal antenna spans.

Assuming the base station is at the centre of the array, four quadrants with $n_q = N_{Ant,tot}/4$ can be defined, so that each quadrant side counts $n = \sqrt{n_q} = \frac{\sqrt{N_{Ant,tot}}}{2}$ elements per side. With this, the total array harness distance can be calculated as:

$$L_{base,ant} = 4 \sum_{i=1}^n \sum_{j=1}^n [d \cdot (i + j)] = 4 \cdot d \cdot (n^2 \cdot (n + 1)) = d \cdot N_{Ant,tot} \cdot \left(\frac{\sqrt{N_{Ant,tot}}}{2} + 1 \right)$$

For the two array topologies provided this yields the following harness distances

- $N_{Ant,tot} = 32 \times 32 \rightarrow L_{base,ant} = 87,040 \text{ m}$
- $N_{Ant,tot} = 128 \times 128 \rightarrow L_{base,ant} = 5,324,800 \text{ m}$

Just for reference, considering a specific mass of about 10 kg/km for the needed harness between each antenna and the base station, this yields an extremely high total harness mass of 870.4 kg and 53,248 kg.

8.2.1 Antennas to Hubs to Base Station

Since connecting a large amount of antennas to the base station appears infeasible, a different approach was investigated. Here, the different antenna units are first bundled in a hub forming an antenna cluster and then the hub is connected to the base station.

For the connection of the antenna units to the hub, in line with the deployment strategy presented in Sections 12.2.3.3-Antenna deployment and 12.3.2-Different deployment pattern

it is assumed that a) every antenna has a dedicated connection to the hub, and b) the antennas are deployed in a continuous sequence, one after the other at a distance equal to their tip-to-tip distance, with the hub been deployed last at a distance d_{Hub} , assumed to be approximately the antennas' tip-to-tip distance too. With this, the total cluster harness distance can be calculated as:

$$L_{hub,ant} = \sum_{i=1}^{N_{Ant,hub}} [d_{Hub} + (i - 1) \cdot d] \approx d \cdot \frac{N_{Ant,hub} \cdot (N_{Ant,hub} + 1)}{2}$$

For the connection of the hubs to the base station, the same formula defined in previous section for the antennas to base station case can be reused by replacing a) number of antennas with number of hubs, and b) distance between antennas with side length of the hub cluster.

The number of hubs is $N_{Hub} = N_{Ant,tot} / N_{Ant,hub}$, thus the quadrant side counts now $n_H = \frac{\sqrt{N_{Hub}}}{2}$ elements per side. And the side length of each hub cluster is $l_{cluster} = \sqrt{N_{Ant,hub}} \cdot d$.

$$L_{base,hub} = 4 \sum_{i=1}^{n_H} \sum_{j=1}^{n_H} [l_{cluster} \cdot (i + j)] = (\sqrt{N_{Ant,hub}} \cdot d) \cdot N_{Hub} \cdot \left(\frac{\sqrt{N_{Hub}}}{2} + 1 \right)$$

For the two array topologies provided this yields the following harness distances when considering e.g. 16 antennas per hub

- $N_{Ant,hub} = 16 \rightarrow L_{hub,ant} = 680 \text{ m/hub}$
- $N_{Ant,tot} = 32 \times 32 \rightarrow N_{Hub} = 64 \rightarrow L_{base,hub} = 6,400 \text{ m}$
- $N_{Ant,tot} = 128 \times 128 \rightarrow N_{Hub} = 1024 \rightarrow L_{base,hub} = 348,160 \text{ m}$

Considering again a specific mass of about 10 kg/km for the needed harness between each antenna and its hub and about 7 kg/km between each hub and the base station, this yields a total reference harness mass of 480 kg and 9,400.32 kg.

8.2.1.1 Results comparison and conclusions

Table 8-3 shows the comparison of the total harness distance for the direct connection between antennas and the base station, as well as the connection of antennas via hubs to the base station.

Total Harness Distance	Array – 32 x 32	Array – 128 x 128
Without Hubs [m]	87,040	5,324,800
With Hubs [m]	49,920	1,044,480

Table 8-3: Comparison of Harness Distance for Array with and without Hubs

In both cases, the solution with hubs promises shorter total harness distances which leads to smaller harness masses although in both cases, in terms of feasibility, figures indicate the need for yet better solutions to the harness issue.

There is still the potential to optimise the cable sizing using series instead of parallel connection for power, or combining data and power harness, which could yield an even greater mass

advantage for the solution with hubs but still they all seem unlikely to completely avoid harness to remain a major driver.

8.2.2 Antenna concept

For system level considerations the antenna was treated as a black box. Due to the large number of antennas required by the observatory and the long length of the dipoles, a very effective way to store and deploy each antenna is necessary. Different technical implementations of this concept are possible (see chapter 11-Mechanism for antenna concepts and chapter 12-Robotics for the deployment strategy).

In the following, the system level assumptions are presented. A single antenna unit consists of two orthogonally crossed conductors (5 m tip-to-tip) and, at least, one Low-Noise Amplifier (LNA) per dipole, which provide the two raw analogue signals of each antenna. In agreement with the concepts proposed by mechanisms and the deployment strategy proposed by robotics, a stowed unit volume of 200 x 200 x 200 mm³ was assumed as representative reference to accommodate any antenna unit electronics and the stowed antenna conductors. This implies that the conductors can be compactly stored within such a volume and can be deployed out of this stowed configuration. Each unit is supplied with power from the base station (see Power chapter-section 14.2) and has a data connection to the hub or the base station depending on the observatory architecture of choice.

8.3 Observatory architecture

Different observatory architectures for a generic array of antennas were formulated based on a functional decomposition of the end-to-end science data processing flow over the following three subsystems:

- The Antenna subsystem
- The Network subsystem
- The Base Station subsystem

The list of identified functions and their descriptions, as well as their possible allocation to each of the subsystems is provided in Table 8-4.

		Possible Allocation		
Function	Description	Antenna	Network	Base Station
Signal Reception	Receiving the science signal	✓		
Signal Pre-Processing	Amplifying, filtering, etc. the received signal	✓		
Signal Digitization	Discretizing/digitizing the analog signal, so it can be transferred and processed by digital means	✓	✓	✓
Signal Transfer	Transmission/Reception of analog/digital signals to and from other subsystem	✓	✓	✓
Signal Bundling	Bundling multiple analog/digital signals into one analog/digital signal		✓	

Partial Data Reduction	Partial processing/combining/correlating data from a cluster of antennas (subset of the full array)	✓
Final Data Reduction *	Final processing/combining/correlating the data products from all clusters of antennas (full array)	✓
Processing **	Processing/combining/correlating all signals from all antennas (full array)	✓
Compression	Compressing science data for optimized storage and transfer to Earth (reducing science data volume)	✓
Communication to Earth	Sending science data via relay to Earth	✓

* Final Data Reduction only applicable if Partial Data Reduction has been performed per cluster (potentially beneficial in case of regular arrays)

** Processing only applicable if data from all antennas are processed at once, i.e. without any Partial Data Reduction

Table 8-4: Functional Decomposition of the System

Based on this decomposition and possible allocations, the following scenarios were derived:

- **Scenario 1:** Network w/o hubs, Digitization at base station, Processing at base station
 - Each antenna sends analog signals to the base station
 - All digitization and data processing is done at the base station
- **Scenario 2:** Network w/o hubs, Digitization at antenna, Processing at base station
 - The antenna analog signals are digitized at the antenna
 - Each antenna sends a digital signal to the base station
 - All data processing is done at the base station
- **Scenario 3:** Network w/ hubs, Digitization at base station, Processing at base station
 - Each antenna within a cluster sends analog signals to a hub
 - Each hub bundles all analog signals of the cluster and sends them to the base station
 - All digitization and data processing is done at the base station
- **Scenario 4:** Network w/ hubs, Digitization at hub, Processing at base station
 - Each antenna within a cluster sends analog signals to a hub
 - Each hub digitizes all analog signals of the cluster, bundles them, and sends a digital signal to the base station
 - All data processing is done at the base station
- **Scenario 5:** Network w/ hubs, Digitization at antenna, Processing at base station
 - The antenna analog signals are digitized at the antenna
 - Each antenna within a cluster sends a digital signal to a hub
 - Each hub bundles all digital signals of the cluster and sends them to the base station
 - All data processing is done at the base station
- **Scenario 6:** Network w/ hubs, Digitization at hub, Processing split between hub and base station
 - The antenna analog signals are digitized at the antenna
 - Each antenna within a cluster sends a digital signal to a hub

- Each hub pre-processes all digital signals of the cluster, produces some intermediate science data products, and sends them to the base station
- The final processing of the cluster data products is done at the base station
- **Scenario 7:** Network w/ hubs, Digitization at antenna, Processing split between hub and base station
 - Each antenna within a cluster sends analog signals to a hub
 - Each hub digitizes all analog signals of the cluster, pre-processes all digital signals to produce some intermediate science data products, and sends them to the base station
 - The final processing of all cluster data products is done at the base station

Table 2-1 summarises these scenarios.

		Network has Hubs		Digitization			Processing	
		NO	YES	@ antenna	@ hub	@ base	@ hub	@ base
Scenario	1	✓				✓		✓
	2	✓		✓				✓
	3		✓			✓		✓
	4		✓		✓			✓
	5		✓	✓				✓
	6		✓		✓		✓ (pre)	✓ (final)
	7		✓	✓			✓ (pre)	✓ (final)

Table 8-5: Main Features of each System Architecture Scenario

Pre-processing of the data at the hubs (**Scenarios 6 & 7**) promised a reduction of data rate between hub and base station although, during the study, it was deemed infeasible by the ALO topical team. **Therefore, Scenarios 6 and 7 were discarded.**

Connecting every antenna with a dedicated line to the base station (**Scenarios 1 & 2**) requires more harness than using hubs to bundle the antenna signals (see section 8.2.1.1). Furthermore, it is foreseen that each antenna would need a larger amplifier to reach the base station, which increases power needs and signal noise. The power supply harness for the antennas would also be oversized to compensate for the voltage drop, which further increases the mass. The problems with decentralised power supply are discussed in the Power chapter. **Due to these disadvantages, Scenarios 1 and 2 were also discarded.**

The remaining options (**Scenarios 3, 4 & 5**) only differ in the allocation of the digitizer. Having the digitizer at the base station (Scenario 3) requires complex multiplexing of the antennas RF signals, with increasing difficulty as the number of signals to be bundled at the hubs increases. Furthermore, it can introduce distortions into the signal. Having the digitizer at the antenna (Scenario 5) also means that some kind of controller is necessary to send the data to the hub. This hardware is more sensitive to the lunar night conditions and potentially increases the noise

at the antenna unit. Instead, grouping all sensitive hardware at hub level (Scenario 4) makes the antenna units as simple as possible while also simplifying thermal control of sensitive hardware. **Therefore, Scenarios 3 and 5 were discarded while Scenario 4 was selected as the preferred for the observatory architecture.**

8.3.1 Observatory architecture baseline

A diagram of the observatory architecture baseline (consistent with preferred Scenario 4) is shown in Figure 2-1.

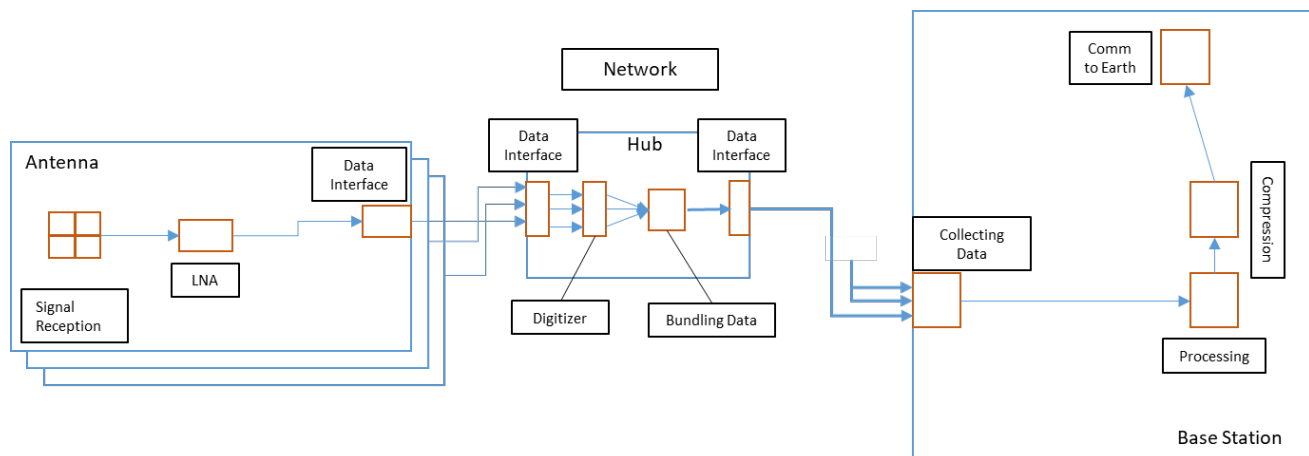


Figure 8-1: Observatory Architecture Baseline

The antenna unit is as simple as possible, which minimizes noise level and makes it less sensitive to lunar night survival. The hub collects the analogue signals from all antennas, digitizes them and bundles them. Grouping the sensitive hardware in the hub makes lunar night survival easier. Furthermore, it allows for a highly integrated hardware solution that can save power and mass. Additionally, the antenna-to-hub harness and the hub-to-base station harness can be selected optimal for the order of length they are operated in. The bundled signal is then sent to the base station for processing. After processing, the science data product may be further compressed (if possible) before it is sent to Earth via relay.

8.3.2 Observatory data resources

A summary of the scaling laws for the observatory data processing needs and data generation rates (see section 4.2) is presented in Table 8-6.

Antennas and Hubs	
Data rate per antenna unit (2 dipoles)	$B_{Antenna} = 200 \text{ Msps} \cdot 8 \text{ bit} \cdot 2 = 3600 \text{ Mbps}$
Data rate per hub	$B_{Hub} = N_{Ant-per-Hub} \cdot B_{Antenna}$

Imaging Array	
Maximum integration time	$T_{int} = 1760 \text{ s} \cdot \sqrt{16384/N_{Ant}}$
Processing power	$367 \text{ TFlops} \cdot (N_{Ant} \cdot \log_2 \sqrt{N_{Ant}}/114688)$
Processed data rate	$19.5 \text{ Mbit/s} \cdot (N_{Ant}/16384) \cdot (1760/T_{int})$
Global Detection (per Antenna)	
Maximum integration time	$T_{int} = 1 \text{ s}$
Processing power *	$2.6 \text{ GFlops} \cdot \log_2(N_{chan})/13$
Processed data rate	$1 \text{ Mbit/s} \cdot (1/T_{int})$

* Processing power required to compute the FFT of each antenna signals (assumed the same for each antenna of the Imaging Array experiment) in which $N_{chan} = 8192$ has been chosen

Table 8-6: Observatory Data Resources

8.4 Observatory description

Based on the initial assumptions for the mass and power needs of a single antenna unit (i.e. 1-2 kg, 1-2 W), the foreseen total mass and power budgets will be huge. For the smallest option (32 x 32, i.e. 1024 antennas), the antennas alone could have a mass up to 2 t and power needs up to 2 kW. While for the optimal option (128 x 128, i.e. 16384 antennas), the antennas alone could have a mass up to 33 t and power needs up to 33 kW. In addition, kilometres of harness for power and data, plus the rest of support subsystems make it obvious that a single EL3 with a payload capacity of 1.8 t would not be sufficient to bring such observatory to the lunar surface.

In order to better understand the challenges, drivers and scaling considerations for the deployment and operation of such observatory, the study was reoriented to define the “smallest reasonable observatory”, still fully representative of a larger scale one, and then identify the different design thresholds as function of the observatory size (even if only in terms of orders of magnitude given the low level of definition of most elements of the system).

8.4.1 Baseline observatory – Single EL3

From a first sizing iteration, the following system level assumptions were made for an observatory compatible with a single EL3 mission:

- One single Imaging Array cluster of 16 antennas and 1 hub, with Global Detection experiment done with some antenna(s) of the array (different operation mode)

- Wired power and data transfer between antennas and hub, and between hub and base station, plus wireless data transfer between hub and base station as demonstrator
- Central power supply with solar panels and Regenerative Fuel Cell (RFC) (see the Power chapter for more details)
- Lunar night survival with heaters and hibernation (see the Thermal chapter for more details)
- One single rover using a magazine-like concept for deployment of the antennas (after antennas are deployed, the magazine is also deployed remaining as hub of the cluster)

8.4.1.1 Baseline observatory needs

Based on the formulas presented in Section 8.3.2, the following data volumes are produced.

Imaging Array (16 Antennas)	
Integration time required per cycle	56320 s (15.64 h)
Science data rate generated	0.6 kbit/s
Science data generated per cycle	33.5 Mbit
Max. science data generated per lunar day*	720 Mbit
Global Detection (1 Antenna)	
Integration time required per cycle	1 s
Science data rate generated	1000 kbit/s
Science data generated per cycle	1 Mbit
Max. science data generated per lunar day *	1,209,600 Mbit

* For 100% observation duty cycle, which is not realistic. Desired observation duty cycle > 25% (with Imaging Array and Global Detection experiments not performed in parallel).

Table 8-7: Baseline Observatory Needs

8.4.1.2 Baseline observatory modes

The observatory modes defined to account for the required resources during each observatory operation cycle are described in Table 8-8.

Mode	Description
Standby (Day STBY)	Only necessary units active. Antennas and hubs off.
Observation (Day OBS)	Science operation. Imaging Array as sizing case (larger number of active antennas and resources needs).
Communication (Day COMMS)	Transmitting science data and mission housekeeping to Earth and receiving mission telecommands from Earth via relay.
Hibernation (Night HIB)	Hibernation for lunar night survival. All units off except for thermal control (i.e. PCDU, RFC and OBC/RTU at minimum).

Table 8-8: Baseline Observatory Modes

8.4.1.3 Baseline observatory conceptual schedule

The observatory conceptual scheduled considered for the observatory operations is described in Table 2-3.

Mode	Duration [h]	Rationale
Day STBY	35	Residual buffer.
Day OBS	288	Max. time window for science including time to charge fuel cell for lunar night survival.
Day COMMS	15	Accumulated window for Science Data and TT&C communications.
Night HIB	370	Lunar night duration including margin.
	<i>Total: 708</i>	

Table 8-9: Baseline Observatory Conceptual Schedule

At near-equatorial locations, the lunar daylight and night period have about the same duration of ~ 354 h. Local sun visibility might be shortened by lunar topology which could cause shadowing on the solar panels. Therefore, some margin must be considered at the beginning and at the end of the lunar night phase. The science operation is restricted by the power available from the solar panels to operate the full array and recharge the RFC for night survival. For a large observatory, the available communication bandwidth could be a further restriction on the available time for science operation. But for the reduced baseline observatory, the expected science data is in the order of 0.1 to 1000 kbps compared to an expected relay link capability of 25 to 43 Mbps, which is not a limitation. A placeholder of 15 h is chosen to provide enough link time to transmit all science data and TT&C. Rover operation is not considered, as deployment phase takes place before the observatory operation phase starts and the rover is assumed to require significantly less resources. Therefore, 288 h can be used for science operation (~ 40% duty cycle). The remaining time of 35 h is considered as standby buffer.

8.4.1.4 Baseline observatory budgets

An overview of the baseline observatory budgets, based on the equipment breakdown provided in section 8.4.2) is presented in Table 8-10.

#	Element	Nominal Mass [kg]	Nominal Power [W]			
			Day STBY	Day OBS	Day COMMS	Night HIB
16	Antenna	1.85	0	2.2	0	2.7
1	Network Hub	50.4	0	79	0	90
-	Network Harness	7.6	-	32	-	32
1	Base station / CPE	503.5	36.5	105.5	257.3	60.9
1	Rover	393.5	-	-	-	-
	TOTAL	984.6	36.5	251.7	257.3	226.1

Table 8-10: Baseline Observatory Budgets

For the network harness estimation, in accordance with the approach discussed in Section 8.1.2, an average harness length of 43 m per antenna is required (in particular 32 lines for data signal at 3.5 kg/km and 16 lines for power at 3.9 kg/km), plus an average harness length of 30 m per hub is required (in particular 1 line for data signal at 3.5 kg/km and 1 line for power at 3.9 kg/km). An average power loss of 2 W per antenna is considered for the complete network harness.

The rover payload consists of the antennas, the hub, and the network harness with a total aggregated nominal mass of about 90 kg.

8.4.2 List of Equipment

8.4.2.1 Antenna subsystem

Unit	#	Size [mm]	Nominal Mass [kg]	Nominal Power [W]			
				Day STBY	Day OBS	Day COMMS	Night HIB
Antenna assembly	1	200 x 200 x 200	1.000	0.0	0.0	0.0	0.0
LNA	2		0.050	0.0	0.1	0.0	0.0
RFOverFiber transmitter	2		0.200	0.0	1.0	0.0	0.0

Thermal Control	1		0.350	0.0	0.0	0.0	2.7
Total		250 x 250 x 250 *	1.85	0.0	2.2	0.0	2.7

* A volume margin (25% in all dimensions) was accounted on top of the selected reference antenna concept volume

Table 8-11: Antenna Subsystem – List of Equipment

Unit	TRL	Heritage considerations
Antenna assembly	5	TRL 8 for JUICE, TRL 5 for lunar environment
LNA	6	COTS for space, not lunar qualified. May be qualified for lunar environment on board Chinese mission Chang'e 4
RFOverFiber transmitter	3	COTS for terrestrial applications
Thermal Control	9	MLI, Heaters, Washers, White paint/SSM/OSR

Table 8-12: Antenna Subsystem – Technology Readiness

8.4.2.2 Network subsystem

8.4.2.2.1 Harness Element

Unit	#	Average Length [m]	Nominal Mass [kg]	Nominal Power [W]			
				Day STBY	Day OBS	Day COMMS	Night HIB
Antenna-to-Hub Data *	32	43	0.149	0.0	0.0	0.0	0.0
Antenna-to-Hub Power **	16	43	0.166	0.0	2.0	0.0	2.0
Hub-to-Base Data *	1	30	0.105	0.0	0.0	0.0	0.0
Hub-to-Base Power **	1	30	0.117	0.0	0.0	0.0	0.0
Total			7.6	0	32	0	32

* For data harness, a specific mass of 3.5 kg/km is assumed

** For power harness, a specific mass of 3.9 kg/km is assumed

Table 8-13: Network Subsystem – Wires – List of Equipment

8.4.2.2.2 Hub Element

Unit	#	Size [mm]	Nominal Mass [kg]	Nominal Power [W]			
				Day STBY	Day OBS	Day COMMS	Night HIB
ADC++ (double channel, TBC)	16		0.20	0.0	2.0	0.0	0.0
RFOverFiber Receiver	32		0.200	0.0	1.0	0.0	0.0
Hub Control Unit + Fiber Transceiver	1		3.000	0.0	10.0	0.0	0.0
Wireless Transceiver	1		2.50	0.0	5.0	0.0	0.0
Thermal Control	1		5.50	0.0	0.0	0.0	90.0
Structure	1		20.00	0.0	0.0	0.0	0.0
Roll for antenna wires	16		0.30	0.0	0.0	0.0	0.0
Roll for hub wires	1		0.50	0.0	0.0	0.0	0.0
Harness *	1		4.51	0.0	0.0	0.0	0.0
Total		1500 x 750 x 750	50.41	0.0	79.0	0.0	90.0

* Hub internal harness is assumed as 10% of the hub mass.

Table 8-14: Network Subsystem – Hub – List of Equipment

Unit	TRL	Heritage considerations
ADC++ (double channel, TBC)	6	COTS for space, not lunar qualified
RFOverFiber Receiver	3	COTS for terrestrial applications
Hub Control Unit + Fiber Transceiver	6	COTS for space, not lunar qualified
Wireless Transceiver	3	Terrestrial Applications
Thermal Control	3	MLI, heaters, washers, white paint/SSM/OSR: TLR 9 Louvers: TRL 3
Structure	6	Standard elements (panels, struts, etc.)
Roll for antenna wires	6	Standard elements
Roll for hub wires	6	Standard elements

Table 8-15: Network Subsystem – Technology Readiness

8.4.2.3 Base station subsystem

Unit	#	Size [mm]	Nominal Mass [kg]	Nominal Power [W]			
				Day STBY	Day OBS	Day COMMS	Night HIB
Science Data Processing Unit	1	100 x 100 x 100	1.00	0.0	20.0	0.0	0.0
Data Storage	1	230 x 200 x 150	12.00	0.0	44.0	44.0	0.0
OBC&RTU	1	200 x 200 x 200	3.00	6.5	6.5	6.5	6.5
S-band Transponder	2	290 x 110 x 197	3.74	0.0	0.0	0.0	0.0
S-band Amplifier	2	340 x 88 x 70	1.38	0.0	0.0	0.0	0.0
S-band RFDN	1	N/A	3.60	0.0	0.0	0.0	0.0
LGA (S)	2	100 x 100 x 285	0.28	0.0	0.0	0.0	0.0
K-band Transponder	2	215 x 140 x 175	3.30	0.0	0.0	33.4	0.0
K-band Amplifier	2	340 x 88 x 70	1.10	0.0	0.0	45.0	0.0
K-band RFDN	1	N/A	2.40	0.0	0.0	0.0	0.0
HGA (K)	1	Ø 550 x 140	1.47	0.0	0.0	0.0	0.0
HGA APM	1	450 x 450 x 500	12.00	0.0	0.0	0.0	0.0
HGA APM EU	1	100 x 100 x 50	4.00	0.0	0.0	20.0	0.0
Wireless Transceiver	1	6.5 x 6.5	2.50	0.0	5.0	0.0	0.0
Rover deployment system (TBC)	1	L x W x H	0.00	0.0	0.0	0.0	0.0
Hubs deployment system (TBC)	1	L x W x H	0.00	0.0	0.0	0.0	0.0
Thermal Control	1	TBD	41.20	0.0	0.0	0.0	24.4
Solar Panels	1	80.91	60.68	0.0	0.0	0.0	0.0
Battery	1	260 x 240 x 270	15.00	0.0	0.0	0.0	0.0
PCDU	1	450 x 240 x 160	8.08	30.0	30.0	30.0	30.0
RFC	1	L x W x H	76.65	0.0	0.0	0.0	0.0
Structure	1	N/A	190.00	0.0	0.0	0.0	0.0
Harness	1	N/A	50.35	0.0	0.0	0.0	0.0
Total			503.53	36.5	105.5	257.3	60.9

* Base station internal harness is assumed as 10% of the overall mass.

Table 8-16: Base Station Subsystem – List of Equipment

Unit	TRL	Heritage considerations
Science Data Processing Unit	6	Satellites by SPIRE (flying on LEO)
Data Storage	3	Lunar Gateway
OBC&RTU	6	MASCOT-2
S-band Transponder	9	
S-band Amplifier	9	Earth Obs Missions (Thales Alenia Spain)
S-band RFDN	9	
LGA (S)	9	
K-band Transponder	6	TRL 9 for Tx at the end of this year TRL 6 due to Rx chain
K-band Amplifier	9	
K-band RFDN	9	
HGA (K)	9	
HGA APM	5	Heritage with TRL 9 exists but not for lunar environment, e.g. KARMA7-FG from KDA; additional mass margin added for orbital loads and dust protection
HGA APM EU	6	Elektra SG
Wireless Transceiver	3	Terrestrial Applications
Rover deployment system (TBC)	TBD	
Hubs deployment system (TBC)	TBD	
Thermal Control	3	MLI, heaters, washers, White paint/ssm/osr, heat pipes: TRL 9 Possibly loop heat pipes: TRL 5 IF RHU needed: TRL 4 Louvers: TRL 3
Solar Panels	4	
Battery	6	
PCDU	3	
RFC	3	
Structure	6	Standard elements (panels, struts, etc.) (Heritage from previous EL3 mission?)

Table 8-17: Base Station Subsystem – Technology Readiness

8.5 Considerations for scalability

This section presents and discusses the system budgets of different scaled arrays based on the extrapolation of the baseline system presented in Section 8.4.1. Given that not all design assumptions can be directly extrapolated, these results shall be considered in terms of orders of magnitude and not as precise results of additional design iterations.

8.5.1 General considerations and known limitations

Volume available and required for accommodation of units has not been assessed in scaled missions. Therefore, while mass-wise a certain array might be compatible with a given number of EL3s, accommodation feasibility has not been confirmed for such system in that number of EL3s.

The mass of the power subsystem is scaled with the power demand, although the baseline solution (solar panels plus RFC) is not suitable for large arrays with demands above ~ 1 kW during lunar night.

Similarly to the volume, the thermal control of the base station has not been assessed in scaled missions since geometric impact cannot be directly extrapolated.

The potential need or benefits of using a larger number of rovers has not been assessed in scaled missions (maintained at 1 for all cases). This is expected to be sufficient for small arrays but not likely for large arrays if deployment time wants to be kept to a reasonable minimum.

The harness length is approximated (as discussed in section 8.1.2) only in orders of magnitude, while the thresholds –assuming feasibility- to implement some wireless solutions could not be established.

The number of antennas per hub is fixed at 16 based on the selected reference antenna unit concept (see Section 11.2.1) and the observatory deployment strategy (see Sections 12.2.3.3 and 12.3.2), but larger arrays would require more efficient and compact stowed configurations with likely larger number of antennas per hub.

8.5.1.1 Scaling law for data budgets

Table 8-18 shows the evolution of the processing power needs and data generation budgets, derived from the formulas presented in 8.3.2, as the observatory array grows in size.

Array Size	Comp. Power [GFlops]	Data Rate [kbit/s]	Data per Cycle [Mb]	Data per LDay [Mb]
4 x 4 = 16	102	0.6	34	720
8 x 8 = 64	614	5	130	5800
16 x 16 = 256	3,277	40	540	46,000
32 x 32 = 1024	16,384	300	2,200	370,00
64 x 64 = 4096	78,643	2,400	8,600	3,000,000
128 x 128 = 16384	367,000	19,500	34,300	23,500,000
Global Detection: 1x Antenna	2.6	1000	1	1,209,600

Table 8-18: Data Budgets Scaling with Array Size

The comparison of the different array sizes with the Global Detection antenna shows that the Imaging Array is the main driver for computing power. But for data generation, the Global Detection experiment is the driver, at least when comparing to small and medium size arrays, while for full scale arrays it becomes less of a driver.

8.5.1.2 Scaling law for mass budget

Table 8-19 shows the evolution of the mass budget, as the observatory array grows in size. The observatory mass always includes the rover mass of 393.5 kg.

Array Size	Antennas Mass [t]	Hubs Mass [t]	Harness Mass [t]	Base Station Mass [t]	Observatory Mass [t]
4 x 4 = 16	0.03	0.05	0.01	0.50	0.98
8 x 8 = 64	0.12	0.20	0.03	0.69	1.43
16 x 16 = 256	0.5	0.8	0.1	1.4	3.2
32 x 32 = 1024	1.9	3.2	0.5	4.5	10.5
64 x 64 = 4096	7.6	12.9	2.2	16.6	39.7
128 x 128 = 16384	30.3	51.6	10.2	65.4	157.8

Table 8-19: Mass Budgets Scaling with Array Size

For easier comparison of the relative growth, Table 8-20 shows each mass contribution to the overall observatory excluding the rover.

Array Size	Antennas Share [%]	Hubs Share [%]	Harness Share [%]	Base Station Share [%]
4 x 4 = 16	5.01	8.53	1.29	85.17
8 x 8 = 64	11.36	19.35	2.96	66.33
16 x 16 = 256	16.61	28.28	4.41	50.71
32 x 32 = 1024	18.72	31.89	5.16	44.23
64 x 64 = 4096	19.26	32.80	5.69	42.25
128 x 128 = 16384	19.25	32.78	6.46	41.51

Table 8-20: Mass Shares Scaling with Array Size excl. Rover

For small arrays, the base station is the dominant factor of the total mass budget. For larger arrays, the base station remains an important driver, but antenna and hub mass becomes much more relevant. The harness, although it is -in absolute terms- a significant contributor for large arrays, has the smallest relative contribution to the overall mass budget.

8.5.1.3 Scaling law for power budget

Table 8-21 shows the evolution of the power budget, as the observatory array grows in size.

Array Size	Day STBY [kW]	Day OBS [kW]	Day COMMS [kW]	Night HIB [kW]
4 x 4 = 16	0.036	0.25	0.260	0.23
8 x 8 = 64	0.036	0.7	0.260	0.7
16 x 16 = 256	0.036	2.6	0.260	2.7
32 x 32 = 1024	0.036	10	0.260	11
64 x 64 = 4096	0.036	42	0.260	42
128 x 128 = 16384	0.036	170	0.260	170

Table 8-21: Scaled Observatory Power Budget

The power consumption during standby and communications corresponds exclusively to the base station and therefore it is independent of the number of antennas. For communications, the same configuration and operational approach is considered in all modes, i.e. the only difference would be the time required to transmit the increasing amount of science data, which would eventually impact the observation duty cycle and the mission efficiency. Finally, it is not casual that the power demand during observation and during hibernation are of the same order of magnitude. Due to the similar operational and non-operational temperatures of most units, the thermal control power is of the same order magnitude as the power dissipated during nominal operation. This underlines the challenge of ensuring units survival during night when solar power is not available.

8.5.1.4 Scaling law summary and conclusions

Table 2-4 presents a summary of all budgets and -as reference- a simple estimation, based on the overall observatory mass, of the potentially required number of EL3 missions.

Array Size	Mass [t]	Max. Power [kW]	Comp. Power [Mflops]	Data Rate [kbit/s]	Number of EL3s
4 x 4 = 16	0.98	0.25	102	0.6	1
8 x 8 = 64	1.43	0.7	614	5	~ 1
16 x 16 = 256	3.2	2.7	3,277	40	~ 2 – 3
32 x 32 = 1024	10.5	11	16,384	300	~ 7
64 x 64 = 4096	39.7	42	78,643	2,400	~ 25
128 x 128 = 16384	157.8	170	367,000	19,500	~ 90

Table 8-22: Summary of Observatory Budgets Scaling with Array Size

Considering, that these numbers are nominal values without system margins and limited redundancy (e.g. no redundancy for harness), the baseline observatory (4 x 4) is likely the largest array that can be delivered by a single EL3 without any significant improvement of the assumptions considered for this study. Therefore, it is well suited as a precursor mission to demonstrate feasibility of instruments and the observatory architecture.

For the slightly larger case of 8 x 8, in addition to the potential accommodation feasibility issues, the available capacity of 1.8 t per EL3 might be quickly reached once all margins and redundancy requirements are considered. For even larger arrays, multiple EL3s are required. Since all data must be delivered to and processed at a single base station, this requires different dedicated EL3s designs (one as base station, the others just providing additional antenna and hubs to be deployed and connected to the common base station). These alternative mission concepts were not assessed in this study.

This Page Intentionally Blank

9 DATA HANDLING

The following chapter describes Data-Handling Subsystem (DHS) of Astrophysical Lunar Observatory (ALO).

9.1 General considerations and initial assumptions

Table 9-1 presents assumptions toward DHS.

Initial assumptions	
Ref.	Assumption
1.	All the presented hardware solutions are based on existing developments/state-of-art. In 5-10 year perspective the performance of subsystems will improve - this is not considered for baseline design.
2.	In terms of radiation properties, both rad-tolerant and rad-hard solutions should be considered, depending on sub-system criticality and redundancies (i.e. On-Board Computer shall be rad-hard since it is a critical part of data-handling)
3.	Mass Memory will be sized on the assumption that at least 1-year storage is needed.
4.	It is assumed that from the DHS point of view the observatory will contain the following building blocks: <ul style="list-style-type: none"> • On-Board Computer controlling the instrument. • Payload Processing Unit for scientific data processing. • Mass Memory for storage of scientific data. • HUB Electronics together with Transceivers and related electronics used to transfer data (both analogue and digital) from Antenna via HUB to Base Station.

Table 9-1: Initial assumptions

9.1.1 Key drivers and challenges

The key drivers considered in the design of ALO are presented in Table 9-2. They are based on selected scenario of operation (so called Scenario 4), and associated scaling (i.e. number of antennas) assumed for this study.

Key drivers		
Ref.	Key driver	Impact
1.	DHS shall be able to store 720Mb of science data per day.	Relatively big Mass Memory needs to be considered. (i.e. 256Gb for one-year storage)
2.	DHS shall provide 102 GFLOPS of computational power.	Computational power needed for processing of scientific data will require state-of-art processing capabilities suitable for space environment.

3.	DHS shall provide 3200 Gbps of throughput from each antenna to processing unit.	In order to meet those requirements, data from antenna to base station (both analogue and digital) will have to use fibre optics.
4.	Analogue signal from 16 antennas (in two axis) needs to be transferred to Hub for potentially long distance.	Copper-based cables are not considered due to size and possible introduction of noise. RF-over-Fibre is considered.
5.	Digitalization of analogue signal is performed in the Hub.	Hub will have to include sufficient “intelligence” to digitalize the signal and transfer it via high-speed digital link.
6.	Base Station gathers the data, processes them and stores in Mass Memory for downlink.	Base Station will include Mass Memory and high performance Payload Processing Unit.

Table 9-2: Key drivers

9.2 Baseline Description

Description of the proposed solution is based on selection of operational scenario of ALO (Scenario 4). The concept is presented in Figure 9-1.

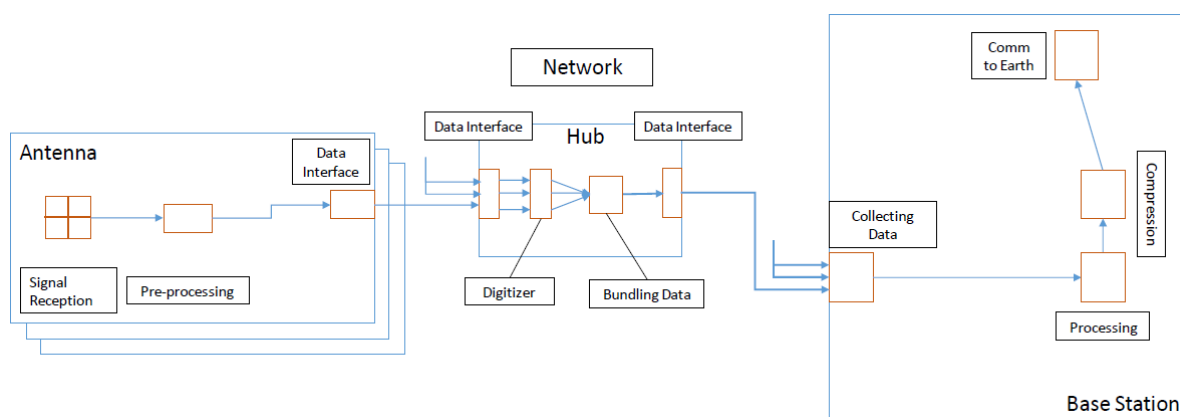


Figure 9-1: Scenario 4 being the baseline for DHS design

The hardware solution proposed below for the DHS design is based on existing technologies. 5-10 year perspective will only improve performance characteristics of subsystems (i.e. bigger mass memories will be available, more efficient solutions for science data processing will become available etc.).

9.2.1 On-Board Computer

The On-Board Computer (OBC) will be used to control the instrument, collect housekeeping data, parse telecommands etc. The proposed compact design is based on the MASCOT-2 design RD[67], including:

- Processor board with LEON3FT, GR712 (fully redundant)
- I/O module with mass memory and Remote Terminal Unit (RTU), 2GB BOL storage, 32 + 32 interfaces for thermal/separation sensors (fully redundant)

- CAN network for platform (redundant)
- Set of interfaces for communicating (RS422/SpW etc...)

The estimated total mass would be below 3 kg and the assumed total power consumption would be below 6.5 W.

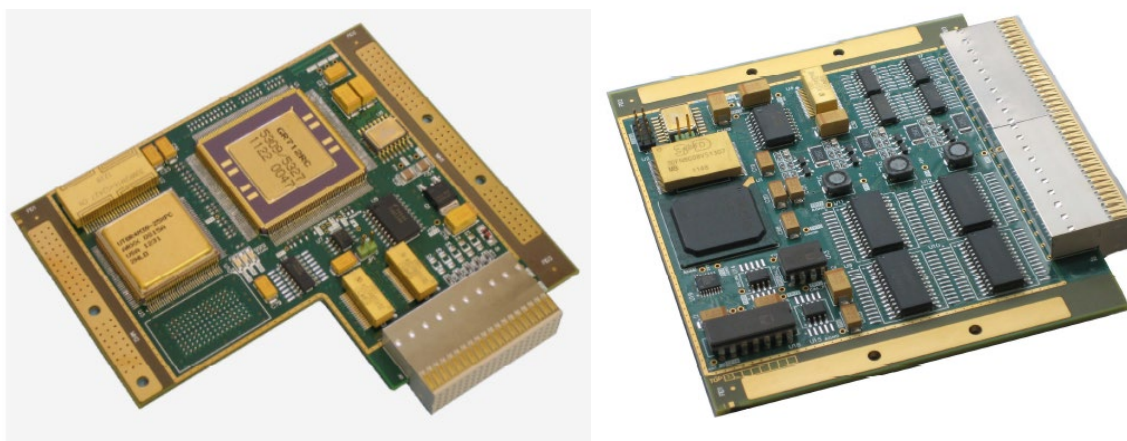


Figure 9-2: Picture of MASCOT-2 Boards

9.2.2 Payload Processing Unit

Payload Processing of the scientific data will be the key aspect of DHS. It will allow generation of scientific products from analogue data coming from Antennas.

In the current scaled configuration (16 Antennas), ~100 GFLOPS of processing power is needed. Based on available solutions (as per Figure 9-4), Tegra 2 chip from NVIDIA could be considered for this application. It is a Commercial Of The Shelf (COTS) high-performance processor (Graphics Processing Unit) already flying on commercial satellites.

The proposed solution would provide 750GFLOPS of processing power, consume 20W, weight 1kg and would fit into 10x10x10 cm box.

9.2.3 Mass Memory

Mass Memory will be used to store scientific data until it can be downloaded to the Ground Station. It is assumed that 720 Mb of data is produced per day (giving roughly 256 Gb of data per year).

The proposed baseline solution is based on High Capacity Mass Memory for Lunar Gateway project, where environmental requirements for the hardware are similar. It will provide 5TBytes of storage (EOL), will consume 44W and weight 12kg.

9.2.4 HUB Electronics and Data Transfer hardware

Transfer of data from Antenna to Base Station, as per Scenario 4, would be distinguished between analogue signal and digital data.

- In order to minimize the noise, Analogue signal will be transferred from Antenna to HUB with RF-over-Fibre. Such solutions are available (also for military applications). The baseline design is based on Transmitters/Receivers from Glenair RD[68].
- HUB electronics will collect analogue signal, digitalize it and send it with digital link to Base Station. Considering that 3200Gbps of bandwidth is needed per one antenna, digital transmission on fibre optics is considered. Such a solutions exist, also for space market. Current design is based on solutions from Smith Interconnect RD[69].

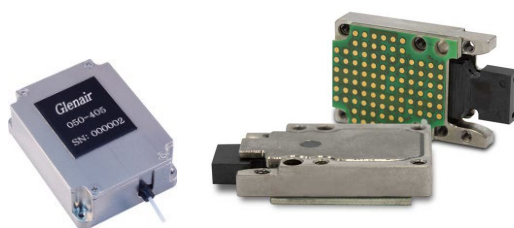


Figure 9-3: Example of RF-Over-Fibre transmitter/receiver (on the Left) and example of digital fibre transceiver proving up to 120Gbps of bandwidth (on the Right)

On top of that, HUB will have to include “intelligence” capable of collecting the data from ADCs and sending it via digital link to the Base Station. For the purpose of this study, FPGA based solution is assumed to be enough to perform this task. Budgets are scaled on a design based on Xilinx Ultrascale KU60 FPGA.

9.2.5 List of Equipment

Unit	#	Size [mm]	Nominal Mass [kg]	Power Consumption [W]			
				Day STBY	Day OBS	Day COMMS	Night HIB
On-Board Computer	1	200x200x200	3	6.5	6.5	6.5	6.5
Mass Memory	1	230x200x150	12	0	44	44	0
Science Data Processing Unit	1	100x100x100	1	0	20	0	0
HUB Electronics	1	TBD	4	0	10	0	0
ADCs	16	TBD	0.2	0	2	0	0
RF-Over-Fibre	32	TBD	0.2	0	1	0	0

Table 9-3: List of Equipment

Unit	TRL	Heritage considerations
On-Board Computer	6	MASCOT-2 Heritage might require requalification.
Mass Memory	3	Mass Memory being developed for Lunar Gateway.

Unit	TRL	Heritage considerations
Science Data Processing Unit	6	Flying on SPIRE satellite (LEO), might require requalification.
HUB Electronics	6	COTS for space available might require qualification for Moon environment.
ADCs	6	COTS for space available might require requalification for Moon environment.
RF-Over-Fibre	3	COTS available, requires qualification for Moon environment.

Table 9-4: Technology Readiness

9.3 Trade-Offs and alternative options

From the DHS point of view, the following alternatives/trade-offs were considered:

- On-Board Computer – no alternatives were considered in this study as this subsystem is not considered to be technologically challenging
- Payload Processing Unit – although the baseline solution is based on Tegra 2 chip, other single chip solutions can be presented

Name	Vendor	Device class	Qual.	Process node	# of cores	Max Frequency (MHz)	Peak Performance	Power (W)
Keystone II	TI	DSP SoC	COTS	28 nm	8 (DSP)	1,250 (DSP)	198.4 GFLOPS	21.69
Myriad 2	Intel	VPU SoC	COTS	28 nm	12 (DSP)	600 (DSP)	1 TOPS (DSPs)	1
Myriad X	Intel	VPU SoC	COTS	16 nm	16 (DSP)	700 (DSP)	4 TOPS (total), 1 TOPS (NPU)	<2
Tegra X1	NVIDIA	GPU SoC	COTS	20 nm	256 (GPU)	1,000 (GPU)	512 GFLOPS	15
Tegra X2	NVIDIA	GPU SoC	COTS	16 nm	256 (GPU)	1,300 (GPU)	750 GFLOPS	15
Xavier	NVIDIA	GPU SoC	COTS	12 nm	384 (GPU)	1,377 (GPU)	21 TOPS (total)	15
Steppe Eagle	AMD	GPU SoC	COTS	28 nm	4 (CPU)	2,000 (CPU)	87 GFLOPS	7-25
V1605B	AMD	GPU SoC	COTS	14 nm	4 (CPU)	3,600 (CPU)	3.6 TFLOPS	12-25
V2718	AMD	GPU SoC	COTS	7 nm	8 (CPU)	4,150 (CPU)	1.43 TFLOPS	10-25
i.MX 8M Plus	NXP	Media SoC	COTS	14 nm	4 (CPU)	1,800 (CPU)	2.3 TOPS (NPU)	<2
MPPA3-80	Kalray	Manycore	COTS	16 nm	80 (DSP)	1,200 (DSP)	25 TOPS, 4 TFLOPS	-
Coral Edge TPU	Google	AI accel.	COTS	-	-	-	4 TOPS	2

Figure 9-4: Comparison of high-performance COTS processors (either used for space or planned to be used).

In case more computational power is needed, FPGA-based solution could be implemented. An array of FPGAs (i.e. Xilinx Ultrascale KU60) could be potentially used to implement specific operations needed for science data processing. This solution requires further study.

- Mass Memory – a number of other solutions are available depending on required size and radiation tolerance. As an example, HERA Mass Memory has the following properties: 256 Gbit EOL size, below 15W power consumption, 4.9kg of mass.
- HUB and Transceivers – no trade-offs were provided. Technology capable of fulfilling the requirements was presented. Further study might be needed to properly select hardware (i.e. in context of Moon environment) and communication protocol (i.e. Ethernet or SpaceFibre)

9.4 Considerations for scalability

Scalability of the instrument will have following impact on DHS:

- On-Board Computer – no/minor impact coming from increased number of antennas/HUBs
- Payload Processing Unit – an increase in the number of antennas could result in significantly higher computational needs (and increased power consumption). In such a case, assessment has to be done to choose an optimal solution. As mentioned in 9.3, array of FPGAs might be a better solution in case significant computational power is needed.
- Mass Memory – increased number of antennas will result in high data to be stored. Baselined solution has already significant margin, nevertheless, the choice of Mass Memory might be adapted to fit scaled requirements.
- HUB and Transceivers – scalability might some have impact. Bandwidth/number of digital fibre optics transceivers might be adapted to fulfil higher bandwidths.

9.5 Technology Needs

In the current Scenario 4 no show stoppers were identified from DHS point of view.

Potential investigation could be done in case increased computational power is needed to process scientific data (as mentioned in chapter 9.3).

10 TELECOMMUNICATIONS

10.1 General considerations and initial assumptions

Initial assumptions	
Ref.	Assumption
1.	Return link is through the relay satellite from the lunar surface to the orbit
2.	Forward link is through the relay satellite from the orbit to the lunar surface.
3.	Relay satellite has constant communication with Earth.
4.	Two links necessary, one for TT&C and another one for High Data Rate (HDR).

Table 10-1: Initial assumptions

10.1.1 Subsystem Requirements

Subsystem Requirements	
Req. ID	Statement
COM-010	The ALO Communications Subsystem shall be independent from the LDE after landing.
COM-020	The selected frequency bands, modulation, and coding schemes shall comply with the international standards and recommendations (IAOG RD[70], SFCG RD[71], CCSDS RD[72] and RD[73], and ICSIS RD[74]).
COM-030	The ALO communications shall support lunar relay link.
COM-040	The communication link shall be closed with a nominal margin of at least 3dB.
COM-050	TT&C link with 10 kbps in forward and return link.
COM-060	High data rate with 43 Mbps in the return link and 8 Mbps in the forward link.

Table 10-2: Subsystem requirements

10.1.2 Key drivers and challenges

Key drivers		
Ref.	Key driver	Impact
1.	LDE Communications Subsystem cannot be used post-landing.	ALO needs its own communications subsystem.
2.	ALO Communications Subsystem will only be used from Early surface Operations phase onwards.	No communications requirements before post-landing.
3.	Direct to Earth (DTE) link not available.	Relay link must be considered.

4.	LCNS, Lunar Gateway or Pathfinder available for LS – LO link.	Relay to GW/LP/LCNS then substitute DTE link.
5.	LCNS, Lunar Gateway and Pathfinder already have DTE link implemented.	No DTE link budget considered in this study for these satellites.

Table 10-3: Key drivers

10.2 Baseline Description

Given that the mission landing on the far-side of the moon, and as per RD[70] and RD[71], the proposed TT&C communications is via S-band and Ka-band. The mission architecture in Figure 10-1 presents the communications links in the aforementioned frequency bands, with the considered relays, and typical data rates expected.

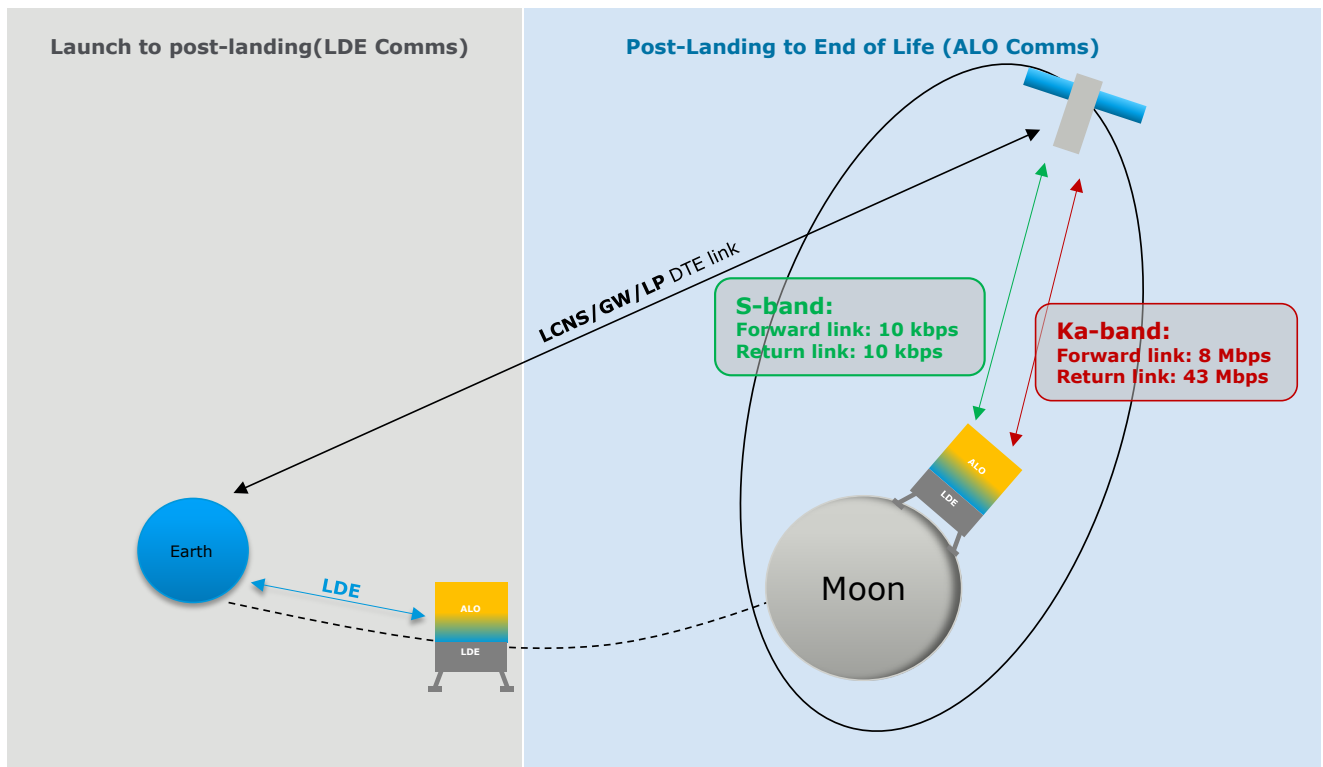


Figure 10-1: Mission architecture and assumptions

The communications subsystem is based on S-band for TT&C link and Ka-band for high data rate link. As stated in Table 10-3, no DTE link is available, and therefore all links must be established through a relay satellite.

Three possible relays were considered: Gateway (GW), Lunar Pathfinder (LP) and Lunar Communications and Navigation Services (LCNS). Each link budget will be presented for all three of them to better explain the advantages and disadvantages of each.

10.2.1 S-band Link

Two possibilities have been considered for the S-band link: optimal- and worst-case scenario. In the optimal scenario, maximum antenna gain is assumed, as well as no additional interferences or losses. This yields a higher data rate in both forward and return link.

RETURN LINK				
PARAMETER	GATEWAY	LCNS	PATHFINDER	Notes
ALTITUDE [AU]	-	-	-	-
ALTITUDE [km]	71770.0	14000.0	9000.0	Distances
ELEVATION ANGLE [deg]	90.0	90.0	90.0	Estimation
RANGE [km]	71770.0	14000.0	9000.0	Calculated
FREQUENCY [MHz]	2290	2290	2290	S-band
TX POWER [W]	20	20	20	TWTA
TX ANTENNA GAIN [dB]	5	5	5	LGA 10° off boresight
TX LOSSES [dB]	4	4	4	3dB Coupler
TX EIRP [dBW]	14.01	14.01	14.01	Calculated
PATH LOSSES [dB]	196.76	182.56	178.72	Calculated
ATMOSPHERE LOSS [dB]	0.00	0.00	0.00	Not applicable
RX POL. LOSS [dB]	0.50	0.50	0.50	Estimation
RX G/T [dBK]	-5.80	-6.80	-10.00	Estimation
DEMOD. LOSS [dB]	2.00	2.00	2.00	Estimation
MOD. LOSS [dB]	0.00	0.00	0.00	Estimation
S/NO [dB]	37.55	50.75	51.39	Calculated
REQUIRED Eb/No [dB]	1.30	1.30	1.30	LDPC1/2(8192, 4096) , FER=10 ⁻⁶
Eb/No LOSS [dB] (Solar Plasma)	0.00	0.00	0.00	No solar effect
MINIMUM MARGIN [dB]	3.00	3.00	3.00	Nominal Value
MAX BIT RATE [dBHz]	33.25	46.45	47.09	Result
MAX BIT RATE [kbps]	2.11	44.15	51.13	RESULT
DESIRED BIT RATE [kbps]	2.00	40.00	50.00	Required
Rx Eb/No [dB]	4.54	4.73	4.40	Calculated
MARGIN AT DESIRED BITRATE [dB]	3.24	3.43	3.10	Calculated

Figure 10-2: S-band Optimal Return Link

FORWARD LINK				
PARAMETER	GATEWAY	LCNS	PATHFINDER	Notes
ALTITUDE [AU]	-	-	-	-
ALTITUDE [km]	71770.0	14000.0	9000.0	Distances
ELEVATION ANGLE [deg]	90.0	90.0	90.0	Estimation
RANGE [km]	71770.0	14000.0	9000.0	Calculated
FREQUENCY [MHz]	2025	2025	2025	S-band
MOD. INDEX [RAD/PK]	1.25	1.25	1.25	Estimation
TX EIRP [dBW]	38.50	29.80	21.00	Estimation
PATH LOSSES [dB]	195.69	181.49	177.66	Calculated
ATMOSPHERE LOSS [dB]	0.20	0.20	0.20	S-band, 99% availability
RX G/T [dBK]	-24.50	-24.50	-24.50	Estimation
DEMOD. LOSS [dB]	2.00	2.00	2.00	Estimation
MOD. LOSS [dB]	0.45	0.45	0.45	Estimation
REQUIRED Eb/No [dB]	3.30	3.30	3.30	LDPC1/2(512, 256) , FER=10 ⁻⁶
Eb/No LOSS [dB] (Solar Plasma)	0.00	0.00	0.00	No solar effect
MINIMUM MARGIN [dB]	3.00	3.00	3.00	Nominal Value
MAX BIT RATE [dBHz]	37.96	43.45	38.49	Result
MAX BIT RATE [kbps]	6.25	22.14	7.06	RESULT
DESIRED BIT RATE [kbps]	6.00	20.00	7.00	Required
Rx Eb/No [dB]	6.47	6.74	6.34	Calculated
MARGIN AT DESIRED BITRATE [dB]	3.17	3.44	3.04	Calculated

Figure 10-3: S-band Optimal Forward Link

For the return link, a maximum of 50 kbps could be achieved using the Lunar Pathfinder and a maximum of 40 kbps can be achieved using the LCNS constellation. However, in the forward link the Lunar Pathfinder would yield only 7 kbps as opposed to LCNS which would yield a maximum data rate of 20 kbps. Using the Gateway only 2 kbps and 6 kbps could be reached for the return and forward link, respectively. It can be then concluded that LCNS would be the preferred option for this scenario.

For the worst-case scenario, it is assumed that the antenna is 90° off boresight with respect to the relay satellite. This means that the antenna would provide its the minimum gain, resulting in lower data rates.

RETURN LINK				
PARAMETER	GATEWAY	LCNS	PATHFINDER	Notes
ALTITUDE [AU]	-	-	-	-
ALTITUDE [km]	71770.0	14000.0	9000.0	Distances
ELEVATION ANGLE [deg]	90.0	90.0	90.0	Estimation
RANGE [km]	71770.0	14000.0	9000.0	Calculated
FREQUENCY [MHz]	2290	2290	2290	S-band
TX POWER [W]	20	20	20	TWTA
TX ANTENNA GAIN [dB]	-3	-3	-3	LGA 90° off boresight
TX LOSSES [dB]	4	4	4	3dB Coupler
TX EIRP [dBW]	6.01	6.01	6.01	Calculated
PATH LOSSES [dB]	196.76	182.56	178.72	Calculated
ATMOSPHERE LOSS [dB]	0.00	0.00	0.00	Not applicable
RX POL. LOSS [dB]	0.50	0.50	0.50	Estimation
RX G/T [dBK]	-5.80	-6.80	-10.00	Estimation
DEMOD. LOSS [dB]	2.00	2.00	2.00	Estimation
MOD. LOSS [dB]	0.00	0.00	0.00	Estimation
S/NO [dB]	29.55	42.75	43.39	Calculated
REQUIRED Eb/No [dB]	1.30	1.30	1.30	LDPC1/2(8192, 4096) , FER=10 ⁻⁶
Eb/No LOSS [dB] (Solar Plasma)	0.00	0.00	0.00	No solar effect
MINIMUM MARGIN [dB]	3.00	3.00	3.00	Nominal Value
MAX BIT RATE [dBHz]	25.25	38.45	39.09	Result
MAX BIT RATE [kbps]	0.34	7.00	8.10	RESULT
DESIRED BIT RATE [kbps]	0.30	7.00	8.00	Required
Rx Eb/NO [dB]	4.78	4.30	4.36	Calculated
MARGIN AT DESIRED BITRATE [dB]	3.48	3.00	3.06	Calculated

Figure 10-4: S-band Worst Return Link

FORWARD LINK				
PARAMETER	GATEWAY	LCNS	PATHFINDER	Notes
ALTITUDE [AU]	-	-	-	-
ALTITUDE [km]	71770.0	14000.0	9000.0	Distances
ELEVATION ANGLE [deg]	90.0	90.0	90.0	Assumed
RANGE [km]	71770.0	14000.0	9000.0	Calculated
FREQUENCY [MHz]	2025	2025	2025	S-band
MOD. INDEX [RAD/PK]	1.25	1.25	1.25	Estimation
TX EIRP [dBW]	38.50	29.80	21.00	Estimation
PATH LOSSES [dB]	195.69	181.49	177.66	Calculated
ATMOSPHERE LOSS [dB]	0.20	0.20	0.20	S-band, 99% availability
RX G/T [dBK]	-30.50	-30.50	-30.50	Estimation
DEMOD. LOSS [dB]	2.00	2.00	2.00	Estimation
MOD. LOSS [dB]	0.45	0.45	0.45	Estimation
REQUIRED Eb/No [dB]	3.30	3.30	3.30	LDPC1/2(512, 256) , FER=10 ⁻⁶
Eb/No LOSS [dB] (Solar Plasma)	0.00	0.00	0.00	No solar effect
MINIMUM MARGIN [dB]	3.00	3.00	3.00	Nominal Value
MAX BIT RATE [dBHz]	31.96	37.45	32.49	Result
MAX BIT RATE [kbps]	1.57	5.56	1.77	RESULT
DESIRED BIT RATE [kbps]	1.50	5.00	1.75	Required
Rx Eb/NO [dB]	6.50	6.76	6.36	Calculated
MARGIN AT DESIRED BITRATE [dB]	3.20	3.46	3.06	Calculated

Figure 10-5: S-band Worst Forward Link

For the return link, a maximum of 8 kbps could be achieved using the Lunar Pathfinder and a maximum of 7 kbps could be achieved using the LCNS constellation, therefore having similar values. The Gateway on the other hand would provide only 0.3 kbps, a much slower data rate. In the forward link, LCNS could reach a maximum of 5 kbps, much higher than the 1.75 kbps provided by the Lunar Pathfinder and the 1.5 kbps provided by the Gateway. This leads to the conclusion that LCNS would be the preferred option also for this scenario.

The S-band TT&C architecture shown in Figure 10-6 consists of the transponders, power amplifiers, Radio Frequency Distribution Network (RFDN), and the antennas. The transponders and TWTAs are redundant, with hot redundancy in the receiver chain and cold in the transmitter chain. The RFDN consists mainly of the isolators, diplexers, couplers, and coaxial cables/waveguides. The antenna part consists of two LGAs placed in opposite sides of the spacecraft for a quasi-omnidirectional coverage.

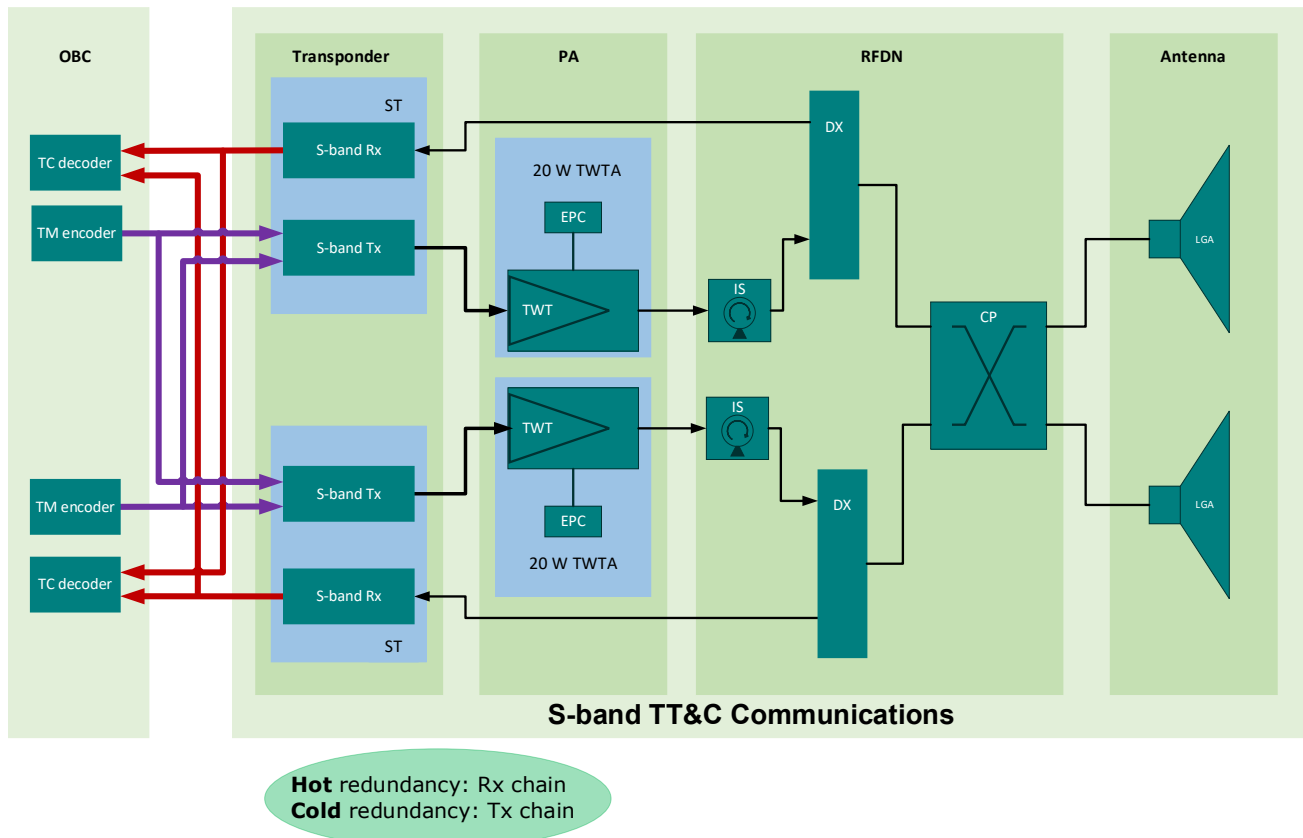


Figure 10-6: S-band Architecture

10.2.2 Ka-band Link

Ka-band will be used for the high-data rate link. Therefore, the data rate is assumed to be limited by the relay satellite capacity, not by the ALO communications subsystem itself.

RETURN LINK				
PARAMETER	GATEWAY	LCNS	PATHFINDER	Notes
ALTITUDE [AU]	-	-		-
ALTITUDE [km]	71770.0	14000.0		Distances
ELEVATION ANGLE [deg]	90.0	90.0		Estimation
RANGE [km]	71770.0	14000.0		Calculated
FREQUENCY [MHz]	27500	27500		K-band
TX POWER [W]	60	5		TWTA
TX ANTENNA GAIN [dB]	41	41		0.55m HGA
TX LOSSES [dB]	1.5	1.5	ONLY S-BAND AND UHF	Switch
TX EIRP [dBW]	57.28	46.49		Calculated
PATH LOSSES [dB]	218.35	204.15		Calculated
ATMOSPHERE LOSS [dB]	0.00	0.00		Not applicable
RX POL. LOSS [dB]	0.50	0.50		Estimation
RX G/T [dBK]	16.20	16.90		Estimation
DEMOD. LOSS [dB]	2.00	2.00		Estimation
MOD. LOSS [dB]	0.00	0.00		Estimation
S/NO [dB]	81.23	85.34		Calculated
REQUIRED Eb/No [dB]	1.30	1.30		LDPC1/2(8192, 4096) , FER=10 ⁻⁶
Eb/No LOSS [dB] (Solar Plasma)	0.00	0.00		No solar effect
MINIMUM MARGIN [dB]	3.00	3.00		Nominal Value
MAX BIT RATE [dBHz]	76.93	81.04	-	Result
MAX BIT RATE [kbps]	49365.65	127020.39	-	RESULT
DESIRED BIT RATE [kbps]	43000.00	50000.00	-	Required
Rx Eb/NO [dB]	4.90	8.35	-	Calculated
MARGIN AT DESIRED BITRATE [dB]	3.60	7.05	-	Calculated

Figure 10-7: Ka-band Return Link

FORWARD LINK				
PARAMETER	Value	LCNS	PATHFINDER	Notes
ALTITUDE [AU]	-	-		-
ALTITUDE [km]	71770.0	14000.0		Gateway
ELEVATION ANGLE [deg]	90.0	90.0		Assumed
RANGE [km]	71770.0	14000.0		Calculated
FREQUENCY [MHz]	27000	27000		K-band
MOD. INDEX [RAD/PK]	-	-		Estimation
TX EIRP [dBW]	55.00	48.90		Estimation
PATH LOSSES [dB]	218.19	203.99	ONLY S-BAND AND UHF	Calculated
ATMOSPHERE LOSS [dB]	0.00	0.20		Not applicable
RX G/T [dBK]	12.00	12.00		Estimation
DEMOD. LOSS [dB]	2.00	2.00		Estimation
MOD. LOSS [dB]	0.00	0.00		Estimation
REQUIRED Eb/No [dB]	3.30	3.30		LDPC1/2(512, 256) , FER=10 ⁻⁶
Eb/No LOSS [dB] (Solar Plasma)	0.00	0.00		No solar effect
MINIMUM MARGIN [dB]	3.00	3.00		Nominal Value
MAX BIT RATE [dBHz]	69.11	77.01	-	Result
MAX BIT RATE [kbps]	8151.01	50215.91	-	RESULT
DESIRED BIT RATE [kbps]	8000.00	50000.00	-	Required
Rx Eb/NO [dB]	6.38	6.32	-	Calculated
MARGIN AT DESIRED BITRATE [dB]	3.08	3.02	-	Calculated

Figure 10-8: Ka-band Forward Link

The Lunar Pathfinder does not support Ka-band, only S-band and UHF. It will be therefore not considered for the preliminary link budget assessment. For the return link, a maximum of 43 Mbps could be achieved using the Gateway and a high power TWTA given that this is the maximum data rate supported by it. This upper limit is set at 50 Mbps for the LCNS constellation, which would be then reached without the need for the high power TWTA. In the forward link, LCNS could reach a maximum of 50 Mbps once again, opposed to the 8 Mbps provided by the Gateway. It can be then concluded that both relay satellites would be suitable for the return link, but LCNS would again be the preferred option considering the forward link as well.

The Ka-band TT&C architecture shown in Figure 10-9 consists of the transponders, power amplifiers, RFDN, and the antenna. The transponders and TWTAs are redundant, with hot

redundancy in the receiver chain and cold in the transmitter chain. The RFDN consists mainly of the isolators, diplexers, switches, and coaxial cables/waveguides. The antenna section consists of a HGA to optimize for the high data rate in Ka-band.

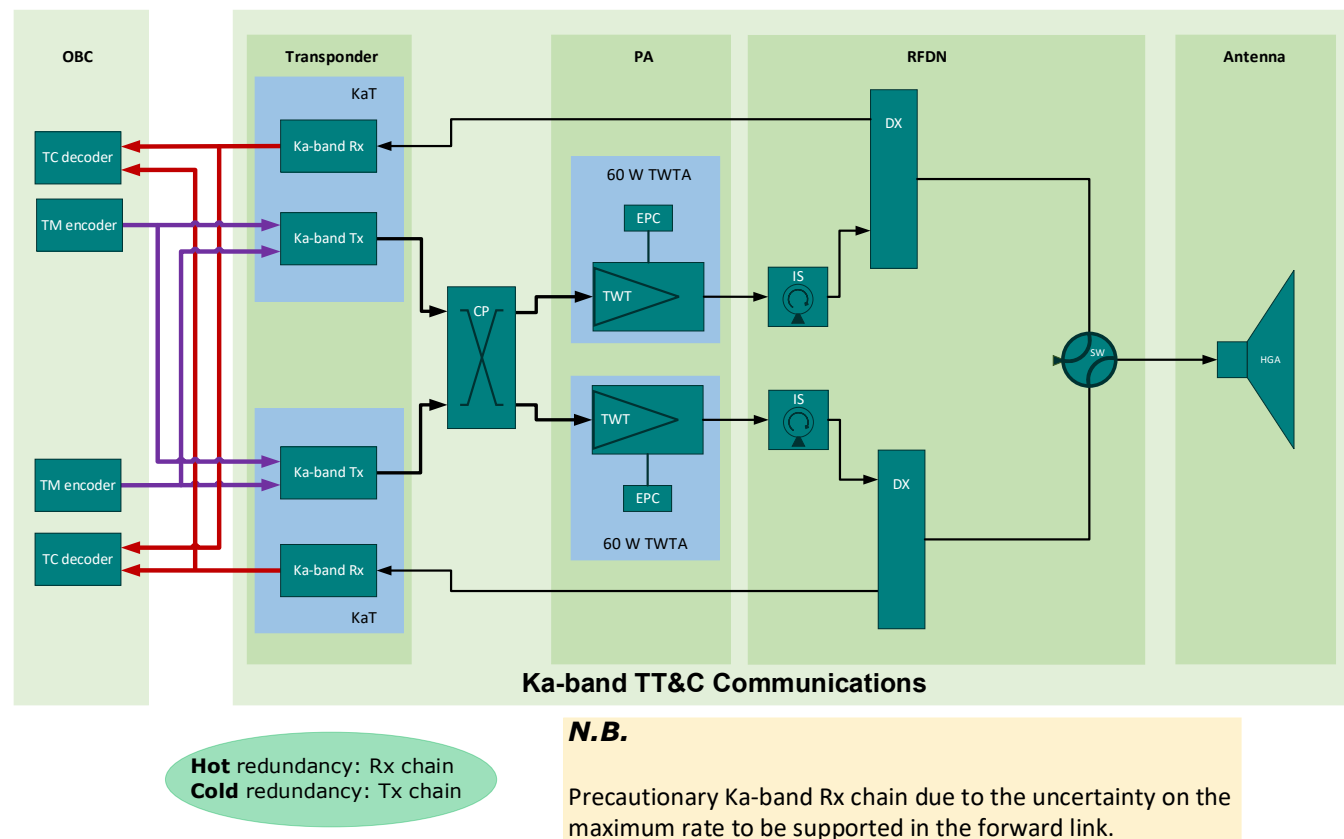


Figure 10-9: Ka-band Architecture

10.2.3 List of Equipment

Unit	#	Size [mm]	Nominal Mass [kg]	Power Consumption [W]		
				GW	LCNS	PF
S-band LGA	2	100x100x285	0.25	0	0	0
S-band RFDN	1	-	3	0	0	0
S-band TWTA*	2	340 x 88 x 70	1.25	30	30	30
S-band Transponder (Tx)*	2	290 x 110 x 197	3.4	24	24	24
S-band Transponder (Rx)**				6.7	6.7	6.7
Ka-band HGA	1	Ø 550 x 140	1.34	0	0	0

Ka-band RFDN	1	-	2	0	0	0
Ka-band TWTA*	2	175x215x140	1	90	7.5	0
Ka-band Transponder (Tx)*	2	70x340x88	3	16.9	16.9	0
Ka-band Transponder (Rx)**				16.5	16.5	0

* TWTA and Tx Transponder in cold redundancy

** Rx Transponder in hot redundancy.

Table 10-4: List of Equipment

Unit	TRL	Heritage considerations
S-band LGA	9	
S-band RFDN	9	
S-band TWTA	9	Earth Obs Missions (Thales Alenia Spain)
S-band Transponder (Tx)	9	
S-band Transponder (Rx)	9	
Ka-band HGA	9	
Ka-band RFDN	9	
Ka-band TWTA	9	
Ka-band Transponder (Tx)	9	
Ka-band Transponder (Rx)	6	

Table 10-5: Technology Readiness

10.3 Trade-Offs and alternative options

From the development of the project, two alternatives were considered as options.

10.3.1 Ka-band transmit-only

As previously stated in Figure 10-9, and given the uncertainty around the maximum rate needed in the forward link, a HDR architecture was proposed for both forward and return. However, in the case of not needing a HDR forward link, a transmit-only architecture with TM only capability is proposed as shown in Figure 10-10. With this simplified architecture, both the mass and the power consumption decrease, as well as having an increase in the TRL from 6 to 9. The disadvantage would be the limited data rate in the forward link, which might be deemed as unnecessary in future phases of this mission.

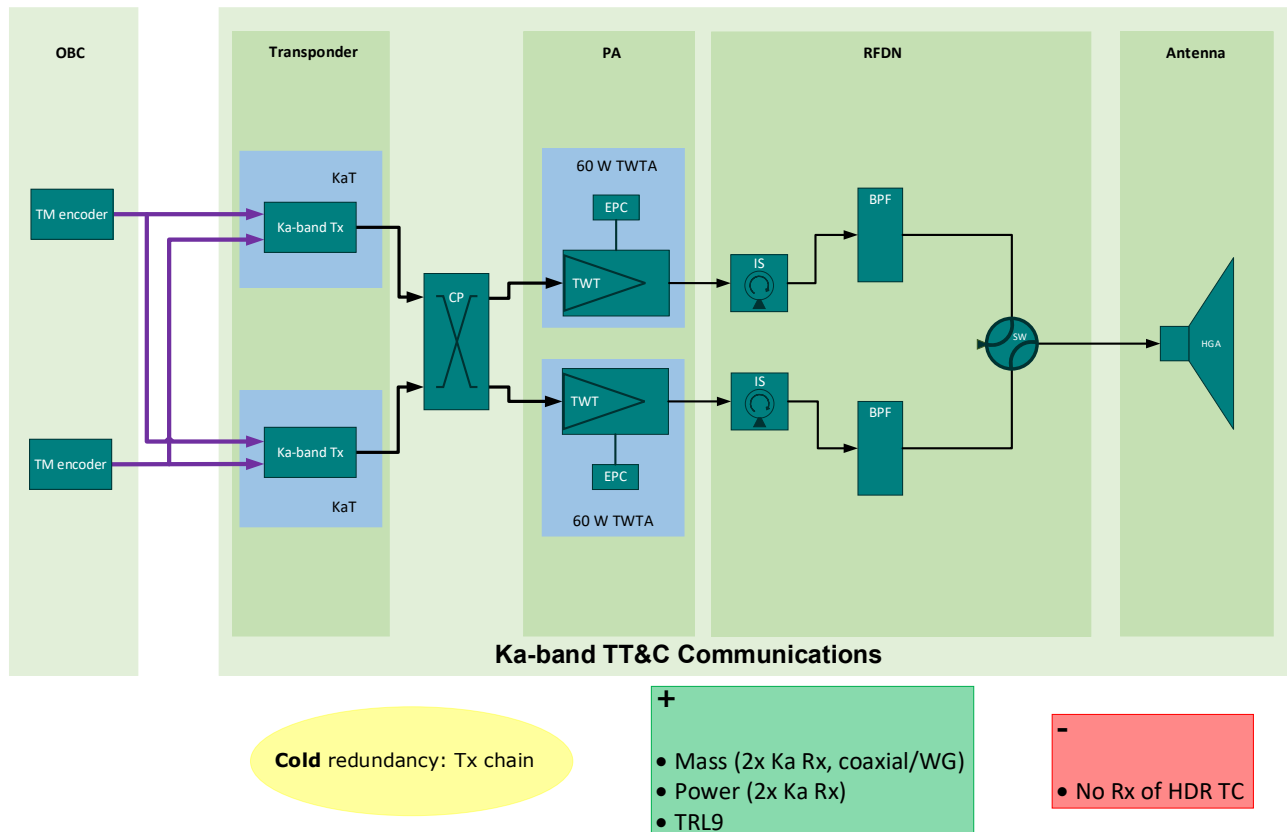


Figure 10-10: Ka-band TM only option

10.3.2 Ka-band multiple antennas

A second alternative proposed here is a multiple-antenna architecture comprising an MGA and a HGA as shown in Figure 10-11. The MGA would provide wider coverage in addition to the directivity of the HGA, as well as adding a contingency structure in case of failure of the APM for the HGA. This would allow the system to maintain higher rates in comparison to the S-band as contingency architecture. The disadvantages would be an increase in the total mass introduced by the MGA, and additional losses in switches and RFDN components.

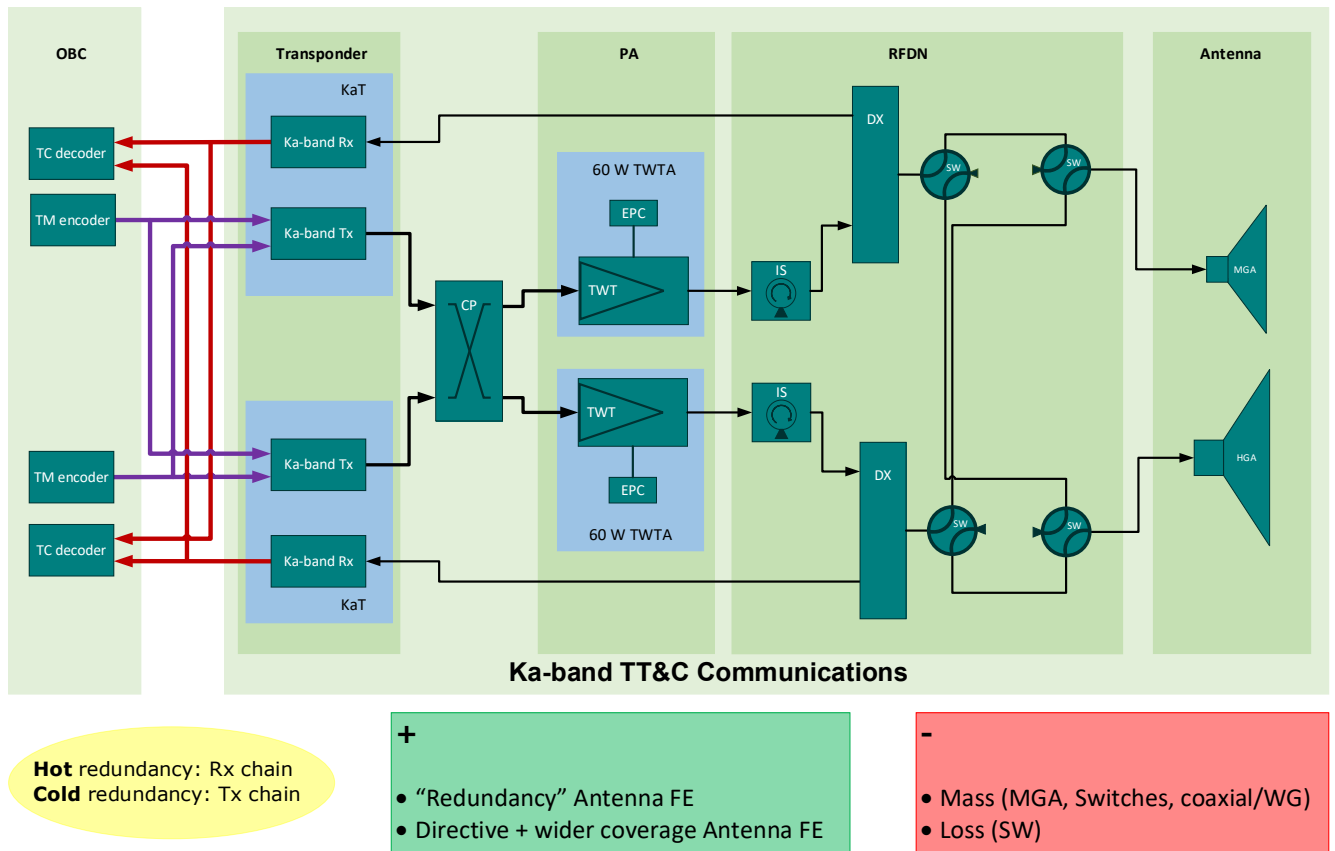


Figure 10-11: Ka-band multiple antennas option

10.4 Wireless communication proposal

For the transmission of the scientific data collected by ALO from the hub to the base station, a local network based on a wireless communication link is proposed. As shown in Figure 10-12 the Draft Recommended Standard RD[73] presents the current technology capabilities and limitations in terms of the achievable data rates as function of the transmission distance.

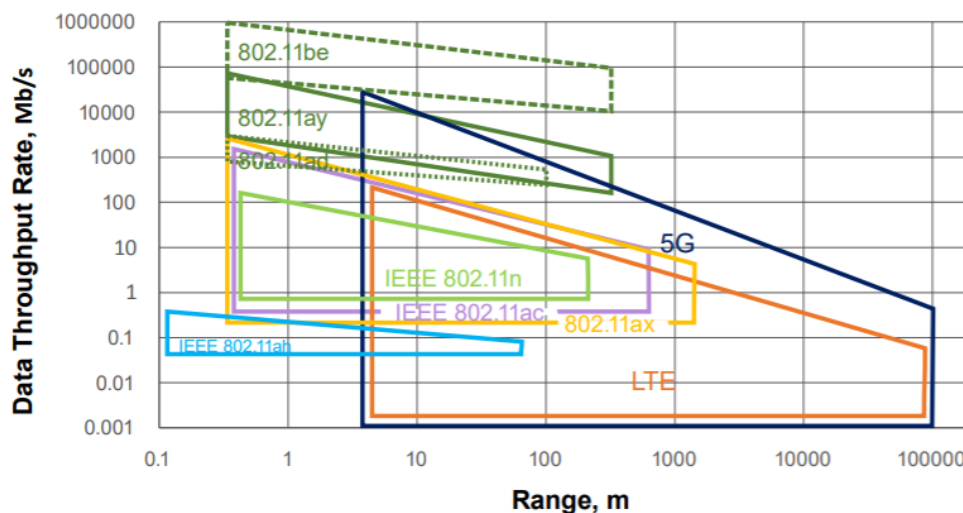


Figure 10-12: Wireless technologies throughput rates as function of range

The foreseen distance between the antenna hub and the base station ranges between 100 m and 1 km. With a simplified scenario of 16 antennas per hub and a transfer rate of 3.2 Gbps for 2 channels per antenna, the suitable technologies are: 802.11be, 802.11ay, 5G for one antenna; and 802.11be as shown in Figure 10-13.

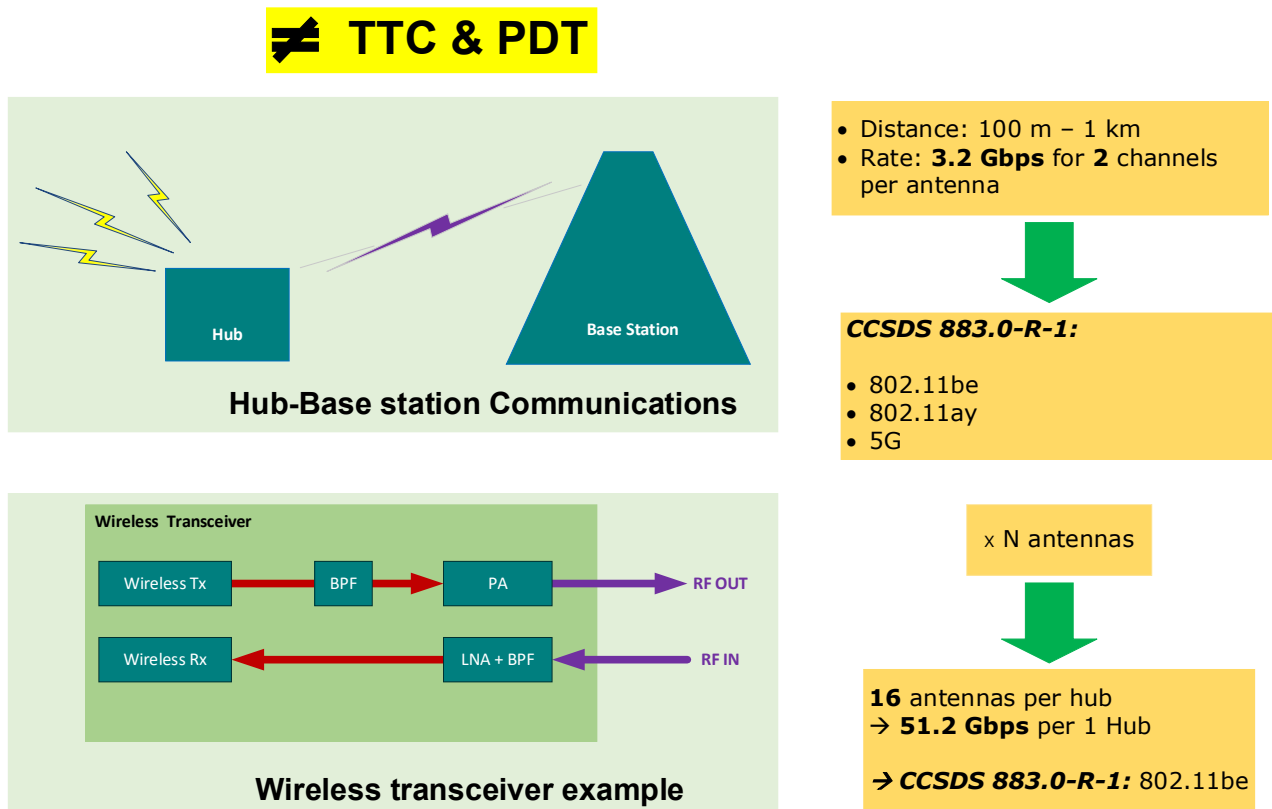


Figure 10-13: Wireless communication candidates: Hub—Base Station

Figure 10-13 illustrates a simple example architecture of a transceiver that could be used for the wireless transmission. The transceiver's transmission chain consists of the transmitter, a band-pass filter and a power amplifier whilst the reception consists of the low-noise amplifier with a band-pass filter and a receiver. Both chains are then interface to the front-end for RF signal input/output. Note that this is intended to have a redundant concept on the transceiver, both on the hub and on the base station.

Given the presented needs and technology status, it can be seen that the requirements are situated at the boundary of existing technology as shown in Figure 10-14.

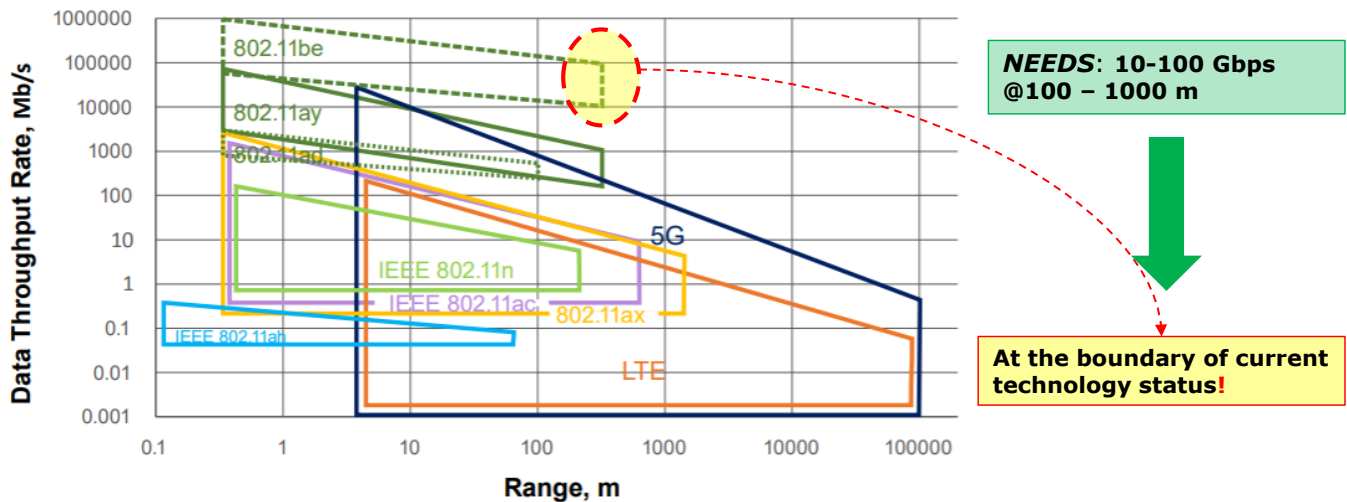


Figure 10-14: Wireless needs and technology status

Please note that the current proposal for wireless communication is not part of the TT&C Communications subsystem, and the solution described above rather an attempt to provide some immediate information on the topic. For an in-depth study, an expert in this field, especially in wireless networks, should be consulted.

10.5 Considerations for scalability

For the lunar wireless communication of this study, the case of a 16-antenna per hub was analysed. The proposed solution is therefore designed considering this size. In the case of full deployment with many hubs, possibly with more than 16 antennas each, the current solution would have to be re-analysed and re-assessed. This is because the base station would need to be able to simultaneously receive and support a larger number of input signals.

10.6 Technology Needs

In addition to the technology needs of the communications architecture, it is important to mention that the most critical technology need for the success of this mission is the launching and correct functioning of the relay satellites, that is, Gateway, LCNS and Lunar Pathfinder. As of the date of the writing of this report, none of them has been finished and/or launched, meaning that by the time of the launch of ALO, any of these three should already be in orbit to provide quality communications from LS to LO and from LO to the ground stations in Earth.

Technology Needs						
Technology is baselined	Equipment Name & Text Reference	Technology	Supplier (Country)	TRL	Funded by	Additional Information
	S-band LGA		Ruag (SE), Ryma (IT)	9		
	S-band RFDN			9		
	S-band TWTA		Tesat (DE) TAS-B (BE)	9		For TWT only: TAS-Ulm (DE)
	S-band Transponder		TAS-I (IT) TAS-E (ES)	9		
✓	Ka-band HGA		Ruag (SE)			
✓	Ka-band RFDN			9		
✓	Ka-band TWTA		Tesat (DE) TAS-B (BE)	9		
✓	Ka-band Transceiver		Tesat (DE), Kongsberg (NO) TAS-I (IT)	6		Developments are ongoing

Table 10-6: Technology Needs

This Page Intentionally Blank

11 MECHANISM

11.1 General considerations and initial assumptions

Initial assumptions	
Ref.	Assumption
1.	Antenna Pointing Mechanism (APM) for High Gain Antenna (HGA) – size of HGA: diameter 500mm, mass 1.5kg
2.	Large number of payload antennas (minimum 16 in the first EL3 mission, full scale observatory with ~16000 antennas)

Table 11-1: Initial assumptions

11.1.1 Key drivers and challenges

Key drivers		
Ref.	Key driver	Impact
1.	Payload antenna in a form of cross-dipole, each dipole 5m long	<i>Limited number of mechanisms which can deploy to such large structure</i>
2.	Payload antenna system compliant with “black box” solution	Deployment from large-roll removed from the baseline
3.	Possibility of deployment of payload antennas from magazine	Lightweight and compact design of payload antennas in the stowed configuration
4.	Dusty environment on the Moon	Need of additional protection for mechanisms, especially APM, which leads to higher mass margins

Table 11-2: Key drivers

11.2 Baseline Description

11.2.1 Cross-dipole payload antenna

Payload antennas are the main payload for ALO. The nominal configuration was chosen as cross-dipole antenna with 5m length of each dipole, see schematic view on single antenna in deployed configuration presented in Figure 11-1.

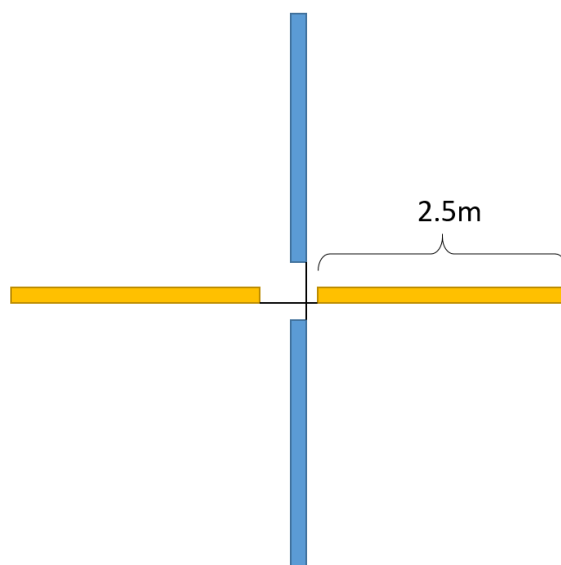


Figure 11-1: Schematic of cross-dipole antenna for ALO

The main design drivers for payload antenna's design were:

- Lightweight and compact design to achieve a high number of antennas for single EL3 mission
- Compatibility to Lunar environment (dust, temperature range, gravity loads)
- Reliable and low power consumption deployment
- Possibility to fit into magazine on the rover

Several designs were analysed (further information on trade-offs in chapter 11.3.1) and the baseline solution is based on tubular boom technology, already used on several missions, including JUICE [RD[75]]. In the baseline design, each half of dipole is made of CuBe thin-wall tapes, which are preformed into the tube-shape and folded onto a reel. It allows to occupy the very small volume in the stowed configuration even for very long tubes. After deployment, tubes are unfolded to its nominal, tubular shape, which provide very good stiffness to mass ratio. Tubular boom concepts are used in space since 60's, Figure 11-2 shows NASA concept of Astro Aerospace's Storable Extendible Tubular Member (STEM) [RD[83]].



Figure 11-2: Astro Aerospace's Storable Extendible Tubular Member (STEM), NASA

Tubular boom antennas can fit into a "black box" solution and as a result to the concept of deployment from the magazine, performed by the rover. It is possible to adjust the angle of deployment (angle between dipole arm and Lunar surface) to prevent from clash with rocks or

dust, similarly to the concept presented in Figure 11-3, which shows the Radio Frequency Analyser (RFA) instrument for Russian RELEC mission built in the Space Research Centre Polish Academy of Sciences (CBK PAN) [RD[76]]. The picture on the left shows RFA in fully deployed configuration, angle of antenna arms wrt. ground is close to 40°. The picture on the right shows the same instrument in the stowed configuration.

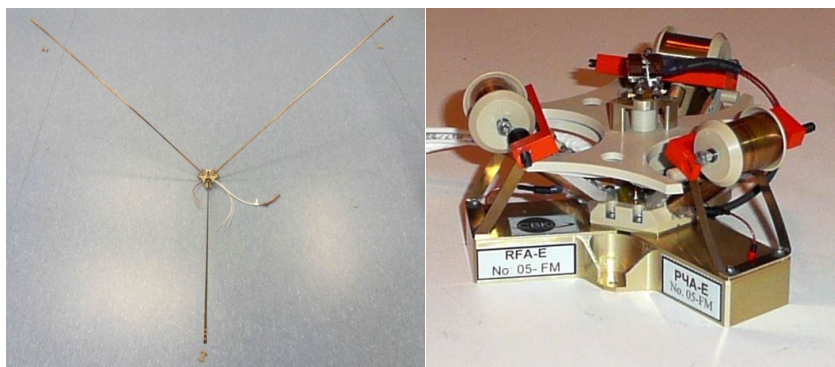


Figure 11-3: Radio Frequency Analyser (RFA) instrument for Russian RELEC mission(CBK PAN). Picture on the right in deployed configuration on the left in stowed configuration.

The assumed mass of single antenna (cross-dipole) with its deployment mechanism, and base structure (without electronics and thermal shielding) is 1kg and the maximum size is 20x20x20cm.

Deployment can be performed using simple HDRM, e.g. based on Vectran melting or simple pin-puller, which result in low power consumption for the deployment operation. The alternative solution may be to use Shape Memory Alloy HDRM to obtain fully passive deployment (concept described in chapter 11.3.2). This solution however has some drawbacks, mainly the lack of control for deployment moment (driven by the increase of temperature during Lunar day) and necessity to thermally control antennas which are not yet deployed to the surface of the Moon. Despite the chosen deployment actuation the big advantage of the baseline solution is that the unfolding of tubular booms is rapid and does not require any additional support from e.g. electric motors, which provide high reliability of the process and reduce the mass of the antenna. It is possible to deploy every half of the dipole one-by-one or all 4 simultaneously.

The similar design is used for RWI instrument on-board JUICE mission (presented in Figure 11-4) and has already reached TRL8. The non-operation temperature for JUICE RWI mechanism is in range -200°C to +200°C which proves suitability of the design to Lunar temperature range. Some redesign is needed to adjust the CuBe tape thickness and length to ALO requirements which reduce the TRL level to TRL5 for ALO.

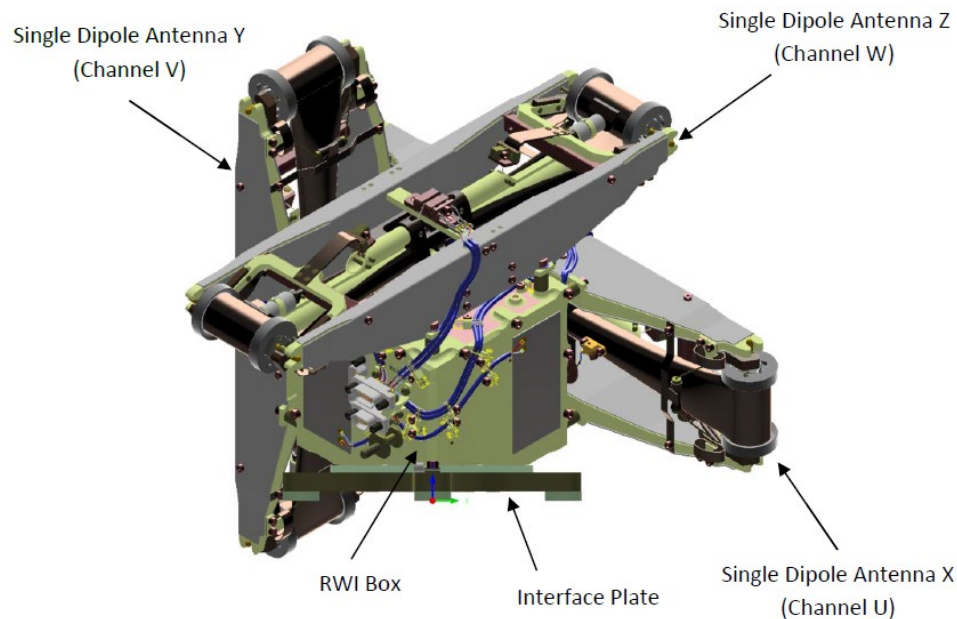


Figure 11-4: RWI antenna for ESA JUICE mission

Figure 11-5 shows preliminary concept of “black box” with cross dipole antennas for ALO. In this concept each antenna is placed inside the box with preamplifiers inside and covered with MLI. Several boxes can fit into the magazine. Deployment of boxes from magazine to Lunar surface is performed by separate mechanism (design TBD, probably similar to CubeSat deployers [RD[77]]) and/or robotic arm on board the rover.

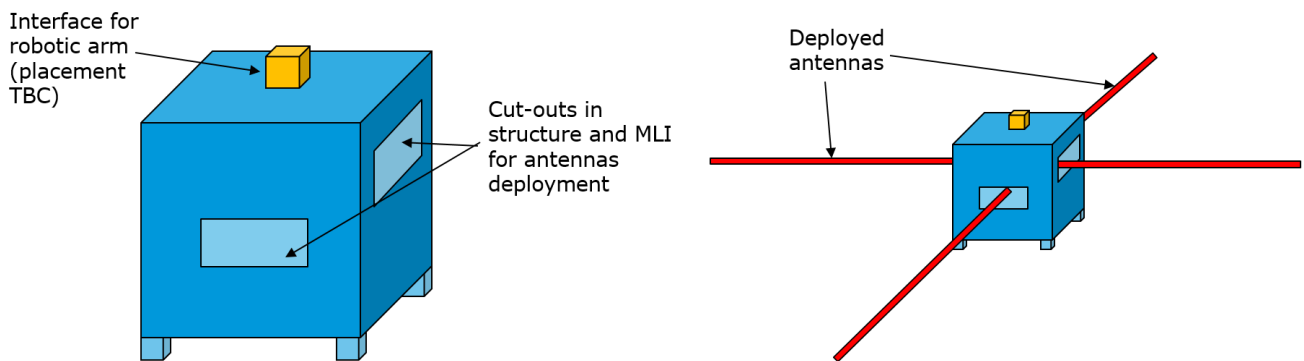


Figure 11-5: Concept of ALO payload antenna inside the “black box”

11.2.2 Antenna Pointing Mechanism

It is assumed that a least one High Gain Antenna (HGA) is needed for ALO mission. The HGA will be located on a lander, the size of a HGA dish was calculated as 500mm (diameter) and mass of 1.5kg. APM shall allow to position HGA in two axes (azimuth and elevation) to achieve contact with constellation of communication satellites on Lunar orbit.

There are already several APMs designs available which are used on satellites and other spacecraft, however ALO environment requires redesign and requalification of available APMs

(mainly very low temperatures during Lunar night, abrasive effects of Lunar dust and Moon loads have to be taken as main design drivers).

The proposed baseline for APM is KARMA-7 FG developed by Kongsberg [RD[78]], already used on MetOP-SG satellites and presented in Figure 11-6. Design has TRL9 for this particular mission, however the adjustment of APM will have to be performed to withstand additional loads (Moon gravity), larger reflector size (0.5m) and protection from dust. These redesign impact is reflected in increased mass margin for the design and reduction of the TRL level for ALO to TRL5.



Figure 11-6: Karma-7 FG by Kongsberg

The baseline for the APM Electronic Unit (APM EU) is Kongsberg's Elektra-5 [RD[79]], which is dedicated to the baselined APM. Nominal mass of this APM EU (without margins) is 3.3kg and assumed TRL level for ALO is TRL6.



Figure 11-7: Elektra by Kongsberg

11.2.3 List of Equipment

The following equipment has been identified:

- 16 cross-dipole payload antennas
- 1 Antenna Pointing mechanism (with EU)
- Several HDRMs and deployment mechanisms (hinges) for Solar Arrays

Unit	#	Size [mm]	Nominal Mass [kg]	Power Consumption [W]			
				Day STBY	Day OBS	Day COMMS	Night HIB
Cross-dipole antenna	16	200x200x200	1		*		
APM	1	450x450x500	12			20	
APM EU	1	100x100x50	4	5			

* one-time power consumption of 10W (TBD) for deployment of each antenna

Table 11-3: List of Equipment

Unit	TRL	Heritage considerations
Cross-dipole antenna	5	RWI on board JUICE (TRL 8)
APM	5	Karma-7 FG (TRL 9)
APM EU	6	Elektra-5

Table 11-4: Technology Readiness

11.3 Trade-Offs and alternative options

11.3.1 Cross-dipole payload antennas trade-off

Several ideas were analysed during trade-off for mechanism of cross-dipole payload antennas deployment, including revising of already stated concepts. During first CDF sessions the desired shape (cross-dipole) and number of antennas (min. 16) was established which led to analysing the most promising solutions (also taking into consideration current TRL available).

The four types of mechanisms were considered in the analysis:

- Antennas made of Shape Memory Alloy (SMA) tapes, passively deployed during hottest part of Lunar day
- Antennas printed on a film (Kapton/Mylar/other), stored in a form of a roll in stowed configuration or cross-dipoles made of film stripes
- Tubular boom technology (actual baseline)
- Sail-like structure with motorised and non-motorised deployment

11.3.1.1 Antennas made of SMA tapes

In this solution, the main antenna structure is made of 4 SMA tapes which are rolled in the stowed configuration. When subjected to high temperature (above transition temperature) tapes will move to their original pre-deformed shape (flat tapes) and will form a shape of cross-dipole. This solution requires large amount of power if passive deployment scenario is not used. Also, it is not clear if deployment of such long tapes (2.5m long) will be fully successful in Lunar conditions (possibility of not fully unrolling or “banana-shape” of tapes). The TRL is very low for this concept (TRL < 3) which provides a high risk for supplantation of SMA technology for ALO.

Figure 11-8 presents SMA tapes concept: on the left the deformed, rolled SMA tape is shown; the central picture shows SMA tape in unfolded state, after heating; the right picture depicts the schematic configuration of 4 SMA rolls for ALO antenna. Left and central pictures present the prototype developed by Center for Astronomical Instrumentation (CAI) [RD[80]].

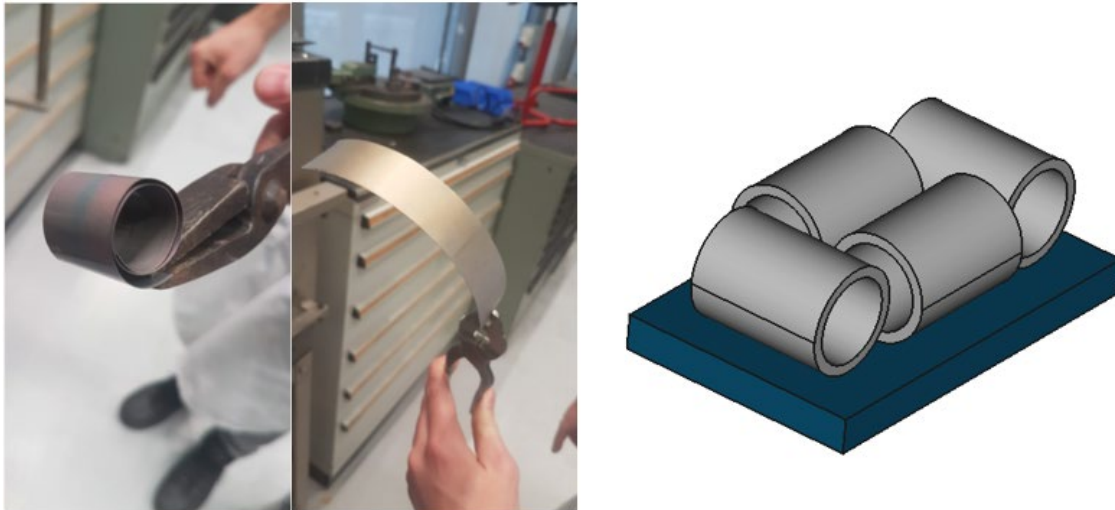


Figure 11-8 Antenna concept based on SMA tapes

11.3.1.2 Antennas printed on a film or made of film stripes

In this concept several antennas are printed on a film (e.g. Kapton) which is then folded and rolled. Rover is used for unrolling process.

The main drawback of this concept is the size of the roll – to be able to print 5m-long cross dipole the roll itself has to have a width of at least 3.5m. Such large roll will not fit into the rover which adds more complexity to the system – the wide tape needs to be folded on the sides before rolling it up. An additional mechanism for unfolding will have to be introduced (which has influence on mass, size and reliability of the system). The additional problems might be connected with susceptibility of the system to abrasive environment and raptures during deployment. Thin foils like Mylar are fragile to cuts and raptures which can be caused by rocks and micrometeoroids. Thicker foils (e.g. Kapton) have greater resistance to raptures but usually are more stiff which will have large influence on deployment process and roll size. In both cases the film needs to be unrolled directly on Moon surface.

It is still an interesting technology and the only one in this trade-off which uses the concept of unrolling of the antennas. The TRL level however is still very low (TRL < 3).

Figure 11-9 presents the prototype antenna made of polyimide film, which was deployed at NASA/GSFC [RD[81]], [RD[82]].



Figure 11-9: A prototype polyimide film antenna deployed at NASA/GSFC

11.3.1.3 Sail-like structures

These concepts rely on deployment mechanisms used mainly in drag and solar sails. Four arms (made of e.g. CFRP), with C- or O-shaped cross-section, are rolled around the main reel. Deployment can be provided by a centrally placed electrical motor or can be fully passive when using only energy stored in folded arms. The motorised solution is heavy (needs to accommodate electrical motor), less reliable (risk of failure of electrical motor) and needs powering for longer time. The non-motorised solution (e.g. PW-Sat2) eliminates these drawbacks however it is not clear if it can be up scaled to ALO needs, especially taking into consideration Moon gravity loads. TRL level is ~5 for ALO, impact of dust and gravity loads might be design driver for ALO needs.

Figure 11-10 depicts 2 example solutions. On the left the motorised concept from DLR is presented [RD[83]]; on the right the non-motorised solution of PW-Sat2 drag sail in the deployed (top) and stowed (bottom) configuration is shown [RD[84]].

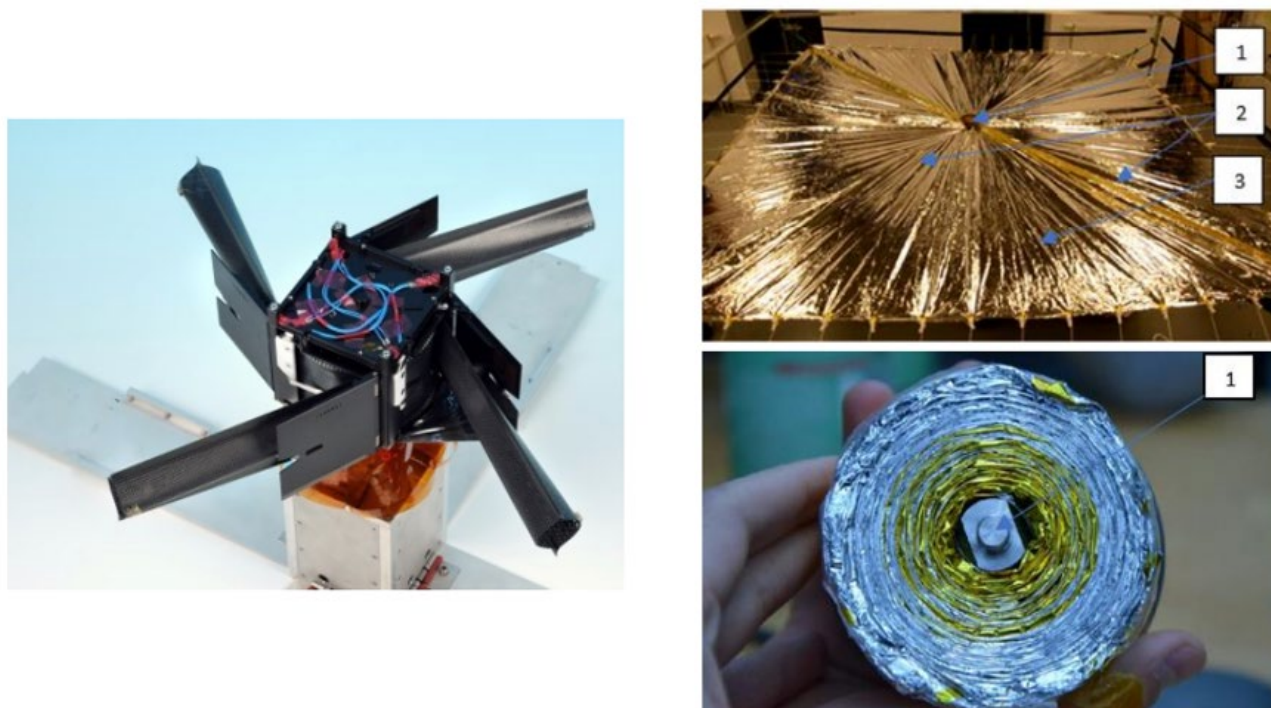


Figure 11-10: Deployment mechanisms for drag sails (motorised and non-motorised concepts)

11.3.2 Passive deployment trade-off

During the ALO CDF study the possibility of using SMA technology was analysed, mainly for a deployment of cross-dipole antennas. The idea was to use advantages of the temperature profile on the landing site to provide fully passive deployment of SMA antennas (concept described in detail in 11.3.1.1) or to use HDRM based on SMA for other antennas concepts (including the baseline concept with tubular booms).

During Lunar day we can observe that temperature gradually increases up to over 90°C and then is falling down to -170°C during Lunar night. By adjusting the SMA transition temperature it is possible to achieve deployment of antennas during hottest part of Lunar day, without any additional power source (relying only on SMA shape transition). In this scenario antennas need to be deployed during the Lunar day phase (Phase 1) when temperature is increasing. All antennas which will not be deployed during this phase will have to be stored under some thermal shield (e.g. on a lander) to be sure that non-deployed antennas will not deploy before placement on Lunar surface. The second deployment phase (Phase 2) is available when temperature falls below SMA transition temperature and lasts until it reaches minimum operation temperature for the rover.

The main advantage of this solution is fully passive deployment – there is no need to power any HDRM to deploy cross-dipole antennas, which has a high impact on power budget with high number of antennas. The main drawback is that there is no possibility to control the moment of antennas deployment and non-deployed antennas needs to have additional thermal control while waiting for phase 2.

Figure 11-11 shows the temperature plots for two possible landing sites with indication of 2 deployment phases of antennas on the Lunar Surface and the phase when SMA will transition under hottest temperature range.

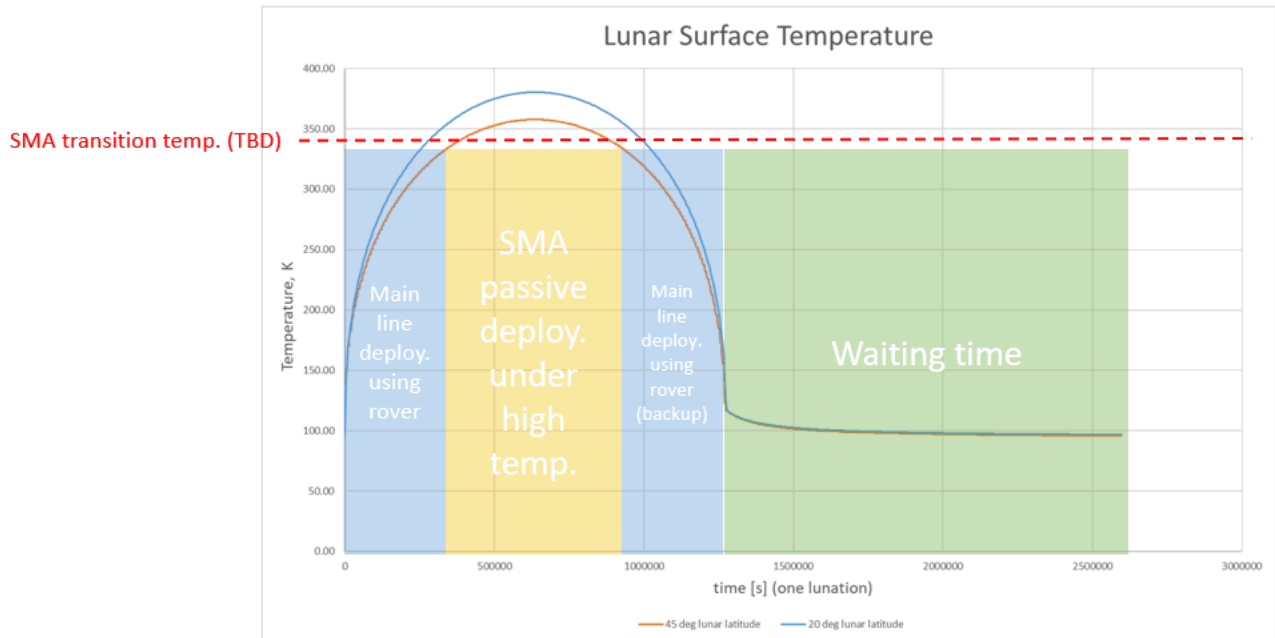


Figure 11-11: Temperature plot on landing sites with proposed phases for passive deployment of payload antennas

11.4 Considerations for scalability

The baseline concept for payload antennas assumes 16 antennas during single EL3 mission, however it seems possible (by mass and volume available on the lander) that larger number of antennas could fit in the single launch. From mechanism point of view there is no major difference in the design of single payload antenna for scenario with 16,000 of antennas (pattern of 128x128) but in this case antenna design starts to affect other subsystems significantly.

The current baseline concept requires large amount of harness which connects antennas to the hub. With a large number of antennas on single EL3 mission the mass of harness becomes unbearable by the lander, also distribution of all antennas will not be possible during single Lunar day (and rover will probably not survive Lunar night). To handle the harness problems it might be useful to reconsider antenna mechanism solution with the use of polyamide film rolls. This concept has several major drawbacks (as described in section 11.3.1.2 but the possibility to reduce the amount of harness might be a design driver. Also using of passive deployment with the use of SMA technology might solve some issues with limited time available for antennas deployment during Lunar day.

For a full scale observatory several EL3 missions will have to be used which implicates that antenna design needs to withstand conditions implicated by landing of next EL3 missions in the close range (especially additional dust deposition).

11.5 Technology Needs

ALO mission is very demanding in terms of size and number of payload antennas needed for fully operational observatory. Deployment of large number of antennas (~16000), without help from humans (astronauts) was never performed even on Earth. In this case the main driving factor for ALO is to choose the optimized solution for payload antennas design and deployment.

The chosen baseline has high TRL for other missions and technology is widely used for space applications. Other trade-off solutions have much lower TRLs and would require intensive development programme.

Technology Needs						
Technology is baselined	Equipment Name & Text Reference	Technology	Supplier (Country)	TRL	Funded by	Additional Information
✓	Cross-dipole antenna	Tubular boom	Astronika (PL), CBK PAN (PL)	5	ESA	TRL 8 for JUICE
	Cross-dipole antenna	SMA tapes	CAI (NL)	3		
	Cross-dipole antenna	Antennas printed on a film	NASA (USA)	3	NASA	
	Cross-dipole antenna	Non-motorized deployment of 4 arms mechanism	DLR (DE), Warsaw University of Technology (PL),	5	ESA	
✓	APM	Dust protection for rotary mechanisms	Leonardo (IT)	5	ESA	

Table 11-5: Technology Needs

This Page Intentionally Blank

12 ROBOTICS

12.1 General considerations and initial assumptions

The overall assumptions and approach is based on ESA system developments of robotic components – however this complexity and scale is unprecedented. Additional influences originate from studies of other lunar exploration activities like the Polar Explorer RD[92].

Initial assumptions	
Ref.	Assumption
1.	Constant rover speed = 360 m/h
2.	One hub consists of 16 antennas and is deployed using a magazine which fits on the rover
3.	Distance between antennas = 5.15 m
4.	Shortest distance from the station to the edge of the antenna matrix = 350 m
5.	Time required to put an antenna on the ground = 0.5 h
6.	Time required to load a magazine onto the rover = 1 h
7.	Rover mass = 350 kg w/o margin

Table 12-1: Initial assumptions

12.1.1 Key drivers and challenges

Key drivers		
Ref.	Key driver	Impact
1.	Estimate deployment time of antennas	Time needed can be very long if a lot of antennas are deployed (16384) and considering that the rover may not be operable during lunar night
2.	Estimate travelled distances of the rover	Distance travelled can be very long if a lot of antennas are deployed (16384)
3.	Number of antennas / rover speed does not allow quick completion of the task	Rover has to survive a lunar night
4.	Required precision in placement or measurement of actual placement of the antennas	Sophisticated deployment/positioning mechanism required and/or high precision rover localisation

Table 12-2: Key drivers

12.2 Baseline description

12.2.1 Approach

In this study, the robotic asset fulfils the role of a logistics element and construction machine. The analysis is based on a step-by-step analysis starting from after landing until the last antenna is deployed. In brief, a rover will carry a magazine with 16 antennas and deploys them step by step, after the magazine is empty it is placed on the lunar surface remaining as hub for the deployed antennas cluster, and then the rover will return to the lander to pick up a new magazine.

12.2.2 High level subsystem components

The major robotic element is the rover. This rover itself is equipped with a robotic arm. Those components are illustrated in detail in the paragraphs below. Strictly spoken the arm and rover are the major concerns from the robotics group but due to the tight system integration and the deployment strategy with a magazine with its own actuators and systems it is listed here as well.

12.2.2.1 Magazine

This is not strictly part of the robotics subsystem or consideration but plays a major role in the development and deployment concept so it is listed here.

Due to the large amount of antennas to deploy and scalability considerations, a magazine based deployment strategy was proposed as baseline for this study. The detailed design of the magazine was not addressed during the study, instead some assumptions were made at system level to allow the assessment and characterisation of the robotic needs.

Table 12-3 summarises the relevant antenna magazine assumptions.

Antenna magazine assumptions	
Ref.	Assumption
1	The magazine is connected to the lander via a harness
2	One magazine houses 16 antennas
3	The magazine dimensions are 1500 x 750 x 750 mm
4	The magazine mass is 108 kg (90 kg + 20% margin)
5	The rover has to carry a single magazine at a time
6	One magazine constitutes 1 row of the 16 x 16 antenna array

Table 12-3: Antenna magazine assumptions

Note that assumption 2 and 6 are listed separately, since the first addresses the number of antennas, while the latter is relevant for the deployment layout.

12.2.2.2 Robotic arm on the rover

Various factors have an impact on the selection of a method for the array deployment. The factors with highest relevance that could be potential showstoppers for the deployment method option are the following:

- Scalability of the mission:
- Whether the deployment subsystem needs to be operational for several missions e.g. for potential array extensions.
- Mass and volume of the magazine:
- The mass and volume of the magazine may vary depending on the array size to be deployed (e.g. 4x4, 16x16, ...)
- Magazine loading from the lander to rover:
- Either the magazine is already mounted on the rover (possibility for single magazine mission) or the rover needs to be capable of fetching magazines from the lander (requirement for multi-magazine mission)

Taking into account these factors, two major options were analysed as possible solutions:

Option 1

The first option is having a dispenser mechanism in the rover that would simply drop the antenna from the rover/magazine directly to the ground. This option would be the simpler approach from the point of view of robotics complexity; however, it would not provide solutions for all the factors detailed above. Going for this option would then require the development of other solutions for the deployment of the magazine from the lander to the rover. In addition, the precision of the planar placement of the antennas would be restricted to the precision of the location of the rover at a given time. Nevertheless, this option is to be further explored in the subsequent studies.

Option 2

The second option is to have a robotic arm mounted on the rover. If dimensioned properly, the robotic arm could provide solutions to all the factors.

In order to have an estimation for the robotic arm size, we have assumed as starting point a robotic arm from a study and concept from the company LEONARDO, the Dextrous Lightweight Arm for Exploration (DELIAN). This robotic arm also served as a starting point for a previous CDF study, Polar Explorer RD[92].

In the DELIAN study, several scenarios were defined for sample acquisition, sample retrieval, and instrument deployment on Moon and Mars.

One of the scenarios was the placement of a 6 kg seismometer in Martian gravity at a distance of 1.7 m from the lander (Scenario B, see Figure 12-1). The arm configuration derived for this scenario was a four degree of freedom arm with 2 m length and 5.1 kg mass. Four families of joints were identified that serve as building blocks for different arm configurations. The joints use brushed DC motors with planetary and harmonic drive gearboxes and are foreseen to be heated through thermistors. The links are made out of titanium.

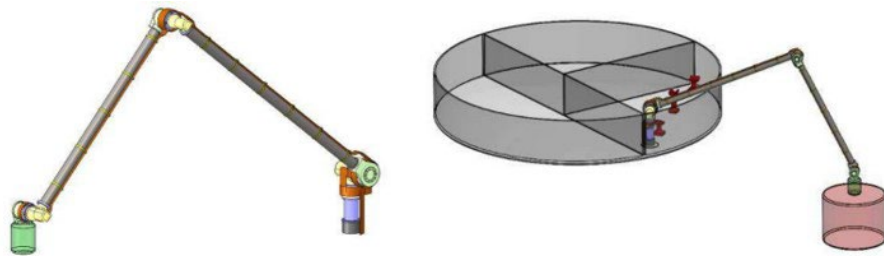


Figure 12-1: DELIAN Scenario B

For end-to-end verification of the arm in laboratory conditions, a development model was designed (see Figure 12-2 and Figure 12-3). Using a deflection compensation algorithm, the arm achieved an accuracy of 4.9 mm and a repeatability between 0.3 and 2 mm RD[85].

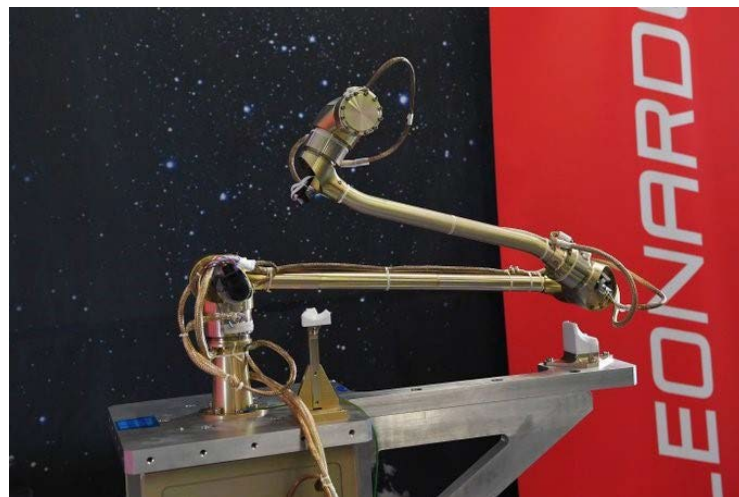


Figure 12-2: DELIAN development model

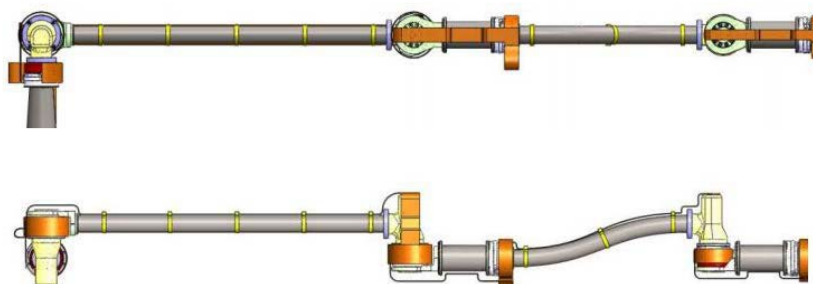


Figure 12-3: DELIAN development model CAD drawing

The relevant DELIAN specifications for Scenario B were taken from RD[86] and are listed in Table 12-4.

Lift Mass	Surface Gravity (Mars)	Arm Length	Reach Distance	First Link Diameter	Min shoulder torque	Motor Mass	Structure Mass	Max power
9 kg	0.379 g	2.0 m	1.7 m	0.037 m	37.9 Nm	2.6 kg	1.6 kg	37 W

Table 12-4: DELIAN Scenario B specifications

To be in accordance with the above factors mentioned for ALO, the scaled robotic arm is required first of all to be capable of operating in a multi-mission scenario, being a requirement to be operational for several years. Secondly, it is required to have a reach of at least 3 meters in order to be capable of reaching the magazine in the lander and carry it to the rover. Lastly, the robotic arm needs to be able to carry up to 108 kg (see Table 12-3) at the maximum reach.

Motor Mass Scaling

According to RD[87], a simple approximate correlation exists between torque T and mass m for the same family of motors:

$$\frac{T}{m^{\frac{3}{2}}} = \text{const.}$$

A scaling factor was determined based on the minimum required shoulder torque to lift a 108 kg payload in Moon gravity at a reach distance of 3 m and was applied to all motor masses. The DELIAN Scenario B motor mass is 2.6 kg. It is also taken into account the scaling of the number of motors. The DELIAN Scenario B has 4 motors while in ALO we are assuming 6 motors in order to provide more degrees of freedom given that multiple different motions are required for the robotic arm (e.g. picking magazine from lander, mounting magazine in the rover, deploying antennas from the magazine). Scaling this up leads to a total motor mass of 22.5 kg for ALO.

12.2.2.2.1 Link Mass and Diameter Scaling

To scale the link mass and diameter, it was assumed that the deflection at the tip of the robotic arm while lifting the desired payload should remain the same. With regard to link stiffness, the arm was modelled as a single circular tube with a 108 kg mass hanging at its end at a reach distance of 3 m. It was assumed that the link material remains unchanged and the inner and outer tube radii are scaled uniformly.

The DELIAN Scenario B structural mass is 1.6 kg. Assuming the bulk of that mass stems from the links, scaling this up leads to a structural mass of 21 kg for ALO. The DELIAN Scenario B first link diameter is 3.7 cm. Scaling this up leads to a first link diameter of 9.5 cm for ALO.

12.2.2.2.2 Motor Power Scaling

Under the assumption that the joint speeds remain the same, motor power is proportional to torque. The DELIAN Scenario B peak power is 37 W. Scaling this up leads to a peak power of 512 W for ALO.

With the scale parameters defined, Table 12-5 includes all the initial specifications of the robotic arm on-board the rover for ALO.

Lift Mass	Surface Gravity (Moon)	Arm Length	Reach Distance	Min Shoulder Torque	First Link Diameter	Motor Mass	Structure Mass	Max power
108 kg	0.165 g	4 m	3 m	525 Nm	0.095 m	22.5 kg	21.0 kg	512 W

Table 12-5: ALO robotic arm up-scaled specifications without margin

The arm total mass is composed of motor mass, structural mass and end-effector mass. The unknown end-effector mass as well as other uncertainties are covered by an additional 20% margin. As a result, the total mass is estimated at **52.2 kg** including margin.

The arm peak power is composed of peak motor power and control electronics power. The unknown control electronics power as well as other uncertainties are covered by an additional 20% margin. As a result, the peak power is estimated at **614 W** including margin. However, if the joints are never used all at once, at maximum torque, this value can be lowered significantly.

Please note that these values are intended as rough estimates. In depth analysis is required for more accurate values.

12.2.2.3 Rover

In this study, the rover has been looked at as a “black box” to carry out the mission. Initial estimates of rover-level volume, mass and power budgets are provided, based on the given mission scenario. These are driven by the high-level rover interfaces with the environment and payloads – driving on the lunar surface, carrying the antenna magazine, and deploying the antennas.

Rovers are complex systems which consist of a multitude of subsystems to fulfil their functionality:

- Structure and Mechanisms
- Power System
- Thermal Control System
- Communication System
- Locomotion System
- Navigation
- Control and Data Handling System
- Payloads

The complete design of a rover would require a separate study by itself, involving specialists for the individual subsystems and disciplines.

In terms of heritage, so far ESA has neither flown nor built a lunar rover. Looking at Mars, the ExoMars rover has been built and qualified and is expected to fly to the red planet in 2022. The Sample Fetch Rover, as part of the NASA-ESA Mars Sample Return programme, is currently being designed. However, the lunar environment differs significantly from Mars, in terms of

atmosphere, temperature, gravity, length of day, distance to earth, etc. Thus, technologies and concepts cannot simply be carried over.

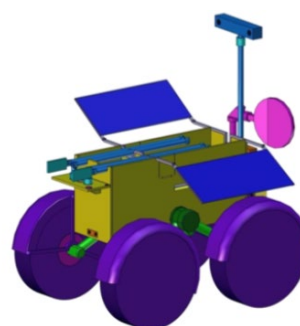
Several early-phase studies involving lunar rover concepts have been carried out by ESA in the past. These can serve as a starting point for more detailed designs in the future. It is worth mentioning the HERACLES CDF study (RD[94], RD[95]), which included a tele-operated rover for lunar surface exploration and sample collection, and the Lunar Volatiles Prospector industry study, which included the Lunar Prospecting Rover (LPR) to drill for ice samples at the lunar poles. A vehicle with a high payload capacity that has already been flown to and operated on the moon is the Lunar Roving Vehicle (LRV) as part of NASA's Apollo missions. Main specifications and illustrations of LRV and HERACLES can be found in Table 12-6 and Figure 12-4.

Rover	Mass (kg)	Payload (kg)	Size (LxWxH) mm	Top Speed (m/s)	Drivetrain power consumption (W)
Lunar Roving Vehicle (LRV)	209	490	3100 x 1830 x 1140	3.61	760 (4 wheel)
HERACLES Surface Mobility Element	506 (17 % margin) Including payload		2000 x 1500 x 1000 Body: (1500 x 520 x 700)	0.84	900 (4 wheel)

Table 12-6: Rover specifications



(a) Lunar Roving Vehicle (LRV)



(b) HERACLES Surface Mobility Element

Figure 12-4: Lunar rover illustrations

Drivetrain Power Estimation

The drivetrain power estimation applies the same approach as the drivetrain power estimation in the LunarCaves CDF of 2021 (RD[93]). Note that this approach is highly dependent on soil properties such as resistances when driving in lunar soft soil. All assumed parameters take the Apollo LRV landing sites as reference, since the lunar properties are well known for that specific location.

Apart from the specific soil properties, the following assumptions were made to enable an estimation of the drivetrain power consumption:

Drivetrain assumptions	
Ref.	Assumption
1.	Assumed mobile mass: 580 kg (rover mass of 350 kg + robotic arm of 43.5 kg + magazine of 90 kg + 20% margin)
2.	4 wheels of 0.81 m diameter and 0.27 m width
3.	Maximum continuous speed: 0.1 m/s
4.	Maximum slope: 5 degrees
5.	Slow accelerations
6.	Contact grousers per wheel: 3
7.	Grouser height: 0.01 m

Table 12-7: Drivetrain assumptions

The “mobile mass” is composed of a rover (i.e. mobile platform including avionics), a robotic arm (Section 12.2.2.2) and an antenna magazine (Section 12.2.2.1), and includes a 20% margin. The number of wheels and wheel dimensions in assumption 2 are taken from the Apollo programme’s Lunar Rover Vehicle (LRV).

The drive train power estimation from the LunarCaves CDF is based on the highly parametrized computations according to RD[88] which in turn are based on the normal and shear stress-based Bekker model RD[89] for traction in soft soils. As previously stated, this approach has been informed by the LRV data; a rover of reasonably similar dimensions. Note that the computations are highly dependent on soil properties. In the present calculations, these are taken from LRV landing sites, but they may deviate from the ALO landing site to an unknown extent. It is also assumed a maximum of 5 degree slope for the surface for the antenna array deployment and therefore rover traversable area.

Parameter	Symbol	Value	Unit
Number of wheels	n	4	-
Vehicle mass	m	580	kg
Vehicle speed	v	0.1	m/s
Wheel nominal width	B	0.27	m
Wheel diameter	D	0.81	m
Contact grousers per wheel	N_g	3	-
Grouser height	h	0.01	m
Slope angle of the ground	θ	0.08726	rad
Gravitational acceleration	g	1.63	m/s ²
Soil cohesion	c	170	N/m ²

Internal friction angle	φ	0.610865	rad
Shear deformation slip modulus	κ	0.018	m
Soil specific mass	γ	1680	kg/m ³
Modulus of cohesion of soil deformation	k_c	1400	Pa/m ^{n'-1}
Modulus of friction of soil deformation	k_φ	820000	Pa/m ^{n'}
Soil deformation exponent	n'	1	-
Coefficient of passive earth pressure	n_c	1.5	-
Coefficient of passive earth pressure	n_γ	25	-

Table 12-8: Model inputs for rover drivetrain power estimation

The estimation is based on the tractive wheel thrust H needed to overcome resistances R when driving in soft soil. The resistances taken into account here are compaction resistance R_c due to load sinkage of the wheels, bulldozing resistance R_b due to soil displacement in front of the wheels, and gravitational resistance R_g when driving up slopes. Effects of slip-induced sinkage and multi-passing of the wheel tracks are neglected. In a steady state (no acceleration or deceleration), wheel thrust is equal to the sum of the resistances:

$$H = R_c + R_b + R_g$$

This thrust relates directly to the output torque per wheel as:

$$\tau_w = \frac{H D}{n 2}$$

with n the number of wheels and D the wheel diameter. Thrust can only be generated when there is slip between wheel and ground. The ideal tractive thrust available H_0 for a wheel can be evaluated given the wheel geometry and the soil parameters. The wheel slip S can then be computed by numerically solving the thrust slip relationship, generically written here as $H = H_0 \cdot f(S)$, for S . This leads to an angular wheel velocity of:

$$\omega = \frac{v}{1 - S} \frac{2}{D}$$

for a given vehicle speed v . The output power for all wheels combined can then directly be computed as:

$$P_{out} = n \tau_w \omega.$$

Evaluating this for the given inputs leads to an output power of $P_{out} \approx 25 \text{ W}$. However, since we are interested in the power consumption of the electric motors, additional friction losses in bearings and gears as well as the motor efficiency need to be taken into account. From RD[90], estimates on the gearbox efficiency in a cold environment were taken to be around 50 % and an ECSS friction factor of 1.5 is applied (RD[91]). A motor efficiency of 80 % is assumed. This leads to an overall efficiency of approximately 25 %, or an efficiency factor of 4, and thus to an input power of:

$$P_{in} = 4 \cdot P_{out} \approx 100 \text{ W}.$$

On top of this, a system margin of 20% is applied, leading to a final estimated drive train power consumption of:

$$P_{drive_train} = 1.2 \cdot P_{in} \approx 120 \text{ W}.$$

The power consumption scales linearly with the vehicle speed and also approximately linearly with the vehicle mass.

Preliminary rover characteristics estimations

Assuming a 16x16 array deployment with magazine containing 16 antennas:

Preliminary robotic elements characteristics	
Ref.	Robotic elements characteristics
1	Rover mass: 420 kg incl. 20% margin
2	Payload capacity: 160 kg (robotic arm + magazine with 16 antennas incl. 20% margin)
3	Mobile robotics total mass: 580 kg incl. 20% margin
4	Size: 2200 x 2000 x 1000 mm
5	Maximum driving power consumption from drivetrain: 120 W (estimated incl. margin)
6	Maximum power consumption on robotic arm operation: 614 W (estimated incl. margin)

Table 12-9: Preliminary robotic elements characteristics

12.2.3 Deployment steps

12.2.3.1 Egress from the lander

The baseline of the mission is to use the EL3 Lander. This means that the rover needs to be deployed to the lunar surface from a height of 3 meters. There are several concepts from cranes to ramps with rails and rope systems which would allow the rover to reach the lunar surface. In this study however, the exact mechanism is left open.

In the Polar Explorer study (RD[92]), which is also based on the EL3 lander, a spring-loaded passive mechanism is presented for deploying a 330 kg rover. The rover, sitting on a deployment platform or attached to cables on the side, is lowered vertically to the surface. Figure 12-5 shows an illustration of the deployment steps. The solution is simple, robust and lightweight and uses space-qualified components. Compared to more complex deployment solutions like a robotic arm; however, the deployment location next to the lander is fixed, which could be a risk in the presence of large boulders.

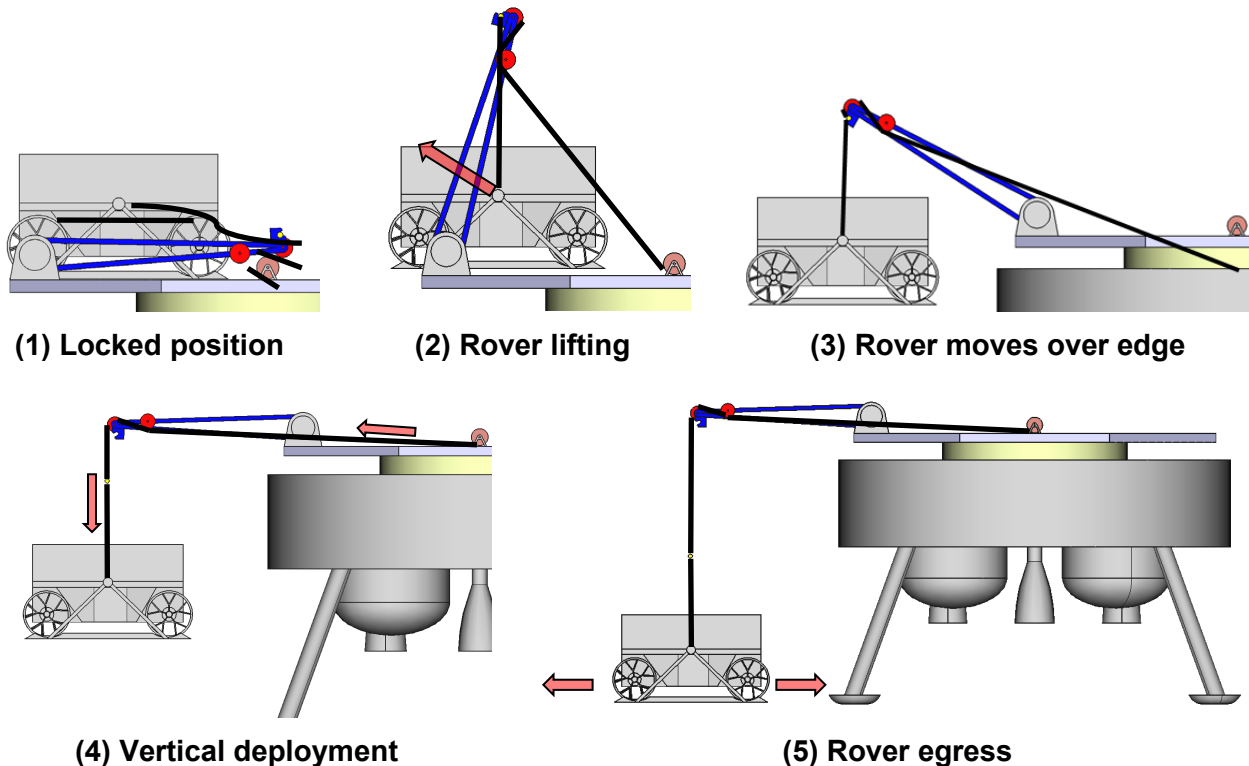


Figure 12-5: Spring-loaded rover deployment mechanism

Other options for rover deployment include ramps and robotic arms or cranes. Due to the height of the lander, regular ramps that allow the rover to drive down to the surface unaided would be long and heavy, needing significant stowage space and an unfolding mechanism. Shorter ramps on the other hand would be very steep, needing additional arresting devices on the rover to safely descend from the lander.

A robotic arm or crane would be the most flexible solution to deploy the rover to a suitable spot on the surface. Its drawbacks are a complex design with multiple motorized joints and a heavy structure to support lifting and moving the rover weight. However, synergies of such a solution could be exploited, if the robotic arm is also used to deploy the antenna magazines from the lander to the rover during its surface operations (see Section 12.3.1).

12.2.3.2 Loading the magazine onto the rover

The rover will load a magazine, deploy the antennas from inside that magazine, and return to the lander to load another magazine. With the issue risen in the previous step of the lander height, a more detailed trade-off is presented in Section 12.3.1; here we will describe the concept that assumes the loading of the magazines onto the rover is performed with a robotic arm that is part of the rover itself.

12.2.3.3 Antenna deployment

With the rover on the lunar surface, the antennas need to be deployed in an optimal way to save energy and operating time. In the following, estimates on the travelled distance are made

by analysing a baseline deployment. A second approach is also presented in Section 12.3.2 as an alternative. In both cases, the rover will deploy antennas one magazine at a time before returning to the base station to repeat the process. It is assumed that the distance between the antennas is constant and that the rover will travel at a fixed speed of 360 m/h. The tool that was used to calculate the deployment time was a python script written in Jupyter Notebook. A number of assumptions were parametrized which are summarized in the Table 12-1.

For the baseline deployment, a matrix of dimension $[m, a+1]$ is deployed with m being the number of magazines and a being the number of antennas in a magazine. For example, if 64 antennas are to be deployed, the resulting matrix will have a dimension of $[4,17]$ as shown in Figure 12-6 below.

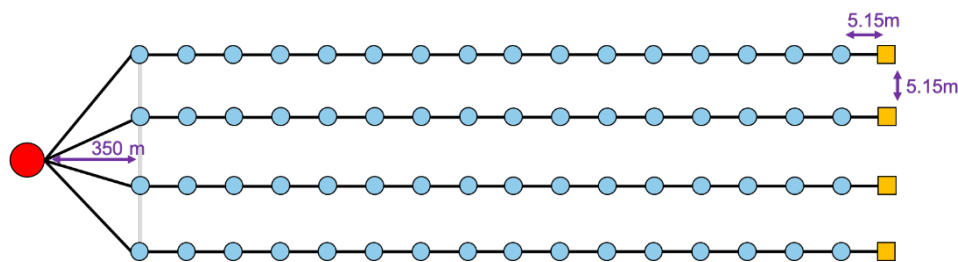


Figure 12-6: Illustration of the deployment pattern
(red: lander, blue: antennas, yellow: magazines)

Table 12-10 shows the travelled distance and the necessary deployment time for different number of antennas. The advantage of this scenario is that the deployment is very simple as the rover has to perform the same task a number of times. This makes the approach very scalable where several EL3 missions can be planned to lay out several matrices of different dimensions.

Matrix dimension	1x17	4x17	16x17	64x17	1024x17
Total antennas	16	64	256	1024	16384
Total distance	0.865 km	3.5 km	13.9 km	57 km	3021.8 km
Total time *	11.9 h	47.6 h	190.5 h	766.2 h	18121.8 h
	0.5 Ed	1.9 Ed	7.9 Ed	31.9 Ed	755.1 Ed
	0.02 Ld	0.07 Ld	0.28 Ld	1.14 Ld	26.97 Ld

* Measured in Earth days (Ed) and Lunar days (Ld)

Table 12-10: Estimated travel times and distances

12.2.3.4 Unloading the Magazine

After all antennas have been deployed, the magazine also needs to be placed on the lunar surface to remain as hub for the deployed antennas cluster.

If the loading of the magazine is done with a robotic arm on the rover, the unloading follows the same approach. But, as described in the robotic arm trade-off (see Section 12.3.1), when

the rover is not equipped with a strong arm, the magazine unloading has to be solved with different means, e.g. simple mechanism on the rover or the magazine itself.

With this action, the magazine deployment cycle is complete and can be repeated by driving back to the lander and loading a new magazine onto the rover.

12.2.4 Other considerations

12.2.4.1 Autonomy and teleoperation

During the study the discussion on the technical challenges of the deployment strategy were dominant, assessing the problem only at conceptual level. This assessment did not cover the challenges of making this system autonomous or remote operable.

12.2.4.2 Number of rovers

The enormous scale of the full-fledged mission with more than 16000 antennas, corresponding to more than 1000 magazines would require a lot of time for deployment. Therefore, it could be considered to deploy more than one rover in multiple missions to speed up the process and have redundancy in case of failure.

12.2.4.3 Positioning accuracy

One of the major challenges to ensure a good performance of the array (see sections 4.2.3.6 and 4.2.3.7) is to have for each antenna:

- An exact placement and alignment within 0.5 m and respective 1 degree

Or

- A placement within 0.5 m and an alignment of less than 10 degrees which is coupled to an accurate measurement that corrects the inaccuracies (by calibration) to less than 1 degree

To follow with either way, the rover would not only need high precision robotics but also self-localisation within the described parameters. A lunar sat-nav system would be essential here (and is already part of other ESA studies, for example, RD[62], RD[63]).

12.2.4.4 Maintenance of the array

Initial consideration saw the robotic element also as a means to perform maintenance operation on the array. However, with the highly integrated modular approach and the limitations of robotics to perform the required tasks, it has been discarded at the current stage.

12.2.4.5 FARSIDE comparison

NASA's FARSIDE study RD[32] is summarised to have a point of reference on how other institutions would develop a rover to deploy antennas on the moon. A considerable advantage for NASA's development is that they have a remarkable background on developing robotic systems for planetary surfaces. The successful deployment of the Apollo Lunar Roving Vehicle

and their five Martian rovers, all add to a knowledge base that gives them a clear advantage to design a robust and reliable system for a lunar observatory.

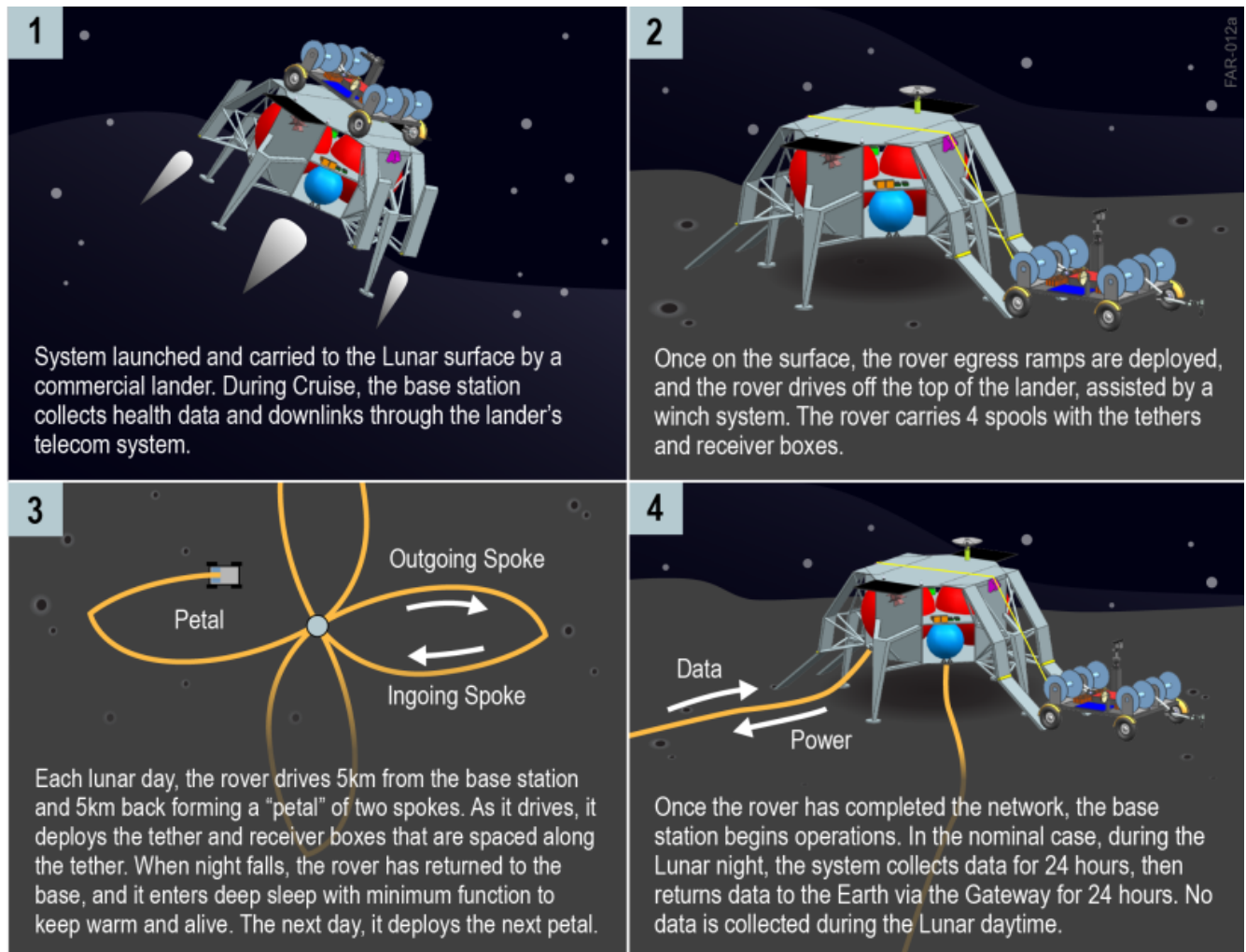


Figure 12-7: Four main stages of the deployment in the FARSIDE study RD[32]

The four main stages of the proposed deployment are summarised in Figure 12-7. A base station is used to provide power from a nuclear energy source, which is needed to survive lunar nights. The station also ensures signal processing and telecommunication via the Lunar Gateway back to Earth. The rover is deployed to the lunar surface via ramps and winch systems, and is designed to install a total of 128 antennas over a distance of 40 kilometres. The antennas are embedded within a tether that connects each node to one another and transports power and signals from the base station. As the rover follows a petal configuration on the landing site, the tether is unrolled and the antennas are deployed using a spring so that no robotic arm is required.

One major question that the FARSIDE study leaves unanswered is how the antennas are actually stored on the roles to assess feasibility regarding e.g. the potential volume and mass of each role in stowed configuration, but also in general to compare this deployment strategy with the magazine-based one.

A summary and comparison of the robotic concepts for this study is given in Table 12-11.

FARSIDE	ALO CDF
No robotic arm	Robotic arm
128 antennas in total	16 antennas for first deployment
Not suitable for scalable deployment	Designed for scalable deployment
Petal shape deployment	Matrix deployment
No hubs	1 Hub serving 16 antennas
Time: 4 lunar days to install 128 antennas	Time: 0.02 lunar days to install 16 antennas
Driving speed: 78 m/h	Driving speed: 360 m/h
Distance travelled: >40 km	Distance travelled: 865 m
Total mass: 420 kg	Total mass: 580 kg
Power consumption from drivetrain: 275 W	Power consumption from drivetrain: 120 W Power consumption for robotic arm operation: 614 W
Size: No specification	Size: 2200 x 2000 x 1000 mm

Table 12-11: Comparison of the robotic requirements with the FARSIDE study

12.2.5 List of Equipment

This section lists the components under the robotics domain. Note that, same as in the rest of the report, the rover denotes the mobile roving platform. The arm and magazine masses are not included in the “rover” mass, but are instead added on top.

Unit	#	Size [mm]	Nominal Mass [kg]	Power Consumption [W]
Rover	1	2200 x 2000 x 1000	420	120
Robotic arm	1	5000	52.2	614

Table 12-12: List of Equipment

The TRL levels and heritage considerations are listed alongside the other driving technology needs in Section 12.5.

12.3 Trade-Offs and alternative options

12.3.1 Robotic arm types on lander and rover

The large versatility of a robotic arm allows to study the possibility of having one on the lander, on the rover, or even on both. To assess the pros and cons of the three options, a trade-off was carried out.

The first option is to have a single, small robotic arm on the rover. This arm would need to be able to carry the weight of a single antenna (including the weight of the respective harness)

and then place it in a precise location on the ground. This translates into a robotic arm with a lifting capacity of around 5 kg and an arm length of up to 2 meters. Having an arm of this size on a rover is a viable solution for setting up the antennas, but it does not solve the two problems of deploying the rover to the ground, and in a later stage, loading the magazines on the rover itself. Nevertheless, this option could be ideal, if in a later stage of the development of the mission, solutions were found to deploy the rover and load the magazines.

The second option is to have a large robotic arm mounted on the rover. It would be responsible to not only carry the magazines from the lander to the rover, but also to deploy the antennas. For these purposes, it would need to be dimensioned to carry magazines up to 108 kg and have a reach distance of at least 3 m to reach them on the lander. Even though the problem of rover deployment is not addressed, this option was selected to provide specifications of a rover robotic arm (see Section 12.2.2.2). An important driver for this option is that from the point of view of mission scalability, the rover would be a stand-alone solution to load the magazines from the lander.

The third option is to have a mixed approach of having a heavy robotic arm mounted on the lander and a specific antenna deployment mechanism on the rover or the magazine itself. The robotic arm on the lander would be responsible to carry the magazine from the lander to the rover and also to deploy the rover. For these purposes, it would need to be dimensioned to carry a rover of at least 420 kg and be able to reach a distance of at least 3 m in order to place the magazine properly on the rover. It should be noted that this reach distance may be dependent on the mounting location of the robotic arm on the lander. To deploy the antennas on the ground, a different solution such as a dispenser mechanism (if on the magazine) or a smaller robotic arm (if on the rover) would be required. Opting for a dispenser mechanism, the antenna deployment would have the disadvantages inherent to this approach mentioned in Section 12.2.2.2. On the other hand, opting for a smaller robotic arm in the rover would increase the robotics complexity for the mission, as more points of failures are added to the lander and rover systems. Even though this option of having two different systems for the deployment of magazines and antennas was not selected for further investigation, in a later stage of the development, it might be a useful alternative.

12.3.2 Different deployment pattern

Another way to deploy the antennas is by following a different matrix shape where the number of columns is fixed and the number of rows varies according to how many antennas should be deployed. If, for example, 64 antennas should be deployed in a matrix of eight columns, nine rows are needed as shown in Figure 12-8.

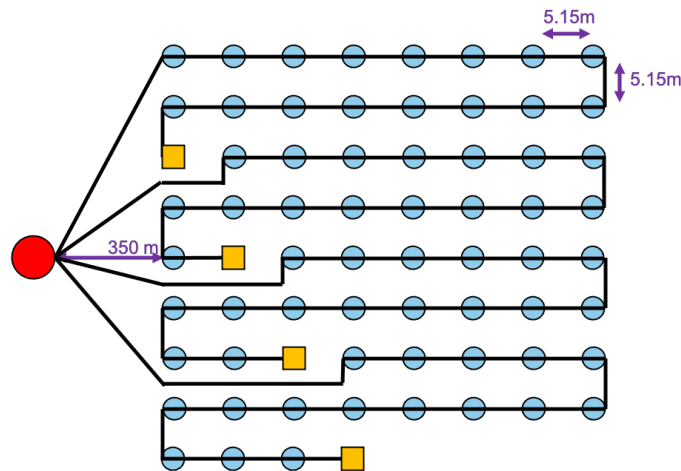


Figure 12-8: Illustration alternative deployment pattern
(red: lander, blue: antennas, yellow: magazines)

Table 12-13 summarizes the travelled distances and required deployment times with the second approach. For this alternative scenario, more control over the shape of the matrix is obtained. In contrast to the baseline deployment, where each row had exactly one magazine, this design lets the operator choose the number of columns and adjust the number of rows.

Matrix dimension	5x4	9x8	17x16	34x32	136x128
Total antennas	16	64	256	1024	16384
Total distance	0.783 km	3.2 km	13.9 km	61.1 km	1582.2 km
Total time *	10.7 h	45.9 h	189.5 h	776.6 h	14122.1 h
	0.4 Ed	1.9 Ed	7.9 Ed	32.4 Ed	588.4 Ed
	0.02 Ld	0.07 Ld	0.28 Ld	1.16 Ld	21.02 Ld

* Measured in Earth days (Ed) and Lunar days (Ld)

Table 12-13: Estimated travel times and distances for alternative deployment approach

Both approaches lead to a similar deployment time for a given number of antennas.

12.4 Considerations for scalability

The deployment strategies were to a large extent driven by scalability considerations. All further work, robotic element selection and sizing, served to conceptualise potential solutions to this end.

Several calculations were made to deploy the antennas in different configurations. Table 12-10 and Table 12-13 summarise these findings and give indications on how the observatory can be scaled to larger arrays with more antennas.

12.5 Technology Needs

Technology Needs						
Technology is baselined *	Equipment Name & Text Reference	Technology	Supplier (Country)	TRL	Funded by	Additional Information
✓	Antenna magazine	N/A	N/A	-	N/A	To be developed from scratch
✓	Moon rover	Lunar Prospecting Rover	Airbus (UK) / TAS-I (Italy)	2	ESA industry study	Individual components might be higher TRL
✓	Heavy duty robotic arm	DELIAN	Leonardo (Italy) / RUAG (Switzerland)	3	ESA TDE activity	Development of stronger actuators for heavy duty arm
	Light weight robotic arm	DELIAN	Leonardo (Italy) / RUAG (Switzerland)	4	ESA TDE activity	Qualification for long-duration moon operations needed
✓	Rover-based payload deployment operations	ROBEX Demonstration Campaign	DLR	3	Helmholtz Association	Deployment of seismometer payload with full ground contact in specific orientation

Table 12-14: Technology Needs

13 THERMAL

The objective of the Thermal Control System (TCS) is to guarantee that all units, equipment, parts and components remain within their design temperature ranges during the mission lifetime. Within this chapter the TCS for ALO mission is presented.

13.1 General considerations and initial assumptions

ALO consists of an array of Antennas connected to the Hub which is connected to the Base module. ALO is planned to operate on far side of the Moon. The location chosen for the study is Tsiolkovskiy crater (20.46° S, 129.06° E). The observatory operates during the lunar day and is OFF during the night (with the exception of few units that may be ON in the Base unit). Planned mission duration is 4 years.

The Antennas and the Hub are directly placed on the lunar surface. The Base is located on top of LDE. Due to its location, it is assumed that the TCS needed for the Base will be very similar to the TCS designs for others EL3 missions, which will be launched before ALO. Therefore the sizing of the Base TCS is based on TCS sizing done for one of the previous studies (Polar Explorer RD[92]).

Initial assumptions	
Ref.	Assumption
1.	ALO location: Tsiolkovskiy crater (20.46° S, 129.06° E).
2.	ALO operates during lunar day, observatory is OFF during lunar night.
3.	Rover and harness TCS is not part of ALO study.
4.	Antennas and hubs are directly placed on the lunar surface, Base is located on top of LDE.
5.	Separate TCS for each unit: antenna, hub, base.
6.	Base TCS design: re-use of TCS designed for previous EL3 missions (which will be launched before ALO).
7.	Lunar surface temperature (Tsiolkovskiy crater location): 380K at noon, 80K during the night.
8.	Thermal surfaces: optical properties are degraded due to the presence of the lunar dust.

Table 13-1: Initial assumptions

TCS sizing is done separately for:

- Antenna
- Hub
- Base

With this approach TCS-related budgets can be easily scaled to the final size of the mission.

TCS for the rover and possible thermal behaviour of the harness between the Antennas, Hub and Base are not assessed in this study.

13.1.1 Thermal lunar surface conditions

The temperature on the surface of the Moon ranges from 30 K in permanently shadowed craters at the poles to about 395 K at the sub-solar point on the lunar equator [RD[96] & RD[97]]. The lunar regolith works as an insulating blanket that covers the Moon. It has a very low thermal conductivity ranging from 0.009 W·m⁻¹·K⁻¹ to 0.035 W·m⁻¹·K⁻¹ [RD[98], RD[99], RD[100]] depending on temperature, local density and mineralogy. The regolith furthermore has a high solar absorptivity of around 0.7 to 0.9 [RD[97], RD[101]] and an emissivity of about 0.92 to 0.98 [RD[97], RD[101]]. Thus the Moon is almost a black body from a thermal perspective with a poor thermal transport on its surface. On top of that, the axis of rotation of the Moon is only inclined by about 1.5 deg, which leads to almost no seasons. The Moon is in a bound rotation with the Earth which leads to a total duration of a lunar day of approx. 29.5 Earth days. The Moon does not have an atmosphere to buffer heat exchange with deep space.

All the factors mentioned above lead to the yields in the fact that the temperature of the lunar surface is driven mainly by the local angle of incident of the Sun. Due to the poor thermal conductivity and the low rotation speed of the Moon, the local temperatures can be assumed to be steady state at any given moment in time with good approximation for the purpose of thermal engineering. This also shows the impact of the local topography on the to-be-expected temperatures. Although global maps of the Moon show a decrease in temperature towards the lunar Poles (see Figure 13-1), local temperatures are dominated by the angle between the local surface normal and the angle of incidence of the Sun.

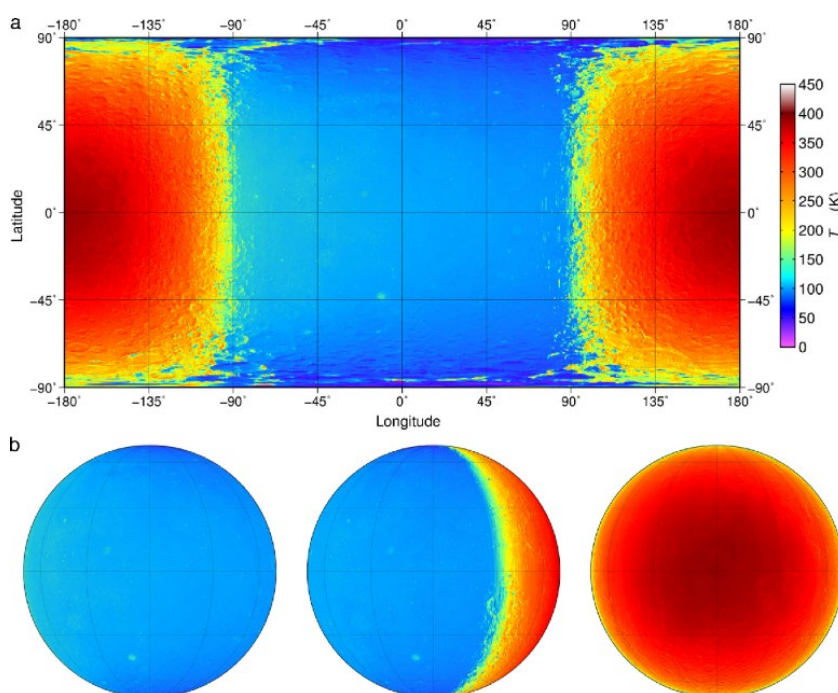


Figure 13-1: Temperature of the Moon as derived by Lunar Reconnaissance Orbit (LRO) Diviner instrument data [RD[102]]

Lunar surface temperature in the location of interest

For ALO study, the temperature of lunar surface in Tsiolkowsky crater has been calculated. The calculation is based on simplified models. The temperature profile is presented in Figure 13-2. As the landing site is located relatively close to the equator, there is a big difference

between surface temperature during the day and night: the temperature rises during the lunar day up to 380K and during the night it drops to 80K. Those extreme temperatures are going to be used for TCS sizing.

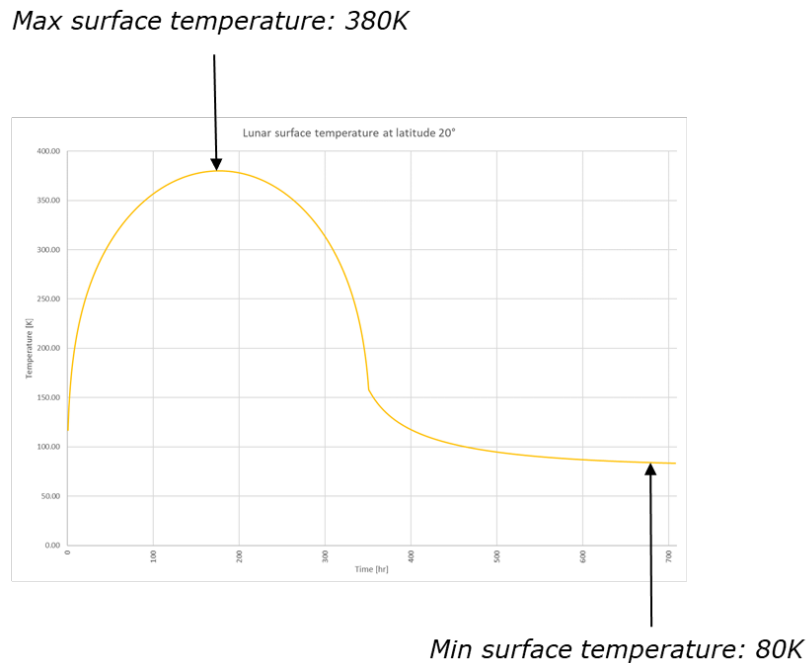


Figure 13-2: Calculated lunar surface temperature profile in Tsiolkowsky crater

13.1.2 Impact of lunar dust on TCS

The challenges of lunar dust in the return to the Moon have been addressed by many authors. For the thermal control subsystem, the biggest impact is the degradation of optical surface properties, such as radiators and MLI outer layers. There are several reports from the Apollo and Luna missions of degradation of radiator performance due to lunar dust, as shown for example in Figure 13-3 on the left for the radiator of the Lunar Roving vehicle. It was also reported how suits of the Apollo astronaut were covered with lunar dust, degrading the optical surface properties (Figure 13-3 on the right). In studies performed to investigate the impact of lunar dust on radiators [RD[103]] it was identified that even small sub-mono layers of lunar dust (simulant material) increased the absorptivity of white paint and second surface mirrors.

To include this effect in ALO TCS sizing, following materials have assumed degraded optical properties: Antenna radiator and external MLI layer for all elements. Detailed values are presented in the baseline TCS description section.



Figure 13-3: Left: Dust on the radiator of the Lunar Roving Vehicle; Right: Impact of lunar dust on the spacesuits of astronauts during Apollo; (credit: NASA)

13.1.3 Key drivers and challenges

ALO needs to survive over its 4 years mission lifetime the cycles of changing thermal conditions between the lunar day and night, including a surface temperature variation of about 300K.

During the lunar day ALO units need to survive long exposure to the Sun and high lunar surface temperatures. Moreover, they need to be able to reject the heat created during their operations not to overheat any of the internal units. Lunar day environmental conditions and the need to reject dissipated heat (to keep the units below their maximum operating temperatures) drive the radiator size needed for each unit.

Especially important for ALO is the survival of the lunar night, which lasts around 350 hours, and the surface temperature drops to 80K. During this time the units of ALO mission need to be kept above their minimum temperature limits. Both lunar night conditions and units thermal requirements (especially minimum temperature) are main drivers of TCS design: they define the need for heating power and thermal insulation from the environment.

TCS design for lunar day and TCS design for lunar night cannot be considered and sized separately: during the lunar night the heating power needs to be high enough to also cover the losses through the radiator. Therefore the bigger radiator is needed, the need for heating power increases. The final TCS design must be a balance between the rejection capabilities during the lunar day and the heating power needed for lunar night survival.

Key drivers		
Ref.	Key driver	Impact
1.	Lunar night conditions: low surface temperature and long night duration	Heater power needs for lunar night.
2.	Lunar day conditions: high surface temperature and long exposure to solar flux	Radiator sizing.
3.	Units thermal requirements	Radiator sizing and heater power needs for lunar night.
4.	Internal dissipation	Radiator sizing.

Table 13-2: Key drivers

13.2 Baseline Description

TCS is designed to keep all units and equipment within their allowable temperature ranges, during all phases of the mission, with minimum heater power and as low as possible mass of the system.

In ALO CDF only high level design is done: no specific geometry of antenna, hub and base have been provided to include it in the initial TCS sizing.

Therefore, each unit is defined as a “box” covered with MLI and with a radiator placed on top of it. This assumption allows to calculate basic budgets: first estimation of the mass of thermal hardware and the input to power budget for lunar night.

TCS sizing has been done in two steps for each ALO unit: first, the radiator size for lunar day operations has been estimated and then the heater power needed for lunar night has been calculated.

Radiator sizing for operations during lunar day

To size the radiator, not only internal dissipation and heat rejection to the deep space have been taken into account, but also the heat exchange with environment including:

- Solar flux reaching the radiator;
- Heat exchange between MLI and deep space;
- Heat exchange between MLI and lunar soil.

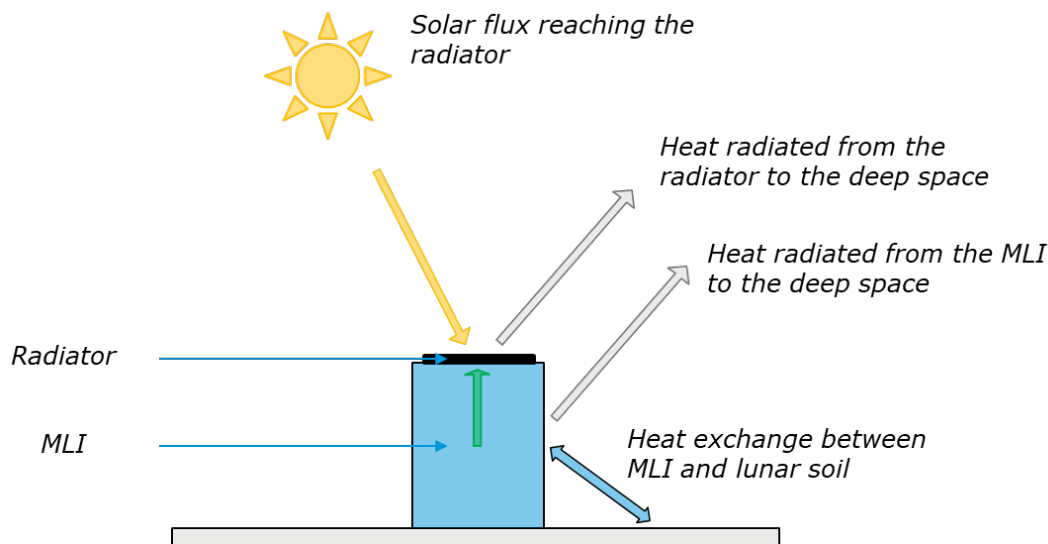


Figure 13-4: TCS sizing: Heat exchange during lunar day

To size it for the worst hot conditions (highest surface temperature (380K) and solar flux to the radiator), radiator sizing is done at lunar noon.

Heater power estimation for lunar night

Once radiator size is calculated, the heater power for lunar night survival is estimated.

In the heater power estimation, the following heat exchange is taken into account:

- Heat radiated from the radiator to the deep space;
- Heat exchange between MLI and deep space;
- Heat exchange between MLI and lunar soil.

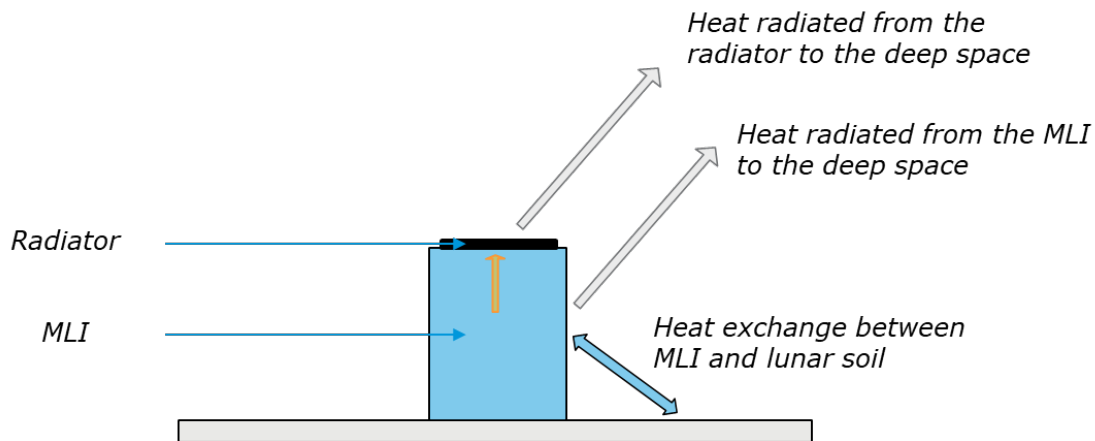


Figure 13-5 TCS sizing: Heat exchange during lunar night

Heating needs are calculated with the assumption that the temperature of the lunar surface is 80K.

13.2.1 Antenna

As explained previously, in this iteration, the antenna unit is assumed to be a box with some electronics inside. Antenna booms are not taken into account in the TCS sizing. The dimensions of the antenna body are 0.2x0.2x0.2m³.

Currently, there is no plan to place batteries inside the antenna. It includes only LNAs and RFoverFiber transmitters. Because of that, it is assumed that the antenna can survive in relatively large thermal range: from maximum operating temperature of 52°C to minimum non-operational temperature of -100°C. The temperature requirement for antenna is based on data collected in ESA activity: Low Temperature Electronics - Thermal Design for future exploration missions SD3 (completed in 2018, Table 13-3).

Mission	Non-operaitonal	Operational
James Webb Telescope		39 K (NIRCam, NIRSpec, FGS/NIRISS) 7 K (MIRI)
Mars Exploration Rovers (outside Rover's warm box)	-110°C to +55°C	-90°C to +40°C, -110°C to +45C (CCDS)
New Horizons (outside warm box)		-100 °C (LORRI) -140°C(LEISA) -100°C (CCDs)

MSL	-120°C to +20°C	-70°C to + 50 °C
MARS 2020	-128°C to +50°C	-55°C to +70°C
Exomars	-120°C to +60°C	-120°C (Optical Head)
Gaia	-110°C	-100°C
Euclid		100 K (detectors) 240K (warm electronics)
HP3	-115°C to 55°C	-45°C to 55°C

Table 13-3: Most significant or extreme temperature values of the missions included in ESA Study: Low Temperature Electronics - Thermal Design for future exploration missions SD3 [RD[104]]

The Antenna box is going to be placed directly on the lunar soil. In order to limit the heat flow between the Antenna and the soil, it is assumed that it will have some small structure support, made from low conductive plastic (for example PEEK, Vespel, Glass Fibre). The exact shape and location of it (if inside or outside of antenna MLI) are not defined in this study – only a thermal link representing reduced connection to the lunar soil is included in the calculations.

To provide heating capability during lunar night, kapton heaters are foreseen in the Antenna design.

Thermal hardware to be used with its properties is summarised in the table below.

Thermal Hardware	Description
MLI	MLI with $\epsilon^* = 0.1$ is assumed for the Antenna. The external MLI layer has a degraded IR emissivity (dust influence taken into account): value 1.0 is used. This value represents all materials that have high epsilon value (Kapton, Black Kapton, Stamet, BetaCloth). Final external layer selection can be chosen based on electrical conductivity needs or solar absorptivity value needed (this value is not used in initial sizing as no solar flux on MLI is calculated). MLI area: 0.24m ² .
Radiator	Radiator is covered with OSR: in the calculations degraded optical properties are assumed UV absorptivity = 0.4 and IR emissivity = 0.9. In case of the radiator, its degraded emissivity actually improves its performance – but the degradation of alpha resulting in increased absorbed solar flux influences more the final radiator performance. Radiator area: 0.036m ² .
Thermal washers/support isolating structure	A structure or simple stand-offs made from low conductive material are foreseen to limit the direct contact of the Antenna with lunar soil. In current iteration it is included by adding very small conductive coupling between lunar soil and the Antenna interior.

Heaters	Kapton heaters are foreseen for lunar night survival as the baseline option. Electric power is assumed to be available from the Hub element. Other option for lunar night heating would be RHU: however as a baseline heaters are considered due to their higher TRL and the fact that it can be easier to accommodate them inside the Antenna and they do not provide waste heat during lunar day. 4 heaters are foreseen: 2 nominal + 2 redundant.
Thermocouples	Thermocouples are foreseen for temperature monitoring inside the antenna. 6 thermocouples are included in initial TCS budget.
Internal Units TCS (paints, washers, thermal fillers)	In the thermal budget 0.1 kg is foreseen for TCS for internal Antenna units.

Table 13-4: Antenna Thermal Hardware

A detailed list of equipment, its mass and heating power needs are included in Table 13-7.

13.2.2 Hub

The Hub is going to be used to store antennas during the cruise to the Moon. After the Antenna array deployment, it will be used to distribute power and to transfer the data between Antennas and the Base.

In case of the Hub, the initial TCS design described previously applies. However, because part of the Hub will be empty after the Antennas deployment, only 25% of its volume is assumed to be thermally controlled. In the controlled volume there will be various electronics and possibly some batteries.

The temperature requirement for the Hub is assumed to be from maximum operating temperature of 30°C to minimum temperature of 0°C. This requirement is driven by the batteries, which have relatively narrow operating thermal conditions comparing to other equipment.

To optimise the radiator size and its performance, it is assumed that the radiator area is divided into two identical radiator panels mounted on the top of the Hub. They are slightly inclined to improve their performance: having two parts of the radiator, which are inclined in different directions decreases the area with worst thermal performance at a time. Therefore, during the lunar day while one part of the radiator is illuminated by perpendicular solar rays (in this set up the biggest amount of solar flux is absorbed), the other half is facing the other direction, so the angle between the solar rays and the radiator surface results in smaller amount of absorbed solar flux. The overall balance of the absorbed/rejected heat flux is better than for the configuration with one “flat” radiator: by absorbing less solar flux, more internal heat can be rejected to the deep space.

Also the configuration with 2 symmetrical inclined radiators is not influenced by the direction of how the Hub is oriented: inclined radiators will keep their overall improved performance with comparison to the one flat radiator configuration. As a baseline, inclination angle of 25° is chosen for the radiators. While sizing the radiators, it is assumed that there are no obstacles around the Hub that could influence the performance of the radiators.

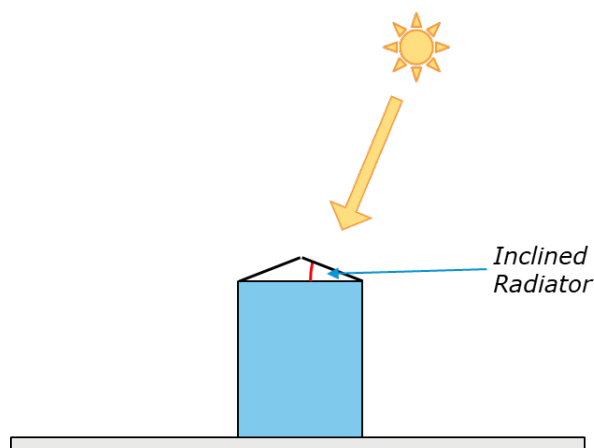


Figure 13-6: Inclined radiators configuration

For lunar night survival, louvres above the radiators are baselined in order to reduce heater power need. As a baseline, use of Kapton heaters is assumed. However, if needed, RHUs can be used inside the Hub as well.

Thermal hardware to be used with its properties is summarised in the table below.

Thermal Hardware	Description
MLI	<p>MLI with $\epsilon_{\text{ps}}^* = 0.05$ is assumed.</p> <p>The external MLI layer has degraded (dust influence taken into account) IR emissivity: 1.0 is used. This value represents all materials that have high epsilon value (Kapton, Black Kapton, Stamet, BetaCloth). Final external layer selection can be chosen based on electrical conductivity needs or solar absorptivity value needed (this value is not used in initial sizing as no solar flux on MLI is calculated).</p> <p>MLI area: 1.7m^2.</p>
Radiator	<p>Radiator is covered with OSR: optical properties assumed UV absorptivity = 0.2 and IR emissivity = 0.85 (those properties are not degraded as radiators are assumed to be protected by the louvres during the system deployment).</p> <p>Radiator area is divided into 2 panels inclined by 25°.</p> <p>Radiator area: 0.51m^2.</p>
Louvres	<p>Louvres are covering the radiator panels during the lunar night. Optical properties assumed: UV absorptivity = 0.2 and IR emissivity = 0.4.</p>
Heaters	<p>Kapton heaters are foreseen for lunar night survival as baseline option. Electric power is assumed to be available. Other option for lunar night heating would be RHU: however, as a baseline heaters are considered due to their higher TRL and they do not provide waste heat during lunar day.</p> <p>In current iteration, it is assumed that mass of all heaters and thermocouples is 1kg.</p>
Thermocouples	<p>Thermocouples are foreseen for temperature monitoring inside the antenna.</p> <p>In current iteration, it is assumed that mass of all heaters and thermocouples is 1kg.</p>

Internal Units TCS (paints, washers, thermal fillers)	In the thermal budget 1 kg is foreseen for TCS for internal Hub units.
---	--

Table 13-5: Hub Thermal Hardware

A detailed list of equipment, its mass and heating power needs are included in Table 13-7.

13.2.3 Base

Base TCS design is different than Antenna and Hub TCS design. Main difference is the unit placement: Antennas and the Hub are placed directly on the lunar soil while the Base is placed on the top of LDE. Therefore, no heat exchange between lunar soil and the Base is included in initial TCS sizing. Also, due to the lack of information about possible “shape” of the base, no heat leaks via MLI are estimated. To cover MLI heat leaks during the lunar night, value from previous CDF lunar studies is estimated: for the first TCS sizing it is assumed that 130W is leaking during the lunar night into the environment.

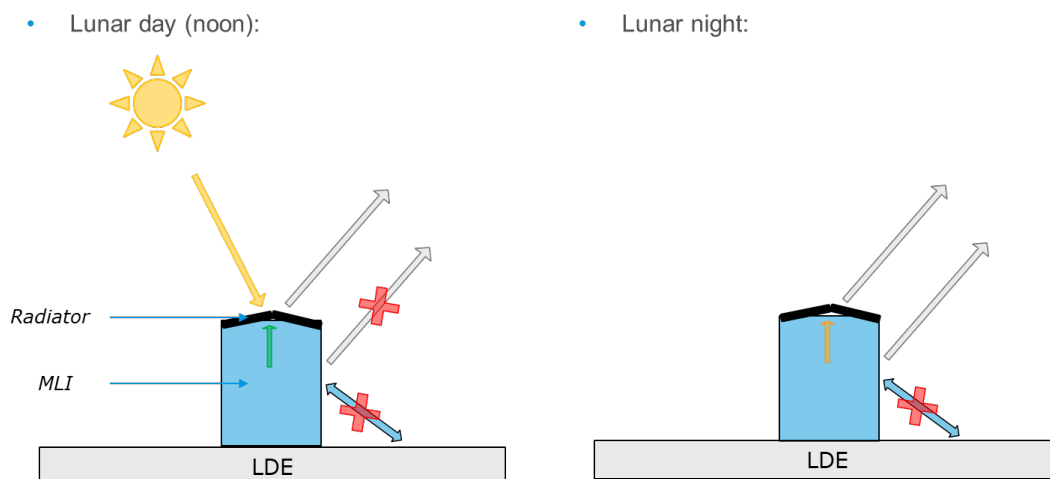


Figure 13-7: Base TCS Concept

Base TCS is close to the Hub TCS design: it also requires inclined radiators (25°) mounted on the top and covered with louvres. The required temperature range is from 0°C during lunar night to 30°C during lunar day.

Base has the highest power dissipation among all ALO units. Big contributor here is the communication subsystem. Because of the foreseen number of internal units and their dissipation, it is foreseen that heat pipes will be needed to transport dissipated heat to the Base radiators or to distribute heat during lunar night. Six heat pipes are included in initial TCS budget.

Current radiator sizing includes only the radiator needed for the currently foreseen internal units. If fuel cells are used in the Base design, an additional radiator will be needed to reject to the environment the waste heat produced by them during the lunar day. During the lunar night the waste heat from fuel cells can be used for heating needs.

Thermal hardware to be used with its properties is summarised in the table below.

Thermal Hardware	Description
MLI	<p>MLI with $\epsilon^* = 0.05$ is assumed.</p> <p>The external MLI layer has degraded (dust influence taken into account) IR emissivity: 1.0 is used. This value represents all materials that have high epsilon value (Kapton, Black Kapton, Stamet, BetaCloth). Final external layer selection can be chosen based on electrical conductivity needs or solar absorptivity value needed (this value is not used in initial sizing as no solar flux on MLI is calculated).</p> <p>MLI area assumed (for mass estimation): 27m^2.</p>
Radiator	<p>Radiator is covered with OSR: optical properties assumed: UV absorptivity = 0.2 and IR emissivity = 0.85 (those properties are not degraded as radiators are assumed to be protected by the louvres during the system deployment).</p> <p>Radiator area is divided into 2 panels inclined by 25°.</p> <p>Radiator area: 1.73m^2.</p>
Louvres	Louvres are covering the radiator panels during the lunar night. Optical properties assumed: UV absorptivity = 0.2 and IR emissivity = 0.4.
Heaters	<p>Kapton heaters are foreseen for lunar night survival as baseline option. Electric power is assumed to be available.</p> <p>Other option for lunar night heating can be RHUs or use of waste heat from fuel cells. Both options can be further explored in the next iteration of ALO TCS design.</p> <p>In current iteration, it is assumed that mass of all heaters and thermocouples is 1kg.</p>
Thermocouples	<p>Thermocouples are foreseen for temperature monitoring inside the antenna.</p> <p>In current iteration, it is assumed that mass of all heaters and thermocouples is 1kg.</p>
Internal Units TCS (paints, washers, thermal fillers)	In the thermal budget 1 kg is foreseen for TCS for internal Base units.
Heat Pipes	<p>Heat Pipes may be needed for heat transport inside the Base. If needed, Loop Heat Pipes may be used as well.</p> <p>In initial TCS sizing 6 Heat Pipes are included in the TCS budget.</p>

Table 13-6: Base Thermal Hardware

A detailed list of equipment, its mass and heating power needs are included in Table 13-7.

13.2.4 List of Equipment

The following equipment has been identified.

Unit	#	Size [m ²]	Nominal Mass [kg]	Power Consumption [W]			
				Day STBY	Day OBS	Day COMMS	Night HIB
Antenna							
MLI		0.24	0.1				
Thermal washers/support isolating structure			0.1				
Heaters + Thermocouples			0.15				2.7
Radiator (OSR)		0.036	0.008				
Internal Units TCS (paints, washers, thermal fillers)			0.1				
Hub							
MLI		1.7	0.7				
Heaters + Thermocouples			1.0				90.0
Louvres		0.51	2.5				
Units TCS (paints, washers, thermal fillers)			1.0				
OSR		0.51	0.25				
Base							
MLI		27.0	10.8				
Heaters + Thermocouples			1.0				350.0
Louvres		1.73	8.7				
Heat pipes			15.0				
Units TCS (paints, washers, thermafillers)			5.1				
OSR		1.73	0.9				

Table 13-7: List of Equipment

Unit	TRL	Heritage considerations
MLI	9	
Thermal washers/support isolating structure	9	
Heaters	9	
Thermocouples	9	
Louvres	3	Louvres have been flown on Rosetta mission, but never used in lunar environment (especially taking into account dust).
OSR	9	
Thermal filler	9	

Thermal paints (for various units): e.g. Black Paint	9	
Heat pipes	9	
Loop Heat Pipes (if needed, TBC)	5	Loop heat pipes have been also flown/designed for ExoMars. However, a development of dedicated configuration of LHP may be needed.

Table 13-8: Technology Readiness

13.3 Trade-Offs and alternative options

Within this section possible improvements of TCS performance are proposed and initially assessed.

13.3.1 Antenna

In case of Antenna, to improve TCS performance, it is worth exploring possible extension of maximum and minimum temperature limit.

This will affect heating power needs: if, for example, Antenna could work at higher temperature (higher maximum operating temperature), less heat would need to be rejected to keep it at appropriate temperature level. That results in the need of smaller radiator. When radiator is smaller, the heat losses during the lunar night will be smaller as well. Therefore, heating power needed for lunar night survival will be lower than current baseline.

Also, if minimum temperature limit can be lowered, less heating power is needed for lunar night survival.

Graphs below show the relationship between temperature limits and possible savings on heating power. The influence is shown by modifying just one parameter at a time. In the future design, the change of the parameters can be combined. For example, expanding maximum operating temperature to 60°C and minimum temperature to -110°C decreases heating power need from current 2.7W to 1.05W.

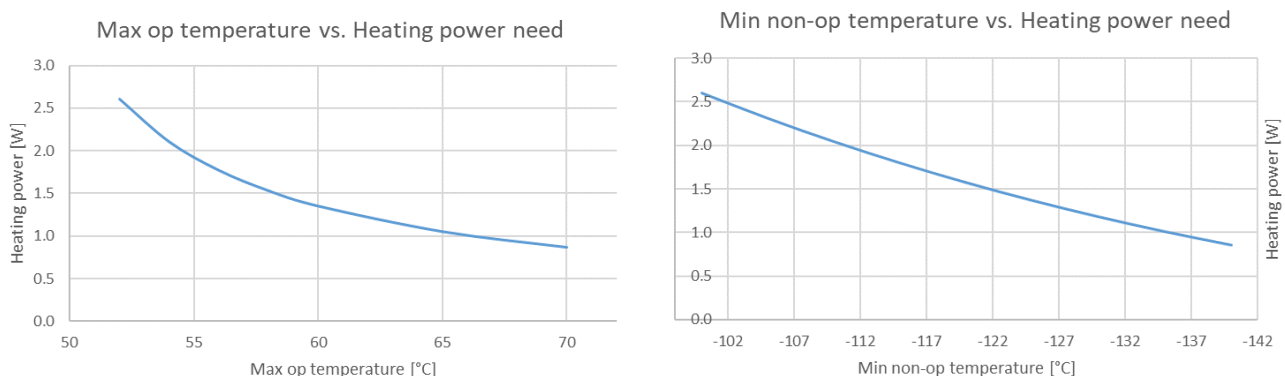


Figure 13-8: Antenna TCS: Influence of maximum and minimum temperature on heater power demand

In the baseline Antenna TCS design, heating power is delivered by kapton heaters. Possible use of RHUs can be also explored. However, RHUs also dissipate the heat during the day and the heat dissipated would need to be also rejected, which will influence radiator size needed for the Antenna. In case of such a small unit as Antenna, this solution may influence significantly its mass budget. However, that needs to be confirmed by making next iteration of TCS sizing.

Another option to save heating power is including in the TCS design a heat switch that can “thermally disconnect” the electronics from the radiator during the lunar night. Also this option and its influence on mass budget can to be reassessed in the next design iteration.

13.3.2 Hub

To explore possible improvements for the Hub TCS design, a similar exercise has been done as for the Antenna design: the influence of extending the temperature ranges for the Hub has been explored and is presented on the graphs below.

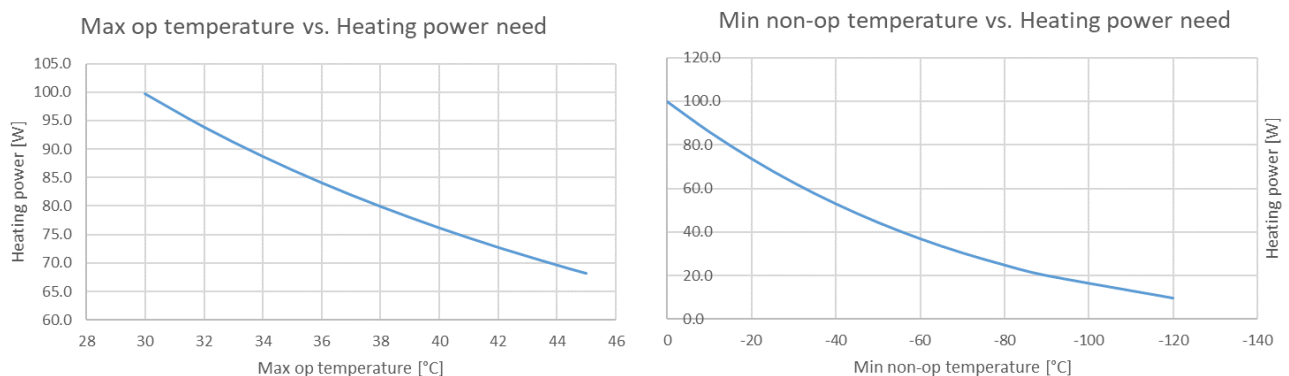


Figure 13-9: Hub TCS: Influence of maximum and minimum temperature on heater power demand

If in the Hub no batteries are present, its minimum survival temperature during the lunar night could be decreased to, for example, -100°C. This decrease will reduce power heating need from currently baselined 90W to 15W.

In case of the Hub, it can be also explored how the radiators’ inclination influences the heating power need. Only inclination up to 45° has been investigated, as above this value, it is possible that the radiator is so much inclined that it can see the lunar soil and have some thermal exchange with it and its efficiency may decrease.

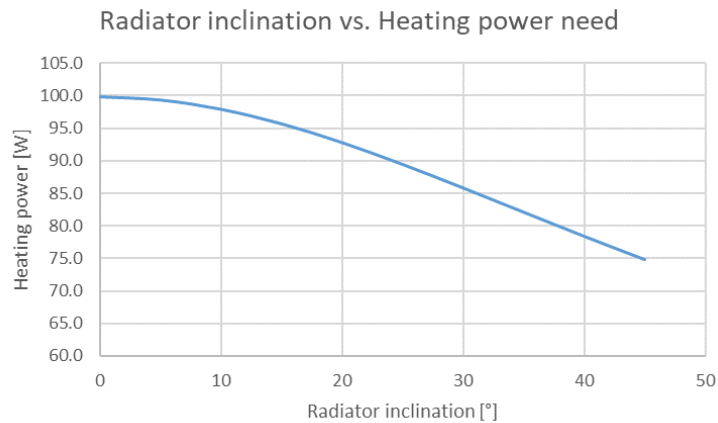


Figure 13-10: Hub TCS: Influence of radiator inclination on heater power demand

Also the influence of amount of thermally controlled volume in the Hub have been explored. As expected, in case where more volume needs to be controlled, increase of heating power need occurs. The trend of this growth can be observed on the graph below.

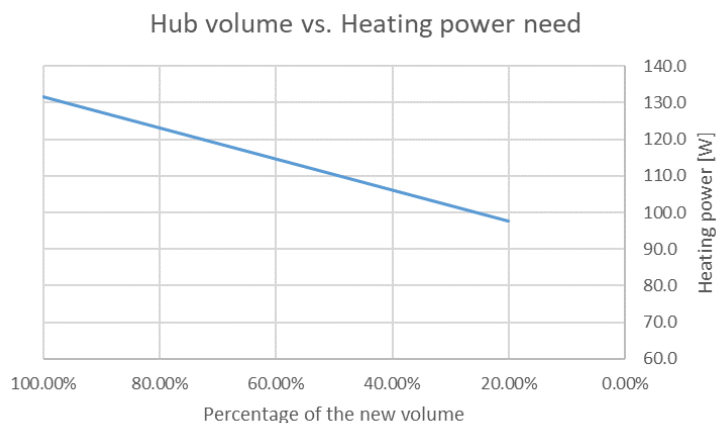


Figure 13-11: Hub TCS: Influence of TCS controlled volume on heater power demand

13.3.3 Base

Base TCS can be also improved by modification of: maximum required temperature, minimum required temperature and radiators' inclination.

Graphs below show the change of heater power need when each of the parameters mentioned above is modified.

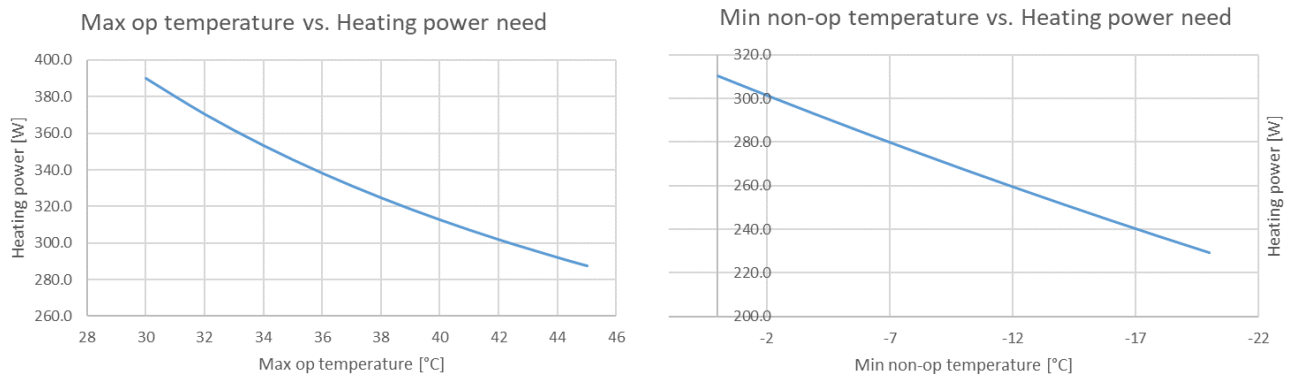


Figure 13-12: Base TCS: Influence of maximum and minimum temperature on heater power demand

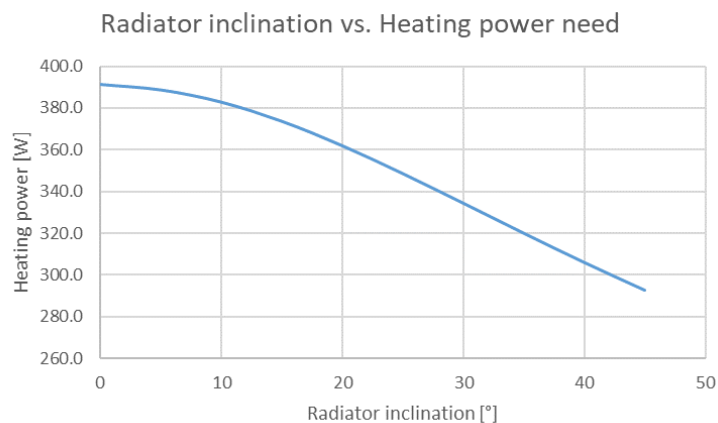


Figure 13-13: Base TCS: Influence of radiator inclination on heater power demand

For example, expanding maximum operating temperature to 35°C and minimum operating temperature to -10°C decreases heating power need from 350W to 290W (almost 20% less compared to current baseline).

In this iteration the options for heating power source during the lunar night have not been explored. Kapton heaters are baselined as electric power is assumed to be available. Other option for lunar night heating can be RHUs or use of waste heat from fuel cells. Both options can be further explored in the next iteration of ALO TCS design.

13.4 Considerations for scalability

In case of TCS, the design is done individually for each type of unit. Therefore to calculate TCS budget for larger amount of units, it is enough to multiply the amount of units by TCS budgets per unit.

13.5 Technology Needs

Thermal design and TCS needs for ALO are in line with the needs identified for previous studies for lunar exploration. As ALO is planned to be launched in second batch of EL3 launches, the development of the technologies needed shall be on good track and the technologies shall be possible to use when needed.

The technologies needed to be developed are: louvered radiators, RHUs (if the need for them is identified in the next design iteration) and Loop Heat Pipes (if they are found to be necessary for the Base TCS). Moreover, in order to have various electronics working in the wide range of temperatures, the qualification of all units and processes (including soldering of the components to the boards) needs to be well planned and defined.

Technology Needs						
Technology is baselined	Equipment Name & Text Reference	Technology	Supplier (Country)	TRL	Funded by	Additional Information
✓	Louvered radiator	Louvered Radiator	SENER (ES), ESR Technologies (UK), CSEM (CH)	3		Rosetta Louvers by SENER TRL 9 / louvered radiator with dust protection and active louvers will need to be developed but components are assumed to be on TRL 3 already
	Loop Heat Pipes	LHP (propylene or ammonia)	IberEspacia (ES) or Euro Heat Pipes (BE)	5		
	Radioisotopic Heater Unit (RHU)	Radioactive Decay of the synthetic radioactive material Americium	University of Leicester (UK)	4	ESA	Qualification needed for all equipment and manufacturing processes
✓	Low Temperature Electronics/Equipment	Low Temperature Electronics / Equipment	TBD	5		

Table 13-9: Technology Needs

This Page Intentionally Blank

14 POWER

14.1 General Considerations and Initial Assumptions

14.1.1 Key Drivers and Challenges

Key drivers		
Ref.	Key driver	Impact
1.	Night survival is compulsory.	Power shall be provided over the lunar night. At least for thermal control, and probably for a minimum level of electrical functionality.
2.	Night operation is highly desirable.	(Higher) power for full operation is desired over the lunar night.
3.	Site is at a lunar mid-latitude (not polar).	No possibility of night duration < 336 hours. Large range of sun elevation during lunar day. Sun azimuth range of 180° over lunar day. These factors strongly impact the solar generation concepts.
4.	EL3 landing attitude is uncontrolled.	Sun azimuth range will be unknown/random w.r.t. landed EL3. This strongly impacts the solar generation concepts.
5.	Electromagnetic quietness for the science instrument is required. (Details are TBD).	Noisy electrical functions such as switching DC/DC converters may be problematic in general and especially at antennas or hubs. It is unclear if sinusoidal AC may also be problematic. This strongly impacts the power subsystem architecture and the power distribution options w.r.t. delivering power to the distant elements.
6.	Powered system elements will be spread over multi-km distances in a full observatory or tens of metres, even for a preliminary demonstration system.	Need to consider if the individual elements (antennas, hubs) can be power-autonomous, with generation and/or storage implemented locally at each element OR if power shall be generated and/or stored centrally and distributed over long distances to the elements.
7.	The ALO system shall be delivered to the moon by EL3, with a payload capability of 1.8 tonnes.	This limits the use of very heavy power system elements such as fission reactor systems and very large energy storage (e.g. battery) units.
8.	The mission duration is 4 years (of operation).	This rules out the use of short-lived energy solutions (e.g. primary batteries or primary fuel cells), and impacts solar cells and secondary batteries in terms of performance degradation.

Table 14-1: Key drivers

14.1.2 Power System Requirements

Qualitative and “soft” requirements are covered above as *key drivers*.

Within the frame of the ALO CDF study, the quantitative requirement that arises as input to the EPS design and sizing is the power and energy requirement budget which is summarised in Table 14-2.

This budget is applicable to a small-scale 16-antenna ALO demonstrator system, which was identified as an achievable mission in the context of a single EL3 lunar delivery.

	Day STBY	Day OBS	Day COMMS	Night HIB
Observatory total power (W)	37	252	257	226
Total power incl. 20% margin (W)	44	302	309	271
Duration per lunar cycle (hrs)	33	290	15	370
Energy per lunar cycle incl. 20% margin (Wh)	1456	87516	4631	100388

Table 14-2: Power and energy load requirements summary for small-scale ALO

14.2 Trade-Offs and Analyses

14.2.1 Local and Central Power System Options

There are three basic element types (“nodes”) in the ALO architecture: base, hubs and antennas. In principle, power could be generated and/or stored locally at all the nodes, or generated/stored at the base and somehow transferred to the numerous remote nodes.

Table 14-3 examines what solutions may be plausible to provide electrical power (and also heat) at each type of node.

	Solar photovoltaic cells / panels	European RTG	Nuclear fission reactor system	Regenerative fuel cell system	Li-ion secondary battery	European RHU (heat only)
Key figure(s) of merit	~10 to 20 g/W.	100 g/W	~10 ² g/W, depends on scale.	~2 to 5 g/Wh. 0.7 to 1.8 kg/W overnight.	7 g/Wh 2.5 kg/W overnight.	70 g/W
Notes	Horizontal panel will provide power for most of the day. Dust may be a problem.	10 W & 10 kg per unit. Launch safety & fuel supply limit max. units per launch: ~10 ¹	Minimum ~10 ³ kg and ~10 ³ W per unit. Small scale is not possible	Minimum mass ~10 ² kg per unit	Require tight thermal control (> 0°C)	~3 W & 200 g per unit. Launch safety & fuel supply limit max. units per launch: ~10 ²
Antenna: day electricity	YES	NO	NO	NO	NO	n/a
Antenna: night electricity	NO	NO	NO	NO	NO	n/a
Antenna: heat	n/a	NO	n/a	n/a	n/a	PERHAPS
Hub: day electricity	YES	PERHAPS	NO	NO	NO	n/a
Hub: night electricity	NO	PERHAPS	NO	NO	NO	n/a
Hub: heat	n/a	PERHAPS	n/a	n/a	n/a	PERHAPS
Base: day electricity	YES	NO	YES	NO	NO	n/a
Base: night electricity	NO	NO	YES	PERHAPS	NO	n/a
Base: heat	n/a	PERHAPS	n/a	n/a	n/a	PERHAPS

Table 14-3: Power source suitability analysis

14.2.1.1 Power source conclusions

For a full-scale ALO that operates at night, electrical power must be generated and fed centrally. There is no night-time power solution compatible with the low-mass / large-number requirements of the hub and antenna elements.

For a small-scale ALO launched on a single EL3, no power solution for sustained night operations is possible.

A small-scale ALO could be centrally powered by a base-mounted Electrical power system (EPS) with solar array and an electrochemical energy storage system (battery or regenerative fuel cell). Radioisotope heaters could provide thermal support if needed. The energy density of an electrochemical system could support night survival, plus possibly brief demonstrations of night operations. Sustained night operations will not be possible. This option is taken forward as the baseline for the design and sizing that follows.

A future full-scale ALO could exploit continuous centrally-provided power from a (yet to be developed) fission reactor system. The reactor power system would itself be a full mission endeavour, requiring a dedicated EL3 (or equivalent) to deliver it to the moon.

14.2.2 Solar Array Attitude Trade-Off

A sun-tracking solar array mounted on the ALO base station (assumed to be accommodated on top of the EL3 platform) will be difficult to achieve. Considering the mid-latitude lunar sites of interest, and the fact that the EL3 (azimuthal) landing attitude is uncontrolled, it follows that the tracking array would require a one-shot rotational adjustment in one axis to account for the landing attitude, plus a SADM tracking the sun around another axis.

Simpler options are to: deploy a fixed array in the horizontal plane (Figure 14-1, on the left); or to deploy a fixed but “optimised” solar array (Figure 14-1, on the right).

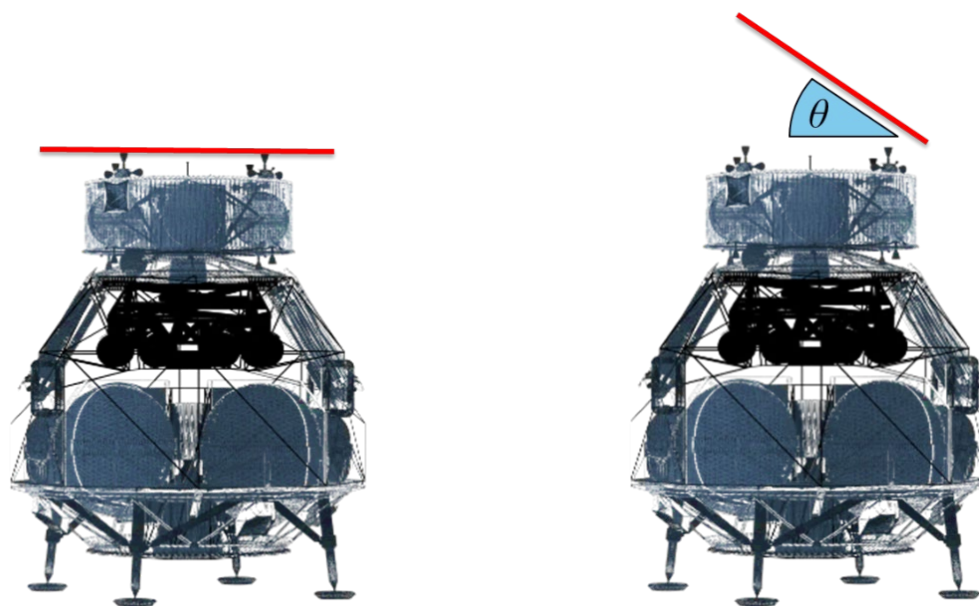


Figure 14-1: Fixed solar array attitude options. Left: horizontal, right: optimised.

For the optimised solar array, the tilt angle θ is equal to the time-averaged sun elevation, which is approximately 44° for the Tsiolkovsky site and 29° for the Von Karman site. The tilt must be azimuthally specific (i.e. looking towards the equator).

This would also be complex to achieve, considering that EL3 (azimuthal) landing attitude is uncontrolled. It would require two rotational deployment/locking mechanisms in orthogonal axes (for azimuth and elevation). The mechanism dealing with the elevation angle could be essentially the array deployment mechanism, as its deployed angle is known in advance (from

the site latitude). However, the second axis mechanism (for azimuth) would have to be capable through 360° to compensate for the unknown landed attitude.

Figure 14-2 compares the performance of a horizontal and “optimised” solar panel at the Tsiolkovsky landing site. The green and blue lines represent the power output of the horizontal and optimised panels as a function of time through the lunar day. Printed on the graph are also the generated energy values (integrated over the full lunar day) for each option. The power and energy data are normalised to the power or energy that would be delivered by a sun-tracking panel. The modelled sun elevation and relative azimuth are also plotted for context, with the azimuth being arbitrarily zeroed at the sunrise direction.

The model used to derive these graphs uses simplified astronomy, in which the Sun is a point source, no topography variation / horizon masking is considered, and the (Night duration) = (day duration) = (synodic_month / 2) = 354 hours. The solar array model does not consider temperature variation along the lunar cycle, and is nominally fixed at an assumed 100°C. This is conservative with respect to the array output near dawn and dusk, where the sun incidence will be oblique and the array will be colder.

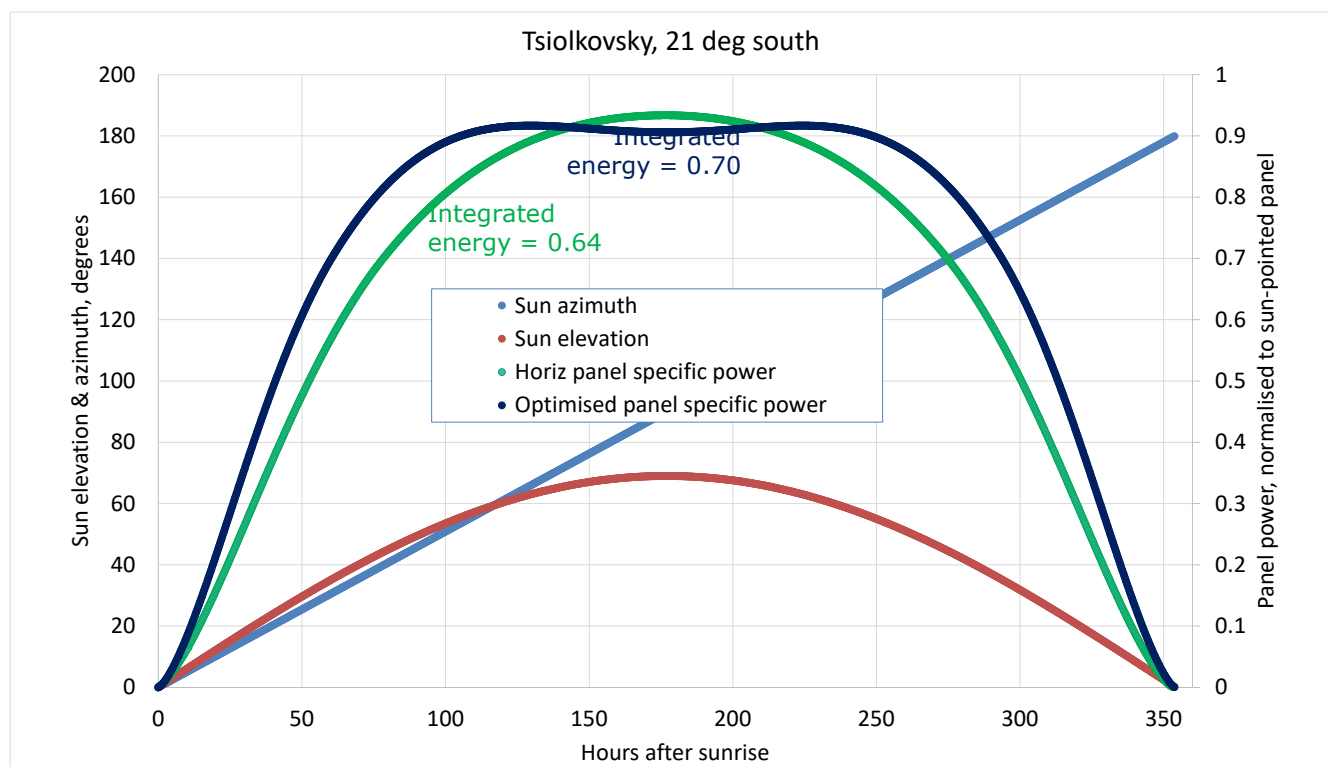


Figure 14-2: Comparison of horizontal and optimised solar array attitudes at Tsiolkovsky site

Figure 14-3 is the equivalent graph for the Von Karman site.

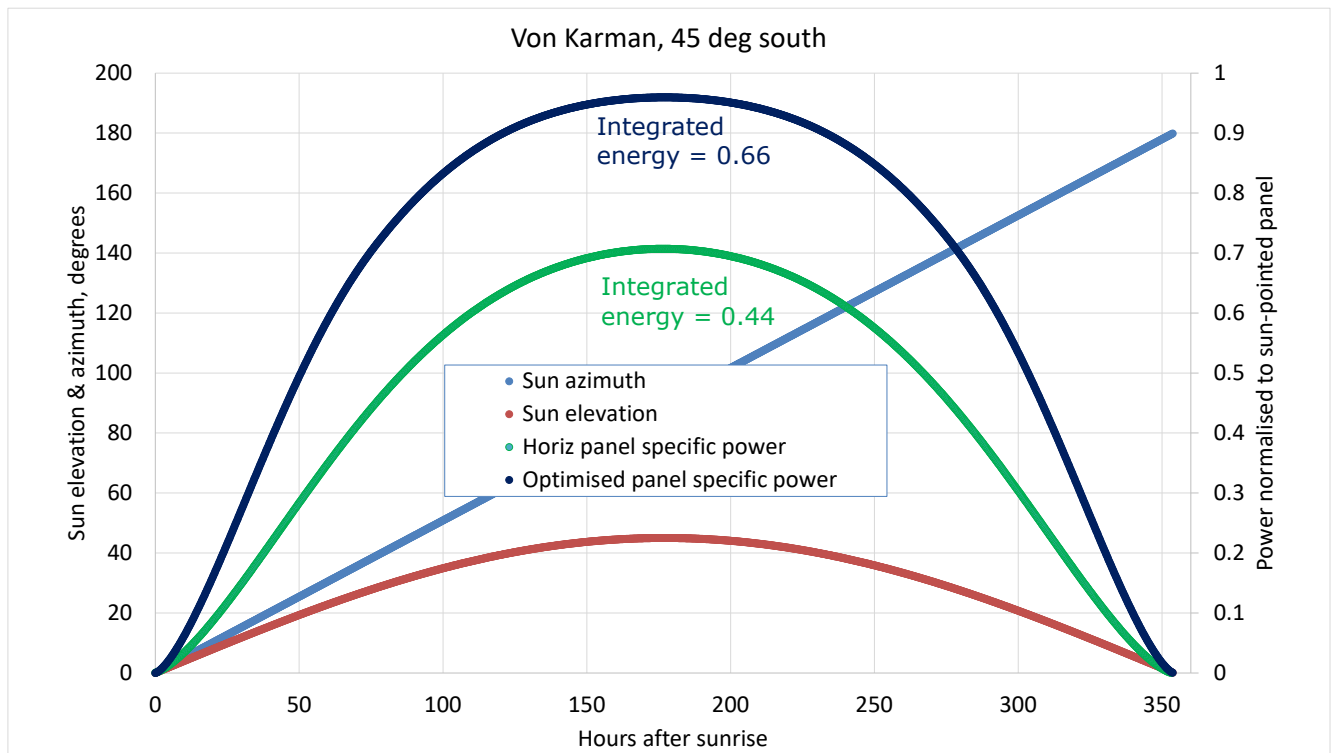


Figure 14-3: Comparison of horizontal and optimised solar array attitudes at Von Karman site

Figure 14-2 shows that, at the Tsiolkovsky site, the power and energy gain from an optimised panel vs. a horizontal one is modest. In the dawn and dusk periods, the optimised panel gives a few hours advantage for achieving a given power level, and the full day integrated energy is a factor $0.7/0.64 = 1.09$ higher. These performance increases are not judged significant enough to justify the extra mass, complexity and operational risk of an additional rotating/locking mechanism.

Figure 14-3 shows that, at the Von Karman site, the power and energy gain from an optimised panel vs. a horizontal one is more significant. In the dawn and dusk periods, the optimised panel gives many (even tens of) hours advantage for achieving a given power level, and the full day integrated energy is a factor $0.66/0.44 = 1.5$ higher.

In the absence of strong external reasons to choose the Von Karman site over the Tsiolkovsky site, the selected baseline for the EPS design and sizing is to assume the Tsiolkovsky site and the simpler horizontal solar array attitude.

14.2.3 Solar Array Mechanical Configuration Trade-Off

14.2.3.1 Conventional rigid solar array

Rigid panel arrays are the most common variant, having flown on countless spacecraft, spanning LEO, GEO and deep space missions. Certain types incorporate lateral panels, hinged to a central row, providing a backbone. Such schemes could be adapted to such a lunar use.

Required modifications would include local reinforcements of the hinges, to support the lateral panels, as well as an increase in deployment system torque margins, to overcome lunar gravity.

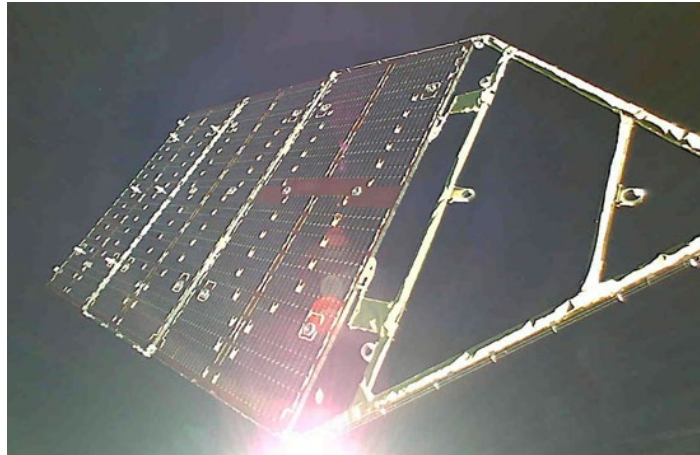


Figure 14-4: Solar Array Comprising Rigid Panels

14.2.3.2 Rollable solar array

Solar arrays, comprising flexible blankets onto which rigid cells are bonded, have been flown in the past (Hubble Space Telescope, ERS-1, ERS-2, Olympus) but became redundant with the advent of lightweight rigid panel arrays. However, in recent years, such a concept has been seeing renewed interest. In particular, Thales Alenia Space is currently developing such an array (RD[107]) for GEO applications. It comprises flexible blankets, onto which the Photovoltaic Assembly (PVA) is bonded, supported by a pair of carbon-fibre tape springs on either side.

All design details are subject to a Non-Disclosure Agreement (NDA). Nevertheless, an empirical assessment can be made as to its suitability for such a lunar application.

Required modifications would include reinforcements of the tape springs, to ensure against buckling under lunar gravity, as well as an increase in deployment system torque margins, to enable the array to deploy vertically.

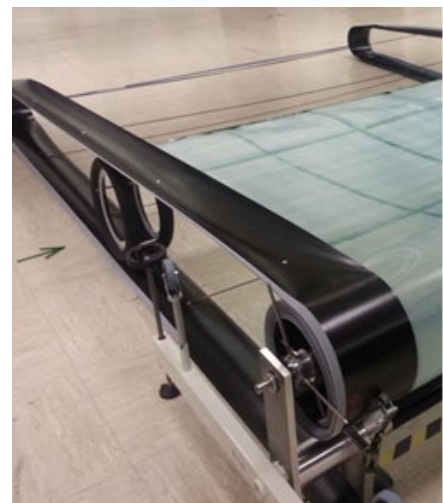


Figure 14-5: Concept illustration (left) and development model (right) of flexible roller array (RD[107])

14.2.3.3 Deployable mast solar array

A solar array, comprising hinged blanket segments, deployed and kept in tension by an extendable central mast, is currently being developed in Europe. All design details are subject to a non-disclosure agreement. Nevertheless, a qualitative assessment can be made as to its suitability for such a lunar application.

Required modifications would include some reinforcement of the central mast, to ensure against buckling under lunar gravity, as well as an increase in deployment system torque margins.



Figure 14-6: Solar Array Design Comprising Deployable Mast

14.2.3.4 Decagonal membrane solar array

A novel array concept, termed the Very Large Solar Array (VLSA), has been devised within ESA. As a patent application is currently underway, design features cannot be disclosed.

When deployed, the array takes the form of a polygonal membrane, onto which PVA is bonded. This solar array concept has been baselined in another ESA lunar mission CDF study *European Charging Station for the Moon* (ECSM) (RD[108]).

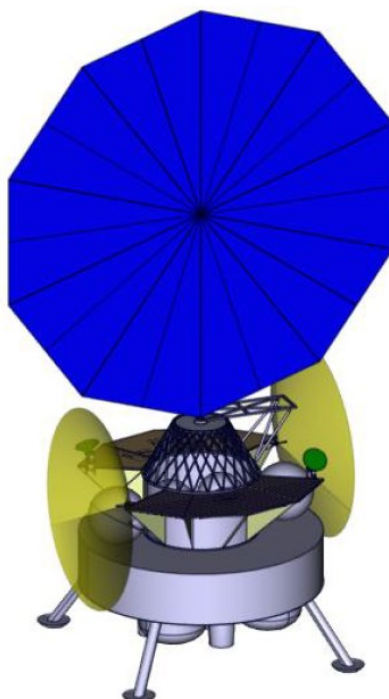


Figure 14-7: Solar Array Concept Design Comprising Decagonal Membrane

14.2.4 Solar Array Concept Trade-off

The parameters derived in the preceding subsections for each concept are summarised in the following table, together with current Technology Readiness Levels (TRL).

	Rigid panel	Rollable flex	Deployable mast	ESA VLSA
Stowed power density, kW/m ³ *	3.2	24	8.4	12
Area-specific power, W/kg*	50	69	99	62
Current TRL for space	9	5	4	2
Current TRL for moon	4-5	4	3	2

*Assuming EOL & operation at ~ 100°C.

Table 14-4: Characteristics of solar array concepts

The latter three concepts are designed for large array applications, and will likely have worse figures of merit than listed at the small scales applicable to a single-EL3 ALO.

For purposes of mass estimation, the traditional rigid panel is taken as baseline. This is a conservative and low-risk option. However, the new flexible array concepts may bring advantages in terms of accommodation and system configuration.

14.2.5 Electrochemical Energy Storage Trade-Off

The high-level trade off in Section 14.2.1 identifies RFCS as a suitable electrochemical storage technology to allow lunar night survival of a small-scale ALO. Table 14-5 gives further detail of the key qualitative and quantitative trade-off parameters that result in the selection of RFCS as opposed to Li-ion battery as the main energy storage device.

Although RFCS is a high-risk option in many areas such as TRL, development risk, reliability, complexity and volume, its far superior mass-specific energy capability is essential to meet the energy budget shown in Table 14-2, so it is selected as the baseline for this design.

However, an RFCS device is not capable of fast response to changes in load. It also may be unsuitable for use in flight, and may require some significant time to commission and activate once on the lunar surface. For all these reasons, a small “auxiliary” Li-ion battery is also included in the baseline EPS design.

	Li-ion battery	Regenerative Fuel Cell System (RFCS)
Maturity	Flight	TRL 3
Complexity	Very Low	Very High (see below)
Failure tolerance	Easily achieved with small addition e.g. extra string	Gas system is a single-point failure (e.g. micrometeorites) unless duplicated with > x1.5 mass impact factor.
Energy efficiency	Close to unity	< 50 %. Causes solar array size increase.
Interface & system	Simple electrical interface, even option of direct-on-bus (unregulated)	Requires auxiliary battery for e.g. load transients. Requires complex (and new) power conditioning functionality.
Thermal aspects	Requires thermal management in tight range (costing power at night or requiring RHUs)	Dissipates heat when discharging. Can be exploited for thermal control.
Mass-specific energy	In region of 120 Wh/kg, effectively, in use, at EOL	Much higher, depends on energy requirement. Approx. 500 Wh/kg for ALO, TBC.
Volume-specific energy	In region of 110 Wh/litre, effectively, in use, at EOL	Lower than batteries. Approx. 80 Wh/litre for ALO, TBC.

Table 14-5: Comparison of secondary Li-ion battery and RFCS (pros are green, cons are red)

14.2.6 Regenerative Fuel Cell System

Detailed consideration of RFCS for lunar surface application on the scale of an EL3 mission can be found in the report of the previous ESA CDF Study “ECSM” (RD[108]).

The key points of greatest relevance for the ALO study are repeated below:

- High temperature PEM technology as most promising technology after PEM (due to the higher reaction temperature of 180°C being advantageous for effective heat rejection in space)

- Possible redundancy approach could comprise three independent RFCS (Apollo style), with a 2/3 redundant power capability allowing failure of one system without loss of mission.
- It appears feasible to launch the RFCS charged although there would be some implications on the launch preparations and procedures. The gas tanks would be pressurised at launch.
- The RFCS is currently being developed in ESA led R&D activities with the TRL expected to be TRL 4 by 2021. TRL 5 is expected to be achieved by 2022. For the following activities high priority will be given to the storage tank development, which have not been treated properly yet for RFCS application.
- Control and software are another important part for RFCS development, which will also be addressed in the following R&D activities.
- Testing capability at ESTEC is needed and currently being analysed. A testing capability at ESTEC will be important to assess different terrestrial candidate technologies, to perform qualification tests as well as long duration lifetime tests.
- The impact of gas leakages in and reactant losses of the RFCS need to be assessed in future studies.
- The RFCS technology is expected to be at TRL 4 towards the end of 2021. Currently, Prototech (Norway) is developing, together with Air Liquide Advanced Technologies (ALAT, France) and Airbus (Germany), an RFCS for lunar night survival (ESA Contract No. 4000127686). A CAD design concept is shown in Figure 14-8.

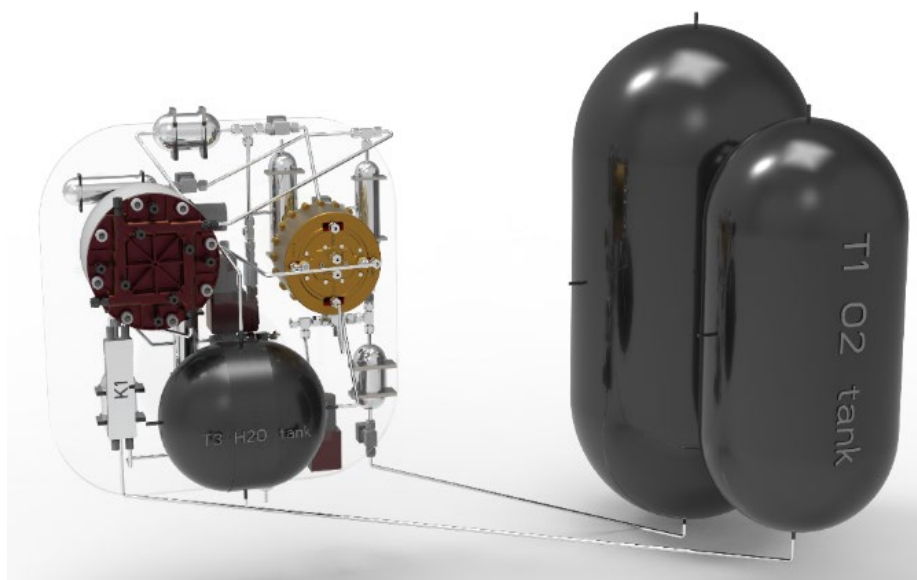


Figure 14-8: RFCS currently under development by Prototech in an ESA-funded activity

The assumptions made in the baseline RFCS sizing calculation are as follows:

- Efficiency of electrolysis assumed to be 87%
- Efficiency of fuel cell assumed to be 54%
- Roundtrip efficiency of RFCS = $0.87 \times 0.54 = 45\%$

- No redundancy is included in the reactant system (gas tanks and piping etc.)
- 10% margin is added for reactant H₂O quantity
- Electrolyser and fuel cell stack power density of 500 W/kg
- Net mass of H₂O stored in full H₂O bladder/tank is 80% of gross tank mass
- Net mass of H₂ stored in full H₂ tank is 10% of gross tank mass
- Mass of O₂ stored in full O₂ tank is 60% of gross tank mass
- Auxiliaries mass of RFCS is 35 kg
- Enclosure mass of 20 kg and MLI of 1 kg

14.2.7 Antenna Power Feed and Cabling Options

Each individual antenna unit requires in the region of 2 to 3 W of electrical power. In Night HIB mode, this is for electrical heaters, so in principle could be consumed at any voltage. In Day OBS mode, however, the power is used by the Low-Noise Amplifier (LNA) and the RF-over-fibre transmitter. These electronic devices (or at least the LNA) require low voltage, e.g. 3 to 5 V DC.

It is understood that the nature of the ALO observatory demands extreme electromagnetic “quietness” from the systems, especially in the vicinity of the antennas. However, quantitative details are TBD.

A most conservative assumption would be to assume that no AC current of any form (including switching converters) is permitted at antennas. This this would demand that the power feed must be DC, at a voltage close to compatible with the antenna electronics (5 V?). Only (lossy) linear regulators could be used to fine-tune voltage at the antenna if required.

However, the ALO concept means that the hub-antenna chain must cover large distances, and ohmic loss in the cabling is proportional to I^2 (or $1/V^2$). This presents a great challenge to feed the antennas with power in an efficient way without excessive mass of cabling.

Four basic power feed options are identified and discussed below:

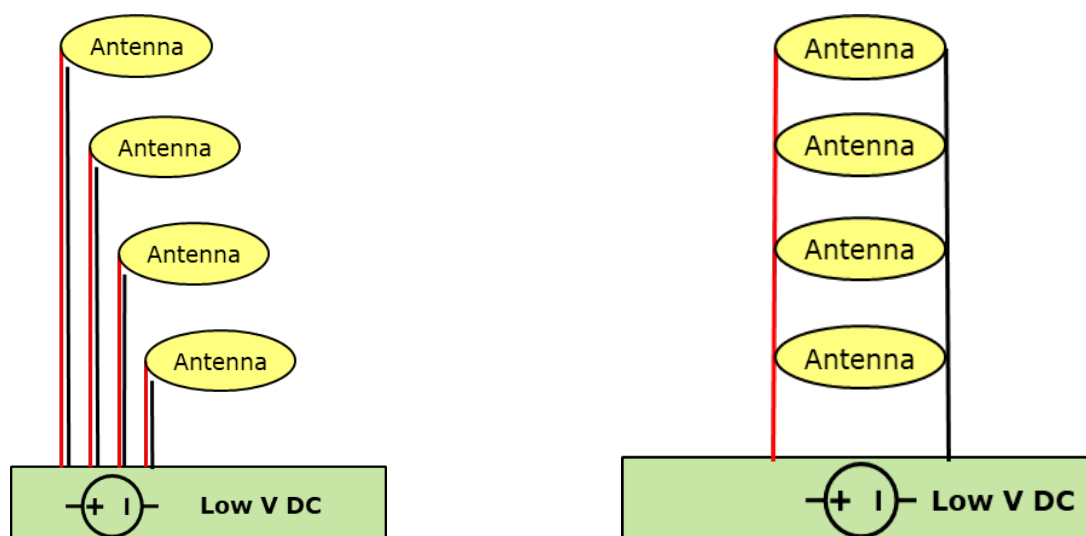


Figure 14-9: Left: parallel individual feed; right: parallel common feed.

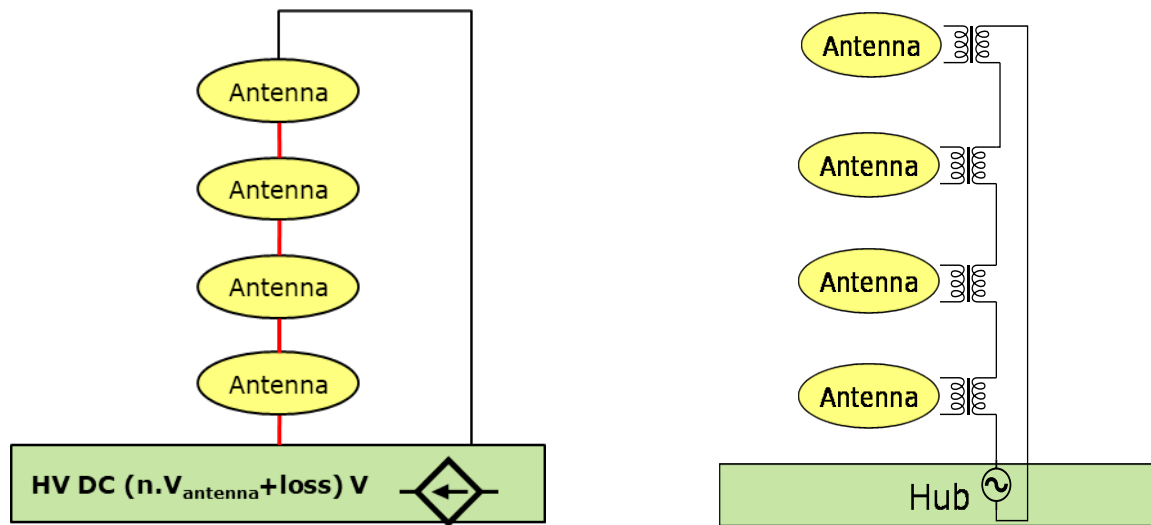


Figure 14-10: Left: series DC feed; right: series AC feed.

14.2.8 Parallel Individual Feed

See Figure 14-9, left. This concept uses individual dedicated cabling (send and return) for each antenna.

- ✗ Very high total cabling length and mass.
- ✓ Cable failure would only affect one antenna, so no further redundancy is needed.
- ✓ Suitable for both “star” or “linear chain” antenna/hub deployment architectures.
- ✗ Varying voltage loss for each antenna depending on cable length, so requires:
 - antenna with very flexible voltage need,
 - or separated feeds at the hub (current source or tailored voltage source), different for each antenna,
 - or linear regulators wasting power at the closer units.
- ✗ High ohmic loss due to low hub feed voltage.

14.2.9 Parallel Common Feed

See Figure 14-9, right. This concept uses common parallel cabling (send and return) for the chain of antennas.

- ✓ Low total cabling length.
- ✗ Cables have varying current (higher near the hub). Will require varying cable thickness to optimise the mass/power trade-off. This will mean high mass cabling, despite the minimum length
- ✗ Cable failure would affect a full antenna chain, so cable redundancy is needed.
- ✗ Only suitable for “linear chain” antenna/hub deployment architecture (not “star”).
- ✗ Varying voltage loss for each antenna depending on cable length, so requires:

- antenna with very flexible voltage need,
- or linear regulators wasting power at the closer antenna units.
- ✗ (Very) high ohmic loss due to low hub feed voltage and high cable current near hub.

14.2.10 Series DC Feed

See Figure 14-10, left. This concept uses series cabling and DC feed for the chain of antennas. The hub voltage output is therefore “shared” by the antennas (and the cable ohmic loss).

- ✓ Low total cabling length.
- ✓ Low cable mass.
- ✗ Cable failure would affect a full antenna chain, so cable redundancy is needed.
- ✗ Only suitable for “linear chain” antenna/hub deployment architecture (not “star”).
- ✗ Feed needs to be high voltage DC [= $(V_{\text{antenna}} \times n) + \text{losses}$]. This may be impossible or impractical for large number of antennas per hub.
- ✗ To be flexible to antenna number (and wire resistance variation with e.g. lunar surface temperature), the feed needs to be a good current source (not a voltage source).
- ✓ Same voltage to each antenna (provided they are identical):
- ✓ Low ohmic loss.

14.2.11 Series AC Feed (as selected in the NASA-JPL FARSIDE study RD[109])

See Figure 14-10, right. This concept uses series cabling and AC feed for the chain of antennas. Each antenna needs a transformer, rectifier and filtering electronics).

- ✓ Low total cabling length.
- ✓ Low cable mass.
- ✓ Allows feed voltage to be freely selected, (higher OR lower than $(V_{\text{antenna}} \times n) + \text{losses}$), so approach is flexible to n .
- ✗ Cable failure would affect a full antenna chain, so cable redundancy is needed.
- ✗ Only suitable for “linear chain” antenna/hub deployment architecture (not “star”).
- ✗ Additional mass of an AC transformer at every antenna, plus rectifier and filters. Lower AC frequency leads to larger/heavier transformers.
- ✗ TBD if the required EMC quietness can be achieved. Use of high quality sinusoidal AC and careful frequency selection may be key.
- ✗ To be flexible to antenna number (and wire resistance variation with e.g. lunar surface temperature), the feed needs to be a good AC current source (not a voltage source).
- ✓ Same voltage to each antenna (provided they are identical):
- ✓ Low ohmic loss.

14.2.12 Antenna Power Feed Conclusions

Both the parallel individual feed and parallel common feed options (Figure 14-9) will be unsuitable for a large array due to excessive ohmic loss and excessive cable mass.

The series AC feed (RD[109]) (Figure 14-10, right) is likely the best all-round option **if** the EMC aspects and the mass of transformers/rectifiers at every antenna can be shown to be acceptable.

Otherwise, the series DC feed (Figure 14-10, left) may be attractive, especially in cases where the number of antennas per hub is less than ~ 50, and therefore the voltage feed at the hub remains within sensible levels (e.g. below ~250 V).

14.3 EPS Model and Baseline Sizing Results

14.3.1 EPS Model Description

In order to estimate the required characteristics, mass and size of the electrical power system components, a bespoke Excel-based power-energy model was created.

In summary, the model calculations are as follows:

1. Consider the Night HIB energy requirement to determine battery or RFCS sizing.
2. Determine energy needed to recharge the battery or RFCS during the day. Then add the Day COMMS & Day OBS energy requirements.
3. Consider the solar array performance at the selected site, in the selected configuration
4. From 2 and 3, determine the solar array area needed (and mass implied, depending on array type).

14.3.2 EPS Model Inputs and Assumptions

Site characteristics	Night Duration	354	hrs				
	Day Duration	354	hrs				
Battery characteristics	Discharge efficiency	0.98					
	Charge efficiency	0.98					
	Battery round-trip efficiency	0.96					
	Mass-specific energy @ EOL	115	Wh/kg				
	Battery density	0.92	g/cc				
	Max DoD @ EOL	0.9					
RFCS characteristics	Fuel cell energy efficiency	0.54					
	Electrolyser energy efficiency	0.87					
	RFCS combined energy efficiency	0.47					
	Fuel cell aux consumption	18.8	W				
	Electrolyser aux consumption	15.3	W				
	Mass-specific energy	466	Wh/kg				
PCDU characteristics	APR efficiency assumed	0.96					
	Distribution efficiency assumed	0.98					
	BCR efficiency	0.95					also applies to RFCS charging
	BDR efficiency	0.95					also applies to RFCS discharging
	Idle consumption	30	W				included in budget
Base internal harness	Harness efficiency	0.98					
Solar array characteristics	Area-specific power @ EOL, 100°C, sun-pointed	212	W/m ²				
	Area-specific mass	4.2					

Table 14-6: EPS model inputs and assumptions

14.3.3 EPS Model Results

14.3.3.1 Li-ion battery option

Battery mass	1165	kg
Solar array area required	4.8	m ²
Solar array mass	22	kg
PCDU mass	17	kg
Total EPS mass	1204	kg

Table 14-7: EPS Model results (Li-ion battery option)

In this case, the EPS mass of 1.2 tonnes is clearly unacceptable, being two-thirds of the entire EL3 capability for this one subsystem alone.

14.3.3.2 RFCS option

Battery mass	17	kg
RFCS main unit mass (with empty water tank)	92	kg
RFCS oxygen tank mass (full with oxygen)	97	kg
RFCS hydrogen tank mass (full with hydrogen)	73	kg
Solar array area required	8.1	m ²
Solar array mass	37	kg
PCDU mass	21	kg
Total EPS mass	336	kg

Table 14-8: EPS Model results (RFCS option)

336 kg is an acceptable subsystem mass in this context. The RFCS option is selected as baseline.

14.3.4 EPS Model Timeline

Figure 14-11 shows how key power subsystem modelled parameters change through the course of a lunar day.

Also shown are the modelled time-points at which the system mode is assumed to change. Exit from, and entry to, Night HIB mode is triggered when the solar power generation (minus losses) equals the demand of Day STBY mode. The (dawn) entry to and (dusk) exit from Day OBS mode is triggered when the solar power generation (minus losses) equals the demand of Day OBS mode.

The EPS model uses simplified astronomy, in which the Sun is a point source, no topography variation / horizon masking is considered, and the (Night duration) = (day duration) = (synodic_month / 2) = 354 hours.

The solar array model does not consider temperature variation along the lunar cycle, and is nominally fixed at an assumed 100°C. This is conservative with respect to the array output near dawn and dusk, where the sun incidence will be oblique and the array will be colder.

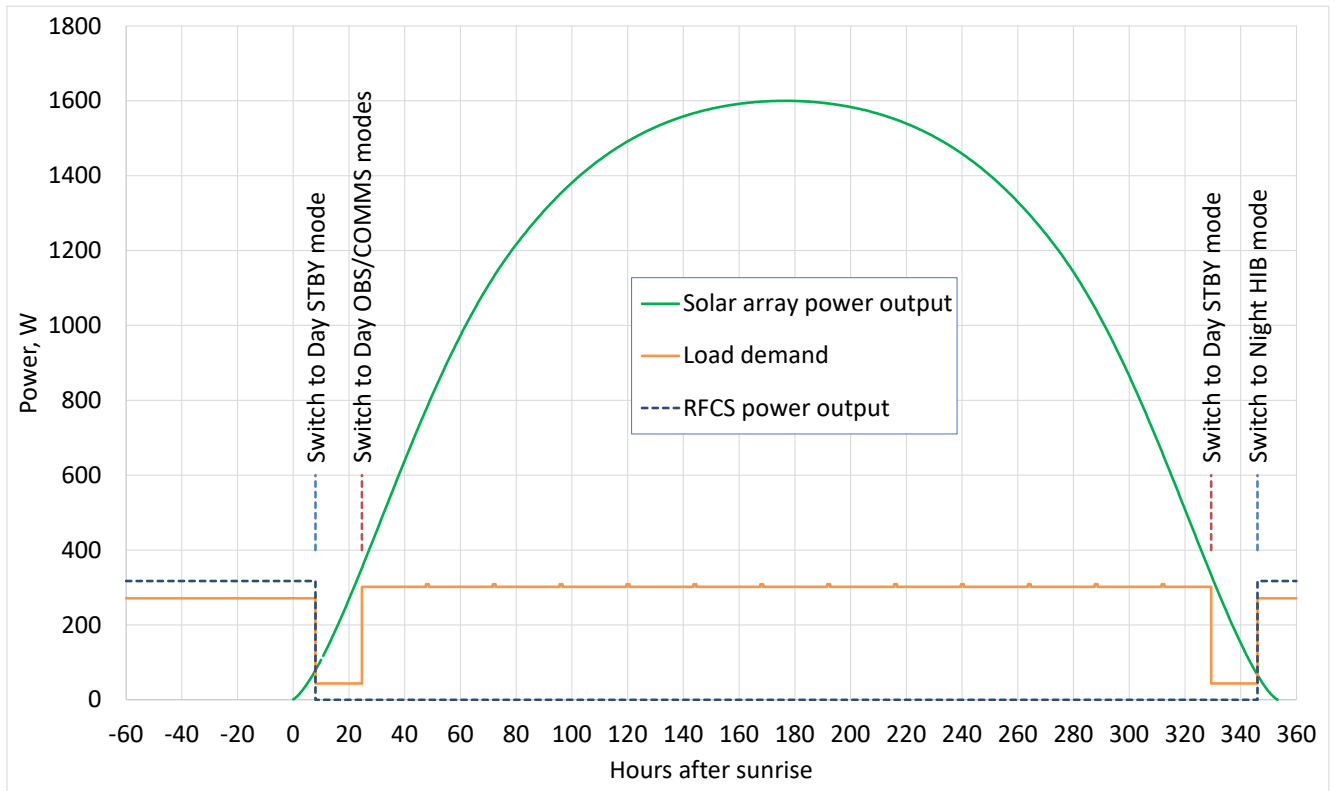


Figure 14-11: EPS model results with baseline design – timeline representation.

14.3.5 List of Equipment

The following equipment has been identified.

Unit	#	Size [mm unless stated]	Nominal Mass [kg]	Power Consumption [W]			
				Day STBY	Day OBS	Day COMMS	Night HIB
PCDU	1	160 x 240 x 450	21	30	30	30	30
Battery	1	270 x 240 x 260	17	-	-	-	-
RFCS main unit	1	Cylinder: height 910 x dia 560	92	15*	19*	19*	15*
RFCS oxygen tank (full)	1	Sphere: dia 910	97	-	-	-	-
RFCS hydrogen tank (full)	1	Sphere: dia 1140	73	-	-	-	-
Solar array	1	Area: 8.1 m ²	37	-	-	-	-

*RFCS electrical consumption is accounted for in the EPS model, but not represented in the system power budget, in order to avoid double counting

Table 14-9: List of Equipment

Unit	TRL	Heritage considerations
PCDU	3	A new and unique PCDU development will be required. The PCDU will need to interface and manage solar array & battery & RFCS.
Battery	6	Mission-specific qualification will be needed, possibly with special thermal considerations (TBC).
RFCS	3	A PEM O ₂ -H ₂ RFCS is currently being developed in ESA-led R&D activities. The TRL is expected to be TRL 4 by end of 2021.
Solar array	4	Regardless of which type of solar array is used (traditional rigid or novel flexible), the lunar surface application will require a specific delta-development and qualification w.r.t lunar gravity and environment. Thermal aspects and dust deposition are key issues.

Table 14-10: Technology Readiness

14.4 Considerations for scalability

14.4.1 Nuclear Power – Radioisotope Systems

Radioisotope thermoelectric generators would provide continuous day and night power at a mass cost of:

- ~1 W/kg with Am-241 fuel (European development, see Figure 14-12 and RD[110])
- ~3 W/kg with Pu-238 fuel (USA devices)

But, the maximum credible power capability to be embarked on a single launch is in the region of 300 W. Future developments of e.g. Stirling-engine-based radioisotope power systems may increase these numbers by e.g. a factor of x1.5 or x2. However, they could not provide the power needed for a full-scale (thousands-of-antennas) system.

European radioisotope heating devices are scheduled to be available before the launch of ALO and may be important for thermal night survival. These units (RHU and ELHS) are shown in Figure 14-13.

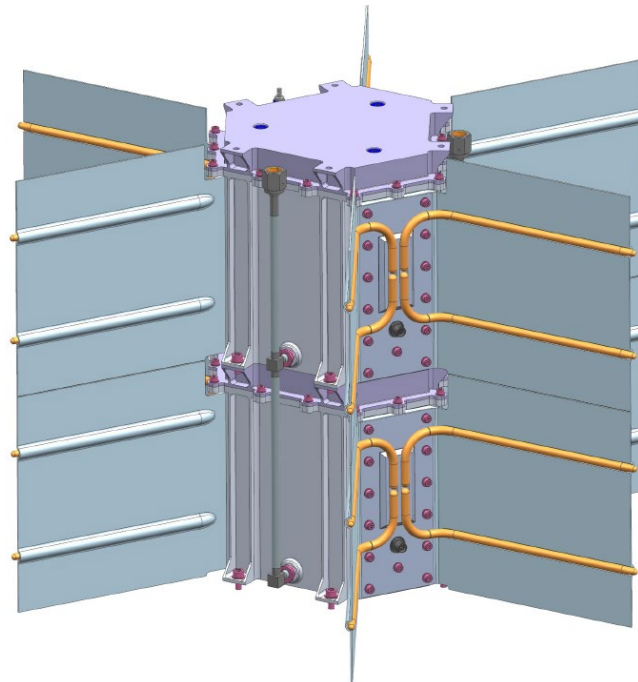
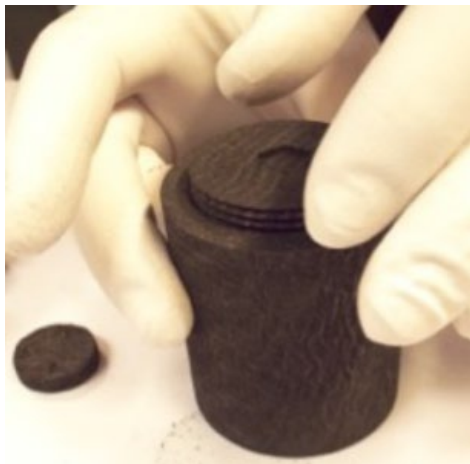
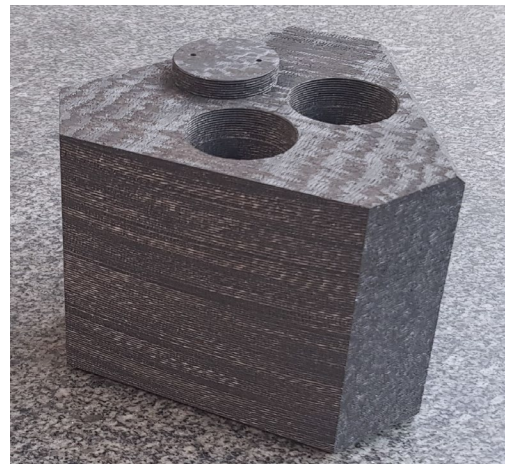


Figure 14-12: European RTG (20 W version). Credit: University of Leicester. RD[110].



Thermal power	3 W
Mass	207 g
Dimensions	42 x 52 mm
Specific power	15 W/kg



Thermal power	200 W
Mass	6.74 kg
Dimensions	113 x 44 x 117 mm
Specific power	30 W/kg

Figure 14-13: European RHU (left) and Large Heat Source (ELHS) (right). Credit: University of Leicester RD[110].

14.4.2 Nuclear Power – Space Fission Reactor Systems

Nuclear fission reactor power generation systems employing known technology are a realistic proposition for the production of power in the range 1 kW to 1 MW.

Full-system specific-power estimates range from less than 2 W/kg for a small ‘low risk’ system up to more than 30 W/kg for a high temperature, high power, performance optimised design. Examples of design concepts from NASA work (RD[111]) are shown in Figure 14-14 and Figure 14-15.

A fission reactor system would need a dedicated EL3 landing, even at the smallest possible scale. A European lunar fission reactor system is technically achievable but no development work is currently underway, and to achieve a flight capability would need major political and financial support, over more than a decade.

However, ESA (HRE directorate) is planning to open a new work-stream in this field, with a new study activity foreseen for implementation in 2022/23.

A nuclear fission reactor system is seen as a key enabling technology for many ambitious lunar surface missions, and ALO (full scale observatory) seems a ideally matched application.

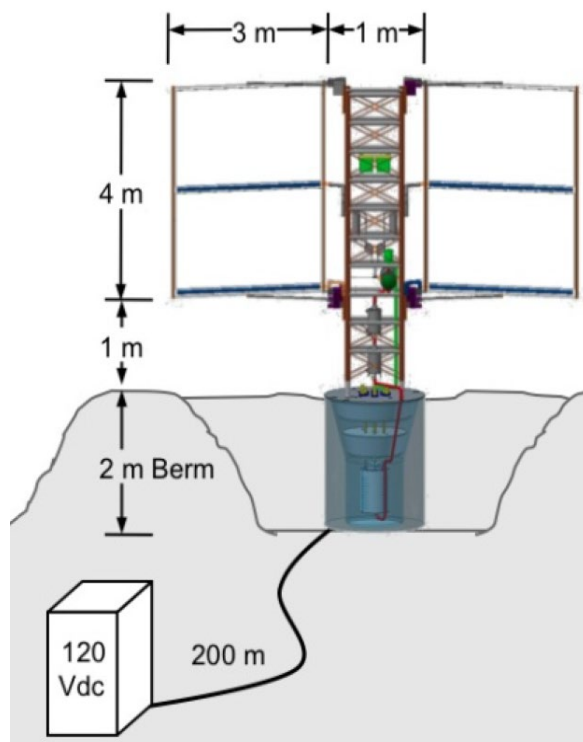


Figure 14-14: NASA Mobile Fission Power System (10 kW, 3340 kg) RD[111]

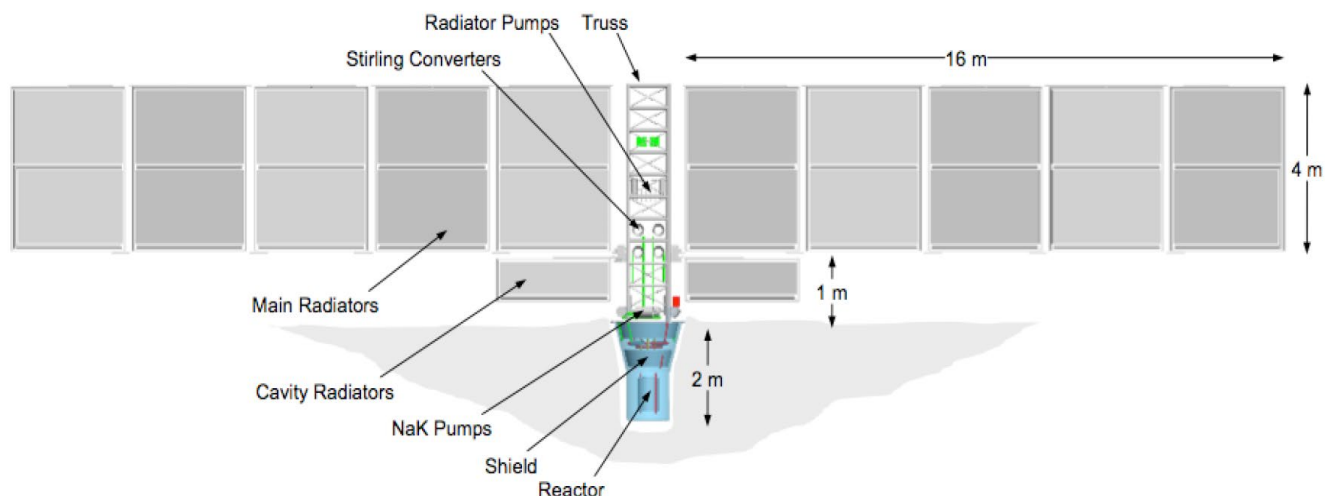


Figure 14-15: NASA Fission Surface Power System (40 kW, 5800 kg) RD[111]

14.5 Technology Needs

Technology Needs						
Technology is baselined	Equipment Name & Text Reference	Technology	Supplier (Country)	TRL	Funded by	Additional Information
✓	PCDU	PCDU	TBD	3	n/a	A new and unique PCDU development will be required. The PCDU will need to interface and manage solar array & battery & RFCS.
✓	RFCS	RFCS	CMR Prototech (Norway)	3	Currently E3P ExPeRT	A PEM O ₂ -H ₂ RFCS is currently being developed in ESA-led R&D activities. The TRL is expected to be TRL 4 by end of 2021.
✓	Solar array	Solar array	TBD	4	n/a	Regardless of which type of solar array is used (traditional rigid or novel flexible), the lunar surface application will require a specific delta-development and qualification w.r.t lunar gravity and environment. Thermal aspects and dust deposition are key issues.

Table 14-11: Technology Needs

15 CONFIGURATION

15.1 General considerations and initial assumptions

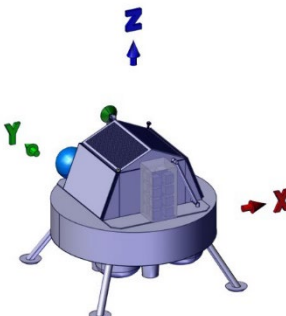
Initial assumptions	
Ref.	Assumption
1.	Payload Lander interface diameter of 2121mm
2.	<p>Coordinate system of the ALO is defined as follow:</p>  <p>Figure 15-1: ALO reference frame</p> <ul style="list-style-type: none"> - X axis is the egress direction of the rover - Z axis: axial direction - Y axis is perpendicular to X and Z axes completing a right-hand coordinate system

Table 15-1: Initial assumptions

SubSystem Requirements		
Req. ID	Statement	Parent ID
CONF-010	Overall assembly of the LDE and ALO should fit inside Ariane 6 fairing envelope	
CONF-020	<p>Configuration shall accommodate the following ALO platform elements:</p> <ul style="list-style-type: none"> - Rover with an envelope volume of 2.2m x 2m x 1m - Regenerated Fuel Cell System: <ul style="list-style-type: none"> o Cylindrical main unit o Hydrogen spherical tank o Oxygen spherical tank - Deployable solar panels with total area of 8.1 m2 - Warm electronics of power, data, communication, etc. subsystem units. - Thermal radiator with a sufficient area to dissipate the thermal heat of the warm electronics. 	

CONF-030	The configuration shall accommodate all payload and equipment required for the mission objectives and requirements	
CONF-040	The configuration shall take into account constraints and limitation due to AIV requirements	
CONF-050	The accommodation and locking of deployable items shall be such that stowage and deployment are reliable and can be tested on ground	
CONF-060	The configuration shall provide unobstructed fields of view and correct pointing direction to antennas: 1 HGA and 2 LGA's	
CONF-070	Optimize the overall design to have a low CoG	
CONF-080	CoG of the launch stack shall stay within a distance $d < 30\text{mm}$ from the launcher longitudinal axis	

15.1.1 Key drivers and challenges

Key drivers		
Ref.	Key driver	Impact
1.	Ariane 6 fairing envelope	ALO overall lateral dimension $<$ fairing diameter = 4.57m
2.	Minimize the CoG axial offset from the centre axis	Include equipment masses in the CAD model
3.	Rover volume envelope: 2200 x 2000 x 1000 mm Mass of 350 kg	Rover driveway path of 2.2m width
4.	Solar array of 8.1m ² without any shadow on the panels	Deployable solar panels on the highest position
5.	Thermal radiator dimension and position	Accommodation of the warm electronics under a thermal louvre Inclined (25deg) thermal louvre on the garage roof
6.	Antenna hub mass and dimension: 100 kg, 1500 x 750 x 750 mm	Antenna hub on one side of the garage
7.	RFCS mass and dimension	RFCS equipment on the opposite side of the Antenna Hub
8.	Robotic arm on the lander	The arm should be placed as closest possible to the Antenna Hub

Table 15-2: Key drivers

15.2 Baseline Description

The ALO configuration is a trapezoidal box mounted on a baseplate with overall dimensions as shown in Figure 15-2:

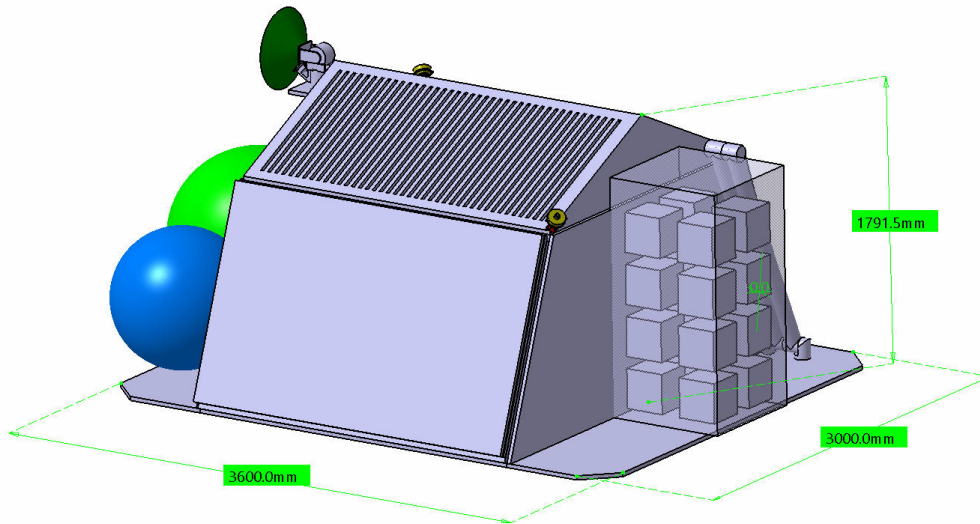


Figure 15-2: ALO overall dimension

The ALO platform, Rover Garage Element (RGE) contains the following elements as shown in Figure 15-3:

- Baseplate, equipped with an interface ring of 2,121 mm diameter to interface with LDE
- Side walls (trapezoid shape)
- Doors (69 deg angled)
- Garage ceiling (horizontal plate)
- Roof (25 deg angled)

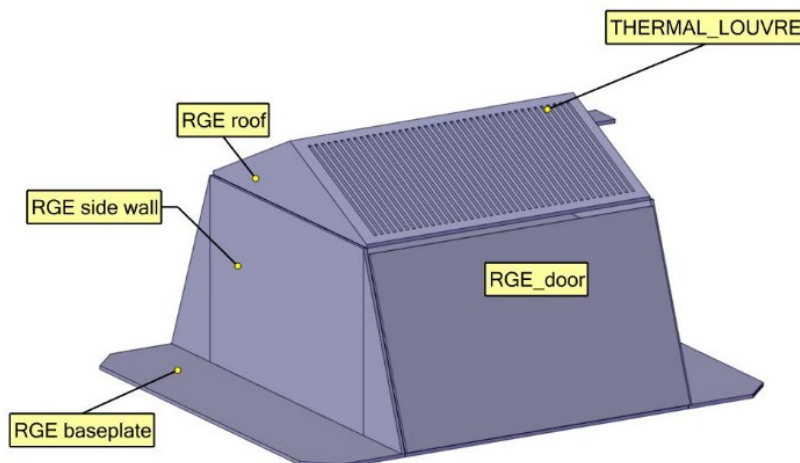


Figure 15-3: ALO platform

The antenna hub is mounted on the Y⁻ of the baseplate. And on the opposite site of the antenna hub, Y⁺, is available for the RFCS equipment. The warm electronics are mounted on the RGE ceiling underneath the RGE roof.

Figure 15-4 shows the ALO deployed configuration.

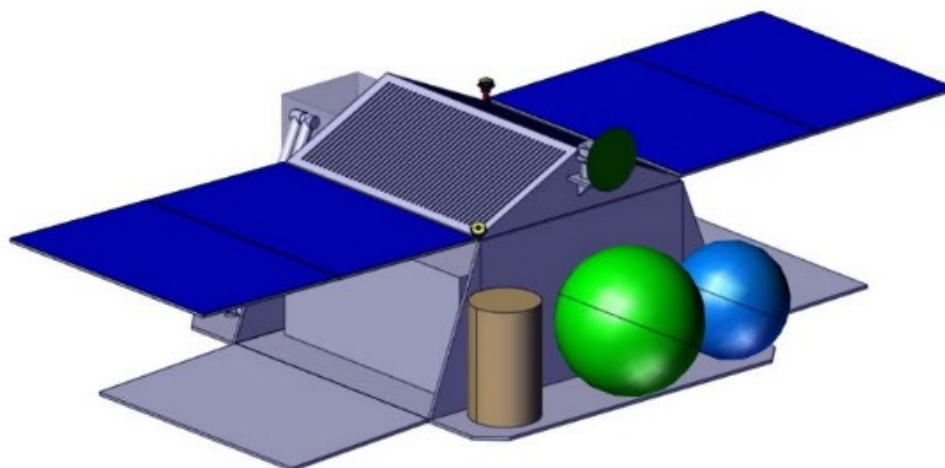


Figure 15-4: ALO deployed configuration

15.3 Internal and External accommodation

The equipment accommodation on the ALO is illustrated in Figure 2-2 and Figure 15-6.

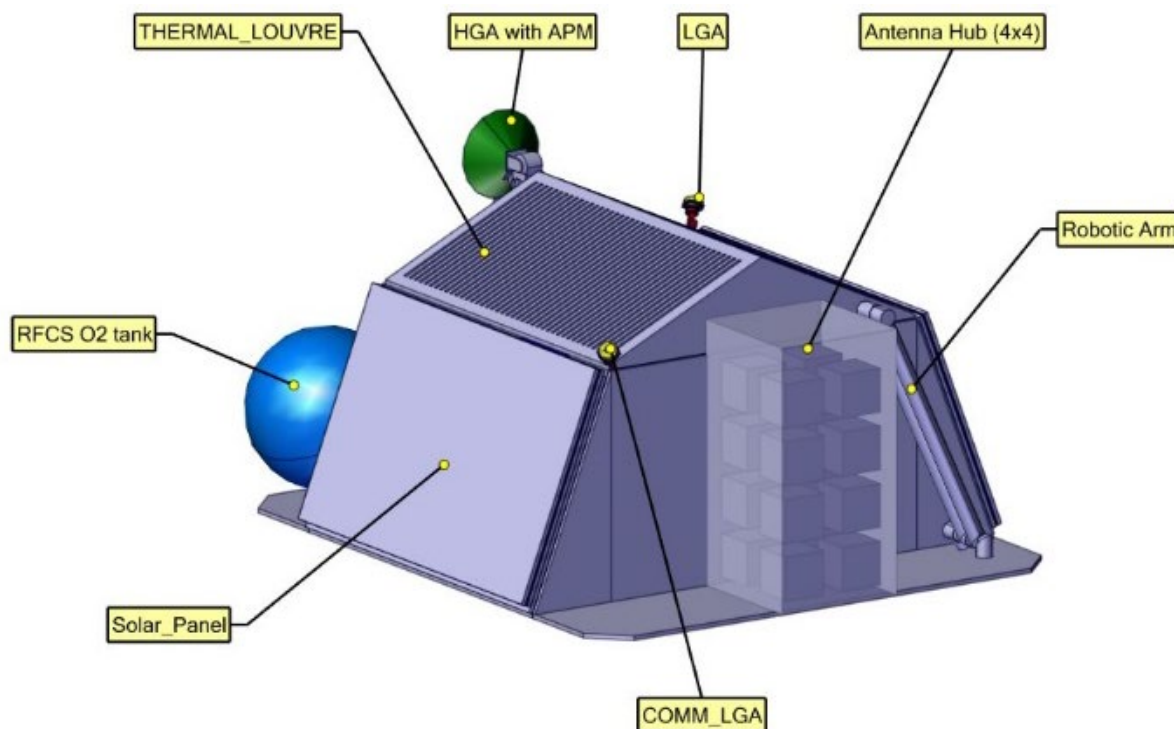


Figure 15-5: ALO external accommodation

Figure 15-6 shows the internal and external accommodation of the ALO configuration.

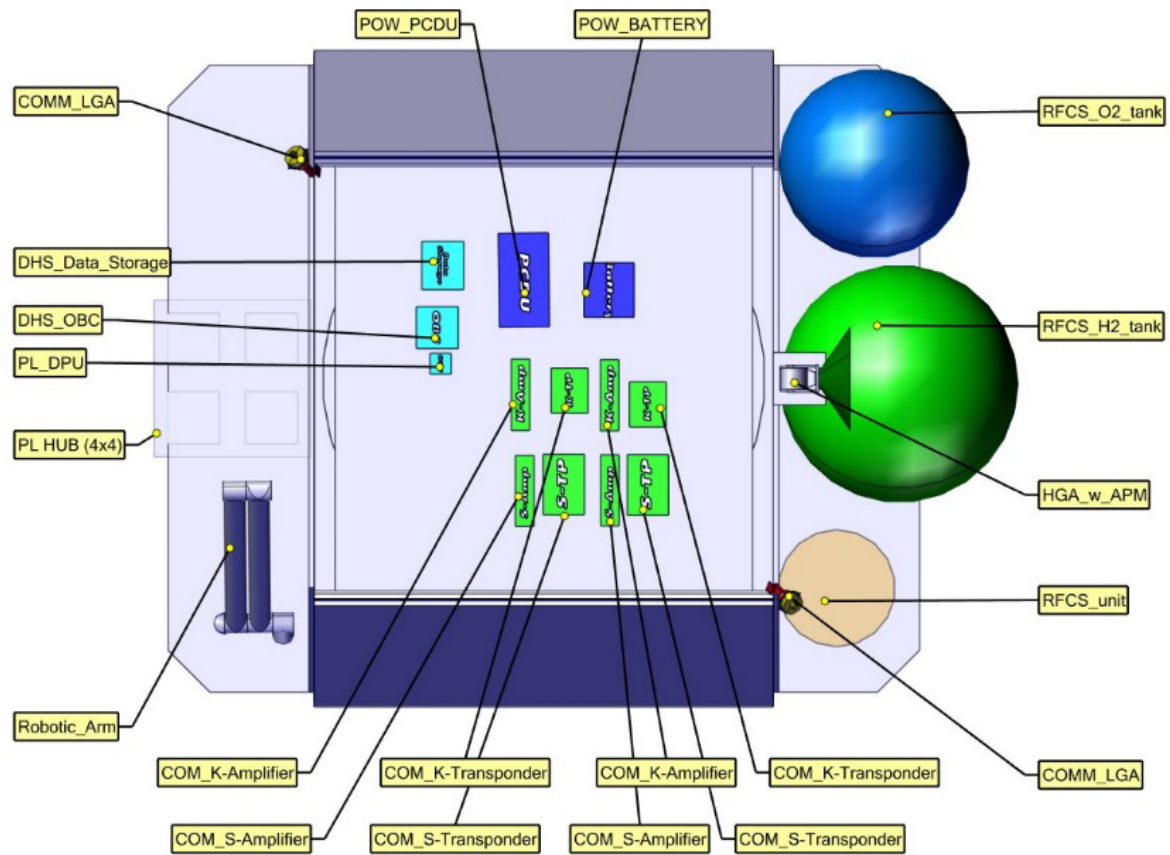


Figure 15-6: ALO equipment accommodation

First CoG estimation of the spacecraft in the launch configuration, stowed solar panel and full tank is shown in Figure 15-7.

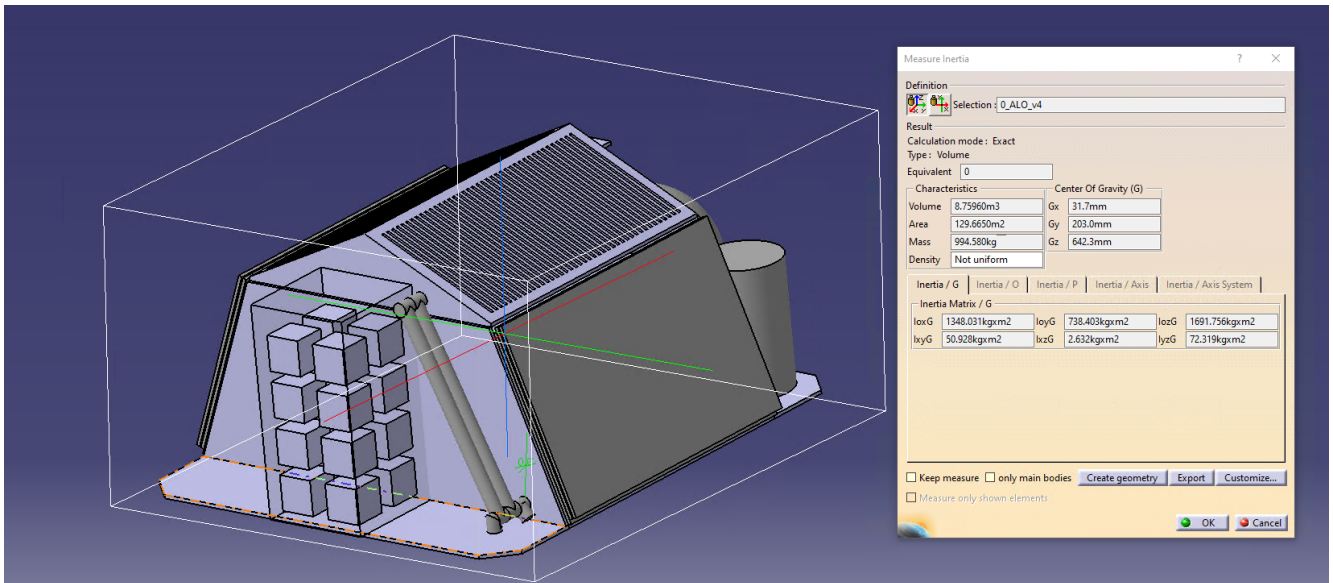


Figure 15-7: ALO – CoG and Mol

Currently the CoG location located at 600mm the LDE/CPE interface and about 30 cm away from the central axis toward the RFCS subsystem location. Further accommodation study needs to be performed in the future to meet the CoG limit of the launcher.

15.4 Overall Dimensions

The overall dimension of the ALO is shown in Figure 15-8.

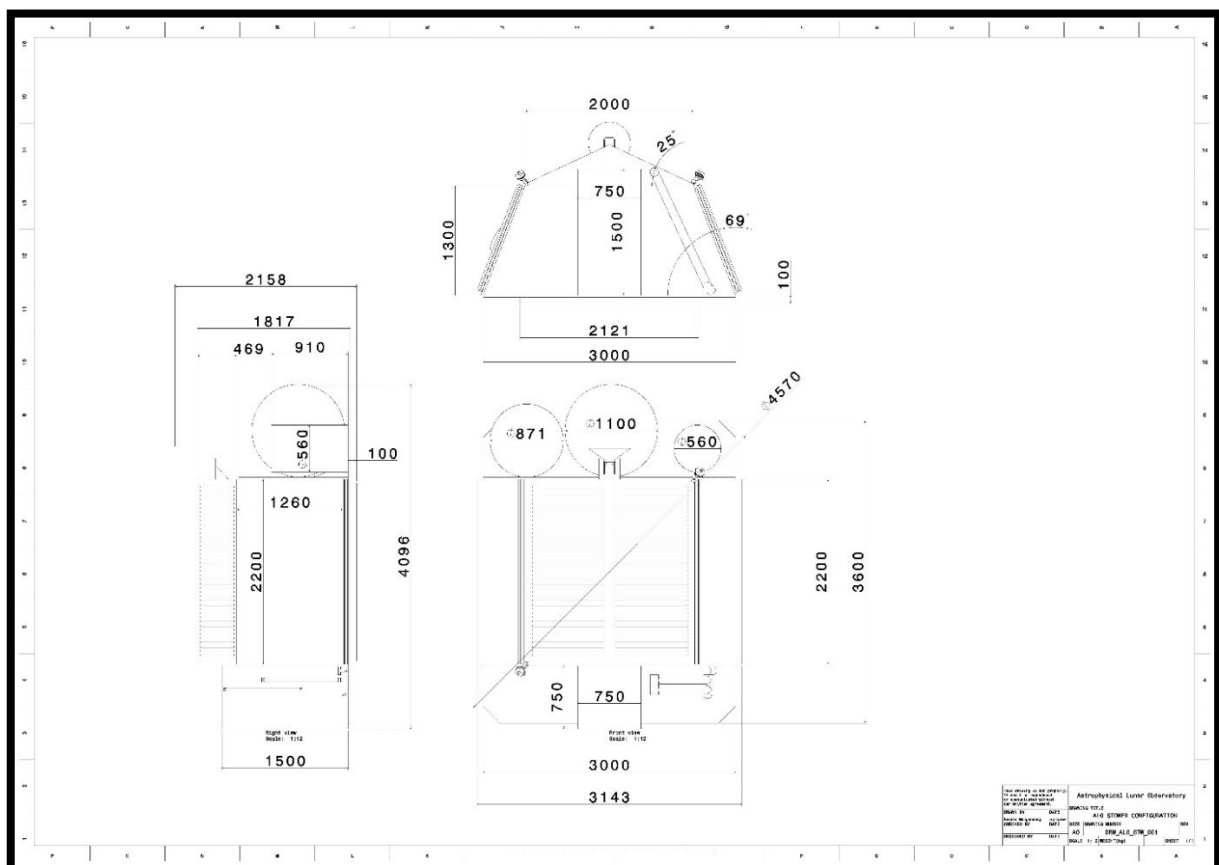


Figure 15-8: ALO – dimensional drawing

16 STRUCTURES

16.1 General considerations and initial assumptions

When talking about the structure of a spacecraft, we typically understand the elements required to provide mounting interfaces (points, surfaces, volumes) for equipment and instruments. In addition, the structure shall survive the launch environment undamaged, and any other event the spacecraft is subjected to; for ALO in particular, this means landing on the Moon. On top of that, there are requirements coming from sub-systems, like thermal, stability, etc. and requirements imposed by the launcher, like minimum stiffness, and a number of dynamic characteristics.

Specifically for ALO, when talking about structure, we do not intend the structural elements of the hub, or the central base, or the antennas. Structure here means the “structure of the ALO-specific CPE”, the CPE being the carrier of the elements to be landed and placed on the Moon surface, i.e. the rover, antennas, etc. Moreover, some equipment will remain on the CPE (robotic arm, etc.) supporting the functioning of the Astrophysical Lunar Observatory.

Initial assumptions	
Ref.	Assumption
1.	The interface provided by the LDE is circular and has a diameter of 2.121 m
2.	The launcher is Ariane 6 and the CPE shall comply with the fairing volume requirements
3.	The CPE needs to comply with all Ariane 6 structural requirements (strength, stiffness, etc.)
4.	No communality with other CPEs of other Lunar projects is required
5.	No separation requirement of the CPE from the LDE after landing
6.	No requirements towards the LDE.

Table 16-1: Initial assumptions

16.1.1 Key drivers and challenges

Key drivers		
Ref.	Key driver	Impact
1.	Low mass	Minimising the number of load paths foreseen (preferably one and identical for launch and landing) Use of high-strength and/or high-modulus and low-mass/-density materials Surface elements made from sandwich panels with CFRP skins
2.	Strength and stiffness	Use of high-strength and/or high-modulus and low-mass materials (note: strength/stiffness requirements not necessarily coupled)

3.	Low COG for safe landing also on inclined lunar surfaces	Heavy items are mounted/placed preferably as low as possible, light(er) items can be mounted/placed higher.
4.	Thermal requirements	Radiator surfaces shall face the cold sky and shall not be close to hot spacecraft elements such as SA. For improved thermal conductivity, heat dissipating equipment is placed preferably on metallic surfaces (i.e. panels with skins from aluminium); aluminium sandwich cores
5.	Rover egress onto Lunar surface	The structure supports rover operations by providing interfaces not only fixation during launch but also during deployment onto the Moon surface
6.	Robotic arm operations	The structure provides stiffness and strength as support of the robotic arm

Table 16-2: Key drivers

16.2 Baseline Description

Based on the assumptions and drivers above, the structural baseline chosen is explained below and shown in Figure 16-1.

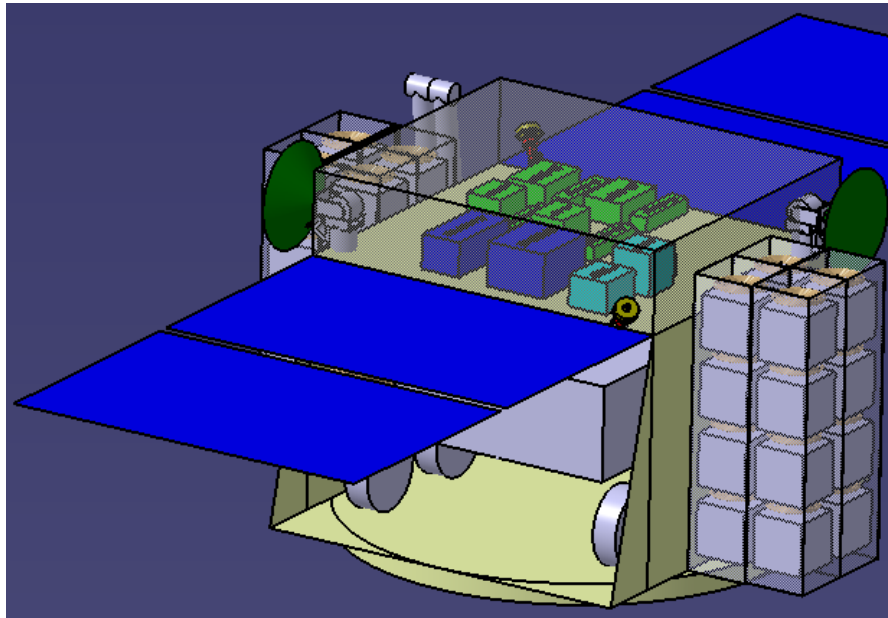


Figure 16-1: Baseline structural design

A short Carbon Fibre Reinforced Plastic (CFRP) sandwich cylinder will interface the LDE and carry a rover garage. For rover egress, a minimum deck surface is foreseen; its size depends on what is required for moving the rover from the CPE onto the lunar surface.

The rover garage provides volume for the rover and a mounting surface on top, for radiators facing the sky. Solar arrays are placed as extensions of the rover garage roof and need to be deployed; structural supports for SAs are foreseen. All surfaces, apart from the mounting

surface for the radiators, are made from CFRP skin / aluminium honeycomb panels. The garage roof on which the radiators are placed is made from aluminium / aluminium honeycomb sandwich panels; equipment, in particular heat-dissipating equipment, can be placed on the same panel as the radiator(s), but opposite side wrt the radiator(s).

The rover garage walls provide supports for placing of the antenna hubs in vertical orientation; the robotic arm can access the magazines and place them on the rover. Robotic arm support makes use of the rover garage wall / base; a stiff base for the arm is provided by local structural re-enforcements where required.

Reasons for not choosing a “Polar Explorer” type (that is, a large-diameter circular or multi-polygonal deck with mounting options below the deck) follow:

1. Mounting surface requirement in terms of area (mainly concerning antenna magazines) is not so big
2. Being rather “heavy”, the rover needs to be placed as low as possible, which means the deck needs to be low; as such mounting of equipment between LDE and a CPE deck is prohibitive
3. Placing radiators on a “low” deck, would not allow mounting hot equipment on the opposite side below
4. Placing solar arrays on a “low” deck would mean more shadowing effects

With the chosen configuration, the primary structure consists mainly of the LDE interface and the rover garage base, significantly reducing the overall surface and mass of the primary structure.

Rover side walls and roof are considered secondary structures and are mainly used to provide mounting surfaces. The robotic arm base is placed close to the LDE interface. That, being a primary structure, already provides a rather stiff base, but will still require some stiffening and a way to sustain the bending moment. Some generic provisions for taking (lateral) shear loads need to be foreseen.

Given the very preliminary structural design, no detailed mass estimation has been performed. Instead, from analogy to similar structures considered for other EL3 studies, a mass of 190 kg for the complete structure is considered.

16.2.1 List of Equipment

Primary structure – Central cylinder with small “rover” deck and interface to LDE

- CFRP/alu core central cylinder 2.121 m diameter, 0.2 m high, 20 mm sandwich, M55J & 3/16-AI 5056 0.0007P
- Aluminium ring interfacing LDE central cylinder top flange
- Circular deck made from CFRP-alu HC sandwich panels

Note: preferably, the central cylinder should be part of the LDE, i.e. the LDE should provide an interface to the CPE with enough clearance to mount a horizontal deck w/o the need for a cylinder.

Secondary structure

- Rover garage CFRP/aluminium (side walls) or aluminium/aluminium (roof) sandwich structures, with shear support
- Deck extension on opposite sides serves as rover driveway (if required)

- Robotic arm supports, interfaces for equipment

Tertiary structure (brackets, cleats, inserts, etc.)

- Equipment interfaces via inserts, brackets, etc.
- Local reinforcements for dispenser mounting, robotic arm, and other equipment

Structural elements are based on technologies well-mastered and flown on many Space missions

- Honeycomb panels are lightweight and exhibit high stiffness, multiple inserts are possible
- Aluminium skin & aluminium core (thermal)
- CFRP skin & aluminium core (weight, stiffness)
- Struts made from CFRP, with CFRP or aluminium or titanium end-fittings
- CFRP central cylinder structure, metallic I/F rings
- TRL 7-9

16.3 Considerations for scalability

For what scalability of the structure is concerned, the current structural baseline design does not offer the option to mount many more magazines, as the bending loads on the garage wall panels will increase and will require reinforcements causing too much of a mass penalty.

Should the available launch mass allow to carry more hubs, antennas, central bases, etc. on one mission (for instance going from 16 to 64 antenna), a larger deck might be the best way to carry such additional modules. However, this will increase the mass; this has been avoided by choosing a compact garage and placement of all equipment around it.

Making use of RFCS:

- RFCS tanks cannot be placed under the deck as for ECSM as rover egress would become more complex due to an increased deck height
- RFCS tanks would need to be mounted on the deck
- A larger CPE deck area would be required

16.4 Technology Needs

In terms of structure, no particular technology needs are identified.

17 GROUND SEGMENT AND OPERATIONS

17.1 General Considerations and Initial Assumptions

Based on the maturity level of the study, an Operations Concept has not yet been defined for this mission. The Ground Segment and Operations section in this report focuses on identifying the elements and issues that would need to be considered for addressing the Operations Concept in a later stage.

The following list summarizes the initial overall assumptions of the ALO mission concerning Ground Segment and Operations.

Initial assumptions	
Ref.	Assumption
1.	ALO is part of the EL3 framework
2.	ALO will launch no sooner than 2029
3.	ALO will be deployed at the EL3 landing site with LDE/CPE as the centrepiece (TBD).
4.	ALO is on the far side of the Moon, therefore relay communications will be needed through the Gateway, LCNS and any other available system.
5.	Once deployed on the lunar surface, ALO is independent of EL3. It is considered a separate mission from a Ground Segment and Operations point of view and will have its own surface operations centre.
6.	<p>The whole mission consists of 3 very distinct phases with very different needs, communications and operations capabilities:</p> <ul style="list-style-type: none"> • The EL3 flight and landing • The rover operations and deployment of the observatory • The operations of the observatory

Table 17-1: Initial assumptions

The 3 distinct mission phases defined in the assumptions can be considered as separate missions from a Ground Segment and Operations perspective.

Anything related to the EL3 phase is considered as a given and it is out of the scope for this study. The other two phases are analysed starting with a list of dedicated assumptions for each of these phases.

17.1.1 Assumptions for the Rover Operations Phase

Assumptions for the Rover Operations phase		
Ref.	Assumptions	Justification
1.	The rover operations will be conducted during lunar day.	There are no power generation, charging, or enough power storage capabilities foreseen to operate during lunar night.
2.	The whole rover operations phase includes the release from the lander, the commissioning and the deployment of the observatory.	These are all the activities where the rover must be active.
3.	The rover has hibernation capabilities for lunar night.	Given the observatory size, its deployment is likely to take several lunar days.
4.	The overall rover activities and observatory deployment are not time critical.	The hibernation capabilities of the rover give flexibility in the duration of the rover mission.
5.	There is no capability in the rover to communicate directly with the relay constellations. The communications with the rover will be transmitted through the lander and then the lunar relay constellations.	Based on other lunar rover designs, the lander is nominally used to relay the communications.
6.	The rover operations phase will require live teleoperations.	Even assuming certain level of autonomy on the rover, it is expected to monitor the rover activities in live and have direct influence in their execution.
7.	During lunar day, two relay passes of 8 hours duration per day are assumed. (TBD)	This assumption is based on a reasonable allocation of lunar relay resources and sizing of the operations team together with the assumption of rover activities not being time critical.
8.	The rover navigation through the terrain will use all the available means. This includes visual navigation capabilities on the rover, relative positioning with the lander and absolute localization systems provided by the lunar constellations.	This assumption considers the high accuracy needs for the observatory deployment location, the necessity to safely navigate through the terrain from the rover perspective and the obligation to maintain the communications link with the lander.
9.	Once the observatory is deployed, the rover has completed its nominal mission and is no longer used, although given the hibernation capabilities, it might still be used for maintenance of the Observatory if it is equipped to do so.	Maintenance operations will require high capabilities in the rover that have not been defined yet in this study but can be considered in a future iteration.

Table 17-2: Assumptions for the Rover Operations phase

The rover operations phase assumption regarding the number and duration of relay passes can be challenged. It might be a requirement to have a 24 hour coverage during this phase to prioritize a rapid deployment of the observatory against the operational costs derived by high availability demands in the relay constellation service and the operations team.

17.1.2 Assumptions for the Observatory Operations Phase

Assumptions for the Observatory Operations phase		
Ref.	Assumptions	Justification
1.	The Operations of the Observatory start once the rover operations have been completed.	The rover needs to complete the observatory construction mission before having a functional observatory.
2.	There will be an initial commissioning phase followed by a nominal operations phase.	Overall system observatory performances are expected to be characterized and calibrated before entering the nominal operations of the observatory.
3.	There are no time critical nominal operations.	The observatory is a fixed asset and there is no need to react rapidly to get the science data that is expected to be collected throughout the mission.
4.	The observatory is expected to have enough redundancy and autonomy to cope with contingencies affecting critical observatory survival systems.	System failures can occur at any time, also outside ground visibility. The system shall be able to rapidly recover or reconfigure to a safe state until the Operations team can get the data to identify, analyse the problem and decide a course of action as needed.
5.	There is no time critical intervention from ground required in case of failure.	In case of failure and science interruption, the rapid recovery of science activities is not considered time critical for the mission success.
6.	The Observatory operations will be conducted off-line.	Since there are no time critical activities, the operations team will operate the observatory off-line. The monitoring activities will also be nominally off-line since no time critical intervention from ground is required upon failure.
7.	Regular relay passes will be needed for commanding and science data download.	The whole observatory is expected to generate a constant volume of science data while in operations. This data will need to be transmitted to ground through regular relay passes before the storage capabilities of the observatory are exceeded.
8.	Planning and commanding operations for the observatory are only needed on a monthly basis (TBD) during the nominal operations phase.	Based on the inputs received during the study, a long term planning approach is sufficient to operate the observatory.
9.	The relay time and Ground Station time allocation is mostly driven by the generation rate of science data (for the full observatory).	The science data volume is expected to be various orders of magnitude larger than the nominal commanding volume, being the driving factor for the relay and ground communications allocation.

Table 17-3: Assumptions for the Observatory Operations phase

17.2 Specific Considerations for Operations

Each of the mission phases identified in the assumptions presented in Table 17-1 will have its own Ground Segment and, in particular, its own Control Centre adapted to the specific needs of each phase. A high level architecture of the Ground Segment for the Rover and Observatory Operations are shown in Figure 17-1 and Figure 17-2 below.

For the communications part concerning both the rover and the observatory, a “communications relay as a service” approach has been assumed. Two relay constellation systems have been considered in this study: the Gateway and LCNS. Both systems are expected to be in place when the ALO mission would be launched. From an operational approach, the use of any of these services (or any other that could be also be available), is simplified by the introduction of ERCO (European Relay Coordination Office). This is a solution that is currently available for Mars assets and initial discussions have started to establish something similar for the Moon.

In practice, ALO would communicate with ERCO about the amount of data that is needed to get down from the Observatory, the applicable time constraints for that data and the various uplink needs for operating ALO. ERCO would then coordinate with the available relay options to fulfil those requirements by allocating the needed relay passes and ground stations.

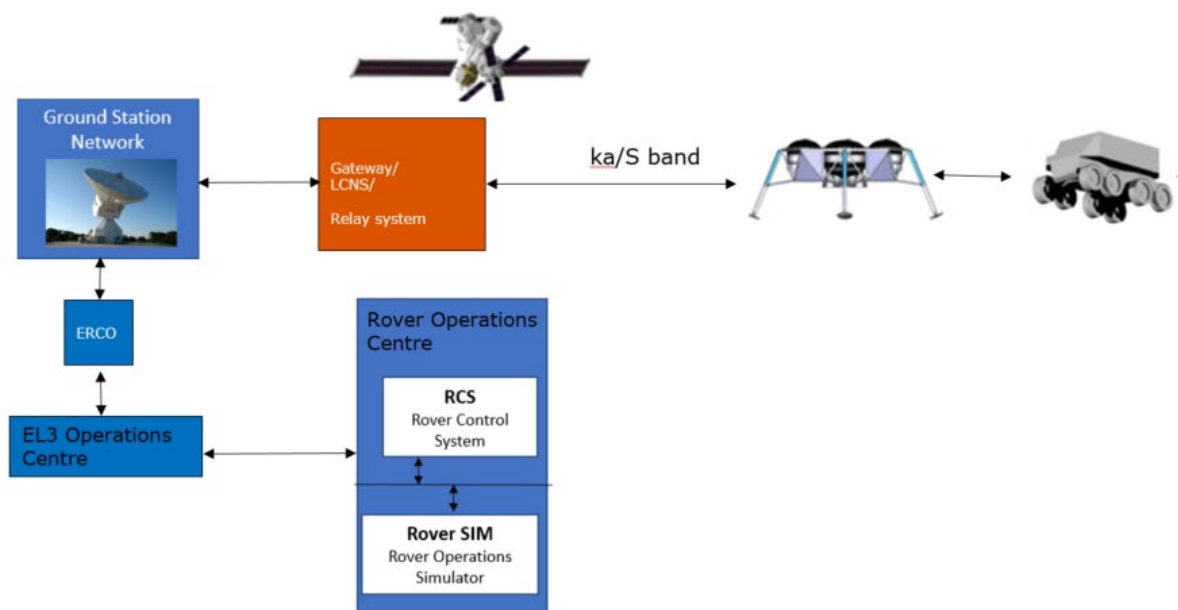


Figure 17-1: Ground Segment architecture for the Rover Operations

During the Rover mission phase, the communications are assumed to go through the lander. This way, the Rover Telecommands and Telemetry would go through the EL3 Operations Centre being the primary link with the Rover Operations Centre.

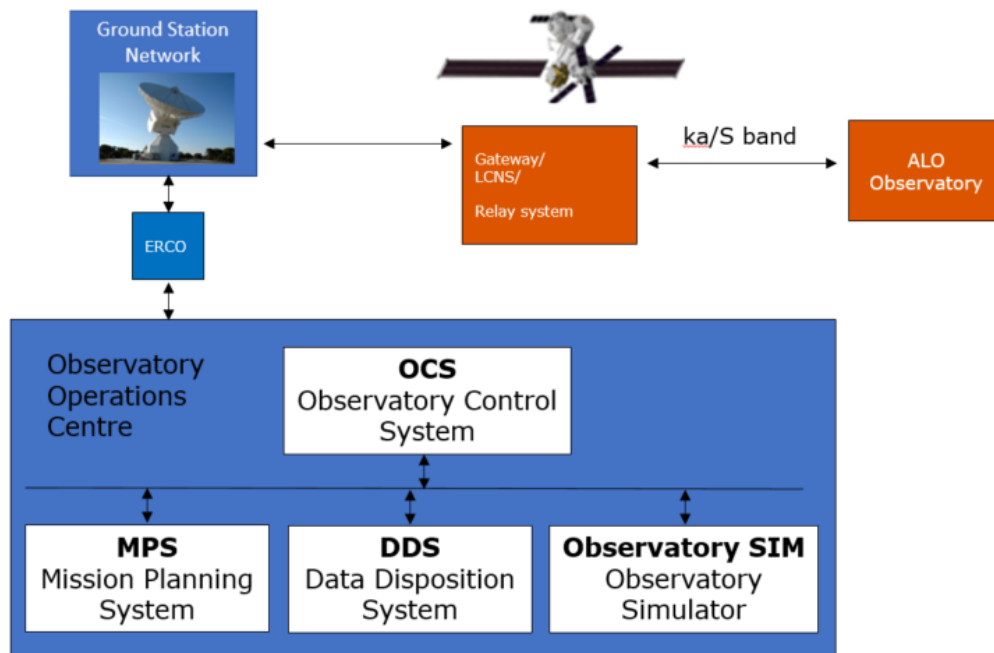


Figure 17-2: Ground Segment architecture for the ALO Observatory Operations

The Observatory Operations Centre is considered independent of any other Operations Centre. The relay constellation system will communicate directly with ALO and therefore a direct link between the Observatory Operations Centre and the ERC0 coordination office is considered in this case.

Low operational intensity for the Observatory is expected. The nominal interactions between ground and the Observatory are minimal and reduced to regular Housekeeping monitoring and commanding of the activities that are pre-planned in advance through long-term planning cycles.

The approach of having separate Control Centres for the EL3, the Rover and the Observatory allows an optimized distribution of the ground maintenance and operational resources, tailoring the support to the needs of each phase. This way, once the specific mission phase is completed, the associated Control Centre can be dismantled and the resources released without affecting the rest of the mission.

17.2.1 Considerations for Contingencies

From a time perspective, the Operations with the Rover and the Observatory are driven by the need of relay communications through a series of pre-scheduled passes and the need to stop all the operations during the Lunar night.

Although the overall timeline of activities are not time critical, this operational time constraints could translate into small blocks of activities that are considered time critical in the sense that a specific block would need to be completed e.g. before hibernation or before the end of a communication pass. This is specially applicable to the rover, for which live operations are envisaged.

If a communications pass is interrupted or if the hibernation starts in the middle of a delicate rover activity, the rover might be left in an inconvenient status for an undefined period of time.

This is a consideration to keep in mind when defining the operations, low level rover activity timelines and the rover autonomy itself.

Moreover, contingencies can occur at any time. Since 24 hours coverage is not guaranteed nor envisaged through all the mission, both Rover and Observatory would need to have enough level of autonomy and redundancy to cope with any contingencies that could put the mission in danger.

When it comes to contingencies in the Observatory, it was agreed in the CDF to not have an Operations team prepared for a fast response to resume the nominal science activities. This stresses the need of a fully autonomous system to react in case of contingency and the need to configure the Observatory to a safe status for an undefined period of time until the Operations team analyses and resolves the situation.

17.2.2 Considerations for Hibernation

The Rover and the ALO Observatory will have hibernation capabilities. Two types of Hibernation/Wake-up systems implementations are considered on-board: Event based and time commanded.

In the first one, the Hibernation/Wake-up is automatically triggered by detection of the system status and/or environment conditions in comparison with a given set of thresholds, while the second one is time controlled by the Operations team.

The adoption of both systems is recommended, so that the hibernation can be actively controlled by Ground while the system is kept safe in case an unforeseen situation occurs.

18 PROGRAMMATICS/AIV

18.1 General considerations and initial assumptions

Initial assumptions	
Ref.	Assumption
1.	Launch mid 2030's (2035)
2.	TRL 6 at Adoption Review (end phase B1)
3.	LDE generic and qualified (no new development)
4.	ALO CPE customized (new development)

Table 18-1: Initial assumptions

18.2 Baseline Description

The ALO system is composed of several elements:

- The Antenna element
- The Hub element
- The Base Station element (including generic CPE functions)
- The Rover element

18.3 Technology Requirements

18.3.1 Generalities

The Technology Readiness Levels (TRL) present a systematic measure, supporting the assessments of the maturity of a technology of interest and enabling a consistent comparison in terms of development status between different technologies.

The definition of the different TRL levels used in ESA are provided in Appendix A - Technology Readiness Levels Table of this report, and the associated models as per RD[112] are shown in Table 18-2:

TRL	ISO Definition	Associated Model
1	Basic principles observed and reported	Not applicable
2	Technology concept and/or application formulated	Not applicable
3	Analytical and experimental critical function and/or characteristic proof-of concept	Mathematical models, supported e.g. by sample tests
4	Component and/or breadboard validation in laboratory environment	Breadboard
5	Component and/or breadboard critical function verification in a relevant environment	Scaled EM for the critical functions
6	Model demonstrating the critical functions of the element in a relevant environment	Full scale EM, representative for critical functions

7	Model demonstrating the element performance for the operational environment	QM
8	Actual system completed and “flight qualified” through test and demonstration	FM acceptance tested, integrated in the final system
9	Actual system completed and accepted for flight (“flight qualified”)	FM, flight proven

Table 18-2: TRL scale

Table 18-3 shows an indication of the development time depending on the current TRL. According to the European Space Technology Master Plan, to prepare the contractual basis for multi-annual programs it takes about 18 months to reach political agreement on financial ceiling. This has also been included in Table 18-3.

TRL	Duration
5-6	4 years + 1.5 year
4-5	6 years + 1.5 year
3-4	8 years + 1.5 year
2-3	10 years + 1.5 year
1-2	12 years + 1.5 year

Table 18-3: TRL – development duration

18.4 TRL Assessment

Table 18-4 presents, for each ALO system element, the breakdown at unit level, the TRL assessment, and the heritage.

Element	Nr	Unit	TRL	Heritage
Antenna	1	Antenna assembly	5	TRL 8 for JUICE, TRL 5 for lunar env
	2	LNA	6	COTS for space, not lunar qualified. May be lunar qualified on board of Chinese mission Chang'e 4
	2	<i>RFoverFiber</i> transmitter	3	COTS for terrestrial applications
	1	Thermal Control	9	MLI, Heaters, Washers, White paint/SSM/OSR
Hub	16	ADC++ (double channel, TBC)	6	COTS for space, not lunar qualified
	32	<i>RFoverFiber</i> Receiver	3	COTS for terrestrial applications
	1	Hub Control Unit + Fiber Transceiver	6	COTS for space, not lunar qualified
	1	Wireless Transceiver	3	Terrestrial Applications

	1	Thermal Control	3	MLI, heaters, washers, White paint/ssm/osr: TLR 9 Louvers: TRL 3
	1	Structure	6	Standard elements (panels, struts, etc.)
	16	Roll for antenna wires	6	Standard elements
	1	Roll for hub wires	6	Standard elements
	1	Harness (10%)	N/A	N/A
Base Station		Science Data Processing Unit	6	Satellites by SPIRE (flying on LEO)
	2	Data Storage	3	Lunar Gateway
	1	OBC&RTU	6	MASCOT-2
	2	S-band Transponder	9	
	2	S-band Amplifier	9	Earth Obs Missions (Thales Alenia Spain)
	1	S-band RFDN	9	
	2	LGA (S)	9	
	2	K-band Transponder	6	TRL 9 for Tx at the end of this year TRL 6 due to Rx chain
	2	K-band Amplifier	9	
	1	K-band RFDN	9	
	1	HGA (K)	9	
	1	HGA APM	5	Heritage with TRL 9 exists but not for lunar environment, e.g. KARMA7-FG from KDA; additional mass margin added for orbital loads and dust protection
	1	HGA APM EU	6	Elektra SG
	1	Wireless Transceiver	3	Terrestrial Applications
	1	Rover deployment system (TBC)	TBD	
	1	Hubs deployment system (TBC)	TBD	
	1	Thermal Control	3	MLI, heaters, washers, White paint/ssm/osr, heat pipes: TRL 9 Possibly loop heat pipes: TRL 5 IF RHU needed: TRL 4 Louvers: TRL 3
	1	Solar Panels	4	
	1	Battery	6	
	1	PCDU	3	
	1	RFC	3	
	1	Structure	6	Standard elements (panels, struts, etc.): Heritage from previous EL3 mission (TBC)
	1	Harness (10%)	N/A	N/A
Rover	1	Rover	TBD	
	1	Robotic arm	TBD	

Table 18-4: Technology Readiness

18.5 Technology Needs

In addition to the TRL assessment, the study highlighted “technologies” which may have a major impact on the feasibility of the overall mission. These technologies are defined as “enablers”.

Table 18-5 presents a summary of the critical technologies for the mission covering low TRL but also additional information discussed during the study.

Critical Technology – ‘Enabler’						
Technology is baselined *	Equipment Name & Text Reference	Technology	Supplier (Country)	TRL	Funded by	Additional Information
✓	RF over Fiber transmitter	Data Handling / Communications		3		COTS for terrestrial applications
✓	RF over Fiber Receiver	Data Handling / Communications		3		COTS for terrestrial applications
✓	Louvers	Thermal control		3		
✓	Data Storage	Data Handling		3		
✓	Wireless Transceiver	Wireless		3		Terrestrial applications
✓	PCDU	Power		3		
✓	RFC	Power		3		
✓	Solar Panels	Power		4		
✓	RHU	Thermal Control		4		
✓	Antenna assembly	Science Payload		5		
✓	Rover			TBD		
✓	Robotic arm			TBD		
✓	Mechanisms					Various mechanisms
	Electronics	Low temperature electronics				

Table 18-5: Critical Technology – ‘Enabler’

18.6 Development Approach

A preliminary concept has been defined based on available technologies/equipment and new technologies (TRL3/4), but with a reduced scientific field.

In this context, it is premature to present a detailed development approach. However, a rough development approach can be assessed based on general assumptions for similar missions based e.g. on a typical ESA space mission as follows:

- Phase A terminating by a PRR
- Phase B1 terminating by a SRR
- Phase B2/C/D (implementation phase) confirmed by CMIN and/or a Mission Adoption
- Phase B2 terminating by a PDR
- Phase C terminating by a CDR
- Phase D terminating by a QR

The Preliminary Phase (A/B1) is also a phase of consolidation of the TRL of the less mature unit/instrument/technology to reach an acceptable maturity before the adoption and the implementation phase.

The units/instruments/technology development approaches need to be aligned with the ALO development and phases. The reviews at lower level (unit/ equipment) must be completed before ALO reviews.

Table 18-6 provides an order of magnitude of the duration of the phases based on similar development. Obviously, this will need to be reassessed with a more detailed definition of the flight system.

	Optimistic		Pessimistic
Pre Phase A / Consolidation			
Technology Development Activities		Pending TRL level	
Phase A	6 months		12 months
Phase B1	6 months		12 months
Adoption		TRL 6	
Phase B2	6 months		12 months
Phase C	18 months		24 months
Phase D1	20 months		24 months
Composite Phase D (coupled LDE-ALO AIT + Launch campaign)	6 months		10 months
Implementation Phase	50 months 4 years + 2 months		70 months 5 years + 10 months

Table 18-6: Phase durations

The schedule can be divided a 2 main parts: Preliminary Phase and Implementation Phase with the Adoption Review in the middle to authorize the Implementation Phase. A rough schedule for both phases is presented hereafter.

• Preliminary Phase:

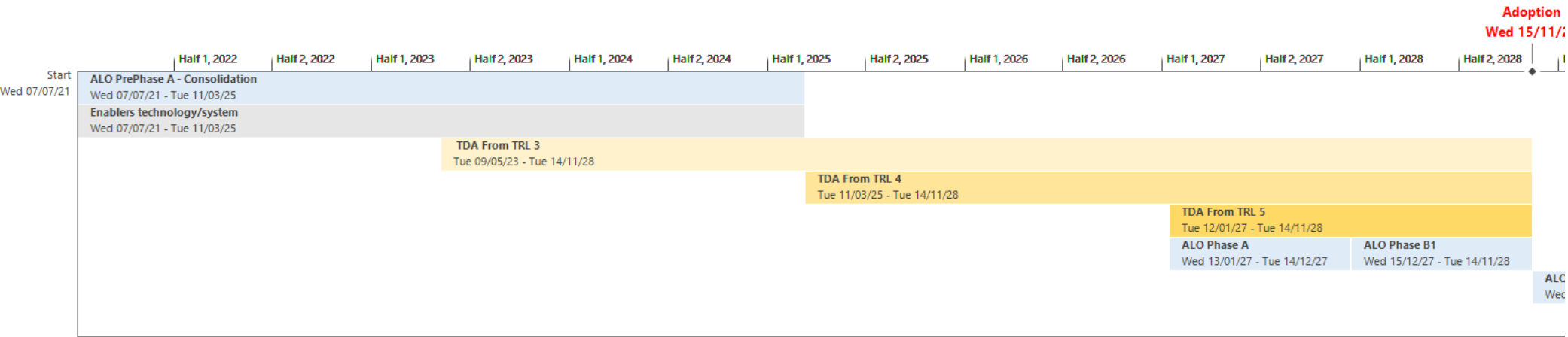


Table 18-7: Preliminary phase

- Implementation Phase:

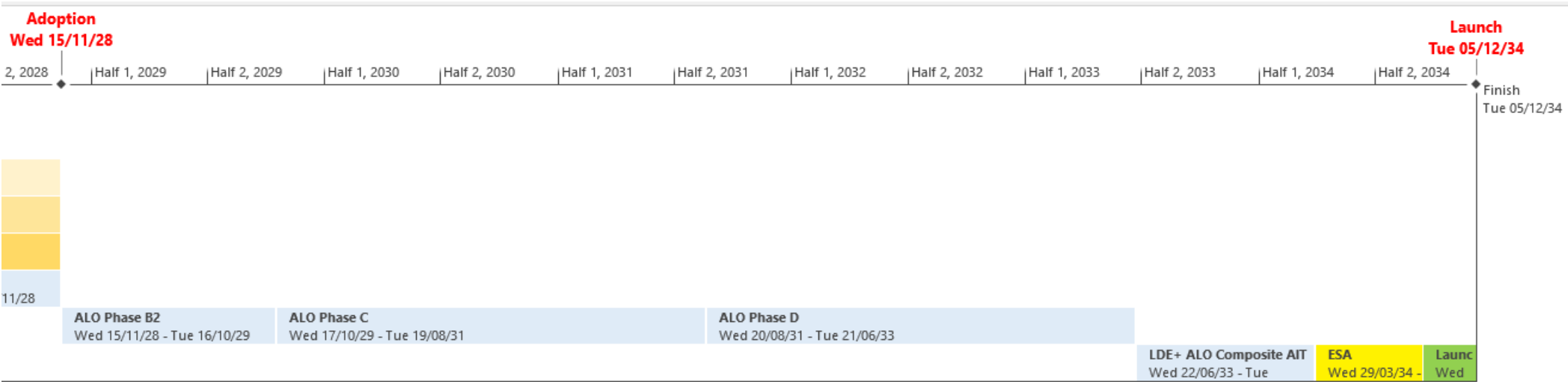


Table 18-8: Implementation phase

18.7 Summary and Recommendations

The ALO CDF study highlighted the difficulties in defining a credible design that meets all scientific expectations.

A preliminary concept has been defined based on available technologies/equipment and new technologies (TRL3/4), but with a reduced scientific field.

In this context a detailed programmatic proposal is not relevant. However based on general assumptions a launch date mid 2030's (2035) seems credible with an adoption review around 2028/2030.

This schedule allows a Preliminary Phase of 6/8 years to answer major questions raised during the CDF study related to scientific objectives and also technology developments.

This Page Intentionally Blank

19 RISK ASSESSMENT

This chapter has been deliberately removed from this version of the report.

20 COST

This chapter has been deliberately removed from this version of the report. Detailed results and cost figures are provided in a restricted dedicated Cost Report RD[2].

21 CONCLUSIONS

The study highlighted the challenges of the ALO mission and could not confirm feasibility for the minimum required observatory size, although it allowed to establish the main drivers and ways forward to mitigate the scale issues. This includes options such as demonstration or precursor missions, or alternative re-scoped mission.

The main feasibility concern lays on the extremely large number of antenna detectors the interferometric array observatory is made of, ranging from ~1,000 antennas for a minimal array size of 32 x 32 to ~16,000 antennas for an optimal array size of 128 x 128.

During the study, it was not possible to identify an antenna detector design nor a deployment strategy that would allow fitting all units in a single EL3 element with its payload mass constraints and the level of available resources.

Therefore, the study was reoriented to define the “smallest reasonable observatory”, still fully representative of a large scale one, and then identify the different design thresholds as function of the observatory size. This allowed to better understand the scaling of these challenges and drivers for the deployment and operation of such observatory.

As consequence of the methodology, the study results do not provide a consolidated detailed baseline design but instead they intent to support establishing a) a long term development plan addressing technology showstoppers and enablers, and b) the scoping of the mission in the overall context of the European Lunar Exploration strategy and, in particular, the EL3 program.

21.1 Representativeness of results

Due to the low maturity of the payload concept, a number of assumptions had to be made to allow progressing on the mission assessment. While a number of technical trades could not be completed due to limited time and expertise within the team.

This section presents the main considerations to be taken into account when assessing the representativeness of the results, especially as they could significantly impact the conclusions.

21.1.1 Dipole/antenna concept

The antenna detector has been specified exclusively from a radiofrequency performance point of view, but no specific physical implementation is prescribed. This of course allows exploring a wide range of solutions that could offer practical benefits from a compact accommodation in stowed configuration and simple deployment point of view.

For the purpose of the study, an implementation concept was chosen with the agreement of the science, mechanisms and robotic deployment teams. Nevertheless, it is not necessarily to be considered the optimal or best possible (e.g. mass, packaging volume,

complexity... they all are exceeding the limits required to achieve the minimum observatory within a single EL3).

21.1.2 Harness budget

Harness was early identified as a potential driver in terms mass, volume and deployment. Still the characterisation of the actual requirements and performances was very preliminary, in addition to very limited availability of relevant specifications from equivalent applications.

Harness budgets are very close coupled with deployment strategy, under the assumption that wireless solutions for the power and data network required by all antennas are infeasible. So results have a significant uncertainty on both, applicability and accuracy.

21.1.3 Magazine concept for deployment

This concept is also very close coupled to the specific antenna design and the deployment strategy, which remains highly uncertain. Ideally, more compact and simpler to deploy antenna units could significantly ease the deployment concept.

Nevertheless, it was considered a convenient way to decouple the overall deployment of antenna clusters from the deployment of each cluster as an independent hub and assess the feasibility of each hub/cluster.

21.1.4 Solutions for power supply and thermal control

Implementation solutions for power supply and thermal control at each level: unit, cluster, central base are very sensitive to power needs. Assumptions regarding power consumption and low temperature tolerance for units are considered too conservative for the needs of this mission.

Pending confirmation of the possibility to further develop the required technologies to mitigate this issue, power need thresholds have been identified to assess impact but uncertainties remain significant.

21.1.5 Communications architecture for relay systems

There is still certain level of uncertainty on the foreseen services and possible architectures required on the Moon to maximise the use of these resources. For this study, S-Band only for European relay constellations and hybrid S/Ka-band have been considered to allow assessing impact.

21.2 Feasibility considerations

As mentioned in the introduction, the feasibility of any full scale observatory could not be confirmed within the study envelope of one single EL3 mission:

- Payload accommodation and mass constraints extremely challenging
- Deployment extremely challenging
- Large power supply (e.g. fission reactor) required
- No solution for decentralised power supply identified yet
- On-ground wireless communications on the edge of foreseen technology
- In-situ data storage and processing on the edge of current technology
- Relay constellations capabilities very limited for foreseen science data volumes

Instead single EL3 mission concepts have been identified able to serve as:

- **Precursor:** small Imaging Array representative of a full scale observatory but potentially supporting both science experiments. Nevertheless power supply and night survival remains a major driver, and deployment is still extremely challenging (with no heritage in Europe).
- **Demonstration:** such as Global Detection mission only potentially easing/removing major feasibility concerns and allowing to test antenna technology and end to end data processing chain

21.3 Main outcome of the study

The study has allowed consolidating the observatory concept:

- Payload performances/resources well characterised and understood
- Support capabilities such as deployment and housekeeping infrastructure needs well identified
- Possible architectures identified and characterised, including feasibility considerations and limitations in terms of both, technology drivers/showstoppers and enabling technologies

And better understanding the scale problem and the impact that the observatory size has on its design and feasibility:

- Models have been developed based on sizing parameters of the Observatory system (number of antennas, use or not of hubs, observatory topology...) including, given the complexity of the system, well identified representativeness limits
- Major impact on feasibility given the large range of resources (and applicable/available technology solutions) across the possible observatory sizes
- Knowledge base has been established to support definition of follow up studies in the context of the EL3 flight opportunities

21.3.1 Technology showstoppers

The following major technology development areas, either limiting or with the potential to enable larger observatories, have been identified

- Low power electronics
- Passive thermal control designs for night survival
 - Tolerance to very low [non-operational] temperatures
- Wireless on-ground comms (10-100 Gbps @ 100-1000m)
- Low mass cryogenic harness for radiofrequency, digital data and power distribution
 - Low power losses and voltage drop over long distances
- Large scale lunar power supply
- Super-computing (data storage and processing) in space

21.4 Study objectives achievement

Despite mission feasibility not been confirmed, all objectives of the study have been achieved:

- The payload concept, needs, and constraints have been consolidated including characterisation of main observatory parameters (topology, performances, etc.) and its impact on the overall science return
- Several possible observatory architectures have been identified and traded, including impact on potential deployment strategies
- Overall mission concept implementing the payload deployment and operation has been defined for a one single EL3 mission, identifying potential gaps with respect to current EL3 capabilities
- Key technology developments to be further addressed through industrial studies have been identified
- Mission risk and schedule risks in the context of the with EL3 programmatic constraints have been assessed
- Areas for potential international cooperation have been identified

21.5 Further study areas

Three main areas for future work have been identified:

1. Payload and mission further consolidation

- Establish antenna specification derived from science requirements, and confirm suitability of a single antenna concept for both science cases
 - Study potential implementation solutions with low mass and compact stowed configuration that allows simpler deployment strategy

- Assess impact of Lunar environment compared to Earth based applications on foreseen performances and constraints
- Alternative deployment strategies for full-scale observatory, and confirm if full autonomous robotic deployment is the way to go or instead potential hybrid approaches involving human supported by robotic assets is more realistic
- Harness characterisation: performances and budgets consolidation
- Relay and navigation services
 - Limited information available from different constellations (specially from European solutions), and in all cases potentially too limiting for [full scale] ALO mission

2. Technology development activities

- In the areas identified in Section 21.3.1

3. Follow up studies

- Global Detection + small array for Imaging Array precursor mission
- Dedicated Global Detection mission
 - Possibility also in coordination with other EL3 missions

22 REFERENCES

Introduction chapter

- RD[1] ALO CDF Study - Internal Final Presentation slides, CDF Team, v1.0, 16/07/2021
- RD[2] ALO - CDF Industrial and Operations Cost Estimate report CDF-219(B) v1.0 , October 2021

Science Objectives chapter

- RD[3] L.V.E. Koopmans et al., “The Cosmic Dawn and Epoch of Reionisation with SKA”, Proceedings of Advancing Astrophysics with the Square Kilometre Array (AASKA14). 9-13 June 2014, Giardini Naxos, Italy. Online at <http://pos.sissa.it/cgi-bin/reader/conf.cgi?confid=215>, id.1. Published April 2015
- RD[4] M. van Haarlem et al., “LOFAR, the Low-Frequency Array”, A&A 556, A2 (2013), doi: 10.1051/0004-6361/201220873.
- RD[5] Rajan, R.T. et al., “Space-based aperture array for ultra-long wavelength radio astronomy”, Exp Astron 41, 271–306 (2016), doi.org/10.1007/s10686-015-9486-6
- RD[6] Thompson et al., “Interferometry and Synthesis in Radio Astronomy”, Springer 2017, ISBN 978-3-319-44431-4
- RD[7] P. Zarka et al, “Planetary and exoplanetary low frequency radio observations from the Moon”, Planetary and Space Science 74 (2012) 156–166, doi.org/10.1016/j.pss.2012.08.004
- RD[8] M. Bentum et al., “A roadmap towards a space-based radio telescope for ultra-low frequency radio astronomy”, Advances in Space Research 65 (2020) 856–867, doi.org/10.1016/j.asr.2019.09.007
- RD[9] Bentum, M.J., Boonstra, A.J., “The RFI situation for a space-based low-frequency radio astronomy instrument”, Proceedings of the 2016 RFI conference, Socorro, New Mexixo, USA, October 2016.IEEE, inspec: 16620879
- RD[10] Alexander, J.K., et al., 1969. “The spectrum of the cosmic radio background between 0.4 and 6.5 MHz”, Astrophys. J. 157, L163.M.J. Bentum et al. / Advances in Space Research 65 (2020) 856–867
- RD[11] Alexander, J.K., Novaco, J.C., 1974. “Survey of the galactic background radiation at 3.93 and 6.55 MHz”, Astron. J. 79, 777–785.

- RD[12] N. Bassett et al., "Characterizing the radio quiet region behind the lunar farside for low radio frequency experiments", *Advances in Space Research*, Volume 66, Issue 6, 15 September 2020, Pages 1265-1275
- RD[13] M.A. Garrett, "Resolving The Sky - Radio Interferometry: Past, Present and Future", *RTS2012*, April 17-20, 2012, Manchester, UK, *Proceedings of Science*, <https://pos.sissa.it/163/050/pdf>
- RD[14] E. de Lera Acedo et al., "SKALA, a log-periodic array antenna for the SKA-low instrument: design, simulations, tests and system considerations", *Experimental Astronomy*, October 2015, Volume 39, Issue 3, pp 567-594, doi 10.1007/s10686-015-9439-0
- RD[15] S.A. Torchinsky et al., "EMBRACE@Nançay: An Ultra Wide Field of View Prototype for the SKA", February 2016, *Astronomy and Astrophysics*, 589, DOI: 10.1051/0004-6361/201526706
- RD[16] G. W. Kant, et al., "EMBRACE: A Multi-Beam 20,000-Element Radio Astronomical Phased Array Antenna Demonstrator," *IEEE Trans. Antenna and Propagat.*, vol. 59, no. 6, pp. 1990–2003, Jun. 2011.
- RD[17] Nivedita Mahesh et al., "Validation of EDGES Low-Band Antenna Beam Model", *arXiv:2103.00423 [astro-ph.IM]*, doi: 10.3847/1538-3881/abfdab
- RD[18] Grant Heiken, David Vaniman, Bevan M French. "Lunar Sourcebook: A User's Guide to the Moon", Cambridge University Press, 1991
- RD[19] T. D. Carozzi, "Intrinsic cross-polarization ratio (IXR) for antenna arrays and improving polarimetry via polarization diversity," 2015 1st URSI Atlantic Radio Science Conference (URSI AT-RASC), 2015, pp. 1-1, doi: 10.1109/URSI-AT-RASC.2015.7303206.
- RD[20] "Wide Field Astronomy & Technology for the Square Kilometre Array", *SKADS 2009*, 4-6 November 2009, *SKADS Proceedings*, editor S. Torchinsky et al., Chateau de Limelette, Belgium, May 23, 2011, <https://pos.sissa.it/132/>, ISBN 978-90-805434-5-4
- RD[21] N. Mahesh et al., "Validation of the EDGES Low-band Antenna Beam Model", vol.162, no.2, *The Astronomical Journal*, 2021, doi: 10.3847/1538-3881/abfdab
- RD[22] A.A. Rogers, Estimates of isolation requirements for EDGES-3 electronics, Edges memo 299, www.haystack.mit.edu/haystack-memo-series/edges-memos
- RD[23] L. Chen et al., Antenna design and implementation for the future space Ultra-Long wavelength radio telescope, vol.45, no.2, *Experimental Astronomy*, 2018, doi: 10.1007/s10686-018-9576-3
- RD[24] ITU, Recommendation ITU-R SM.329-12, Unwanted emissions in the spurious domain, 2012

- RD[25] R.T. Rajan, et al., "Distributed correlators for interferometry in space," 2013 IEEE Aerospace Conference, 2013, pp. 1-9, doi: 10.1109/AERO.2013.6496932.
- RD[26] G.W. Kant et al., EMBRACE System Design and Realisation, SKADS Conference, 4-6 November 2009, Chateau de Limelette, Belgium, PoS (SKADS 2009) 037
- RD[27] J. Hamaker et al. ,Understanding radio polarimetry. I. Mathematical foundations, Astron. Astrophys. Suppl. Ser. 117, 137-147 (1996)
- RD[28] K. M. B. Asad et al., Polarization leakage in epoch of reionization windows – I. Low Frequency Array observations of the 3C196 field, Monthly Notices of the Royal Astronomical Society, Volume 451, Issue 4, 21 August 2015, Pages 3709–3727, <https://doi.org/10.1093/mnras/stv1107>
- RD[29] J. Burns et al, Dark Cosmology: Investigating Dark Matter & Exotic Physics in the Dark Ages using the Redshifted 21-cm Global Spectrum, AAS Bulletin Vol. 51, Nr. 3 (Astro2020 decadal survey on astronomy and astrophysics)
- RD[30] M. F. Morales and J. Hewitt, Toward Epoch of Reionization Measurements with Wide-Field Radio Observations, 2004 ApJ 615 7
- RD[31] J.R. Pritchard, A. Loeb, Constraining the unexplored period between reionization and the dark ages with observations of the global 21 cm signal, 2010, PRD 82 2
- RD[32] J. Burns et al., FARSIDE: A Low Radio Frequency Interferometric Array on the Lunar Farside, arXiv:1907.05407v1
- RD[33] W. van Cappellen et al., "Apertif, Phased Array Feeds for the Westerbork Synthesis Radio Telescope", accepted for publication by A&A, Instrumentation and Methods for Astrophysics (astro-ph.IM), 2021, arXiv:2109.14234 [astro-ph.IM]
- RD[34] Wijnholds, S.J., Ivashina, M., Maaskant, R., Warnick, K.F. (2012) Polarimetry with phased array antennas: sensitivity and polarimetric performance using unpolarized sources for calibration. IEEE Transactions on Antennas and Propagation, vol. 60, no. 10, pp. 4688-4698. <http://dx.doi.org/10.1109/TAP.2012.2207340>
- RD[35] L.V.E. Koopmans et al., Peering into the dark (ages) with low-frequency space interferometers, Experimental Astronomy, 2021, doi.org/10.1007/s10686-021-09743-7
- RD[36] CENELEC, European standard, EN 55022 / CISPR 22, Information Technology Equipment - Radio disturbance characteristics - Limits and methods of measurement

- RD[37] T. D. Carozzi and G. Woan, "A Fundamental Figure of Merit for Radio Polarimeters," in IEEE Transactions on Antennas and Propagation, vol. 59, no. 6, pp. 2058-2065, June 2011, doi: 10.1109/TAP.2011.2123862
- RD[38] Y. Sun, N. B. Agostini, S. Dong, D. Kaeli, "Summarizing CPU and GPU Design Trends with Product Data", arXiv:1911.11313v2
- RD[39] E. Chapman, S. Zaroubi, F. B. Abdalla, F. Dulwich, V. Jelić, B. Mort, "The effect of foreground mitigation strategy on EoR window recovery", Monthly Notices of the Royal Astronomical Society, Volume 458, Issue 3, 21 May 2016, Pages 2928–2939, <https://doi.org/10.1093/mnras/stw161>
- RD[40] F. G. Mertens et al., "Improved upper limits on the 21 cm signal power spectrum of neutral hydrogen at $z \approx 9.1$ from LOFAR", Monthly Notices of the Royal Astronomical Society, Volume 493, Issue 2, April 2020, Pages 1662–1685, <https://doi.org/10.1093/mnras/staa327>
- RD[41] K. M. B. Asad et al., "Polarization leakage in epoch of reionization windows – III. Wide-field effects of narrow-field arrays ", Monthly Notices of the Royal Astronomical Society, Volume 476, Issue 3, May 2018, Pages 3051–3062, <https://doi.org/10.1093/mnras/sty258>
- RD[42] H. K. Vedantham et al., "Lunar occultation of the diffuse radio sky: LOFAR measurements between 35 and 80 MHz", Monthly Notices of the Royal Astronomical Society, Volume 450, Issue 3, p.2291-2305, <https://doi.org/10.1093/mnras/stv746>
- RD[43] A. M. Sardarabadi, L.V.E. Koopmans, "On Identifiability and Estimability of Direction Dependent Calibration of Radio Interferometric Arrays", arXiv:1902.02482v1
- RD[44] J. D. Bowman et al., "An absorption profile centered at 78 megahertz in the sky-averaged spectrum", Nature vol. 555, nr. 7694, pg. 67-70, 2018, <https://doi.org/10.1038/nature25792>
- RD[45] J. Nambissan T. et al., "SARAS 3 CD/EoR radiometer: design and performance of the receiver", Experimental Astronomy vol. 51, pg. 193-234, 2021, <https://doi.org/10.1007/s10686-020-09697-2>
- RD[46] G. J. A. Harker et al., "Parametrizations of the 21-cm global signal parameter estimation from single-dipole experiments", MNRAS vol. 455, issue 4, pg. 3829-3840, 2016, <https://doi.org/10.1007/s10686-020-09697-2>
- RD[47] S. Jester & H. Falcke New Astronomy Reviews 53 (2009) 1–26
- RD[48] A. Loeb & M. Zaldarriaga 2004, Phys. Rev. Lett 92, 211301
- RD[49] A. Liu, J.R. Pritchard, M. Tegmark & A. Loeb 2013, Phys. Rev. D 87, 043002

- RD[50] D. S. Prinsloo et al., "EMI modelling of an 80 kHz to 80 MHz wideband antenna and low-noise amplifier for radio astronomy in space," 12th European Conference on Antennas and Propagation (EuCAP 2018), 2018, pp. 1-4, doi: 10.1049/cp.2018.0820.
- RD[51] Gurnett, D.A., Kurth, W.S., Kirchner, D.L. et al. The Cassini Radio and Plasma Wave Investigation. Space Sci Rev 114, 395–463 (2004).
<https://doi.org/10.1007/s11214-004-1434-0>
- RD[52] Bougeret, J.L., Goetz, K., Kaiser, M.L. et al. S/WAVES: The Radio and Plasma Wave Investigation on the STEREO Mission. Space Sci Rev 136, 487–528 (2008). <https://doi.org/10.1007/s11214-007-9298-8>

Payload Antenna chapter

- RD[53] Preliminary Specifications for the Square Kilometre Array, Technical report, R. T. Schilizzi et al, 2007, Online available:
http://www.skatelescope.org/uploaded/5110_100_Memo_Schikizzi.pdf

Environment chapter

- RD[54] On the origin of the ionosphere at the Moon using results from Chandrayaan-1 S band radio occultation experiment and a photochemical model, R. K. Choudhary, K. M. Ambili, Siddhartha Choudhury, M. B. Dhanya, Anil Bhardwaj, 2016
- RD[55] New views of the lunar plasma environment, J.S. Halekas, Y. Saito, G.T. Delory, W.M Farrell, 2010
- RD[56] Lunar Dust Transport and Potential Interactions With Power System Components, NASA Contractor Report 4404, Cynthia M. Katzan and Jonathan L. Edwards, November 1991
- RD[57] Lunar weather measurements at three Apollo sites 1969-1976, Space Weather Vol. 11, Monique Hollick and Brian J. O'Brien, 2013
- RD[58] In Situ Measurements of Lunar Dust at the Chang'E-3 Landing Site in the Northern Mare Imbrium, Research Article JGR Planets, Detian Li et al., 2019
- RD[59] The Lunar Dust Problem: From Liability to Asset, AIAA Paper, Lawrence A. Taylor et al., January 2005

Mission Analysis chapter

- RD[60] QuickMap, <https://quickmap.lroc.asu.edu>
- RD[61] M.K. Barker et al., *A new lunar digital elevation model from the Lunar Orbiter Laser Altimeter and SELENE Terrain Camera*, Icarus, vol. 273, p. 346-355, July 2016.

- RD[62] ESA CDF Study Team, *Lunar Comms - Assessment of Constellation of Satellites for Lunar Communications and Navigation*, CDF Study Report CDF-180 (A), May 2018.
- RD[63] ESA CDF Study Team, *Lunar Sample Return with LCNS*, October 2020
- RD[64] Surrey Satellite Technology Ltd. , *Lunar Pathfinder Service User Guide v002*, <https://www.sstl.co.uk/getmedia/b492cb63-39de-4801-aabdc004f3aff8a1/LunarPathfinder-UserManual-WebSite-v002.pdf>, July 202

Systems chapter

- RD[65] European Large Logistic Lander (EL3) Generic Mission and System Requirements Document (GMSRD), EL3 Study Team, Issue 1.1, 13-11-2020, ESA-E3P-EL3-RS-002
- RD[66] The Lunar Radio Array (LRA), Lazio, Carilli, Hewit, Furlanetto, Burns, 05-08-2009, <https://lunar.colorado.edu/publicfiles/lazio-SPIE-09.pdf>

Data Handling chapter

- RD[67] Proceedings of the 5th International SpaceWire Conference Gothenburg
- RD[68] Glenair RF-Over-Fiber Media Converters: <https://www.glenair.com/opto-electronic/rf-over-fiber-media-converters.htm>
- RD[69] SpaceABLE 10G SL Series Radiation-Resistant Optical Transceivers: <https://reflexphotonics.com/embedded-transceivers/spaceable-sl-40gfd-120g/>

Telecommunications chapter

- RD[70] The Future Lunar Communications Architecture, IOAG Report V1.2, February 2020
- RD[71] Communication Frequency Allocation and Sharing in the Lunar Region, Recommendation SFCG 32-2R2, July 2019
- RD[72] Proximity-1 Space Link Protocol – Physical Layer, CCSDS 211.1-B-4, December 2013
- RD[73] Spacecraft Onboard Interface Services – High Data Rate Wireless Proximity Network Communications, CCSDS Draft Recommended Standard, March 2021
- RD[74] International Communication System Interoperability Standards (ICSIS), ICSIS Standard Rev. A, September 2020

Mechanisms chapter

- RD[75] Inertial damping system for deployment speed reduction of tubular boom antenna unit for JUICE mission, ESMATS 2019, M. Tokarz et al, <https://esmats.eu/esmatpapers/pastpapers/pdfs/2019/tokarz.pdf>
- RD[76] Innovative Escapement-Based Mechanism for Micro-Antenna Boom Deployment, m.Tokarz et al. AMS 2014, <https://esmats.eu/amspapers/pastpapers/pdfs/2014/tokarz.pdf>
- RD[77] Ispispace CubeSat Deployer, <https://www.isispace.nl/product/quadpack-cubesat-deployer/>
- RD[78] Karma-7 FG Antenna Pointing Mechanism from Kongsberg, Product Specification, <https://www.kongsberg.com/globalassets/kda/products/space/products/mechanical-systems/antenna-pointing-mechanisms-apm/karma-7-fg.pdf>
- RD[79] Elektra Drive Electronics for APM from Kongsberg, Product Specification, <https://www.kongsberg.com/kda/products/space/products/space-mechanisms/elektra/>
- RD[80] Novel Antenna Concept, On behalf of Centre for Astronomical Instrumentation (CAI), PDF presentation, https://tec.esa.int/sites/cdfact-5bbAE2/_layouts/15/WopiFrame.aspx?sourcedoc={F5A20580-7AE2-42F8-96EE-E29A44AA86FB}&file=CAI%20Antenna%20Concepts.pptx&action=default
- RD[81] Polyimide Film Antennas for a Lunar Radio Observatory, K.P. Stuart et al, https://lunarscience.nasa.gov/wp-content/uploads/LSF13P/Stewart_nlsf2013.pdf
- RD[82] The Lunar Radio Array (LRA), J. Lazio et al., <https://lunar.colorado.edu/publicfiles/lazio-SPIE-09.pdf>
- RD[83] Advanced deployable structural systems for small satellites, W. Keith Belvin et al., <https://ntrs.nasa.gov/api/citations/20170003919/downloads/20170003919.pdf>
- RD[84] In-orbit performance analysis of the deorbit sail tested on board PW-Sat2 nanosatellite, E. Ryszawa et al., ESMATS 2019, <https://esmats.eu/esmatpapers/pastpapers/pdfs/2019/ryszawa.pdf>

Robotics chapter

- RD[85] Delian Summary Report, DLN-SR-LDO-13, Leonardo S.p.a., 2018
- RD[86] Arm and Joints Preliminary Design Document, DLN-PDD-SES-003, Selex ES S.p.A., 2013
- RD[87] Predicting motor and generator maximum torque as a function of mass, Paper, 10.1109/IEMDC.2017.8002164, Russel H. Marvin; Brian T. Helenbrook; Kenneth D. Visser, 2017 IEEE International Electric Machines and Drives

- RD[88] Wilkinson, A., & DeGennaro, A. (2007). Digging and pushing lunar regolith: Classical soil mechanics and the forces needed for excavation and traction. *Journal of Terramechanics*, 44(2), 133-152.
- RD[89] Bekker, M. G. (1969). *Introduction to terrain-vehicle systems*. Michigan Univ Ann Arbor.
- RD[90] Boesch, C., Langer, U., Zahnd, B., & Bonduelle, B. (2009). *Development of an actuator for solar-array deployment*
- RD[91] ECSS Space engineering – Mechanisms, ECSS-E-ST-33-01C, ECSS, Rev.2, 01/03/2019
- RD[92] Polar Explorer - CDF study report CDF-212(A), April 2021
- RD[93] LunarCaves - CDF Study report CDF-217(A), July 2021
- RD[94] Heracles (HRLPM2) – CDF Study report CDF-151(A), Dec 2014
- RD[95] Heracles (HRLPM2) – CDF Study report CDF-156(A), May 2015

Thermal chapter

- RD[96] Vasavada, A. R., Paige, D. A., and Wood, S. E., 'Near-Surface Temperatures on Mercury and the Moon and the Stability of Polar Ice Deposits', *Icarus*, 141/2: 179–193 <doi:10.1006/icar.1999.6175>. (1999)
- RD[97] Hayne, P. O., et al., "Global regolith thermophysical properties of the Moon from the Diviner Lunar Radiometer Experiment. *Journal of Geophysical Research: Planets*, 122, 2371–2400. <https://doi.org/10.1002/2017JE005387>, (2017).
- RD[98] Keihm, S. J., Peters, K., Langseth, M. G., and Chute Jr., J. L., 'Apollo 15 measurement of lunar surface brightness temperatures. Thermal conductivity of the upper 1 1/2 meters of lunar Regolith', *Earth and Planetary Science Letters*, 19: 337–351. (1973)
- RD[99] Horai, K.-I., Simmons, G., Kanamori, H., and Wones, D., 'Thermal diffusivity, conductivity and thermal inertia of Apollo 11 lunar material', *Proceedings of the Lunar Science Conference*, 3: 2243–2249. (1970)
- RD[100] Cremers, C. J., and Birkebak, R. C., 'Thermal conductivity of fines from Apollo 12', *Proceedings of the Lunar Science Conference*, 3: 2311–2315, (1971).
- RD[101] R. Birkebak, C. Cremers, "Thermophysical Properties of Lunar Materials: Part I", *Advances in Heat Transfer*, Vol. 10. (1974)
- RD[102] Williams, J.-P., Paige, D. A., Greenhagen, B. T., Sefton-Nash, E. "The global surface temperature of the Moon as measured by the Diviner Lunar Radiometer Experiment", *Icarus*, Vol. 283, p. 300-325, 2017. <https://doi.org/10.1016/j.icarus.2016.08.012>

- RD[103] <https://doi.org/10.1029/2019JE006028>Gaier, J. R.; Jaworske, D. A., “Lunar Dust on Heat Rejection System Surfaces: Problems and Prospects”, Space Technology and applications international forum 2007, New Mexico, Feb. 11-15, NASA/TM—2007-214814, 2007.
- RD[104] TN12 – Final Report, rev. B (P5-2-114-TN12), ESA Study : Low Temperature Electronics - Thermal Design for future exploration missions SD3

Power chapter

- RD[105] Dmitry Bokach, Manuel Hempel and Jarle Farnes, “Alternative Energy Storage Solutions for Lunar Night Survival in Human Exploration Scenarios - TN2: Assessment and trade-off of energy storage solutions for HERACLES and long term lunar missions”. CMR Prototech RP_33907_PR_01. ESA Contract No. 4000127686, Alternative Energy Storage Solutions for Lunar Night Survival in Human Exploration Scenarios.
- RD[106] Mathieu Roig, "RFCS Lunar Mission WP2300 Mathematical Model, 03/04/2020, D2079-TN-003-01, Air Liquide Advanced Technologies. ESA Contract No. 4000127686, Alternative Energy Storage Solutions for Lunar Night Survival in Human Exploration Scenarios.
- RD[107] ‘Development of Innovative Mechanical Flexible Solar Array Architecture’, B. Boulanger et al, Proceedings of the European Space Power Conference 2016, Thessaloniki, Greece, 3-7/10/16.
https://www.e3s-conferences.org/articles/e3sconf/pdf/2017/04/e3sconf_espc2017_01005.pdf
- RD[108] CDF Study Report “ECSSM - European Charging Station for the Moon”, CDF-218(A), August 2021.
- RD[109] Jack O. Burns et al. “Farside Array for Radio Science Investigations of the Dark Ages and Exoplanets – Probe study final report” JPL- Caltech. November 2019.
- RD[110] R. M. Ambrosi et al. “European Radioisotope Power Systems Programme: Recent Updates”, Nuclear and Emerging Technologies for Space, Knoxville, TN, April 6 – April 9, 2020, <https://nets2020.ornl.gov>.
- RD[111] Donald T. Palac, “Fission Surface Power Systems (FSPS) Project : Final Report for the Exploration Technology Development Program (ETDP)”, January 2011, NASA/TM—2011-216975.

Programmatics/AIV chapter

- RD[112] Technology Readiness Levels Handbook for Space Applications, TEC-SHS/5551/MG/ap, Issue 1 Revision 6, Dated September 2008

This page intentionally blank

23 ACRONYMS

Acronym	Definition
AIT/V	Assembly, Integration and Test/Verification
AC	Alternating current
ADC	Analogue to Digital Converter
ALO	Astrophysical Lunar Observatory
APM	Antenna Pointing Mechanism
APR	Array power regulator
ATB	Avionics Test Bench
ATV	Automated Transfer Vehicle
AVM	Avionics Verification Model
BCDR	Battery charge-discharge regulator
BOL	Beginning Of Life
BPF	Band-pass Filter
CaC	Cost at Completion
CAD	Computer Aided Design
CAN	Controller Area Network
CBK PAN	Centrum Badań Kosmicznych PAN
CCSDS	Consultative Committee for Space Data Systems
CD	Cosmic Dawn (the range of redshift from $z = 30$ to $z = 15$)
CDF	Concurrent Design Facility
CDR	Critical Design Review
CER	Cost Estimation Relationship
CFI	Call For Ideas
CFRP	Carbon Fibre Reinforced Polymers
CIC	Cost Improvement Curve
CLPS	Commercial Lunar Payload Services
CLTV	Cis-Lunar Transfer Vehicle
CME	Coronal Mass Ejection

CoG	Centre of Gravity
COTS	Commercial Of The Shelf
CPE	Cargo Platform Element
CTP	Science Core Technology Programme
DA	Dark Ages (the range of redshift from $z = 200$ to $z = 30$)
DALI	Dark Ages Lunar Interferometer
DC	Direct current
DDE	Dust Detector Experiments
DELIAN	Dextrous Lightweight Arm for Exploration
DHS	Data-Handling subsystem
DTE	Direct-to-Earth
E3P	European Exploration Envelope Programme
ECSS	European Cooperation for Space Standardisation (Standards)
Ed	Earth Day
EEE	Electrical, Electronic and Electromechanical
EFM	Engineering Flight Model
EL3	European Large Logistic Lander
ELFO	Elliptical Lunar Frozen Orbits
ELHS	European Large Heat Source (large RHU)
EM	Engineering Model
EMC	Electromagnetic Compatibility
EML2	Earth-Moon Libration point 2
EOL	End Of Life
EoR	Epoch of Reionization (the range of redshift from $z = 15$ to $z = 6$)
EPC	Electronic Power Conditioner
EPS	Electrical power system
EQM	Engineering Qualification Model
ESA	European Space Agency
ESCM	European Charging Station for the Moon
ESD	Electrostatic Discharge

ESM	European Service Module
EU	Electronic Unit
ExPeRT	Exploration Preparation, Research & Technology
FARSIDE	Farside Array for Radio Science Investigations of the Dark ages and Exoplanets
FCR	Fuel cell regulator
FFT	Fast Fourier Transform
FM	Flight Model
FoV	field of view
FPGA	Field Programmable Gate Array
FTE	Full Time Equivalent
GSE	Ground Support Equipment
GSP	General Studies Programme
GSTP	General Support Technology Programme
GW	Gateway
HC	HoneyComb
HDR	High Data Rate
HDRM	Hold-Down and Release Mechanism
HERACLES	Human-Enhanced Robotic Architecture and Capability for Lunar Exploration and Science
HGA	High Gain Antenna
HIB	Hibernation (mode)
HLS	Human Landing System
HRE	Human and Robotic Exploration
HV	High voltage
HW	HardWare
I/F	Interface
I/O	Input/Output
IAOG	Interagency Operations Advisory Group
ICISIS	International Communication System Interoperability Standards

ISRU	In-Situ Resource Utilisation
IXR	intrinsic cross-polarization ratio
LCL	Latching current limiter
LCNS	Lunar Communication and Navigation Service
Ld	Lunar Day
LDE	Lunar Descend Element
LGA	Low Gain Antenna
LHP	Loop Heat Pipe
LNA	Low Noise Amplifier
LO	Lunar Orbit
LOFAR	Low Frequency Array
LP	Lunar Pathfinder
LPR	Lunar Prospecting Rover
LRV	Lunar Rover Vehicle
LS	Lunar Surface
MAIT	Manufacturing Assembling Integrating Testing
MEO	Medium Earth-Orbit
MeVs	Million Electron Volts
MLI	Multi-Layer Insulation
Mol	Moments of Inertia
MPPT	Maximum power point tracker
Nb	Number
NDA	Non-Disclosure Agreement
NID	Non-Ionizing Dose
NRHO	Near Rectilinear Halo Orbit
OBC	On-board Computer
OBS	Observation (mode)
OSR	Optical Solar Reflectors
PA	Product Assurance
PCDU	Power Conditioning and Distribution Unit

PCU	Power Conditioning Unit
PDR	Preliminary Design Review
PDU	Power Distribution Unit
PFM	Proto Flight Model
PO	Project Office
PRR	Preliminary Requirement Review
PVA	Photovoltaic assembly
QM	Qualification Model
QR	Qualification Review
RAMS	Reliability, Availability, Maintainability and Safety - 'Dependability'
RF	Radio Frequency
RFA	Radio Frequency Analyser
RFC	Regenerative Fuel Cell
RFCS	Regenerative Fuel Cell System
RFDN	Radio Frequency Distribution Network
RFI	radio frequency interference
RFOF	RFOverFiber
RGE	Rover Garage Element
RHU	Radioisotopic Heater Unit
RISK	Risk related requirement ID
ROM	Rough Order of Magnitude
RTG	Radioisotope thermoelectric generator
RTU	Remote Terminal Unit
RX/TX	Receiver/Transmitter
S/C	Spacecraft
SA	Solar Array
SADA	Solar Array Drive Assembly
SADM	Solar Array Drive Mechanism
SEP	Solar Energetic Particles
SFCG	Space Frequency Coordination Group

SKA	Square Kilometre Array
SMA	Shape Memory Alloy
SPF	Single Point Failure
SRR	System Requirement Review
SSM	Secondary Surface Mirrors
SSMM	Solid State Mass Memory
STEM	Storable Extendible Tubular Member
STM	Structural Thermal Model
TBC/ TBD	To Be Confirmed/ Defined
TC	Telecommand
TCS	Thermal Control System
TDA	Technology Development Activity
TID	Total Ionizing Dose
TM	Telemetry
TMTC	Telemetry and telecommand
TRL	Technology Readiness Level
TT&C	Telemetry, Tracking, and Command
TWT	Traveling Wave Tube
TWTA	Traveling Wave Tube Amplifier
VLSA	Very Large Solar Array

A APPENDIX A - TECHNOLOGY READINESS LEVELS TABLE

The different levels used in ESA, defined in an internal working group based on NASA's Technology Readiness Levels and ECSS-E-HB-11A RD[121] are provided in Table A-1.

Technology Readiness Level	Milestone achieved for the element	Work achievement (documented)
TRL 1 – Basic principles observed and reported	Potential applications are identified following basic observations but element concept not yet formulated.	Expression of the basic principles intended for use. Identification of potential applications.
TRL 2 – Technology concept and/or application formulated	Formulation of potential applications and preliminary element concept. No proof of concept yet.	Formulation of potential applications. Preliminary conceptual design of the element, providing understanding of how the basic principles would be used.
TRL 3 – Analytical and experimental critical function and/or characteristic proof-of-concept	Element concept is elaborated and expected performance is demonstrated through analytical models supported by experimental data/characteristics.	Preliminary performance requirements (can target several missions) including definition of functional performance requirements. Conceptual design of the element. Experimental data inputs, laboratory-based experiment definition and results. Element analytical models for the proof-of-concept.
TRL 4 – Component and/or breadboard functional verification in laboratory environment	Element functional performance is demonstrated by breadboard testing in laboratory environment.	Preliminary performance requirements (can target several missions) with definition of functional performance requirements. Conceptual design of the element. Functional performance test plan. Breadboard definition for the functional performance verification. Breadboard test reports.
TRL 5 – Component and/or breadboard critical function verification in a relevant environment	Critical functions of the element are identified and the associated relevant environment is defined. Breadboards not full-scale are built for verifying the performance through testing in the relevant environment, subject to scaling effects.	Preliminary definition of performance requirements and of the relevant environment. Identification and analysis of the element critical functions. Preliminary design of the element, supported by appropriate models for the critical functions verification. Critical function test plan. Analysis of scaling effects. Breadboard definition for the critical function verification. Breadboard test reports.

TRL 6: Model demonstrating the critical functions of the element in a relevant environment	Critical functions of the element are verified, performance is demonstrated in the relevant environment and representative model(s) in form, fit and function.	Definition of performance requirements and of the relevant environment. Identification and analysis of the element critical functions. Design of the element, supported by appropriate models for the critical functions verification. Critical function test plan. Model definition for the critical function verifications. Model test reports.
TRL 7: Model demonstrating the element performance for the operational environment	Performance is demonstrated for the operational environment, on the ground or if necessary in space. A representative model, fully reflecting all aspects of the flight model design, is build and tested with adequate margins for demonstrating the performance in the operational environment.	Definition of performance requirements, including definition of the operational environment. Model definition and realisation. Model test plan. Model test results.
TRL 8: Actual system completed and accepted for flight ("flight qualified")	Flight model is qualified and integrated in the final system ready for flight.	Flight model is built and integrated into the final system. Flight acceptance of the final system.
TRL 9: Actual system "flight proven" through successful mission operations	Technology is mature. The element is successfully in service for the assigned mission in the actual operational environment.	Commissioning in early operation phase. In-orbit operation report.

Table A-1: Definition of Technology Readiness Levels